DOCTOR OF PHILOSOPHY

Exploring the contribution of SGK isoforms to signalling and mediating resistance to Akt inhibitors in breast cancer cells

Sommer, Eeva

Award date:
2013

Awarding institution:
University of Dundee

DOCTOR OF PHILOSOPHY

Exploring the contribution of SGK isoforms to signalling and mediating resistance to Akt inhibitors in breast cancer cells

Eeva Sommer

2014

University of Dundee

Exploring the contribution of SGK isoforms to signalling and mediating resistance to Akt inhibitors in breast cancer cells

Eeva M. Sommer

A thesis submitted for the degree of Doctor of Philosophy

University of Dundee

August 2013

I. Contents

II. List of Figures

III. List of Tables

IV. Acknowledgements

First and foremost I would like to thank my advisor Professor Dario Alessi for giving me the opportunity to work in his laboratory and for all of his enthusiasm, encouragement, patience, and guidance that have greatly helped me to complete this PhD. I would also like to thank Hannah Greenwood and Darren Cross from AstraZeneca who followed this project with special attention and gave many useful suggestions.

In addition, a big thank you to everyone in the DSTT for reagents and inhibitor screening, in particular I would like to thank Tom Macartney for cloning and Fiona Brown for raising antibodies. Big thanks also to the MRC PPU support staff Judith Hare, Alison Hart, Allison Bridges, Rachel Naismith, Kirsten Airey and Janis Stark for making my life a lot easier. I would also like to thank David Campbell and Bob Gourlay for mass spectrometry analysis.

I would like to thank all members of Dario's lab, both past and present with special thanks to: Ayaz and Laura – thank you for welcoming me to work on your projects and letting me learn by your side. Helen & Esther – thank you for being my "PhD buddies", we all embarked on this process during Summer 2010 and I cannot emphasise enough how important your support through all the ups and downs has been. Esther – these acknowledgements would not be complete without me thanking you for being my loyal running buddy. Agne – thank you for all the chats, the endless giggles and the good old rants. Sourav – thank you for being my bay mate for the whole duration of my PhD and thank you for remaining calm and relaxed even when all the three girls went hysterical in Bay 3. Kristina – thanks for keeping us young and laughing. Chandana – thank you for being a wonderful fellow PhD student.

I would like to thank my mother Marja and my grandmother Kerttu for their love and for supporting me throughout my 20 years of education and pursue of knowledge.

Last but not least I would like to thank my husband Morgen for his kindness, love and support and for always being there for me.

V. Declarations

I hereby declare that the following thesis is based on the results of investigations conducted by myself, and that this thesis is of my own composition. Work other than my own is clearly indicated in the text by reference to the researchers or their publications. This dissertation has not in whole, or in part, been previously presented for a higher degree.

Eeva M. Sommer

I certify that Eeva Sommer has spent the equivalent of a least nine terms in research work in the College of Life Sciences, University of Dundee, and that she has fulfilled the conditions of the Ordinance General No. 14 of the University of Dundee and is qualified to submit the accompanying thesis in application for the degree of Doctor of Philosophy.

Dario R. Alessi

VI. List of Publications

Sommer, E.M., Bago R., Cross, D., Davies, B.R., and Alessi, D.R. Sustained Akt inhibition leads to up-regulation of SGK3. *Manuscript in preparation*

Sommer, E.M., Dry, H., Cross, D., Guichard, S., Davies, B.R., and Alessi, D.R. (2013). Elevated SGK1 predicts resistance of breast cancer cells to Akt inhibitors. Biochem J *452*, 499-508.

Gan, X., Wang, J., Wang, C., **Sommer, E**., Kozasa, T., Srinivasula, S., Alessi, D., Offermanns, S., Simon, M.I., and Wu, D. (2012). PRR5L degradation promotes mTORC2-mediated PKC-delta phosphorylation and cell migration downstream of G alpha(12). Nature Cell Biology *14*, 686-696.

Pearce, L.R., **Sommer, E.M**., Sakamoto, K., Wullschleger, S., and Alessi, D.R. (2011). Protor-1 is required for efficient mTORC2-mediated activation of SGK1 in the kidney. Biochem J *436*, 169-179.

Najafov, A., **Sommer, E.M**., Axten, J.M., Deyoung, M.P., and Alessi, D.R. (2011). Characterization of GSK2334470, a novel and highly specific inhibitor of PDK1. Biochem J *433*, 357-369.

VII. Abbreviations

4EBP1	eukaryotic translation initiation factor 4E-binding protein
AGC	protein kinase A, protein kinase G, protein kinase C
Akt	v-akt murine thymoma viral oncogene homologue 1 (PKB)
AMPK	AMP-activated protein kinase
AS160	Akt substrate of 160kDa
ATP	adenosine triphosphate
Bad	Bcl-2 antagonist of cell death
BSA	bovine serum albumin
cAMP	cyclic adenosine monophosphate
CHAPS	3-[(3-Cholamidopropyl)dimethylammonio]-1-propanesulfonate
C. elegans	*Caenorhabditis elegans*
cpm	counts per minute
C-terminal	carboxy-terminal
Da	Dalton
Deptor	DEP domain containing mTOR interacting protein
DMEM	Dulbecco's Modified Eagle's Medium
DMP	dimethyl pimelimidate
DMSO	dimethyl sulphoxide
DNA	deoxyribonucleic acid
DSTT	Division of Signal Transduction Therapy
DTT	dithiothreitol
E. coli	*Escherichia coli*
ECL	enhanced chemiluminescence
EDTA	ethylenediamine tetra acetic acid
EGF	epidermal growth factor
EGTA	ethyleneglycol bis (2-aminoethylether)-N, N-tetra acetic acid
ERK	extracellular signal regulated kinase
FBS	foetal bovine serum
ENaC	epithelial sodium channel
FOXO	forkhead box O
GPCR	G-protein coupled receptor
GSK	glycogen synthase kinase
GST	glutathione S-transferase
HA	YPYDVPDYA peptide (haemagglutinin)
HEK293	human embryonic kidney 293
HeLa	Henrietta Lacks
HPLC	high performance liquid chromatography
HRP	horseradish peroxidase
IB	immunoblot
IC50	concentration required for 50% inhibition of enzyme activity
IGF1	insulin-like growth factor
IGFR	insulin-like growth factor receptor
IgG	immunoglobulin G
IP	immunoprecipitation
IRS	insulin receptor substrate
ki	kinase inactive

LPA	lysophosphatidic acid
MAGI	membrane-associated guanylate kinase, WW and PDZ domain-containing protein
MDM2	mouse double minute 2 homolog
MEF	mouse embryonic fibroblast
Mg-ATP	magnesium adenosine 5'-triphosphate complex
mLST8	mammalian lethal with SEC13 protein 8
mRNA	messenger ribonucleic acid
MS/MS	tandem mass spectrometry
mTOR	mammalian target of Rapamycin
NDRG1	N-myc downregulated protein 1
Nedd	Neural Precursor Cell-Expressed Developmentally Down-Regulated Protein
NHE	sodium hydrogen exchanger
N-terminal	amino-terminal
PBS	phosphate buffered saline
PDGFR	platelet-derived growth factor receptor
PDK1	3-phosphoinositide-dependent kinase 1
PH	pleckstrin homology
PI3K	phosphoinositide 3-kinase
PIF	PDK1 interacting fragment
PKA	protein kinase A (cAMP-dependent protein kinase)
PKB	protein kinase B (also known as Akt)
PKC	protein kinase C
PMSF	phenylmethanesulphonylfluoride
PPAR	peroxisome proliferator-activated receptors
PRAS40	proline-rich Akt substrate of 40 kDa
Protor	protein observed with Rictor
PtdIns	phosphatidylinositol
PTEN	phosphatase and tensin homolog
PX	phox homology domain
qRT-PCR	quantitative reverse transcription-polymerase chain reaction
Raptor	regulatory associated protein of mTOR
Rictor	Rapamycin-insensitive companion of mTOR
rpm	revolutions per minute
RTK	receptor tyrosine kinase
S6	ribosomal S6 protein
S6K	p70 ribosomal S6 kinase
S. cerevisiae	*Saccharomyces cerevisiae*
SDS	sodium dodecyl sulphate
SDS-PAGE	sodium dodecyl sulphate polyacrylamide gel electrophoresis
SGK	serum- and glucocorticoid-regulated protein kinase
Sin1	SAPK-interacting protein 1
shRNA	short hairpin RNA
TBST	Tris-buffered saline/tween
TFEB	transcription factor EB
Tris	Tris(hydroxymethyl)methylamine
TSC	tuberous sclerosis
Tween	polyethylene glycol sorbitan monolaurate
UTR	untranslated region
wt	wild type
w/v	weight to volume

VIII. Amino Acid Code

Amino acid	Three letter symbol	One letter symbol
alanine	Ala	A
arginine	Arg	R
asparagine	Asn	N
aspartate	Asp	D
cysteine	Cys	C
glutamate	Glu	E
glutamine	Gln	Q
glycine	Gly	G
histidine	His	H
isoleucine	Ile	I
leucine	Leu	L
lysine	Lys	K
methionine	Met	M
phenylalanine	Phe	F
proline	Pro	P
serine	Ser	S
threonine	Thr	T
tryptophan	Trp	W
tyrosine	Tyr	Y
valine	Val	V
any amino acid	Xaa	X

IX. Summary

Phosphatidylinositide 3-kinase (PI3K) signalling pathway is a pivotal regulator of cell growth, proliferation and survival and over 70% of breast cancers harbour mutations within this pathway. Accordingly, key components of this pathway have emerged as promising targets for cancer drug discovery. Much research has focused on the role of Akt as being the major mediator of PI3K in driving proliferation of tumour cells and by comparison the closely related serum- and glucocorticoid-regulated kinase (SGK) isoforms have received little attention. Understanding signaling mechanisms that have the potential to confer resistance to cancer therapies is of great clinical relevance. The central theme of my PhD work has focused on studying the roles that SGK isoforms play in breast cancer cells that are either sensitive or resistant to Akt inhibitors.

In the first part of this thesis I describe the development of tools that were instrumental in enabling the study of endogenous SGK isoforms in subsequent parts of my work. I first utilized the novel antibody tools to the study the role of Protor, a recently identified component of mTOR complex 2 (mTORC2), in the activation of SGK by mTORC2. I demonstrate that in mice lacking both Protor isoforms activation of SGK is significantly impaired in the kidney but not in other tissues or cells studied. mTORC2 kinase activity is not affected by the loss of Protor suggesting that Protor may act as a scaffold that presents SGK for mTORC2 *in vivo*.

In the second part of the present thesis I show that breast cancer cells that possess elevated levels of SGK1 mRNA and protein are inherently resistant to Akt inhibitors. These findings indicate that elevation of SGK1 expressions represents a mechanism of predicting

Akt inhibitor resistance and is therefore of significant relevance to the ongoing development of Akt inhibitors for the treatment of cancer. Patients whose tumours possess elevated levels of SGK1 might be better treated with a combination of inhibitors that suppress the activation of both SGK and Akt isoforms. I also show that in the absence of significant SGK activity Akt can mediate phosphorylation of NDRG1, which has previously been reported to comprise an SGK-specific substrate. Therefore my work emphasises that caution is required when employing NDRG1 as a surrogate marker for SGK activity.

In the third part of this thesis I show that Akt negatively regulates the levels and activity of SGK3. Consequently, following prolonged Akt inhibition the activity and levels of SGK3 are elevated. Furthermore, I also present evidence that the induction of SGK3 as a response to chronic Akt inhibition represents a compensatory signaling mechanism as SGK3 induction reduces the ability of Akt inhibitors to suppress cell proliferation. Finally, my work presented in Chapter 5 also indicates that the precise molecular mechanisms of SGK3 activation may need to be re-evaluated in future work.

1. Introduction

1.1 Regulatory role of reversible protein phosphorylation

1.1.1 The role of protein phosphorylation in signal transduction

Living cells must appropriately receive and respond to extracellular signals in order to undergo process such as cell differentiation, division or death. To achieve this, a cellular signalling cascade is typically initiated by the binding of an external signalling molecule such as a growth factor to a receptor embedded in the cell's plasma membrane. Subsequent activation of the receptor triggers activation of cellular enzymes ultimately leading to a response. In order to propagate signals, activated enzymes frequently modify cellular substrates by, for example, proteolytic cleavage or the covalent attachment of, for instance, phosphate or carbohydrate groups. Phosphorylation is a key component of most signal transduction cascades and is carried out by a group of enzymes termed kinases. Typically protein kinases catalyse the transfer of γ-phosphate of ATP to a Ser, Thr or Tyr residue within the substrate protein. The global importance of protein phosphorylation is illustrated by the facts that majority of human proteins are expected to be phosphorylated, phosphorylation is an evolutionarily conserved mechanism found amongst bacteria, archaea and eukaryotes and many diseases are caused by perturbations of protein phosphorylation.

Phosphorylation is involved in the regulation of every conceivable cellular process. Despite being a very simple process, phosphorylation is an excellent means for signal transduction. Firstly, phosphorylation is reversible because the action of kinases can be reversed by

another class of enzymes, termed phosphatases (Figure 1.1A). Secondly, because a phosphate group carries two negative charges, the addition of a phosphate group introduces a considerable local charge change in the substrate protein. Phosphorylation can thereby induce a conformational change that may affect the substrate in a number of ways (Figure 1.1B). For instance, if the substrate itself is an enzyme, phosphorylation can alter its activity. In fact, the activity of many kinases is regulated by phosphorylation. In addition phosphorylation may affect the ability of the protein to interact with other proteins leading to altered localisation, stability or function (Figure 1.1B).

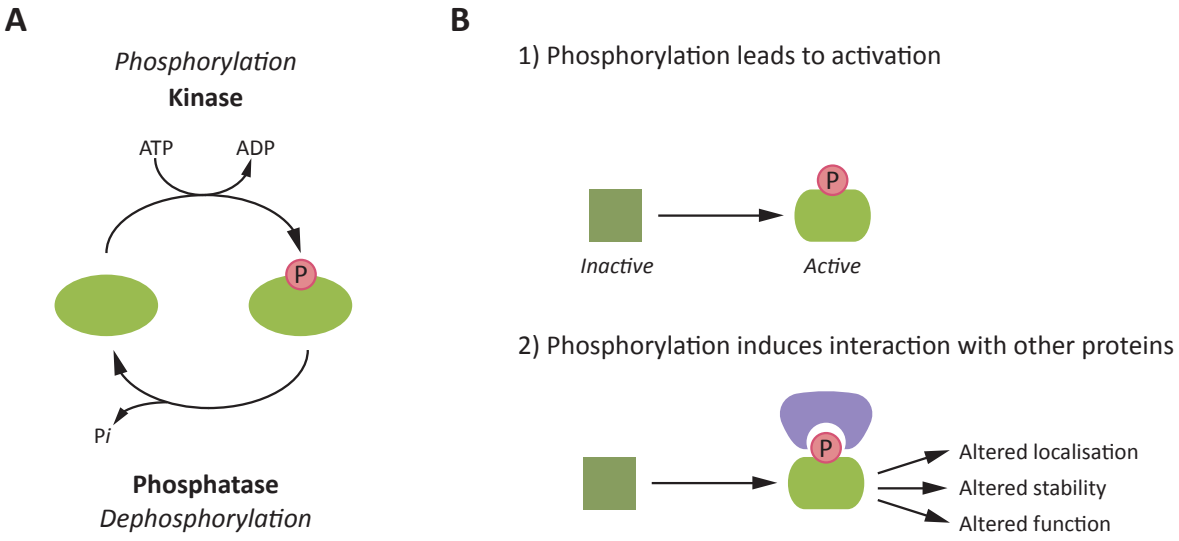

Figure 1.1 Protein phosphorylation and its consequences on target proteins

(**A**) Protein kinases catalyse the transfer of the γ-phosphate of ATP to an amino acid side chain. The reverse reaction is catalysed by protein phosphatases. (**B**) Protein phosphorylation can have wide-ranging effects on the target protein including a change in catalytic activity, protein:protein interactions, stability, function or localisation.

The first description of a signalling system controlled by phosphorylation dates back to 1955. Initially phosphorylase kinase was found to phosphorylate and activate an enzyme

termed glycogen phosphorylase (Fischer and Krebs, 1955; Krebs and Fischer, 1956; Sutherland and Wosilait, 1955). Subsequently Protein kinase A (PKA) was shown to act upstream of phosphorylase kinase (Walsh et al., 1968) thus explaining how adrenaline can trigger glycogen breakdown in the muscle (Figure 1.2). Analogous roles for protein phosphorylation in controlling signal transduction cascades have since been widely described.

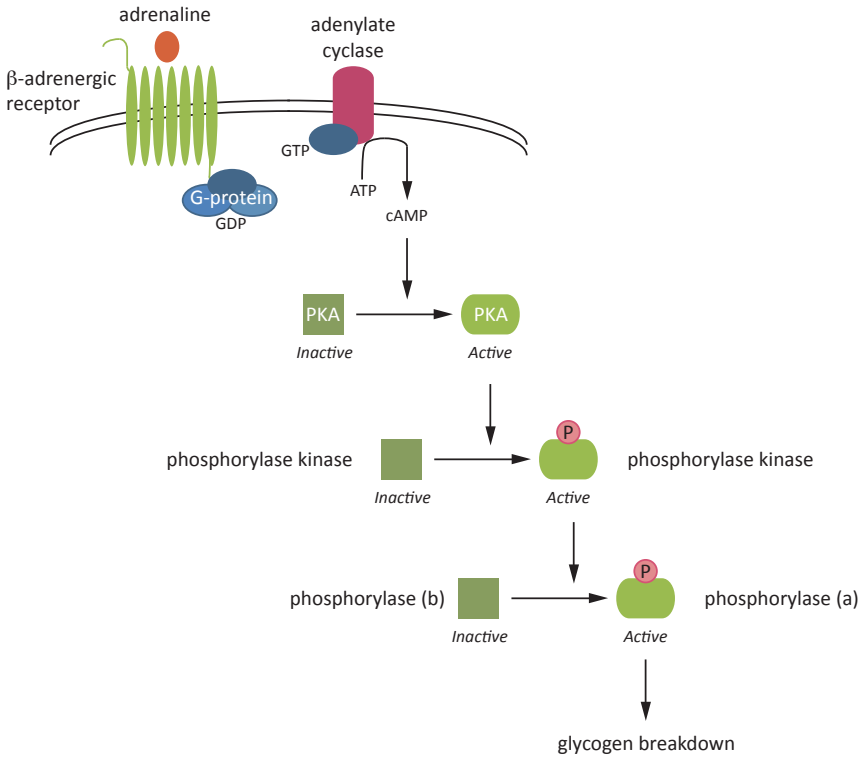

Figure 1.2 Signalling cascade leading to glycogen breakdown

Adrenaline binds to β-adrenergic receptor, a G protein-coupled receptor triggering GTP loading of the α-subunit of heterotrimeric G proteins. GTP loaded α-subunit associates with and activates adenylate cyclase. The resulting cAMP activates PKA, which phosphorylates and activates phosphorylase kinase, which in turn phosphorylates and activates glycogen phosphorylase leading to stimulation of glycogen breakdown.

1.1.2 Protein kinases – the human kinome

The human genome contains more than 500 protein kinases that comprise the kinome (Figure 1.3). Kinases share a similar catalytic region of approximately 250-300 residues (kinase domain) (Hanks et al., 1988) but vary considerably outside the kinase domain and these variable regions tend to contain additional domains that frequently dictate specificity, localisation and regulation. Based on sequence similarity the kinome is divided into eight groups: AGC (PKA, PKG and PKC family), CAMK (Ca^{2+}/Calmodulin-dependent kinases), CK1 (Casein kinase 1 family), CMGC (CDK, MAPK, GSK3 and CLK family), STE (homologues of the yeast *Sterile* kinases family), TK (Tyrosine kinases family), TKL (Tyrosine kinase-like kinases family) and atypical kinases family (Manning et al., 2002b). Members of the same group typically have similar substrate preferences and may be regulated similarly. The atypical kinases do not share significant similarity with the kinase domain but do posses kinase activity. One such kinase is the mammalian target of rapamycin (mTOR). Interestingly, approximately 10% of members of the human kinome are pseudokinases that have retained the kinase fold but have lost residues that are required for catalysis.

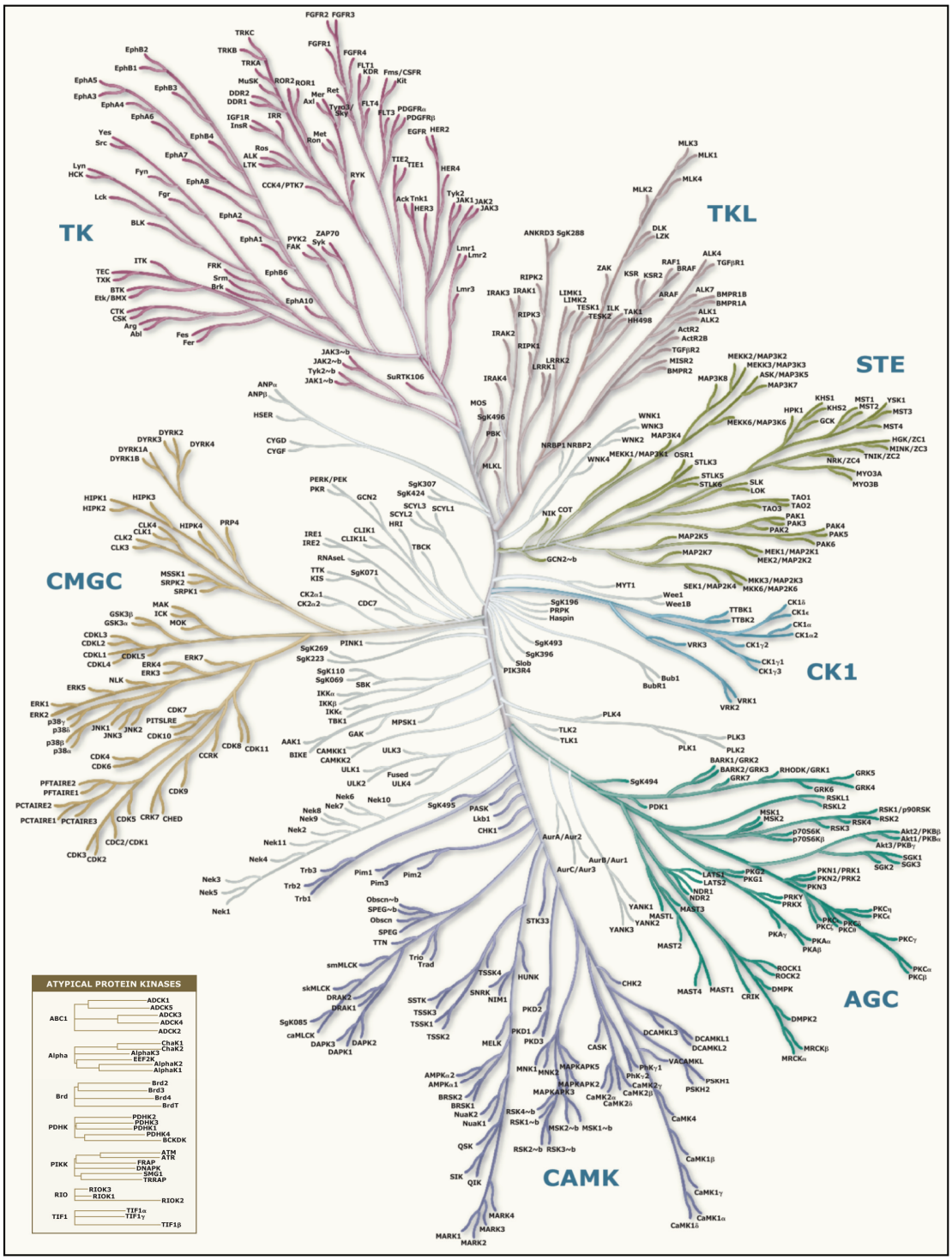

Figure 1.3 The human kinome

About 500 kinases constitute the human kinome. This phylogenetic tree of the kinome is based on the similarity of the kinase domains. Adapted from (Manning et al., 2002b).

1.1.3 General features of a protein kinase

Structural insights into protein kinases were first gained when the catalytic domain of PKA was crystallised (Knighton et al., 1991). Subsequent studies have found that the kinase fold is remarkably well conserved. The kinase domain consists of 12 subdomains organised into two lobes (Figure 1.4). The smaller N-terminal lobe (N-lobe) (subdomains I-IV) is composed of a five-stranded β-sheet and one α-helix (C-helix) while the C-terminal lobe (C-lobe) is α-helical. A hinge region links the two domains and the interface between the two lobes forms an important part of the active site. The N-lobe is involved in the binding and coordination of ATP and the C-lobe plays a role in substrate binding and provides residues that are essential for catalysis [reviewed in (Endicott et al., 2012)].

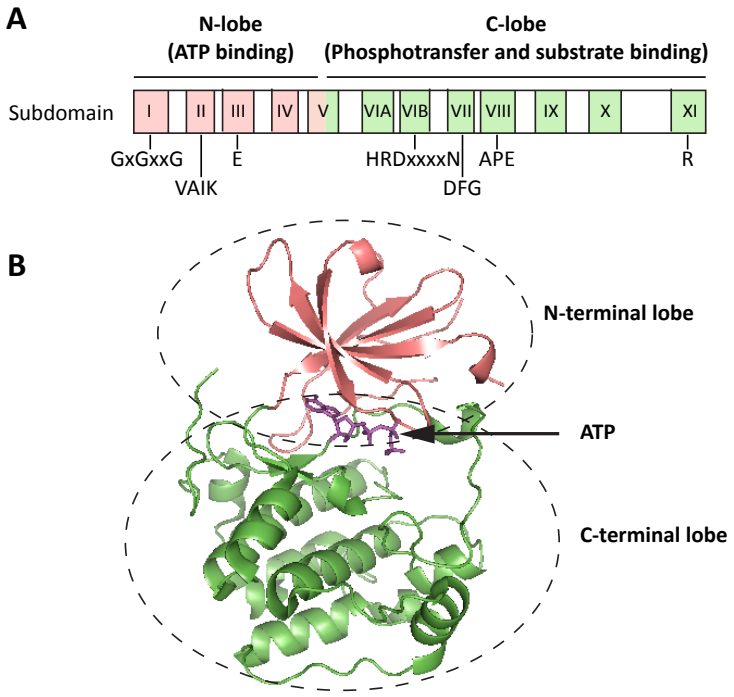

Figure 1.4 General features of a kinase domain and structure of SGK1 kinase domain

(A) Subdomain organisation of protein kinases and key residues and motifs. **(B)** Structure of SGK1 catalytic domain. N-lobe is shown in pink, C-lobe in green and ATP in purple.

Figure 1.4B shows the crystal structure of inactive SGK1 kinase domain. The structure of SGK1 catalytic domain closely resembles the canonical kinase domain fold but the structure around the active site is unusual (discussed below) (Zhao et al., 2007). Within the N-lobe subdomain I contains a conserved a GxGxxG motif that binds to the non-transferable α- and β- phosphates of ATP. Subdomain II contains VAIK motif whose Lys (Lys127 in SGK1) binds and positions ATP, an interaction stabilised by residues within subdomain III. Within subdomain VIB the C-lobe contains the catalytic loop HRDxxxxN motif, whose Asp functions as a proton acceptor for the phosphotransfer and the Asn coordinates an Mg^{2+} ion. Within subdomain VII the C-lobe also contains DFG motif, which coordinates a second Mg^{2+} ion thereby facilitating the orientation of the γ-phosphate of ATP for transfer, and APE motif whose Glu forms a salt bridge with a conserved Arg in subdomain XI, to promote stability of the C-lobe. Between the DFG and APE motifs there is a regulatory region called the activation loop (or T-loop). Kinases are frequently activated by phosphorylation within the T-loop, which allows for the displacement of αC-helix and stabilisation of the N- and C-lobes in the active conformation permitting the proper orientation of the substrate (Hanks and Hunter, 1995; Johnson et al., 1998). For SGK1 and other related AGC-family kinases phosphorylation of a conserved residue within the T-loop is required for activation. In SGK1 the residue is Thr256 and is phosphorylated by 3-phosphoinositide dependent protein kinase-1 (PDK1) (Kobayashi and Cohen, 1999). A striking difference between structure of SGK1 and that of other AGC kinases is the absence of a clearly defined αC-helix in SGK1 (Zhao et al., 2007). A further unique feature of SGK1 is the conformation around the T-loop. The conserved DFG motif of SGK1 forms a short β-sheet with a region that corresponds to a part of αC-helix of other kinases. The key

residue required for activation of SGK1, Thr256, is located on the surface of SGK1. In the inactive SGK1 structure the T-loop is in a conformation that would be expected to hinder the binding of the substrate (Zhao et al., 2007). As of now it is unclear whether the unusual features described are a true representation of the *in vivo* fold of SGK1 or whether they represent crystallisation artifacts.

In order to create kinase inactive mutants by site-directed mutagenesis a number of approaches can be taken. Commonly either (1) the Lys of VAIK motif, (2) the Asp of DFG or (3) the Thr/Ser of T-loop is mutated to an alanine. For example, for SGK1 Lys127Ala (VAIK motif) mutation is used in this study.

1.1.4 Phosphorylation and human disease

Regulation of signal transduction by protein and lipid phosphorylation affects probably every conceivable cellular process. Accordingly, mutations within enzymes that control phosphorylation are linked to a wide spectrum of diseases. A number of hereditary conditions are linked to mutations in kinases and these are listed in Table 1.1. Furthermore, sporadic and hereditary mutations in protein and lipid kinases are extremely frequent in cancers and commonly described mutations are listed in Table 1.2. The initial observations linking kinases and human disease came from studies with viral oncogenes. For example, v-Src encoded by the Rous sarcoma virus is the constitutively active version of the human proto-oncogene c-Src, which is a Tyr kinase (Hunter and Sefton, 1980; Stehelin et al., 1977). The importance of protein phosphorylation in human disease is highlighted by the significant effort that has been devoted for the development of protein

kinase inhibitors for the treatment of cancer and many “druggable” kinase targets have also been identified to play critical roles in inflammation, auto-immunity, hypertension and Parkinson’s disease (Cohen and Alessi, 2013).

Gene	Protein name/function	Disease
ACVR1	ALK2 (receptor Ser/Thr kinase)	Fibrodysplasia ossificans progressiva
ACVRL1	ALK1 (receptor Ser/Thr kinase)	Hereditary haemorrhagic telangiectasia type 2
AKT2	Akt2 (Ser/Thr kinase)	Atypical lipodystrophy
ALK	ALK (receptor Tyr kinase)	Neuroblastoma
AMHR2	AMHR2 (receptor Ser/Thr kinase)	Persistent Mullerian duct syndrome type 2
ATM	ATM (Ser/Thr kinase)	Ataxia telangiectasia
ATR	ATR (Ser/Thr kinase)	Seckel syndrome
BMPR1B	ALK6 (receptor Ser/Thr kinase)	Brachydactyly type 2A
BMPR2	BMPR2 (receptor Ser/Thr kinase)	Primary pulmonary hypertension 1
BRAF	B-Raf (Ser/Thr kinase)	Cardio–facio–cutaneous syndrome
BTK	BTK (Tyr kinase)	Agammaglobulinemia
CASK	CASK (Ser kinase)	X-linked mental retardation
CDKL5	CDK5 (Ser/Thr kinase)	Early infantile epileptic encephalopathy type 2
CHEK2	CHK2 (Ser/Thr kinase)	Li–Fraumeni syndrome 2
EIF2AK3	EIF2AK3 (Ser/Thr kinase)	Wolcott-Rallison syndrome
ERBB3	ErbB-3 (receptor Tyr kinase)	Lethal congenital contractural syndrome type 2
FGFR1	FGFR1 (receptor Tyr kinase)	Osteoglophonic dysplasia, Pfeiffer syndrome and hypogonadotropic hypogonadism
FGFR2	FGFR2 (receptor Tyr kinase)	Pfeiffer syndrome, Apert syndrome, Crouzon syndrome and lacrimoauriculodentodigital syndrome
FGFR3	FGFR3 (receptor Tyr kinase)	Achondrodysplasia, thanatophoric dysplasia types 1 and 2 and Muenke syndrome
FLT4	FLT4 (VEGFR3 receptor Tyr kinase)	Hereditary lymphedema type 1A
GRK1	GRK1 (Ser/Thr kinase)	Oguchi disease 1
GRK4	GRK4 (Ser/Thr kinase)	Hypertension
ICK	ICK (Ser/Thr kinase)	Endocrine–cerebro–osteodysplasia
IKBKG	NEMO (regulatory subunit of IκB kinase)	Hypohidrotic ectodermal dysplasia and incontinentia pigmenti type 2
INSR	InsR (receptor Tyr kinase)	Insulin-resistant diabetes with acanthosis, Donahue syndrome
IRAK4	IRAK4 (Ser/Thr kinase)	Invasive pneumococcal disease and pyogenic bacterial infections
JAK3	JAK3 (Tyr kinase)	Severe combined immunodeficiency
KIT	KIT (Tyr kinase)	Piebaldism
LRRK2	LRRK2 (Ser/Thr kinase)	Parkinson disease
LTK	LTK(receptor Tyr kinase)	Systemic lupus erythematosus
MAPK10	JNK3 (Ser/Thr kinase)	Epileptic encephalopathy Lennox–Gaustaut type
MAP2K1	MEK1 (dual specificity protein kinase)	Cardio–facio–cutaneous syndrome
MAP2K2	MEK2 (dual specificity protein kinase)	Cardio–facio–cutaneous syndrome
MERTK	MERTK (receptor Tyr kinase)	Retinitis pigmentosa 38
MUSK	MuSK (receptor Tyr kinase)	Myasthenic syndrome
NTRK1	TrkA (receptor Tyr kinase)	Congenital insensitivity to pain with anhidrosis
NTRK2	TrkB (receptor Tyr kinase)	Early obesity, hyperphagia, developmental delay

PDGFRA	PDGFRA (receptor Tyr kinase)	Gastrointestinal stromal tumour
PHKA2	Phosphorylase kinase α subunit	Glycogen storage disease type 9A (types 1 and 2)
PHKG2	Phosphorylase kinase γ subunit	Glycogen storage disease type 9C
PINK1	PINK1 (Ser/Thr kinase)	Early-onset Parkinson disease
PRKAA1 *PRKAA2*	AMPK α1/ α 2 catalytic subunit (Ser/Thr kinase)	Wolff-Parkinson-White syndrome
PRKAR1A	PRKAR1A (regulatory subunit of cAMP-dependent protein kinases)	Primary pigmented nodular adrenocortical disease and Carney complex
PRKCG	PKC-γ (Ser/Thr kinase)	Spinocerebellar ataxia type 14
RAF1	c-Raf (Ser/Thr kinase)	Noonan syndrome type 5 and LEOPARD syndrome type 2
RET	RET (receptor Tyr kinase)	Multiple endocrine neoplasia type 2B, familial medullary thyroid carcinoma, familial pheochromocytoma and Hirschsprung disease, Congenital failure of autonomic control, renal dysplasia
ROR2	ROR2 (receptor Tyr kinase)	Robinow syndrome
RPS6KA3	RSK2 (Ser/Thr kinase)	Coffin–Lowry syndrome
STK11	LKB1 (Ser/Thr kinase)	Peutz–Jeghers syndrome
TEK	TEK/Tie-2 (receptor Tyr kinase)	Cutaneous and mucosal venous malformations
TTBK2	TTBK2 (Ser/Thr kinase)	Spinocerebellar ataxia type 11
TGFBR1	TGFβ receptor 1 (Ser/Thr kinase)	Loeys–Dietz syndrome (types 1A and 2A)
TGFBR2	TGFβ receptor 2 (Ser/Thr kinase)	Loeys–Dietz syndrome (types 1B and 2B)
TRPM7	TRPM7 (ion channel and kinase)	Amyotrophic lateral sclerosis–Parkinsonism
WNK1/4	WNK1/4 (Ser/Thr kinase)	Pseudohypo-aldosteronism type 2
ZAP70	ZAP70 (Tyr kinase)	Severe-combined immunodeficiency (T cell-negative)

Table 1.1 Kinases mutated in human disease

Adapted from (Lahiry et al., 2010; Ortutay et al., 2005).

Gene	**Protein name/function**	**Alteration**
AKT1/2/3	Akt1/2/3 (Ser/Thr kinase)	Activation
ALK	ALK (receptor Tyr kinase)	Activation
BCR-ABL	BCR-ABL (fusion Tyr kinase)	Activation (translocation)
BRAF	B-Raf (Ser/Thr kinase)	Activation
CDK4/6	CDK4 (Ser/Thr kinase)	Activation
CDK12	CDK12 (Ser/Thr kinase)	Inactivation
EGFR	EGFR2 (receptor Tyr kinase)	Activation
ERBB2	HER-2 (receptor Tyr kinase)	Activation
FGFR2	FGFR2 (receptor Tyr kinase)	Activation
FGFR3	FGFR3 (receptor Tyr kinase)	Activation
FLT3	Fms-related tyrosine kinase 3	Activation
ITK	ITK (Tyr kinase)	Activation
JAK1/2/3	JAK2 (Ser/Thr kinase)	Activation
KDR	VEGFR2 (receptor Tyr kinase)	Activation
KIT	SCFR (receptor Tyr kinase)	Activation
LCK	LCK (Tyr kinase)	Activation

MAP2K1/2	MEK1/2 (dual specificity kinase)	Activation
MAP2K4	MEK4 (dual specificity kinase)	Inactivation
MET	HGFR (receptor Tyr kinase)	Activation
NTRK1/3	Trk-A/C (receptor Tyr kinase)	Activation
PDGFRA	PDGFRA (receptor Tyr kinase)	Activation
PI3KCA	PI3K (Catalytic subunit of Phosphoinositide-3 kinase)	Activation
PI3KR1	PI3K (Regulatory subunit of Phosphoinositide-3 kinase)	Inactivation
PTEN	PTEN (phospholipid PtdIns(3,4,5)P_3 3-phosphatase and dual-specificity protein phosphatase)	Inactivation
STK11	LKB1 (Ser/Thr kinase)	Inactivation
SYK	SYK (Tyr kinase)	Activation

Table 1.2 Protein and lipid kinases and phosphatases frequently mutated in cancer

Adapted from (Forbes et al., 2011; Futreal et al., 2004).

1.2 Overview of breast cancer

1.2.1 Acquired capacities of cancer cells

A seminal review published in 2000 proposed six acquired capacities that are fundamental for the development of malignancies: (1) self-sufficiency in growth signals, (2) insensitivity to anti-growth signals, (3) evasion of apoptosis, (4) tissue invasion & metastasis, (5) limitless replicative potential and (6) sustained angiogenesis (Hanahan and Weinberg, 2000). Over the last decade four new hallmarks have emerged to complement earlier understanding: (7) deregulation of cellular energetics, (8) evasion of immune destruction, (9) genomic instability and (10) tumour promoting inflammation (Hanahan and Weinberg, 2011). These hallmarks, illustrated in Figure 1.5, represent acquired alterations of cell physiology that collectively enable the multistage development of malignant growth. Genomic instability enables the phenotypic changes that give a selective advantage to cancer cells to be acquired via a number of ways including: (1) mutations within gene coding DNA sequences, (2) genomic alterations such as deletions, amplifications or

translocations that result in altered gene expression, (3) epigenetic changes such as changes to DNA methylation or histone acetylation that alter gene expression or (4) other non-mutational changes affecting gene expression.

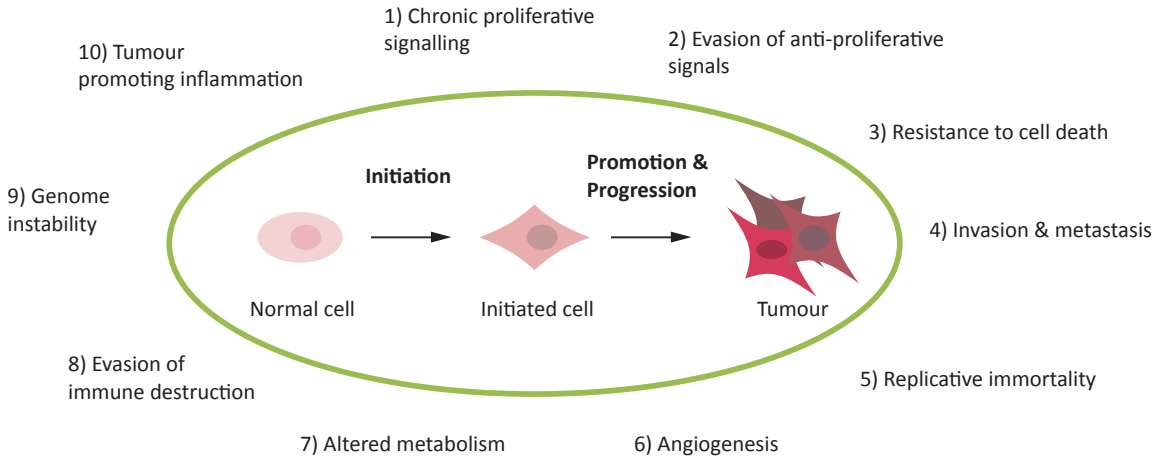

Figure 1.5 Multistage development of cancer

Ten hallmarks of cancer cells, adapted from (Hanahan and Weinberg, 2011).

One of the fundamental properties of cancer cells is the ability sustain chronic proliferation. In normal tissues the release of growth promoting signals and the signal transduction pathways activated by them are tightly controlled to ensure that cells progress through the cell division cycle appropriately. This ensures the maintenance of normal tissue architecture and function. In order to evade normal control of proliferation cancer cells may, for example, produce their own growth factors for which they express cognate receptors, stimulate normal cells within the tumour-surrounding stroma to supply them with growth factors, elevate the expression and/or activity of growth factor

receptors or downstream signalling pathways or alter negative feedback loops which self-limit proliferative signal transduction (Figure 1.6) (Hanahan and Weinberg, 2011).

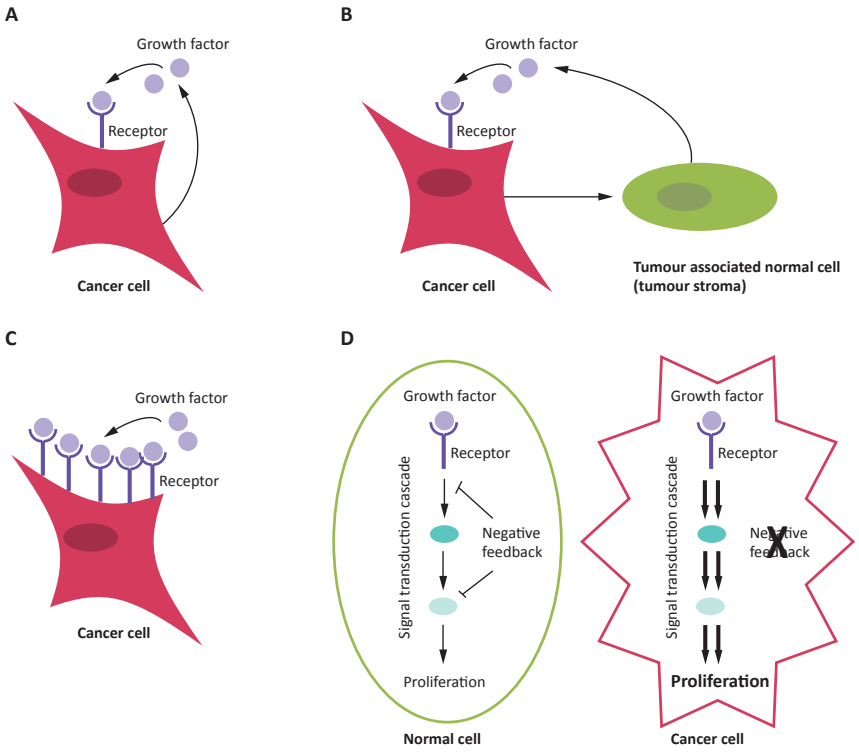

Figure 1.6 Cancer cells acquire the capacity to sustain limitless proliferation

In order to sustain limitless proliferation cancer cells may (**A**) produce their own growth factors (**B**) stimulate surrounding stromal cells to supply growth factors (**C**) elevate the expression and/or activity of growth factor receptors (**D**) elevate activity of downstream signalling pathways or alter negative feedback loops that limit signal transduction.

1.2.2 Classification and mutation analysis of breast cancers

Breast cancer is the most common cancer and remains the principle cause of cancer-related mortality in women worldwide accounting for 23% of cancer diagnoses and 14% of cancer deaths globally in 2008 (Ferlay et al., 2010; Jemal et al., 2011). Like most cancers, breast cancer represents a heterogeneous group of tumours but they can be classified

according to their characteristic molecular features. The gene-expression profiles that breast cancers are most commonly classified according to are: luminal A, luminal B, Her2-enriched (human epidermal growth factor receptor 2, also known as Neu or ERBB2) and triple negative (also known as basal-like) (Sorlie et al., 2001; Sorlie et al., 2003). This classification, however, is not exhaustive and in reality many subclasses with distinctive characteristics are proposed to exist. The key features of the main subtypes are summarised in Table 1.3. Understanding the driving genetic alterations of breast cancer subtypes has led to the development of targeted therapies, some of which are currently used in the clinic. The first targeted therapy for breast cancer dates back to the 1970s when a failed contraceptive ICI46474 (Harper and Walpole, 1966), which is an anti-oestrogenic, was reinvented as tamoxifen and targeted towards oestrogen receptor (ER) positive tumours (Jordan and Koerner, 1975). Since the development of tamoxifen many other endocrine therapies that target the action of oestrogen have been described but their efficacy is often found to be limited due to the emergence of resistance [reviewed in (Musgrove and Sutherland, 2009)].

Historically over-expression of the receptor Tyr kinase Her2 has been linked to poor prognosis of breast cancer patients (Slamon et al., 1987). Survival of Her2 over-expressing patients has improved with the development of drugs such as Trastuzumab (Herceptin). Trastuzumab is a recombinant humanised anti-Her2 monoclonal antibody (Carter et al., 1992). Subsequently other antibody-based therapies as well as catalytic inhibitors (e.g. lapatinib) of Her2 and other related receptors have been developed. Whilst such therapies improve the survival of patients over-expressing Her2, acquisition of resistance to these therapies is frequent [reviewed in (Arteaga et al., 2012; Baselga and Swain, 2009)].

Subtype	Gene expression signature	Approximate prevalence	Available targeted therapy
Luminal A	ER and/or PR positive Her2 negative	40%	ER modulators such as tamoxifen
Luminal B	ER and/or PR positive Her2 amplified	20%	ER modulators such as tamoxifen
Her2-enriched	Hormone receptor negative Her2 amplified	10-15%	Her2 inhibitors such as trastuzumab
Triple negative	Hormone receptor negative Her2 negative	15-20%	none

Table 1.3 Breast cancer classification according to gene expression profiles

Abbreviations not defined in text: oestrogen receptor (ER), progesterone receptor (PR). Adapted from (Sorlie et al., 2001; Sorlie et al., 2003) for the gene expression signatures, prevalence data adapted from (Carey et al., 2006; Fan et al., 2006a).

A recent study by the Cancer Genome Atlas Network determined the most significantly altered genes in breast cancer patients by an exhaustive combination of copy number analysis, DNA methylation analysis, exome sequencing, messenger RNA arrays, microRNA sequencing and reverse-phase protein arrays (Network, 2012). Data is summarised in Table 1.4. Both this study and many others [recently reviewed (Miller et al., 2011; Polyak and Metzger Filho, 2012)] have found that phosphoinositide 3-kinase (PI3K) pathway mutations are frequent in breast cancer with over 70% of breast cancers being estimated to harbour over-activated PI3K pathway signalling. Notably, whilst the comprehensive study of over 800 patient derived tumour samples revealed PI3K pathway mutations to be most frequent in luminal and Her2-enriched cancers, activity of the pathway was conversely found to be highest in triple negative cancers (Network, 2012). This observation illustrates the importance of this pathway in all breast cancer subtypes. Regulation of PI3K signalling and the consequences of mutations on the pathway are considered in Section 1.3.

Gene	Protein	Alteration	Mutation frequency
I. Genes involved in the PI3K Pathway			
PI3KCA	PtdIns(4,5)P_2 3-kinase catalytic subunit	Mutation, amplification	49% of La 32% of Lb 7% of TN 42% of Her2
PI3KR1	PtdIns(4,5)P_2 3-kinase regulatory subunit	Mutation	3% of all 8% of Her2
PTEN	PtdIns(3,4,5)P_3 3-phosphatase and dual-specificity protein phosphatases	Mutation, deletion or loss of expression	13% of La 24% of Lb 35% of TN 19% of Her2
INPP4B	PtdIns(3,5)P_2 4-phosphatase	Loss	9% of La 16% of Lb 30% of TN 30% of Her2
II. Genes not directly involved with the PI3K Pathway			
TP53	P53, transcription factor	Inactivation	12% of La 32% of Lb 84% of TN 75% of Her2
CDK4	CDK4, kinase involved in cell cycle	Amplification	14% of La 25% of Lb 24% of Her2
Cyclin D1	Cyclin D1, cell cycle	Amplification	29% of La 58% of Lb 38% of Her2
Cyclin E1	Cyclin E1, cell cycle	Amplification	9% of TN
GATA3	GATA3, transcription factor	Inactivation	11% 14% La
MAP3K1	MAP3K1, kinase, activation of JNK mediated apoptosis?	Inactivation	14% of La 5% of Lb
MDM2	MDM2, E3 ligase, controls P53 stability	Amplification	14% of La 31% of Lb 14% of TN 30% of Her2
MYC	MYC, transcription factor	Amplification	40% of TN
RB1	RB1, cell cycle suppression	Inactivation Deletion	2% of all 20% TN

Table 1.4 Recent advanced in breast cancer mutation analysis

Abbreviations not defined in text: luminal A (La); luminal B (Lb); triple negative (TN); Her2-enriched (Her2). Adapted from (Network, 2012).

1.3 PI3K-mTOR signalling

1.3.1 PI3K

PI3K signalling pathway is one of the many tightly controlled pathways that cells use to respond to external messages in order to perform their normal functions such as glucose metabolism, cell survival and proliferation. PI3 kinases are divided into three classes, as summarised in Table 1.5. Class I PI3Ks are heterodimeric containing a regulatory p85 and a catalytic p110 subunit [reviewed in (Vanhaesebroeck et al., 2010)]. In the canonical Class I PI3K signalling pathway, illustrated in Figure 1.8, PI3K is activated following the binding of growth factors such as insulin like growth factor 1 (IGF1)) and hormones such as insulin to cell surface receptor tyrosine kinases (RTK). Among others, these receptors include Her2. Following binding of the ligand to the receptor a cascade of events comprising of receptor dimerisation, autophosphorylation of Tyr residues and physical association of the receptors with many cytoplasmic substrates is initiated. One such substrate is PI3K regulatory subunit (PI3KR1), also known as p85, which associates with activated RTKs via its SH2 (src homology) domains that bind to phospho-tyrosine (Escobedo et al., 1991; Skolnik et al., 1991). Alternatively, p85 can also be recruited to the plasma membrane via activated G protein coupled receptors (GPCR) (Stephens et al., 1994) or via adaptor proteins that act as intermediates between the activated receptor and p85 such as insulin receptor substrate -1 (IRS1) (Sun et al., 1991). Interaction of the PI3K catalytic subunit p110 with the small G-protein Ras also contributes to the activation of PI3K (Rodriguez-Viciana et al., 1994). Plasma membrane recruitment brings PI3K to where its substrates are and also relieves the inhibitory effect of p85 on p110 (Myers et al., 1998; Stambolic et

al., 1998; Yu et al., 1998). Activated PI3K phosphorylates the membrane phospholipid phosphatidylinositol 4,5-bisphosphate (PtdIns(4,5)P2) in the 3-position to yield phosphatidylinositol 3,4,5-trisphosphate (PtdIns(3,4,5)P3) (Whitman et al., 1988). The action of PI3K is antagonised by the tumour suppressor PTEN (phosphatases and tensin homolog deleted on chromosome 10) which dephosphorylates PtdIns(3,4,5)P3 to yield PtdIns(4,5)P2 (Maehama et al., 1998).

PI3K class	**Preferred substrate**	**Localisation, biological outputs**	**Catalytic subunit**	**Regulatory subunit**
Class I	PtdIns(4,5)P2	Classically activated at the plasma membrane Signalling contributes to for example cellular proliferation, growth, survival and migration	p110α p110β p110γ p110δ	p85 isoform (p85α, p85β, p55α, p55γ or p50α) for p110α, β or δ p101 or p87 for p110γ
Class II	PtdIns, PtdIns(4)P?	Intracellular membranes and plasma membrane Functions poorly characterised, include for example regulation of apoptosis and migration	PI3K-C2 α PI3K-C2 β PI3K-C2 γ	
Class III	PtdIns	Intracellular membranes Autophagy, endocytosis, phagocytosis, potentially amino acid dependent activation of mTORC1	Vps34	Vps15

Table 1.5 Classification of phosphoinositide 3-kinases

Adapted from (Vanhaesebroeck et al., 2010).

The creation of PtdIns(3,4,5)P_3 leads to the recruitment of proteins that contain a PtdIns(3,4,5)P_3 binding pleckstrin homology (PH) domain to the plasma membrane. Two such proteins are 3-phosphoinositide-dependent protein kinase -1 (PDK1) (Alessi et al., 1997a) and Akt (also known as protein kinase B, PKB) (James et al., 1996). Plasma membrane recruitment of PDK1 does not alter its catalytic activity (Currie et al., 1999) but allows for the co-localisation of PDK1 with its substrate Akt whom it phosphorylates at

Thr308 leading to its activation (Alessi et al., 1997b). Akt controls the phosphorylation of numerous substrates thereby influencing several cellular processes. Akt kinases are discussed in more detail in Section 1.4.

1.3.2 mTOR

The mammalian target of rapamycin (mTOR) is a central integrator of cellular nutrient and energy levels that controls cell growth and homeostasis. mTOR is the mammalian homolog of yeast TOR which was identified as the target of the macrolide rapamycin that gained attention due to its anti-proliferative properties (Brown et al., 1994; Heitman et al., 1991; Sabatini et al., 1994; Sabers et al., 1995). mTOR exists in at least two distinct complexes termed mTOR complex 1 (mTORC1) and mTORC2. Both complexes contain the Ser/Thr kinase mTOR and an accessory protein termed mammalian lethal with sec-13 protein 8 (mLST8, also known as GβL) (Jacinto et al., 2004; Kim et al., 2003), DEP domain containing mTOR-interacting protein (Deptor) (Peterson et al., 2009) and Tt1/Tel2 complex (Kaizuka et al., 2010). Components that are unique to mTORC1 are regulatory-associated protein of mammalian target of rapamycin (Raptor) (Hara et al., 2002; Kim et al., 2002), and proline-rich Akt substrate 40 kDa (PRAS40) (Sancak et al., 2007; Thedieck et al., 2007; Vander Haar et al., 2007; Wang et al., 2007). Rapamycin-insensitive companion of mTOR (Rictor) (Jacinto et al., 2004; Sarbassov et al., 2004), mammalian stress-activated map kinase-interacting protein 1 (mSin1)(Frias et al., 2006; Jacinto et al., 2006) and protein observed with Rictor 1 and 2 (Protor1/2) (Pearce et al., 2007; Thedieck et al., 2007; Woo et al., 2007) are unique to mTORC2. Rapamycin can be used to delineate

functions of the two complexes, as mTORC1 is acutely sensitive to rapamycin whereas mTORC2 is only affected by chronic rapamycin treatment. mTORC1 is the better characterised complex and its activity is regulated by a remarkably diverse array of upstream signals. Briefly, mTORC1 is regulated by at least (1) growth factor signalling, (2) cellular stress, (3) cellular energy status, (4) oxygen and (5) amino acids. mTORC1 integrates these signals to control cell growth and proliferation by promoting anabolic processes (for example protein and lipid biosynthesis) and by inhibiting the catabolic process of autophagy [reviewed in (Laplante and Sabatini, 2012)]. The activation of mTORC1 by growth factor signalling is considered in more detail below. mTORC2 is also regulated by growth factors via as-of-yet poorly understood mechanisms. Increased PtdIns(3,4,5)P_3 levels correlate with increased mTORC2 activity and direct activation of mTORC2 by PtdIns(3,4,5)P_3 has been suggested (Gan et al., 2011). mTORC2 has also been shown to associate with ribosomes following PI3K activation and the activation of mTORC2 is suggested to be dependent on ribosomes, but not protein synthesis (Zinzalla et al., 2011). By phosphorylating its best-characterised substrates Akt, SGK and PKC, mTORC2 controls cell survival and proliferation and cytoskeletal organization (Laplante et al., 2012). The compositions of the mTOR complexes, and an overview of their regulation and cellular functions are illustrated in Figure 1.7.

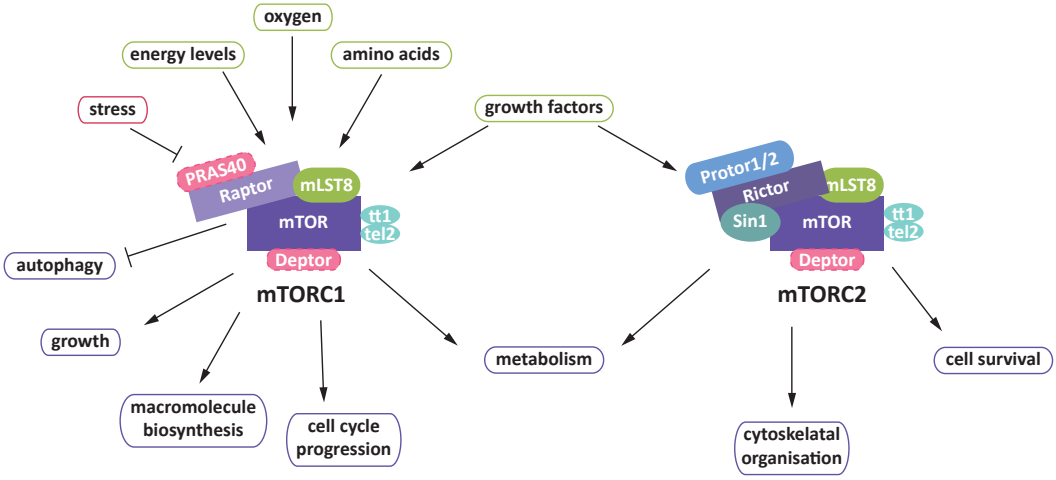

Figure 1.7 Summary of mTOR complexes, their regulation and cellular roles

Adapted from (Laplante and Sabatini, 2012).

Role of PI3K-PDK1-Akt signalling in the growth factor regulation of mTORC1

As illustrated in Figure 1.8, activation of Akt by PDK1 contributes to the activation of mTORC1 by growth factors. Akt phosphorylates PRAS40 leading to its dissociation from mTORC1 thus relieving the inhibitory effect of PRAS40 on mTORC1 (Sancak et al., 2007; Thedieck et al., 2007; Vander Haar et al., 2007; Wang et al., 2007). Furthermore, Akt also phosphorylates and inactivates tuberous sclerosis 2 (TSC2, also called tuberin) in order to activate mTORC1 (Inoki et al., 2002; Manning et al., 2002a). TSC2 is part of a heterodimeric complex together with TSC1. The TSC1/2 complex functions as a GTPase-activating (GAP) for the Ras homolog enriched in brain (Rheb) GTPase. Rheb-GTP stimulates mTORC1 kinase activity and as a Rheb GAP TSC1/2 promotes the conversion of active Rheb-GTP to inactive Rheb-GDP thereby inhibiting mTORC1 (Inoki et al., 2003; Tee et al., 2003). TSC1/2 complex is phosphorylated and inactivated also by other effector kinases of alternative growth factor activated signalling pathways such as the

extracellular-signal-regulated kinases 1/2 (ERK1/2) (Laplante and Sabatini, 2012; Ma et al., 2005). Rheb-GTP is only able to stimulate mTORC1 in the presence of amino acids. According to the current model, amino acids that have accumulated in the lysosome signal via vacuolar v-ATPase and a protein termed Ragulator to promote GTP binding to the heterodimeric RagA/B GTPase and GDP binding to RagC/D heterodimer (Bar-Peled et al., 2012; Kim et al., 2008; Sancak et al., 2010; Sancak et al., 2008; Zoncu et al., 2011). mTORC1 is recruited to the activated GTP-RagA/B heterodimer and is activated at the lysosomal surface by GTP-Rheb. During amino acid starvation mTORC1 is diffuse in the cytosol [reviewed in (Jewell et al., 2013; Laplante and Sabatini, 2012)].

1.3.3 Hyperactivation of PI3K signalling in breast cancer

As discussed in Section 1.2.2, activity of the PI3K pathway is frequently up-regulated in breast cancer and this can be achieved by a number of ways, as illustrated in Figure 1.9. Briefly, frequently observed alterations include, but are not limited to, amplification of RTKs, loss of PTEN or $INPP_4B$ (inositol polyphosphate-4-phosphatase) function, activating mutations of p110 catalytic subunit of PI3K, inactivating mutations of p85 regulatory subunit of PI3K or activating mutations of Akt or Ras. Interestingly $INPP_4B$, which preferentially dephosphorylates PtdIns(3,4)P_2 to yield PtdIns(3)P, is considered to be a tumour suppressor that inhibits PI3K signalling through reducing Akt activation suggesting that PtdIns(3,4,5)P_3 and PtdIns(3,4)P_2 may cooperate in Akt activation (Gewinner et al., 2009).

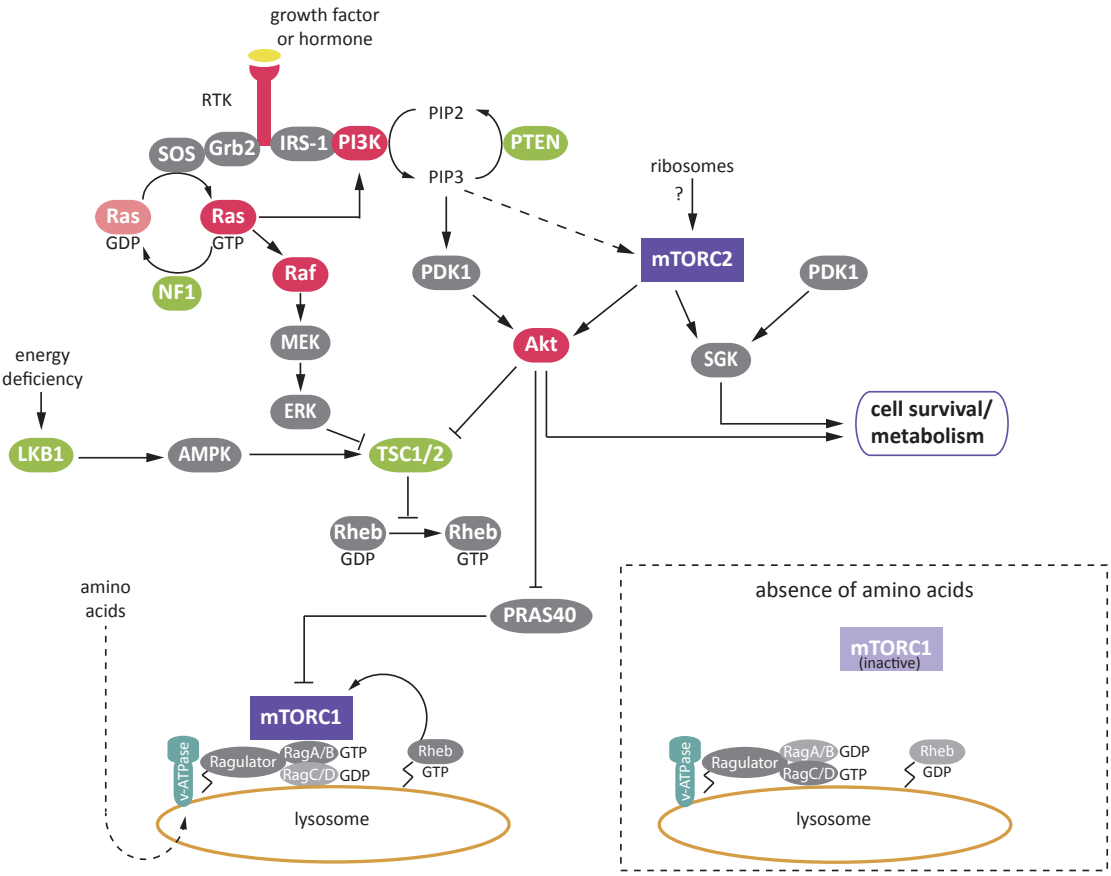

Figure 1.8 An overview of PI3K-mTOR signaling

PI3K is activated downstream of receptor tyrosine kinases (RTK) either directly or via the adaptor protein IRS1. PI3K is also stimulated by the small G-protein Ras. PI3K phosphorylates the membrane phospholipid PtdIns(4,5)P_2 (PIP2) to yield PtdIns(3,4,5)P_3 (PIP3). The reverse reaction is catalysed by PTEN. PtdIns(3,4,5)P_3 generation stimulates the activation of Akt by PDK1 and mTORC2. mTORC2 and PDK1 also activate SGK family members. Akt contributes to growth factor stimulated activation of mTORC1 by relieving the inhibitory effect of PRAS40 on mTORC1. Akt also phosphorylates TSC2 to inhibit the TSC1/2 complex leading to increased association of the small G-protein Rheb with GTP. GTP-Rheb stimulates mTORC1. TSC1/2 is also negatively regulated by the Ras-Raf-MEK-ERK pathway. During energy starvation AMP activated protein kinase (AMPK), which is activated by the tumour suppressor LKB1, inhibits mTORC1 by positively stimulating the GAP activity of TSC1/2. At the lysosome amino acids signal via vacuolar v-ATPase and Ragulator to promote GTP binding to RagA/B and GDP binding to RagC/D. mTORC1 is recruited to the activated GTP-RagA/B heterodimer and is activated at the lysosomal surface by GTP-Rheb. During amino acid starvation mTORC1 is diffuse in the cytosol. Tumour suppressors are indicated in green and oncogenes are indicated in red. mTORC2 is activated downstream of PI3K via poorly defined mechanism that may involve ribosomes. NF1 (Neurofibromin 1) Adapted from (Jewell et al., 2013; Laplante and Sabatini, 2012).

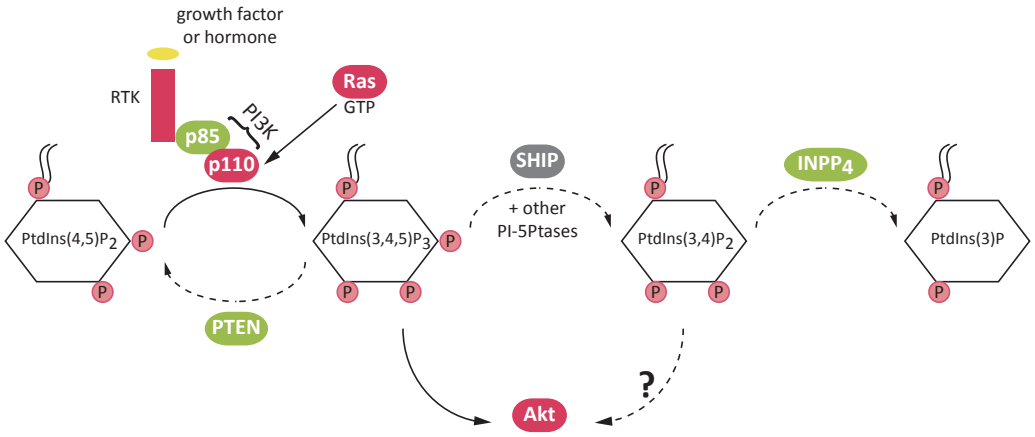

Figure 1.9 Up-regulation of PI3K signalling

PI3K pathway can be up-regulated by activating mutations or over-expression of receptor tyrosine kinases (RTK), p110 catalytic subunit of PI3K, the small G-protein Ras or the kinase Akt. Alternatively PI3K pathway can be activated by loss of function or expression of the p85 regulatory subunit of PI3K, the PtdIns(3,4,5)P_3 3-phosphatase PTEN or the inositol polyphosphate-4-phosphatase ($INPP_4$). Proteins that are frequently activated in cancer are in red and those whose function is frequently lost in cancer are in green.

1.4 The Akt family of protein kinases

Members of the Akt Ser/Thr kinase family are well characterised as downstream effectors of PI3K signalling. The three Akt (Akt1/2/3) isoforms belong to AGC family of kinases and they all contain an N-terminal PtdIns(3,4,5)P_3 binding PH domain. Akt was initially discovered as the oncogene in within the mouse leukemia virus AKT8 (Staal, 1987). The generation of PtdIns(3,4,5)P_3 co-localises PDK1 and Akt kinases at the plasma membrane due to their PtdIns(3,4,5)P_3 binding PH-domains and induces a conformational change in Akt that allows for the phosphorylation and activation of Akt by PDK1 (Alessi et al., 1997b; Calleja et al., 2007; Milburn et al., 2003). Besides the PDK1 site (Thr308 in Akt1), Akt also contains a second growth factor regulated phosphorylation site, termed the hydrophobic motif site (Ser473 in Akt1). Phosphorylation of Ser473 downstream of PI3K signalling is

mediated by mTORC2 (Sarbassov et al., 2005) and it contributes to the efficient activation of Akt (Hers et al., 2011; Najafov et al., 2011). A number of direct targets of Akt have been identified and consequently Akt has been implicated in a number of cellular processes. The best-characterised substrates of Akt are summarised in Table 1.6 [reviewed in (Manning and Cantley 2007)].

Target	Biological output of Akt-mediated phosphorylation
TSC2	Activation of mTORC1: cell growth (promotion of anabolic processes)
PRAS40	"
BAD	Inhibition of apoptosis
Caspase 9	"
ASK1	"
FoxO	Inhibition of apoptosis through transcriptional regulation
MDM2	Down-regulation of P53 leading to for example inhibition of apoptosis through transcriptional regulation
Raf1	Inhibits ERK signalling
eNOS	Stimulation of angiogenesis
AS160	Increased glucose uptake
GSK3	Promotion of proliferation
$p21^{Cip1/WAF1}$	Promotion of progression through the cell cycle
$p27^{Kip1}$	"
Chk1	Blocks cell cycle checkpoint

Table 1.6 Best characterised Akt substrates

Only the most extensively characterised cancer relevant substrates are presented here. Adapted from (Hers et al., 2011; Manning and Cantley, 2007).

Akt and cell survival

To promote cell survival Akt blocks the function or expression of many pro-apoptotic proteins (Hers et al., 2011; Manning and Cantley, 2007). Akt for example directly phosphorylates and inhibits the pro-apoptotic Bcl-2 family member BAD (Datta et al., 1997; del Peso et al., 1997) and inhibits members of the pro-apoptotic forkhead box O (FoxO) family of transcription factors. Akt phosphorylates FoxOs inducing their binding to the adaptor protein 14-3-3 resulting in nuclear export and increased degradation via the

ubiquitin-proteasome pathway (Aoki et al., 2004; Biggs et al., 1999; Brunet et al., 1999; Cahill et al., 2001; Kops et al., 1999). Akt also promotes survival by negatively regulating p53 levels and function through phosphorylation of the E3 ubiquitin ligase mouse double minute 2 homolog (MDM2) (Mayo and Donner, 2001; Zhou et al., 2001).

Akt and cellular growth and metabolism

As previously described, Akt positively regulates mTORC1. Through phosphorylation of its direct targets eukaryotic translation initiation factor 4E (eIF4E)-binding protein 1 (4E-BP1) and ribosomal protein S6 kinase (S6K), mTORC1 regulates protein translation. In addition to regulation of protein synthesis mTORC1 also regulates the synthesis of lipids required by proliferating cells to generate sufficient membrane levels (Laplante and Sabatini, 2012). Akt activation also stimulates glucose uptake and leads to the translocation of glucose transporter 4 (Glut4) to the plasma membrane (Kohn et al., 1996) through phosphorylation of AS160 (Sano et al., 2003).

Akt and cell proliferation

Akt contributes to promotion of cell proliferation through phosphorylation and inhibition of for example the $p27^{Kip1}$ cyclin dependent kinase inhibitor (Liang et al., 2002; Shin et al., 2002; Viglietto et al., 2002) as well as other targets (Hers et al., 2011; Manning and Cantley, 2007). Glycogen synthase 3 (GSK3) was the first direct target of Akt identified (Cross et al., 1995). Phosphorylation of GSK3 by Akt inhibits GSK3 leading to the stabilisation of many proteins that play key roles in G1-to-S-phase cell cycle transition thereby promoting progression through the cell cycle (Hers et al., 2011; Manning and Cantley, 2007).

Somatic Akt mutations in cancer

Constitutive activation of Akt is associated with cancer. The oncogenic Akt protein from the murine leukaemia retrovirus AKT8 is a Gag-Akt fusion protein that relies on a constitutive membrane targeting myristoylation signal for being transforming in mice (Ahmed et al., 1993). Moreover, a human cancer associated somatic mutation causing Akt1 Glu17Lys substitution within the PH domain causes constitutive Akt1 plasma membrane association and activation, transforms cells and induces leukaemia in mice (Carpten et al., 2007). An analogous Glu17Lys mutation has also been reported to occur in Akt2 and Akt3 (Davies et al., 2008; Stephens et al., 2012). Recently a novel translocation between MAGI3 and Akt3 was described. The translocation leads to constitutive activation of Akt3. The fusion protein retains most of Akt3 but also contains MAGI3 lacking its second PDZ domain that is reported to bind PTEN and to contribute to the inhibitory effect of PTEN on the PI3K pathway (Banerji et al., 2012; Wu et al., 2000).

Physiological roles of Akt isoforms

The three Akt isoforms are likely to posses some redundant functions but they also have certain distinct roles. Akt1 knockout mice have a decreased body size and partial neonatal mortality phenotypes (Chen et al., 2001; Cho et al., 2001b; Yang et al., 2003). Akt2 knockout mice display only a modest growth defect but are impaired in the ability of insulin to lower blood glucose levels due to defects of insulin action on liver and skeletal muscle tissue. Consequently Akt2 knockouts suffer from a type 2 diabetes-like syndrome (Cho et al., 2001a; Garofalo et al., 2003). Akt2 was also recently shown to suppress hepatic glycogenolysis (Wan et al., 2013). Akt3 knockout mice have normal glucose metabolism

and overall body size but present a decrease in brain size (Easton et al., 2005; Tschopp et al., 2005).

1.5 Use of PI3K pathway inhibitors to treat cancer

Due to its frequent aberrant activation in cancers and central role in the control of processes such as cell survival and proliferation, the PI3K pathway is an attractive target for anti-cancer therapies. Many small molecule PI3K, mTOR, PDK1 and Akt inhibitors have been developed over the years. Whilst no oncogenic PDK1 mutations have been reported, the central role of PDK1 in cancer signalling is evidenced by the observations that PDK1 over-expression in cells causes transformation (Zeng et al., 2002) and PDK1 hypomorphic mice are protected from spontaneous tumourigenesis caused by reduced PTEN expression (Bayascas et al., 2005). Despite this, development of PDK1 inhibitors is not currently active. The limited anti-tumour activity of PDK1 inhibitors is likely to be due to insufficiently potent inhibition of Akt activation by PDK1 inhibitors. Whilst PDK1 inhibitors potently suppress the activation of PDK1's cytosolic targets (including SGK and S6K), the efficient co-localisation of Akt and PDK1 at the plasma member renders Akt activation by PDK1 very efficient and hard to fully suppress with PDK1 inhibitors. This is likely to explain why even minimal residual PDK1 activity is sufficient to cause Akt activation (Najafov et al., 2011). With the exception of first-generation mTOR inhibitors including rapamycin (sirolimus) and its derivatives, no drugs targeting the PI3K network have yet been approved for clinical use. Many such compounds are currently in clinical trials, as summarised in Table 1.7. For example, catalytic mTOR inhibitors, which unlike rapalogs

inhibit both mTORC1 and mTORC2 efficiently, have yielded promising pre-clinical results [reviewed in (Willems et al., 2012)].

Compound	Target(s)	Status	Company	Comments
Combined PI3K–mTOR inhibitors				
BEZ235	PI3K, mTOR	Phase I, II	Novartis	
XL765	PI3K, mTOR	Phase I	Exelixis/Sanofi-Aventis	
GDC-0980	PI3K, mTOR	Phase I	Roche/Genentech	
GSK1059615	PI3K, mTOR, DNA-PK	Phase I	GlaxoSmithKline	
PKI-587	PI3K, mTOR	Phase I	Pfizer	
PF-04691502	PI3K, mTOR	Phase I	Pfizer	
Pan-PI3K inhibitors				
BKM120	PI3K	Phase I, II	Novartis	
SF1126	PI3K and mTOR	Phase I	Semafore	
PX-866	PI3K	Phase I	Oncothyreon Inc.	
XL-147	PI3K	Phase I	Exelixis/Sanofi-Aventis	
GSK615	PI3K	Phase I	GlaxoSmithKline	
CH5132799	PI3K	Phase I	Chugai Pharma Europe Ltd	
GDC-0941	PI3K (p110α), Flt3	Phase I	Roche/ Genentech	
BAY 80-6946	PI3K	Phase I	Bayer	
Isoform-specific PI3K inhibitors				
Idelalisib (CAL-101)	PI3K (p110δ)	Phase I,II,III	Gilead Sciences	
BYL719	PI3K (p110α)	Phase I	Novartis	
INK1117	PI3K (p110α)	Phase I	Intellikine	
GSK2636771	PI3K (p110β)	Phase I	GlaxoSmithKline	
Akt inhibitors				
Perifosine	Akt,	Phase I, II, III	AEterna Zentaris	Promiscious. No effect in Phase III colorectal cancer trial (Bendell et al., 2012). Phase III trials for myeloma terminated.
Triciribine (API-2)	Akt	Phase I	VioQuest Pharmaceuticals	
GDC-0068	Akt	Phase I	Roche/Genentech	
AR-67 (DB-67)	Akt	Phase I, II	Arno Therapeutics	
GSK690693	Akt	Phase I	GlaxoSmithKline	
VQD-002 (API-2)	Akt	Phase I, II	VioQuest Pharmaceuticals	
MK-2206	Akt	Phase I	Merck	
AZD5363	Akt	Phase I, II	AstraZeneca	
mTORC1 inhibitors (rapamycin derivatives, rapalogs)				
Sirolimus	mTORC1	Phase I, II	Wyeth/Pfizer	
Temsirolimus	mTORC1	Phase I, II, III	Wyeth/Pfizer	Approved for certain cancers
Everolimus	mTORC1	Phase I, II, III	Novartis	Approved for certain cancers
Ridaforolimus	mTORC1	Phase I, II, III	Ariad/Merck	Minor positive results from phase III (Demetri et al., 2013)
mTORC1/2 inhibitors				
AZD8055	mTORC1/2	Phase I, II	AstraZeneca	
AZD2014	mTORC1/2	Phase I, II	AstraZeneca	
OSI-027	mTORC1/2	Phase I	OSI Pharmaceuticals	Completed, no active trials
INK-128	mTORC1/2	Phase I	Intellikine	
CC-223	mTORC1/2, DNA-PK	Phase I, II	Celgene	

Table 1.7 Compounds targeting the PI3K pathway currently in clinical trials

Adapted from (Rodon et al., 2013; Weigelt and Downward, 2012) and data retrieved from http://www.clinicaltrials.gov/, accessed July 2013.

1.5.1 Feedback regulation of signalling networks

In order to appropriately respond to signal transduction cascades cells must have the capacity to down-regulate and switch off activated signalling pathways. Phosphatases for example reverse the action of kinases and consequently often inactivate signalling cascades. This is true for example in the case of the lipid phosphatase PTEN that catalyses the reverse reaction of PI3K. The importance of appropriate regulation of cellular signalling is highlighted by the notion that *PTEN* null mice are embryonic lethal (Di Cristofano et al., 1998; Podsypanina et al., 1999; Suzuki et al., 1998) indicating that in the absence of this negative regulator development fails to occur normally.

Physiological responses to signalling networks are also regulated and fine-tuned by feedback inhibition of components of the activated networks. Such feedback regulation is a feature of both normal and transformed cells. Negative feedback is a universal mechanism for limiting the duration and strength of signalling output. In cancer cells relief of negative feedback control may be a common response to many anti-cancer drugs that target nodes of signalling pathways. For example the use of mTOR inhibitors has revealed that inhibition of mTORC1 leads to elevated PI3K activation as it relieves negative feedback. Indeed, *in vivo* mTORC1 inhibition has been shown to lead to Akt activation (O'Reilly et al., 2006; Sun et al., 2005) as wells as ERK activation (Carracedo et al., 2008). When active, mTORC1 phosphorylates S6K that subsequently phosphorylates IRS1/2 targeting them for degradation causing down-regulation of the RTK-PI3K signalling (Harrington et al., 2004; Haruta et al., 2000; Shah et al., 2004). mTORC1 also directly phosphorylates adaptor protein Grb10 enhancing its stability and its ability to suppress PI3K activation (Hsu et al., 2011; Yu et al., 2011). Pre-clinical characterisation of mTOR

kinase inhibitors has revealed bi-phasic regulation of Akt. mTORC1/2 inhibition first causes a transient inhibition of Akt due to loss of Akt Ser473 phosphorylation and rapid but transient inhibition of Akt Thr308 phosphorylation. Sustained mTORC1/2 inhibition, due to relieved feedback inhibition, however leads to RTK-PI3K activation and subsequent activation of Akt by phosphorylation of Thr308 by PDK1 (Rodrik-Outmezguine et al., 2011).

Modulation of feedback inhibition is also associated with Akt inhibitors. The FoxO transcription factors comprise a key subset of Akt substrates. Many FoxO targets are pro-apoptotic and via inhibition of FoxOs Akt plays a pro-survival role. FoxOs, however, also transcriptionally up-regulate RTKs. Akt inhibition therefore relieves two negative feedback components of the PI3K pathway. Firstly, due to activation of FoxOs Akt inhibition relieves suppression of RTK expression resulting in increased levels of RTKs (Chandarlapaty et al., 2011). Secondly, as discussed in Section 1.3.2, Akt positively regulates mTORC1 via PRAS40 and TSC2. Consequently Akt inhibition leads to reduced mTORC1 activity and subsequently via IRS1/2 and Grb10 to enhanced RTK-PI3K activation. Figure 1.10 illustrates the current understanding of feedback mechanisms that operate within the PI3K-mTOR pathway.

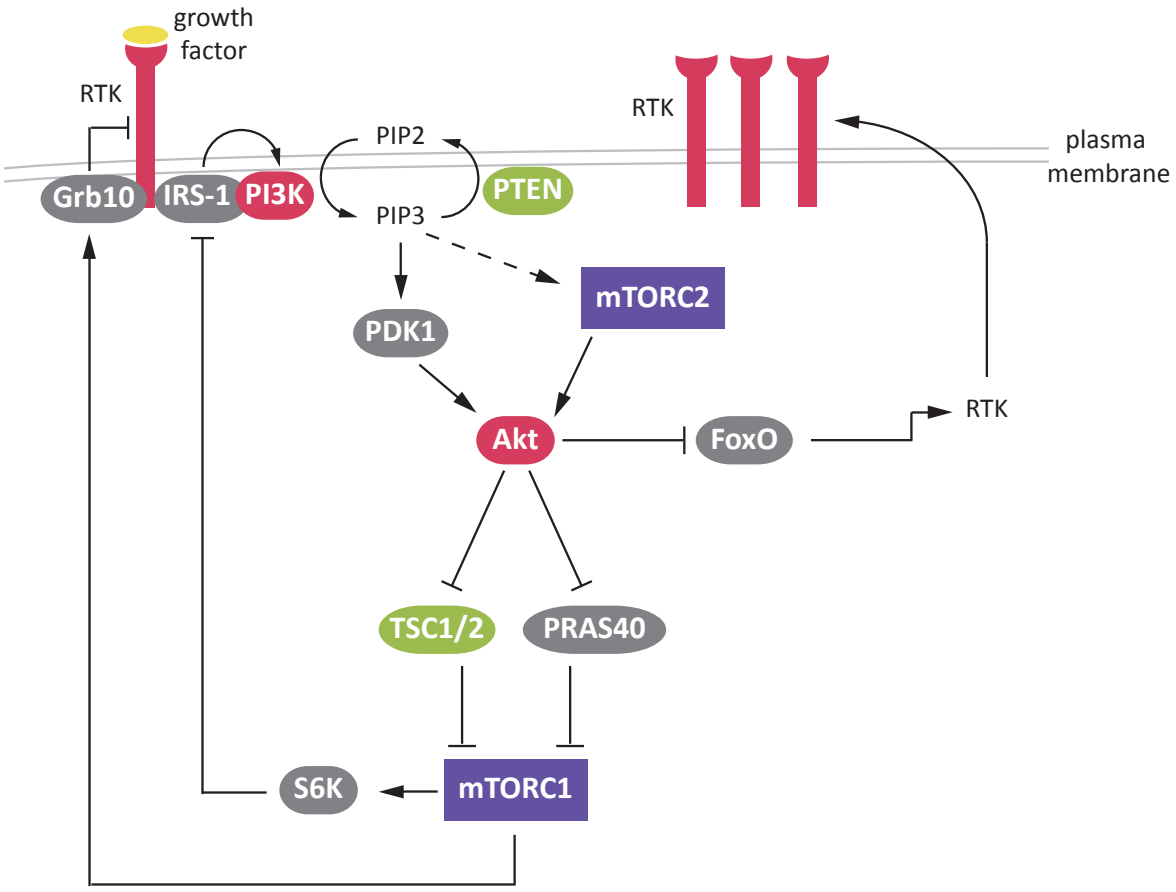

Figure 1.10 Feedback regulation within the PI3K pathway

Receptor tyrosine kinase (RTK) activation stimulates PI3K-AKT activity causing inhibition of FoxO-mediated RTK transcription. RTK stimulation also activates mTORC1, which directs inhibitory feedback to the pathway via S6K-IRS1 and Grb10.

1.6 The SGK family of protein kinases

Most work has focused on Akt as being the key mediator of cell proliferation induced by activation of PI3K. A closely related enzyme termed SGK (serum- and glucocorticoid-regulated kinase) has by comparison received little attention. Three SGK isoforms exist and like Akt, SGKs also belong to the AGC family of kinases. The domain structures of the three SGK isoforms, which share about 80% identity within their kinase domains (Kobayashi et al., 1999), are illustrated in Figure 1.11. All SGK family members contain a

kinase domain that harbours their T-loop phosphorylation site and a conserved AGC kinase C-terminal tail that harbours the second key regulatory site, termed the hydrophobic motif (HM). SGK3 contains an additional phosphoinositide binding Phox homology (PX) domain [reviewed in (Pearce et al., 2010b)]. The SGK family members are closely related to Akt sharing about 45-55% identity within their catalytic domains (Webster et al., 1993b). SGK and Akt kinase phosphorylate substrates within similar consensus sequences: Arg-Xaa-Arg-Xaa-Xaa-Ser/Thr (Alessi et al., 1996; Murray et al., 2005) and are consequently likely to possess some overlapping substrates and functions. SGK kinases are evolutionarily conserved. Yeast contains two SGK orthologues Ypk1 and Ypk2, which are required for endocytosis and proliferation (Casamayor et al., 1999; deHart et al., 2002).

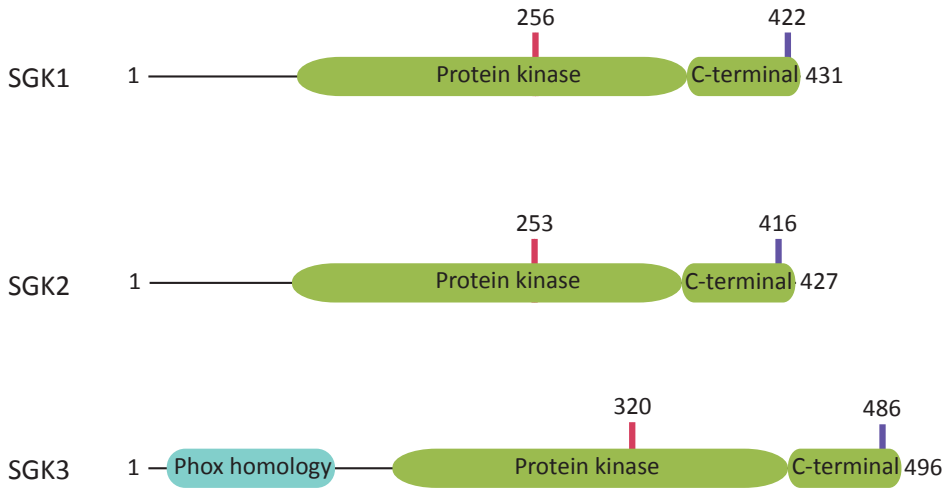

Figure 1.11 The serum- and glucocorticoid-regulated kinases

SGK isoforms share a conserved kinase domain and AGC kinase C-terminal tail. SGK3 additionally contains a phosphoinositide binding Phox homology (PX) domain. The T-loop phosphorylation sites are indicated in red and the hydrophobic motif (HM) phosphorylation sites are indicated in purple.

Mechanism of activation of SGK family members

SGK family members also share their upstream activators with Akt. Like Akt kinases, SGKs too are phosphorylated by PDK1 within their T-loop site (Thr256 in SGK1) (Kobayashi and Cohen, 1999; Park et al., 1999) and by mTORC2 within their HM site (Ser422 in SGK1) (Garcia-Martinez and Alessi, 2008). The molecular mechanism of SGK activation, however, varies from that of Akt kinases because SGKs do not possess a PtdIns(3,4,5)P_3 binding PH domain and therefore their phosphorylation by PDK1 is believed to occur in the cytosol, as illustrated in Figure 1.12. Growth factor signalling activated mTORC2 phosphorylates the HM-site of SGKs (Ser422 in SGK1) allowing the phosphorylated HM to interact with a region termed the PDK1 interacting fragment (PIF)-binding pocket within the catalytic domain of PDK1 (Biondi et al., 2001). HM-site phosphorylation and the integrity of PIF-binding pocket are essential for the phosphorylation and activation of SGKs, but not Akt, by PDK1. This is genetically demonstrated by studies in knock-in embryonic stem (ES) cells in which the PIF-binding pocket of PDK1 is disrupted by Leu155Glu (Collins et al., 2003) or Arg131Met (Collins et al., 2005) mutations that prevent the docking of phosphorylated HM-residue to PDK1 and consequently SGK is not active in these cells. Furthermore, the binding of PDK1 to PtdIns(3,4,5)P_3 is not required for the activation of SGK by PDK1 *in vivo* (Bayascas et al., 2008) or for T-loop phosphorylation *in vitro* (Biondi et al., 2001). The integrity of the PIF-binding pocket is also crucial for the phosphorylation of S6K and p90 ribosomal S6 kinase (RSK) by PDK1 (Collins et al., 2003; Collins et al., 2005). The importance of the preceding HM-site phosphorylation for SGK activation is highlighted by

the fact that in mouse embryonic fibroblast (MEF) cells that lack functional mTORC2 due to either Sin1-, mLST8- or Rictor-deficiency, SGK is not phosphorylated at its HM-site and consequently is not activated (Garcia-Martinez and Alessi, 2008).

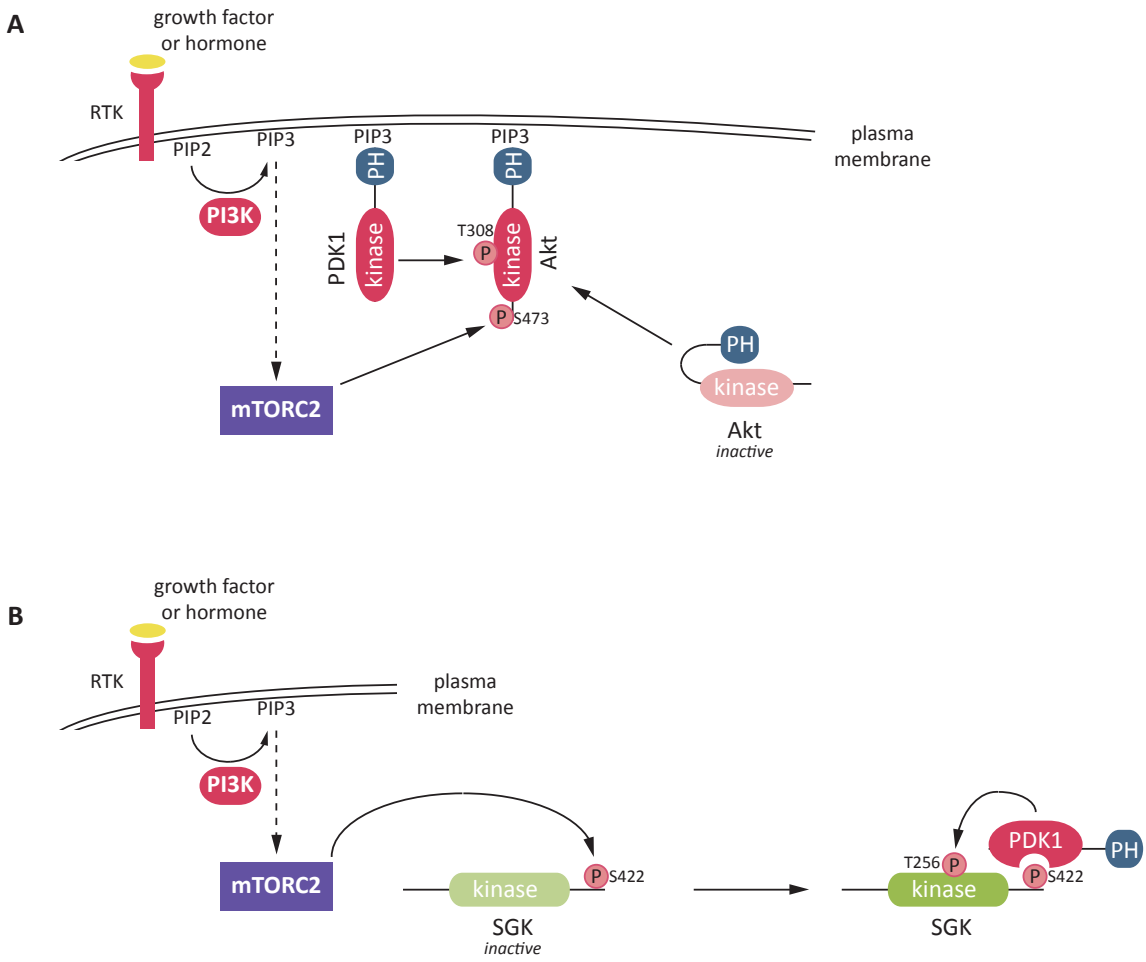

Figure 1.12 Comparison of the activation of Akt and SGK

(**A**) PI3K is activated downstream of RTKs. The generation of PtdIns(3,4,5)P_3 (PIP3) by PI3K, causes the recruitment of Akt to the plasma membrane and a conformational change that enables the phosphorylation of Akt T-loop T308 by PDK1. mTORC2-mediated phosphorylation of the HM-site S473 contributes towards maximal activation. (**B**) mTORC2 is activated downstream of PI3K and phosphorylates the SGK HM-site (Ser422) providing a docking site for PDK1 that then phosphorylates the T-loop Thr256. Residue numbers are shown for Akt1 and SGK1.

1.6.1 SGK1

SGK1 was the first SGK family member characterised and was initially identified as a gene whose expression is regulated by glucocorticoids and serum (Webster et al., 1993b). The *SGK1* gene promoter contains a glucocorticoid-response element that is bound by glucocorticoid receptors (GR) and is sufficient to confer glucocorticoid responsiveness (Webster et al., 1993b). *SGK1* expression is also induced by the mineralocorticoid aldosterone (Chen et al., 1999; Naray-Fejes-Toth et al., 1999) as well as serum and the induction in response to serum is considered to be an immediate-early transcriptional response (Webster et al., 1993a). Multiple other signals including, but not limited to, gonadotrophins, transforming gowth factor beta, cytokines, excessive glucose levels, external stress and changes to cell volume and have been reported to control *SGK1* transcription [reviewed in (Lang et al., 2009; Lang et al., 2006)]. By contrast, *SGK2* and *SGK3* mRNA levels are not increased in response to serum or glucocorticoids, the classic up-regulator of *SGK1* expression (Kobayashi et al., 1999).

SGK1 protein has a half-life of only 30 minutes. The N-terminus of SGK1 contains a motif that targets it ubiquitylation mediated proteasomal degradation and deletion of the first 60 amino acids of SGK1 indeed greatly enhances stability of the kinase (Bogusz et al., 2006; Brickley et al., 2002; Kobayashi and Cohen, 1999). In part SGK1 dictates its own destruction since SGK1 mediated phosphorylation of an E3 ubiquitin ligase termed Neural Precursor Cell-Expressed, Developmentally Down-Regulated Protein 4-2 (Nedd4-2) leads to increased Nedd4-2 mediated ubiquitylation and proteasomal degradation of SGK1 (Zhou and Snyder, 2005). Moreover, also the E3 ubiquiting ligase CHIP has been reported to mediate SGK1 degradation (Belova et al., 2006) and the mTORC2 subunit Rictor has

been shown to associate with Cullin-1 to form a functional E3 ubiquitin ligase complex capable of targeting SGK1 for proteasomal degradation. Phopshorylation of Rictor by activated AGC kinases prevents SGK1 ubiquitylation by Rictor/Cullin-1 (Gao et al., 2010).

Substrates and physiological functions of SGK1

SGK1 has been linked to multiple cellular and physiological processes including, but not limited to, regulation of solute transport, control of blood pressure, memory consolidation and cell survival [reviewed in (Lang et al., 2006)]. SGK1 is thought to participative in the pathophysiology of various conditions as highlighted by the reports that *SGK1* gene variants are associated with for example elevated blood pressure (Busjahn et al., 2002; Rao et al., 2013), increased incidence of ischaemic stroke and type II diabetes (Dahlberg et al., 2011; Schwab et al., 2008) and increased body mass index (Dieter et al., 2004). In *Caernorhabditis elegans* loss of SGK-1 results in a slight developmental delay, smaller body size, defects in reproduction, increased stress resistance and altered metabolism highlighted by increased lipid storage (Hertweck et al., 2004; Jones et al., 2009; Soukas et al., 2009).

SGK1, and to some extent also other SGK family members, have been reported to regulate the activity of a vast number of channels and transporters including sodium, potassium, calcium and chloride channels and amino acid and glucose transporters [reviewed in (Lang et al., 2006; Lang and Voelkl, 2013)]. The mechanistically best-characterised SGK-mediated regulation of a channel is that of the epithelial sodium channel (ENaC) via which SGK1 contributes to the control of renal tubular Na^+ reabsorption. Initially co-expression of SGK1 with ENaC in *Xenopus* oocytes was found to increase ENaC mediated currents due

to increased levels of ENaC at the plasma membrane (Alvarez de la Rosa et al., 1999; Chen et al., 1999; Naray-Fejes-Toth et al., 1999). Subsequently SGK1 was found to phosphorylate the E3 ubiquitin ligase Nedd4-2 that downregulates levels of ENaC at the plasma membrane. Phosphorylation of Nedd4-2 by SGK1 negatively regulates Nedd4-2 by reducing binding of Nedd4-2 to ENaC and inhibiting Nedd4-2 activity by stimulating the binding of Nedd4-2 to 14-3-3 chaperone proteins leading to increased levels of ENaC at the cell surface (Bhalla et al., 2005; Debonneville et al., 2001; Ichimura et al., 2005; Snyder et al., 2002). SGK1 has additionally been suggested to regulate ENaC via the with no lysine kinase 4 (WNK4) (Ring et al., 2007) and transcriptionally (Boyd and Toth, 2005; Zhang et al., 2007).

Many observations link SGK1 to cancer-relevant processes. SGK1 is for example suggested to phosphorylate and inhibit the anti-apoptotic FoxO transcription factors (Brunet et al., 2001). SGK1 has also been linked to for example dexamethasone and GR activation associated breast cancer cell survival (Mikosz et al., 2001; Wu et al., 2004) and in multiple myeloma SGK1 has been identified as a transcriptional target of cytokines that promote proliferation (Fagerli et al., 2011). Furthermore, a role for SGK1 in cell invasion and migration, which are two highly cancer relevant processes, has been reported (Eylenstein et al., 2011; Schmidt et al., 2012a; Schmidt et al., 2012b). An additional substrate of SGK1 is N-myc downstream-regulated gene 1 (NDRG1) and 2 (Murray et al., 2004), but the functional significance of this phosphorylation event remains unknown.

SGK1 knockout mouse models

Whole body SGK1 knockout mice are embryonic lethal in a pure C57BL/6 background due to defects in angiogenesis and heart development presumed to be caused by increased apoptosis in $SGK1^{-/-}$ endothelial and vascular smooth muscle cells (Catela et al., 2010). This observation supports the notion that SGK1 could be a pro-survival kinase. SGK1 knockout mice, however, are viable and seemingly normal in 129/SvJ genetic background. Three different SGK1 knockout mouse models have been described. All three models appear normal when fed a standard diet. The first described constitutive SGK1 knockout mouse model maintains normal sodium and water excretion under normal diet but possesses elevated plasma aldosterone levels suggesting that mechanisms controlling sodium handling and cell volume control are affected. Under sodium deficient diet the SGK1 knockout mice excrete more water and salt than their wild type counterparts, possess highly elevated aldosterone levels and have lowered blood pressure (Wulff et al., 2002). Expression of α-ENaC is only modestly reduced in these mice but the expression levels of the Na^+Cl^- cotransporter (NCC) are drastically reduced (Vallon et al., 2009; Wulff et al., 2002). These mice are resistant to dexamethasone induced increases in blood pressure (Boini et al., 2008) and are also resistant to increases in blood pressure caused by high salt intake in combination with high-fat or high-fructose diet that cause hyperinsulinemia (Huang et al., 2006a; Huang et al., 2006b). A variety of other moderate solute handling defects have been described for these mice, for instance the kidneys of SGK1-/- mice fail to adequately eliminate an acute K+ load (Huang et al., 2004). The second constitutive SGK1 knockout mouse model also displays elevated urinary Na^+ excretion when placed on a low salt diet. Surprisingly, ENaC activity is increased in these SGK1 knockout mice. In

contrast, levels of active form of γ-ENaC are reduced and levels of NCC dimished in these mice (Fejes-Toth et al., 2008). The third SGK1 mouse model, which is a conditional knockout, again, under low-salt diet, exhibits reduced blood pressure and impaired ability to reduce sodium excretion. Whilst only moderate decreases are reported for ENaC levels, the levels of NCC are drastically reduced (Faresse et al., 2012). Based on these observations it appears that whilst SGK1 is involved in ENaC regulation, its primary target may be NCC and possibly other transport systems. The method via which SGK1 controls NCC remains elusive and mechanisms involving with no lysine kinase 4 (WNK4) (Rozansky et al., 2009) and Nedd4-2 (Pablo Arroyo et al., 2011) have been suggested.

SGK1 knockout mice also suffer from reproductive failures (Salker et al., 2011) and recently a role for SGK1 in the control of the immune system was described. SGK1 is suggested to act as a salt-induced gene whose expression directs the induction of pathogenic T_H17 cells that contribute the development of autoimmune diseases (Kleinewietfeld et al., 2013; Wu et al., 2013). To further support the notion that SGK1 might be involved in cancer signalling, $SGK1^{-/-}$ mice are resistant to chemical induction of intestinal tumours (Nasir et al., 2009) and in adenomatous polyposis coli (APC)-deficient background SGK1 absence leads to reduced spontaneous tumourigenesis (Wang et al., 2010).

1.6.2 SGK2

SGK2 is the least studied SGK isoform. SGK2 contains no other distinctive domains beyond the catalytic kinase domain and is not transcriptionally induced in response to

glucocorticoids or serum in cells (Kobayashi et al., 1999). A role for SGK2 in oncogenic signalling has been suggested. An RNA interference (RNAi) screen of human cervical carcinoma cell lines and human papilloma virus (HPV) transformed cells identified SGK2 as a potential proliferation driver (Baldwin et al., 2010). SGK2 knockout mice were described by Schnackenberg and colleagues in a meeting abstract and the authors suggest that SGK2 is not critical for renal salt and water homeostasis during unstressed conditions, but that SGK2 can compensate for the loss of SGK1 during salt deprivation (Schnackenberg et al., 2007).

1.6.3 SGK3

SGK3 (also called SGKL, CISK) was identified as a mediator of interleukin 3 (IL3) -dependent survival in hematopoietic cells and its over-expression was suggested to inhibit FoxO mediated transcription and to inhibit pro-apoptotic Bcl-2 family members in a manner similar to Akt (Liu et al., 2000). These studies did not analyse endogenous SGK3. Unlike the other SGKs, SGK3 possesses and N-terminal lipid targeting domain. The SGK3 PX domain is suggested to primarily bind PtdIns(3)P and to localise to endosomes (Jun et al., 2001; Virbasius et al., 2001).

SGK3 knockout mice (C57BL/6 background) display impaired postnatal hair growth due to a hair bulb keratinocyte proliferation defect (Alonso et al., 2005; McCormick et al., 2004). $SGK3^{-/-}$ mice also display a mild and transient growth defect, normal renal salt handling, subtly decreased locomotion, defective mast cell function, increased gastric acid secretion and decreased intestinal glucose transport (McCormick et al., 2004; Pasham et al., 2011;

Sandu et al., 2005; Zemtsova et al., 2010). SGK3 depletion also further worsens the glucose handling phenotype of Akt2 knockout mice (Yao et al., 2011). SGK1-/-SGK3-/- double knockout mice (mixed 129/SvJ:C57BL/6 background) share the hair growth defect of the SGK3 knockouts and the renal salt retention defect of SGK1 knockouts without showing any novel more severe phenotypes (Grahammer et al., 2006). As indicated by the keratinocyte proliferation defects in the SGK3 knockout mice, SGK3 might play roles in promoting cell survival and proliferation. In fact, many PI3KCA-mutant cancer cell lines have been found to exhibit surprisingly low levels of Akt activation and to depend on SGK3 for their viability (Vasudevan et al., 2009). A further correlation between cancer signalling and SGK3 is provided by the recent observations that SGK3 is transcriptionally regulated by oestrogen and elevated SGK3 levels are found in ER positive breast cancers (Wang et al., 2011; Xu et al., 2012).

1.7 Aims of the study

The key components of the PI3K signalling pathway, PI3K, mTOR and Akt, have emerged as key targets for cancer drug discovery and much previous work as focused on the role of Akt as a major mediator of proliferation- and survival-promoting functions of PI3K. In contrast the closely related SGK isoforms have by comparison received little attention. Owing to the similarity of Akt and SGK isoforms and the potential that these kinases could possess an overlapping set of substrates and functions, the aim of this PhD work was to elucidate whether SGK isoforms could compensate for Akt and represent resistance mechanisms to Akt inhibitors.

2. Materials & Methods

2.1 Materials

2.1.1 Commercial reagents

Acetone, ethanol, formic acid, glycerol, glycine, 4-(2-Hydroxyethyl)piperazine-1-ethanesulfonic acid (Hepes), isopropanol, methanol, 2-mercaptoethanol, orthophosphoric acid, potassium chloride, sodium chloride, sodium ethylenediaminetetraacetic acid (EDTA), magnesium acetate, sodium ethylene glycol tetraacetic acid (EGTA), sodium fluoride, sodium β-glycerophosphate, sodium orthovanadate, pentobarbital, puromycin, adenosine 5'-triphosphate sodium salt (ATP), anti-HA-agarose, ammonium bicarbonate, ammonium persulphate (APS), ampicillin, benzamidine, bovine serum albumin (BSA), bromophenol blue (BPB), dexamethasone, doxorubicin, dimethyl pimelimidate (DMP), dimethyl sulphoxide (DMSO), hydrogen peroxide, iodoacetamide, MISSION™ shRNAs, phenylmethanesulphonylfluoride (PMSF), Ponceau S, sodium dodecyl sulphate (SDS), sodium tetraborate, N, N, N', N'-Tetramethylethylenediamine (TEMED), triethylammonium bicarbonate, Nonidet P40, Triton-X-100 and Tween-20 were from Sigma-Aldrich (Poole, UK). Sucrose and Tris(hydroxymethyl)methylamine (Tris) were from BDH (Lutterworth, UK). Cellophane films, i-Script Kit, SsoFast™ EvaGreen® Supermix, polymerase chain reaction (PCR) plates and Precision Plus protein markers were from BioRad (Herts, UK). 3-[(3-Cholamidopropyl)dimethylammonio]-1-propanesulfonate (CHAPS) was from Calbiochem (Merck Biosciences, Nottingham, UK). Insulin-like growth factor (IGF1) was from Cell Signaling Technology (New England Biolabs, Herts, UK).

Polybrene was from SantaCruz Biotechnology (Heidelberg, Germany). Cell culture dishes and flasks, cryovials and Spin-X columns were from Corning (NY, USA). Cell scrapers were from Costar (Cambridge, USA). 40% (w/v) 29:1 Acrylamide:Bis-Acrylamide solution was from Flowgen Bioscience (Nottingham, UK). Protein A-agarose, Protein G-sepharose, Glutathione-sepharose, Enhanced chemiluminescence (ECL) kit, Hyperfilm MP, Protran nitrocellulose membrane, P81 paper, 3mm chromatography paper and [γ32P]-labelled ATP were from GE Healthcare (Piscataway, USA). Cell dissociation buffer, Dulbecco's modified eagle medium (DMEM), RPMI-1640 medium, Phosphate buffered saline (PBS), Trypsin/EDTA, L-glutamine, Lipofectamine 2000, non-essential amino acids, sodium pyruvate, antibiotic/antimycotic, NuPAGE Novex SDS Bis-Tris gels, NuPAGE MOPS running buffer, NuPAGE reducing agent, NuPAGE LDS sample buffer and primers were from Invitrogen (Paisley, UK). Photographic developer (LX24) and liquid fixer (FX40) were from Kodak (Liverpool, UK). X-ray films were from Konica (Japan). Polyethylenimine (PEI) was from Polysciences (Warrington, PA). Skimmed milk (Marvel) was from Premier Beverages (Stafford, UK). Plasmid Maxiprep and RNeasy kits were from Qiagen Ltd (Crawley, UK). Acetonitrile (HPLC grade) was from Rathburn Chemicals (Walkerburn, UK). Protease inhibitor cocktail was from Roche (Lewes, UK). Horseradish peroxidase (HRP)- and Alexafluor-conjugated secondary antibodies, Bradford reagent and Fetal Bovine Serum (FBS) were from Thermo-scientific (Essex, UK). CellTiter 96® AQueous One Solution Cell Proliferation Assay (MTS) and trypsin (mass spectrometry grade) were from Promega (Southhampton, UK). Matrigel™ invasion chambers were from BD Biosciences #354483 (Oxford, UK). Reastain Quick-Diff kit was from Reagena (Finland). InstantBlue protein staining solution was from Expedeon (Harston, UK).

2.1.2 In-house reagents

Luria Bertani (LB) broth and LB agar plates supplemented with 200 μg/mL ampicillin were from media kitchen. NDRG1 (DU1557) and NEDD4.2 (DU4004) purified from *E.coli* and Crosstide peptide were from the Division of Signal Transduction Therapy (DSTT).

2.1.3 Antibodies

In-house antibodies (Table 2.1) were raised in sheep and affinity purified on the appropriate antigen by the DSTT. In-house antibodies were used at 1 μg/mL in 5% (w/v) skimmed milk in TBST and the in-house phospho-specific antibodies were used at 1 μg/mL in 5% (w/v) BSA -TBST supplemented with 10 μg/mL non-phospho peptide to increase specificity. Commercial antibodies (Table 2.2) were used at 1:1000 dilutions. The α-ENaC antibody was a gift from Dr S. Wilson (University of Dundee).

Antibody	Immunogen	Sheep	Bleed
Akt1	Full-length human Akt1	S742B	3rd
GST	GST (expressed from pGEX4T)	S902A	2nd
HA	HA (YPYDVPDYA)	mouse	-
NDRG1	Full-length human NDRG1	S276B	3rd
PRAS40	Full-length human PRAS40	S115B	1st
PRAS40 pThr246	Human PRAS40 [240-251] (CRPRLNT*SDFQK)	S114B	2nd
Protor-1	Full-length human Protor-1	S020C	3rd
Protor-2	Full-length human Protor-2	S136C	3rd
Rictor (mouse)	Mouse Rictor [6-20] RGRSLKNLRIRGRND	S274C	1st
S6K1	Human S6K1 [25-44] (AGVFDIDLDQPEDAGSEDEL)	S417B	2nd
SGK1+2	Full-length human SGK1	S062D	3rd
SGK2	Human SGK2 [333-346] (KSIGCTPDTVASSS)	S036D	3rd
SGK3	SGK3 PX domain (residues 1-130 of human SGK3)	S037D	3rd
Sin1	Full-length human Sin1	S008C	2nd

Table 2.1 In-house antibodies

Antibody	Catalog #	Source	Species	Blocking buffer
Akt pThr308	4056	CST	Rabbit	BSA
Akt pSer473	9271	CST	Rabbit	BSA
γ-ENaC	E4902	Sigma	Rabbit	milk
Flotillin-1	sc-25506	Santa Cruz	Rabbit	milk
FoxO1	2880	CST	Rabbit	BSA
FoxO3	2497	CST	Rabbit	BSA
FoxO1/FoxO3 pThr24/pThr32	9464	CST	Rabbit	BSA
FoxO1 pSer256	9461	CST	Rabbit	BSA
FoxO3 pSer253	9466	CST	Rabbit	BSA
GAPDH	2118	CST	Rabbit	BSA
GSK3a/ß pSer21/9	9331	CST	Rabbit	BSA
GSK3α/β	44-610	Invitrogen	Mouse	BSA
IGF Receptor β	3027	CST	Rabbit	BSA
IGFR pTyr1135/1136	3024	CST	Rabbit	BSA
mTOR	SC-1549	Santa Cruz	Goat	milk
NDRG1 Thr346	5482	CST	Rabbit	BSA
S6	2217	CST	Rabbit	BSA
S6 pSer235/Ser236	4856	CST	Rabbit	BSA
S6K pThr229	9379	CST	Rabbit	BSA
S6K pThr389	9234	CST	Rabbit	BSA
SGK pT-loop	9379	CST	Rabbit	BSA
Pan-SGK	S5188	SIGMA	Rabbit	milk
PTEN	5384	CST	Rabbit	BSA
SGK pHydrophobic motif	sc-16745	Santa Cruz	Rabbit	BSA
TSC2	3612	CST	Rabbit	BSA
TSC2 pThr1462	3617	CST	Rabbit	BSA

Table 2.2 Commercial antibodies

2.1.4 Plasmids

Dr M. Deak, Dr M. Peggie and Mr T. Macartney performed the cloning, subcloning and mutagenesis of the constructs described in this thesis. Constructs used are shown in Table 2.3. All constructs encoded the human version of the gene. The mammalian expression vector, pEBG6P, was generated by Dr M. Deak. This is a modified version of the pEBG2T vector (Sanchez et al., 1994) that allows the expression of proteins with an N-terminal GST tag followed by a PreScission cleavage site. A mammalian expression vector under the control of the cytomegalovirus promoter called pCMV5A was also utilised, encoding an N-

terminal hemagglutinin (HA)-tag (Andersson et al., 1989). For retroviral transduction of cells pBABE vector encoding puromycin selectable marker was used. The pBABE vector is based on the Moloney murine leukemia virus (MoLV) and the genes are expressed from the MoLV long terminal repeat (LTR) (Morgenstern and Land, 1990).

Construct	Clone number	Vector
GST-Akt1	DU2005	pEBG
GST-Akt1 K179A (Kinase inactive [KI])	DU6191	pEBG
GST-SGK1	DU124	pEBG
GST-SGK1 K127A (KI)	DU125	pEBG
GST-ΔN-SGK1 (61-431)	DU142	pEBG
GST-ΔN-SGK1 (61-431) K127A (residue number for full length) (KI)	DU143	pEBG
GST-ΔN-SGK1 (61-431) T256A (residue number for full length)	DU144	pEBG
GST-ΔN-SGK1 (61-431) S422A (residue number for full length)	DU145	pEBG
HA-SGK1	DU153	pCMV5A
HA-ΔN-SGK1 (61-431)	DU38226	pBABE
HA-ΔN-SGK1 (61-431)	DU163	pCMV5A
HA-ΔN-SGK1 (61-431) K127A (residue number for full length) (KI)	DU41768	pBABE
GST-SGK2	DU176	pEBG
HA-SGK2	DU181	pCMV5A
GST-SGK3	DU410	pEBG
GST-SGK3 K191A (KI)	DU2257	pEBG
HA-SGK3	DU442	pCMV5A
HA-SGK3 shRNA #D resistant	DU44496	pBABE
HA-SGK3 K191A (KI) shRNA #D resistant	DU44538	pBABE

Table 2.3 Constructs

2.1.5 Inhibitors

Inhibitors used in this thesis are shown in Table 2.4. Compounds were dissolved in DMSO and stored at -80°C. The National Centre for Protein Kinase Profiling (http://www.kinase-screen.mrc.ac.uk) performed specificity screens. In-house inhibitors were synthesised by Dr N. Shripo. DSTT SGKi1 and DSTT SGKi2 (unpublished, structures not disclosed) were obtained from collaborations with pharmaceutical companies.

Inhibitor	Target	Source	Reference
AZD5363	Akt	AstraZeneca	(Davies et al., 2012)
AZD8055	mTOR	Axon MedChem	(Chresta et al., 2010)
DSTT SGKi1	SGK	DSTT	Unpublished
DSTT SGKi2	SGK/Akt	DSTT	Unpublished
EMD638683	SGK	Merck	(Ackermann et al., 2011)
GDC-0941	Class I PI3K	In-house	(Folkes et al., 2008)
GSK2334470	PDK1	In-house	(Najafov et al., 2011)
MK-2206	Akt	In-house	(Hirai et al., 2010)
PF-4708671	S6K	Tocris	(Pearce et al., 2010a)
PI-103	Class I PI3Ks & mTOR	In-house	(Fan et al., 2006b)
Rapamycin	mTORC1	Calbiochem	(Vezina et al., 1975)

Table 2.4 Inhibitors

2.1.6 Buffers

Tris lysis buffer: 50 mM Tris-HCl pH 7.5, 1 mM EGTA, 1 mM EDTA, 1% (v/v) Triton-X100, 1 mM sodium orthovanadate, 10 mM sodium-ß-glycerophosphate, 50 mM sodium fluoride, 10 mM sodium pyrophosphate, 0.27 M sucrose, 0.15 M NaCl, 0.1% 2-mercaptoethanol and either 1 mM benzamidine and 0.1 mM phenylmethylsulphonylfluoride (PMSF) or complete protease inhibitor cocktail. For large-scale immunoprecipitations Triton-X100 was replaced with the milder detergent CHAPS (0.3% [w/v]).

HEPES lysis buffer: (for mTOR kinase assays) 40 mM Hepes pH 7.5, 1 mM EDTA, 0.3% (w/v) CHAPS, 0.5 mM sodium orthovanadate, 10 mM sodium-ß-glycerophosphate, 50 mM sodium fluoride, 10 mM sodium pyrophosphate, 0.27 M sucrose, 0.12 M NaCl and 1 mM benzamidine and 0.1 mM PMSF.

Lysis buffer inhibits proteases, kinases, phosphatases and other divalent cation-dependent enzymes ensuring that the phosphorylation and expression levels of proteins are fixed at the levels in which they are found *in vivo*. Benzamidine and PMSF or complete protease

inhibitor tablets prevent the action of metallo, aspartic, cysteine and serine proteases. EDTA chelates Mg^{2+} and EGTA chelates Ca^{2+}. Sodium fluoride, sodium-ß-glycerophosphate and sodium pyrophosphate are Ser/Thr phosphatase inhibitors. Sodium orthovanadate is Tyr phosphatase inhibitor. Sodium orhovanadate was prepared, as recommended by manufacturer, by repeated rounds of boiling and cooling until the solution was colourless at pH10 at room temperature to ensure that it is in the monomeric state that favours Tyr phosphatase inhibition.

Buffer A: 50 mM Tris-HCl pH 7.5, 0.1 mM EGTA, and 0.1% 2-mercaptoethanol

Hepes kinase buffer: (for mTOR kinase assays) 25 mM Hepes pH 7.5, 50 mM KCl

Tris buffered saline (TBS): 50 mM Tris-HCl pH 7.5, 0.15 M NaCl

5x sodium dodecyl sulfate (SDS) sample buffer: 5% (w/v) SDS, 5% (v/v) 2-mercaptoethanol, 250 mM Tris-HCl pH 6.8, 32.5% (v/v) Glycerol, bromophenol blue

Tris-glycine SDS running buffer: 25mM Tris-HCl pH 8.3, 192mM Glycine, 0.1% (w/v) SDS

Tris-glycine transfer buffer: 48mM Tris-HCl, 39mM Glycine, 20% (v/v) Methanol

2.1.7 Cell lines

Wild-type and knockout Rictor mouse embryonic fibroblasts (MEF) (Shiota et al., 2006) were provided by Prof. M. Magnuson (Vanderbilt University School of Medicine, USA). Generation of Protor-1/Protor-2 wild type and double knockout MEFs is described in (2.2.34). BT-474, BT-549, CAMA-1, HCC-1806, HCC-1187, HCC-1937, JIMT-1, MDA-MB-157,

MDA-MB-231, MDA-MB-436, SUM-52-PE, T47D and ZR-75-1 cell lines were provided by AstraZeneca (Alderley Park, Macclesfield, UK). All other cell lines were supplied by the MRC Protein Phosphorylation and Ubiquitylation Unit (University of Dundee).

2.1.8 Animals

Mice obtained from Taconic-Artemis (Cologne, Germany) were maintained under specific pathogen-free conditions and routine animal tail and ear notching was carried out by staff in the College of Life Science Transgenic Unit (University of Dundee). Mrs G. Fraser carried out genotyping from tail biopsies. All procedures were carried out in accordance with the regulations set by the University of Dundee and the United Kingdom Home Office.

2.1.9 Instruments

Centrifuge tubes, rotors and centrifuges were from Beckmann (Palo Alto, USA). Trans-Blot Cells, iQ5 real time PCR detection system and gel dryer apparatus were from BioRad (Herts, UK). SpeedVac was from CHRIST (Osterode, Germany). Thermomixer IP shakers were from Eppendorf (Cambridge, UK). The Biofuge microcentrifuge was from Haraeus Instruments (Osterode, Germany). pH meters were from Horiba (Kyoto, Japan). X-Cell SureLock Mini-cell electrophoresis systems and X-Cell II Blot modules were from Invitrogen (Paisley, UK). Polytron was from Kinematica (Brinkmann, CT, USA). X-omat autoradiography cassettes were from Kodak (Liverpool, UK). The Konica automatic film processor was from Konica Corporation (Japan). Li-Cor Odyssey^{TM} Infrared Imaging System

was from Li-Cor Biosciences (Cambridge, UK). CO_2 incubators were from Mackay and Lynn (Dundee, UK). Tissue culture class II safety cabinets were from Medical Air Technology (Oldham, UK). The PCR thermocycler (PTC-200) was from MJ Research. The 96-well Versamax plate reader was from Molecular Devices (Wokingham, UK). Proxeon EasynLC chromatography system, LTQ-Orbitrap Classic mass spectrometer and Nanodrop were from Thermo Scientific (Essex, UK). Scintillation counter (Tri-Carb 2800 TR) was from Perkin-Elmer.

2.2 Methods

2.2.1 Transformation of chemically competent *Escherichia coli* (*E.coli*)

Calcium competent *E.coli* DH5α (Inoue et al., 1990) cells were provided by the DSTT. Approximately 10-50 ng DNA was added to 50 µl of competent cells and incubated on ice for 5 min. Cells were then subjected to heat shock at 42°C water bath for 90 seconds to induce the uptake of DNA and briefly placed back on ice. Cells were streaked onto LB agar plates containing 200 µg/mL ampicillin and plates incubated at 37°C overnight.

2.2.2 Purification of plasmids from *E.coli*

Transformed DH5α *E.coli* were cultured in 200 mL LB containing 200 µg/mL ampicillin at 37°C while shaking at 200 rpm overnight. Cells were pelleted by centrifugation at 6000 ***g*** for 15 min at 4°C. Plasmid DNA was purified using the Qiagen plasmid Maxiprep kit according to the manufacturer's instructions.

2.2.3 Measurement of DNA and RNA concentration

DNA and RNA concentrations were measured using NanoDrop as per manufacturer's instructions. RNA and DNA absorb at 260 nM. Absorbance was also measured at 280 nM because calculation of 260/280 ratio allows estimation of purity. Ratios of greater than 1.8 are accepted as pure. Lower ratios may indicate the presence of phenol, protein or other contaminants.

2.2.4 DNA mutagenesis

Site-directed mutagenesis was performed using QuikChange kit (Stratagene) and KOD polymerase (Novagen). Mutations were verified by sequencing.

2.2.5 DNA sequencing

Sequencing was performed by DNA Sequencing and Services (www.dnaseq.co.uk) using Applied Biosystems Big-Dye v. 3.1 chemistry on an Applied Biosystems model 3730 automated capillary DNA sequencer.

2.2.6 Cell culture

All procedures were carried out in aseptic conditions meeting biological safety category 2 regulations. Cells were maintained at 37°C in a 5% CO_2 water saturated incubator. For the passaging of cells, cells were washed with PBS and then incubated with Trypsin/EDTA to

detach the cells. Detached cells were resuspended in cell culture medium and split at a 1:2 – 1:20 ratios for continued culture. All breast cancer cell lines were cultured in RPMI-1640 and human embryonic kidney 293 (HEK293), HeLa and MEF cells in Dulbecco's modified eagle medium (DMEM). All cell lines were grown in the presence of 10% (v/v) foetal bovine serum (FBS), 2 mM L-glutamine, 100 U/mL penicillin and 0.1 mg/mL streptomycin. For primary MEF culture medium was additionally also supplemented with 1x non-essential amino acids and 1 mM sodium pyruvate.

2.2.7 Freezing / thawing cells

Detached cells were centrifuges at 1000 rpm for 5 min and resuspended in growth medium supplemented with 10% DMSO. 1 mL aliquots were stored in cryovials at -80°C prior to long-term storage in liquid nitrogen. Cells were thawed in a 37°C water bath, resuspended in growth medium and allowed to adhere overnight prior to medium change.

2.2.8 Transfection of cells using polyethylenimine (PEI)

Cells were transiently transfected using the polyethylenimine (PEI) method (Durocher et al., 2002). 1 mg/mL PEI stock was prepared in 20 mM Hepes (pH 7). For transfection of cells grown on 10 cm dishes, 5 µg of DNA was mixed with 20 µL 1mg/mL PEI and 1 mL serum-free DMEM and left for 15 min at room temperature before being added to cells. Cells were harvested 36 hrs post transfection.

2.2.9 Treatment of cells with growth factors, hormones or inhibitors

In IGF1 stimulation experiments cells were deprived of serum for 16 hrs to induce basal conditions prior to stimulation of the PI3K pathway with 50 ng/mL IGF1 for 30 min. Where indicated a 30 min incubation of cells with inhibitors preceded the addition of IGF1. 50 µg/mL stock of IGF1 was prepared in 20 mM citrate pH 3. For the induction of SGK1, cells were treated with 0.2 µM dexamethasone for 2.5 hrs. Dexamethasone was dissolved in ethanol and diluted in DMEM to prepare 1 mM stock. Inhibitors, along with the equivalent volume of DMSO as a control, were added to the cell culture medium and incubated at 37°C and 5% CO_2 for the times indicated in the figure legends. For chronic inhibitor treatments growth medium was changed to fresh inhibitor or DMSO containing medium approximately every three days. Where cells subjected to chronic treatments needed to be trypsinised and re-seeded, the compounds were added directly to the cell suspension at the time of plating.

2.2.10 RNA interference by small hairpin RNAs (shRNA)

To knockdown the expression of SGK1 and SGK3, the MISSION™ shRNA system obtained from Sigma-Aldrich was utilised. All shRNAs used were in lentiviral pLKO1-puro vector. Sequences of the shRNAs used are shown in Table 2.5. Scrambled shRNA cloned into the same pLK0.1 vector was used as a negative control. To generate lentiviral particles, HEK293T cells grown on 10 cm dishes were transfected with 3 µg of the shRNA-encoding plasmid (pLK0.1), 3 µg of pCMV delta R8.2 (packaging plasmid, Addgene) and 3 µg of pCMV-VSV-G (envelope plasmid, Addgene) using 36 µL PEI. 72 hours post-transfection

virus-containing medium was collected and filtered with a 0.45 µm filter. 2 mL of viral supernatant was used to infect cells cultured in 6-well plates with 8 µg/mL polybrene. After 24 hours, the virus-containing medium was replaced with fresh medium and after next 24 hours cells were seeded for experiments. Protein knockdown was assayed by immunoblotting at 72 hours post infection. No puromycin selection was used as in initial optimisation experiments infection efficiency was found to be near 100%.

shRNA	TRC number	Sequence
SGK1 A	TRCN0000040175	CCGGCGGAATGTTCTGTTGAAGAATCTCGAGATTCTTCAACAGAACATTC CGTTTTTG
SGK1 B	TRCN0000040177	CCGGCATGTCTTCTTCTCCTTAATTCTCGAGAATTAAGGAGAAGAAGACA TGTTTTTG
SGK1 C	TRCN0000010432	CCGGCAATTCTCATCGCTTTCATGACTCGAGTCATGAAAGCGATGAGAAT TGTTTTTG
SGK1 D	TRCN0000196562	CCGGGCAATCTTATTGCACACTGTTCTCGAGAACAGTGTGCAATAAGATT GCTTTTTTG
SGK1 E	TRCN0000194957	CCGGCTGGAAGCTTAGCAATCTTATCTCGAGATAAGATTGCTAAGCTTCC AGTTTTTTG
SGK3 A	TRCN0000001517	CCGGGCGAGACCCTAGTTAAGAGAACTCGAGTTCTCTTAACTAGGGTCTC GCTTTTT
SGK3 B	TRCN0000001518	CCGGGCAGGACTAAACGAATTCATTCTCGAGAATGAATTCGTTTAGTCCT GCTTTTT
SGK3 C	TRCN0000001519	CCGGGAACGTAATGTGCTCTTGAAACTCGAGTTTCAAGAGCACATTACGT TCTTTTT
SGK3 D	TRCN0000001520	CCGGGCATTCGTTGGTTTCTCTTATCTCGAGATAAGAGAAACCAACGAAT GCTTTTT
SGK3 E	TRCN0000001521	CCGGGCCGAGATGTTGCTGAAATGTCTCGAGACATTTCAGCAACATCTCG GCTTTTT
scrambled		CCTAAGGTTAAGTCGCCCTCGCTCTAGCGAGGGCGACTTAACCTTAGG

Table 2.5 shRNA sequences

2.2.11 Transduction with pBABE constructs for stable over-expression

To generate retroviral particles HEK293T cells grown on 10 cm dishes were transfected with 6 µg of pBABE construct, 3.8 µg pCMV-Gag-Pol (packaging plasmid, Addgene) and 2.2 µg pCMV-VSVG (envelope plasmid, Addgene) using 36 µL Lipofectamine 2000 according to

manufacturer's instructions. 72 hours post-transfection virus-containing medium was collected and filtered with a 0.45 μm filter. 2 mL of viral supernatant was used to infect cells cultured in 6-well plates with 8 μg/mL polybrene. After 24 hours, the virus-containing medium was replaced with fresh medium and after next 24 hours transduced cells were selected in the presence of 2 μg/mL puromycin.

2.2.12 Rescue of shRNA mediated knockdown

For rescue experiments cells were retrovirally transduced to stably express wild type or kinase inactive SGK constructs. For rescue of SGK1 knockdown wild-type and catalytically inactive (K127A) SGK1 lacking the N-terminal 1–60 amino acids (ΔN-SGK1) were subcloned into pBABE-puro-HA retroviral vector. ΔN-SGK1 lacks an N-terminal degradation motif that targets SGK1 for proteasomal degradation and allows for higher levels of SGK1 over-expression (Bogusz et al., 2006). For rescue of SGK1 knockdown no silent mutations were introduced into the constructs as one of the shRNAs (SGK1 shRNA #D) targeted the 3' untranslated region (UTR) of the SGK1 gene. Following selection and western blot confirmation of kinase over-expression, cells were infected with either SGK1 shRNA #D or scrambled shRNA. For rescue of SGK3 knockdown three silent mutations (A1449C, C1452T and T1455C, residue numbers correspond to nucleotide numbers in the construct sequence) that alter the nucleotide sequence but not the amino acid sequence of the expressed protein were introduced into full length wild-type and catalytically inactive (K191A) SGK3 in order to create SGK3 shRNA #D resistant constructs. SGK3 shRNA #D

resistant SGK3 constructs were subcloned pBABE-puro-HA retroviral vector and rescue experiments were performed as described above for SGK1.

2.2.13 Cell growth assays

Cells (3,000-4,000 / well) were seeded into the inner 60 wells of 96-well plates and allowed to attach overnight. For inhibitor treatments, cells were treated in triplicates with increasing concentrations (0.01, 0.03, 0.1, 0.3, 1, 3, 10 μM) of inhibitors diluted in DMSO. 72 or 96 hours later cell viability was determined using CellTiter 96® Non-Radioactive Cell Proliferation Assay (MTS), according to manufacturer's instructions. Results were plotted with a best-fit sigmoidal variable slope dose response curve and GI_{50} values were calculated using GraphPad Prism 5.0.

The capacity for proliferation following shRNA mediated knockdown of SGK1 was determined by seeding 2,000 cells / well into the inner 60 wells of 96-well plates 48 hours post transduction with lentiviral shRNAs. MTS assay was then performed 24, 48, 72, 96, 120 and 144 hours post seeding. Results are presented as fold change in absorbance over the five-day period relative to the assay start-point (24 hours post seeding or day 0).

MTS assay is a colorimetric assay for the determination of numbers of viable cells. The reagent contains a stable solution of tetrazolium compound [3-(4,5-dimethylthiazol-2-yl)-5-(3-carboxymethoxyphenyl)-2-(4-sulfophenyl)-2H-tetrazolium, inner salt; MTS] and an electron-coupling reagent (phenazine ethosulfate; PES). Metabolically active, viable cells reduce the MTS tetrazolium compound into a soluble and colored formazan product that

absorbs at 490 nm. The MTS assay is an improved version of the older MTT assay that also utilises the conversion of a tetrazolium compound into a formazan (Mosmann, 1983).

2.2.14 Cell invasion assays

The ability of cells to invade was tested in a growth-factor-reduced Matrigel™ invasion chamber according to manufacturer's instructions. Briefly, cells were serum-deprived for 2 hours, detached with enzyme-free cell-dissociation buffer and 2.5 x 10^5 cells suspended in RPMI-1640 containing 1% (w/v) BSA were added to the upper chambers and chemoattractant (RPMI-1640 containing 10% (v/v) FBS) was added to the lower wells. The chambers were kept at 37°C in 5% CO_2 for 20 hours. Cells that did not invade were removed from the upper face of the filters and cells that had migrated to the lower face of the filters were fixed and stained with Reastain Quick-Diff kit according to manufacturer's instructions and images (×10) were captured.

The growth-factor-reduced Matrigel™ invasion chambers contain polyethylene terephthalate (PET) membrane with 8 micron pores and a layer of growth factor reduced Matrigel Matrix. Matrigel is a solubilized tissue basement membrane matrix containing laminin, collagen type IV, heparan sulfate proteoglycan, entactin and growth factors (Taub et al., 1990). Reduced growth factor Matrigel contains reduced amounts of growth factors that may influence the invasive properties of cells (Vukicevic et al., 1992). The Matrigel layer occludes the 8 micron pores of the membrane thereby blocking non-invasive cells from migrating through the membrane. Cells that invade through the Matrigel layer and

the pores in response to the growth factor containing chemoattractant present beneath the membrane are considered to be invasive in this *in vitro* setting.

2.2.15 Cell lysis

Cells were rinsed with PBS and lysed on ice using lysis buffer. Lysates were snap-frozen in liquid nitrogen and stored at -80°C. Lysates were clarified by centrifugation at 18,000 ***g*** for 15 min at 4°C and the supernatants were used for experiments.

2.2.16 Quantification of protein concentration with Bradford assay

The protein concentration of lysates was estimated using the Bradford assay (Bradford, 1976). Binding of coomassie dye to protein in an acidic medium shifts the absorption maximum from 465 to 595 nm. A standard curve was generated by plotting absorbance against BSA standards. Lysate samples diluted in water were assayed in triplicates using 200 µL of Bradford reagent per sample and absorbance at 595 nM was measured. Sample concentrations were calculated using the standard curve.

2.2.17 Purification of GST-tagged proteins from HEK293 cells

24 hours post-transfection, HEK293 cells that had been transfected with GST-Akt1, GST-ΔN-SGK1 or GST-SGK3 were serum starved for 16 hrs. Cells were treated with 1 µM PI-103 for 30 min (for inactive and dephosphorylated Akt1 or SGK1 for use as substrates in mTORC2 kinase assays) or stimulated with 50 ng/mL IGF1 for 30min (for active Akt1, SGK1

or SGK3) and harvested in Tris-Triton lysis buffer. For the purification of dephosphorylated Akt1 and SGK1 phosphatase inhibitors were omitted from the lysis buffer. 20 µl of glutathione-sepharose beads were used per 5 mg of lysate to bind the GST-tagged protein at 4°C for 2 hrs on a rotating platform. The beads were washed twice with lysis buffer containing 0.5 M NaCl, twice in normal lysis buffer and twice in Buffer A. GST-tagged proteins were eluted from the resin by resuspension in an equal amount of Buffer A containing 0.27 M sucrose and 20 mM glutathione (pH 7.5) for 10 minutes at room temperature. Supernatants were filtered through a 0.22 µm Spin-X column and aliquots snap-frozen and stored at -80°C. Concentration of purified proteins was estimated by Bradford assay and their purity was estimated by SDS-PAGE.

2.2.18 Covalent coupling of antibodies

For the coupling of antibodies, protein G-sepharose and protein A-agarose beads were used. Protein G, isolated from Group G *Streptococci*, binds to the F_c region of IgG-class antibodies and has a high affinity for antibodies generated in many species, including sheep. Protein A, which originates from *Staphylococcus aureus*, also binds F_c region of IgG-class antibodies, particularly those generated in rabbit. Covalent coupling of antibodies was carried out using dimethyl pimelimidate (DMP), a homo-bifunctional imidoester that reacts with primary amine groups, as the cross-linker. Protein A- or G-beads were washed in PBS followed by incubation of 1 µL or resin per 1 µg of antibody for 1-2 hrs at 4°C. Beads were then washed twice with PBS followed by three washes with 0.1 M sodium tetraborate pH 9.3. Beads were then mixed twice for 30 min in sodium tetraborate

containing 20 mM DMP at room temperature followed by four washes with 50 mM glycine pH 2.5 to remove any non-covalently coupled antibody and two washes with 0.2 M Tris-HCl pH 8. Beads were mixed with 0.2 M Tris-HCl pH 8 at 4°C overnight to quench any residual DMP, before storage in PBS at 4°C.

2.2.19 Immunoprecipitation of proteins

3 µL of covalently coupled antibody or for larger sample quantities 1 µL of antibody beads / 1 mg of lysate was mixed with the lysate for 1-4 hrs at 4°C on a rotating wheel. Beads were then washes twice with lysis buffer containing 0.5 M NaCl and twice with lysis buffer containing 0.15 M NaCl followed by 2 washes with buffer A. Reducing agent was omitted from the washes. To elute immunoprecipitates, beads were resuspended in 2x SDS sample buffer (or 2x NuPAGE LDS sample buffer for mass spectrometry) lacking reducing agent for 10 min prior to filtering through Spin-X columns to remove the antibody-bound beads. Reducing agent was added to the eluted samples and the samples were heated.

2.2.20 Resolution of protein samples via SDS-PAGE

Sodium dodecyl sulphate polyacrylamide gel electrophoresis (SDS-PAGE) resolves proteins based on their apparent molecular weight. The anionic detergents SDS and lithium dodecyl sulphate (LDS) bind to proteins giving them a net negative charge that is proportional to the molecular mass of the protein. Consequently, the speed of migration

of proteins through a PAGE matrix is a linear function of the logarithm of their molecular weight.

Resolving gels contained 375 mM Tris-HCl (pH 8.6), 0.1% SDS and 8-10% acrylamide. TEMED and ammonium persulphate (APS) were used to initiate polymerisation. Stacking gels contained 125 mM Tris HCl pH 6.8, 0.1% SDS, 4% acrylamide, TEMED and APS.

Samples were prepared either in 1x LDS sample buffer and 1x sample reducing agent (for use with pre-cast NuPAGE 4-12% Bis-Tris gels) or in 1x SDS sample buffer (for use with homemade gels) and heated at heated at 90°C for 5 min. 5-20 µg of lysate or 10-30 µL of immunoprecipitates were loaded per lane along with protein standards. Electrophoresis was carried out at 80 V until the protein markers started to resolve and then the voltage was increased to 160 – 180 V until the dye front reached the end of the resolving gel.

2.2.21 Coomassie staining of polyacrylamide gels

Polyacrylamide gels were stained in Instant Blue staining solution for 1-2 hrs and destained with MilliQ water.

2.2.22 Dessication of polyacrylamide gels and autoradiography

For drying, gels were incubated in 5% glycerol for 10 min and sandwiched between two sheets of pre-wet cellophane. The gel was then dried in a GelAir Dryer for 1.5 hrs. Dried gels were exposed to Hyperfilm MP for 1-24 hrs in an X-Omat autoradiography cassette. Films were developed using a Konica auto-developer.

2.2.23 Transfer of proteins onto nitrocellulose membranes

Gels were sandwiched between nylon sponges, Whatman 3 mm filter papers and nitrocellulose membrane all soaked in transfer buffer. The transfer cell was submerged in transfer buffer and transfer was carried out at at 750 mA for 1 hour.

2.2.24 Immunoblotting

After transfer, membranes were stained with Ponceau S and destained in distilled water in order to visualise the transferred proteins. Non-specific binding of antibodies was prevented by incubating the membranes with 5% (w/v) skimmed milk in TBST for 1 hour at room temperature. Membranes were then incubated with primary antibodies diluted in either 5% (w/v) skimmed milk or BSA in TBST at 4°C for 16 hrs. Membranes were next washed three times for 10 minutes with TBST. Horseradish peroxidase (HRP)-conjugated secondary antibodies diluted at 1:2500 in 5% (w/v) skimmed milk in TBST were incubated with the membranes for 1 hr at room temperature and the membranes were washed three more times with TBST. Membranes were incubated with the enhanced chemiluminescence (ECL) substrate and exposed to X-ray films for various lengths of time. Films were developed using a Konica automatic developer. Where indicated, signals were visualised using the Odyssey^{TM} Infrared Imaging System instead of ECL. The procedure was the same but the secondary antibodies were labelled with either IRD800 or Alexa680 dyes and the signal captured and quantified with an Odyssey Infrared Imaging System.

2.2.25 Processing protein bands for analysis by mass spectrometry

To minimise contamination with proteins such as keratin, samples were handled in a laminar flow hood. Gels were cut into small pieces. The pieces were sequentially washed for 10 min in 0.5 mL water, 50% (v/v) acetonitrile, 0.1 M NH_4HCO_3 and 50% (v/v) acetonitrile/50 mM NH_4HCO_3. The last step was repeated until the pieces were colourless. Colourless gel pieces were incubated with 0.3 mL acetonitrile for 15 min at room temperature followed by drying in a Speed-Vac at 45°C. Dried gel pieces were incubated with 30 µL 25 mM Triethylammonium bicarbonate buffer containing 5 µg/mL trypsin at 30°C for 16 hrs on a shaking platform. Next an equal volume of acetonitrile was added and the peptides obtained from the digestion were extracted for 15 min on a shaking platform. The supernatant was dried in a clean tube at 45°C using Speed-Vac. To extract further peptides, 100 µL of 50% (v/v) acetonitrile supplemented with 2.5% (v/v) formic acid was added to the gel pieces and incubated for 15 min at room temperature on a shaking platform. The supernatant was combined with the first dried peptide extract and dried using Speed-Vac. Dried peptides were stored at -20°C.

2.2.26 Mass spectrometry

Liquid chromatography–mass spectrometry (LC-MS) was performed by Dr. D. Campbell, and Mr. R. Gourlay. Tryptic peptides were subjected to LC-MS/MS using a Proxeon EasynLC chromatography system coupled with a Thermo LTQ-Orbitrap Classic mass spectrometer. Results were searched against the SwissProt or IPI mouse databases using

Mascot (www.matrixscience.com). Data analysis was performed using Online MassSpec Data Analysis Tool (http://www.proteinguru.com/MassSpec/OLMAT).

2.2.27 mTORC2 kinase assays

Lysates were generated in Hepes-CHAPS lysis buffer. 1-4 mg of lysate was pre-cleared by incubation with 5 µL pre-immune IgG. This was followed by incubation with 5 µg of Sin1 antibody or pre-immune IgG at 4°C for 1.5 hrs. All antibodies were covalently coupled to protein G-sepharose. Immunoprecipitates were washed four times with Hepes-CHAPS lysis buffer and twice with Hepes kinase buffer. Assays were carried out in a final volume of 40 µL Hepes kinase buffer containing 1 µg of substrate (GST-Akt1 or GST-ΔN-SGK1) and kinase reactions were initiated upon addition of 0.1 mM ATP and 10 mM Magnesium acetate. Reactions were carried out for 30 min at 30°C and terminated by SDS sample buffer. Samples were heated to 70°C for 5 min, passed through a Spin-X column and subjected to immunoblot analysis.

2.2.28 Kinase assays employing a protein substrate

Indicated amounts of kinases were incubated with 1 µg of purified protein substrate in the presence of 0.1 mM [γ^{32}P]-ATP and 10 mM Magnesium acetate in Buffer A at 30°C for times indicated in the figure legends. Reactions were terminated with SDS sample buffer.

2.2.29 Kinase assays employing a peptide substrate

In vitro kinase activities were measured using Cerenkov counting of incorporation of radioactive ^{32}P from [$\gamma^{32}P$]-labelled ATP into a peptide substrate. The following conditions were used: 10 mM Magnesium acetate, 0.1 mM [$\gamma^{32}P$]- ATP, 30 μM CROSStide peptide (GRPRTSSFAEG) in Buffer A in a final volume of 50 μL. Control reactions contained a kinase inactive mutant or an IgG immunoprecipitate. Reactions were incubated at 30°C for 30 min and terminated by adding 10 μL of 0.5M EDTA to the reactions. 40 μL of the reactions were spotted onto P81 phosphocellulose paper. Papers were washed five times in 75 mM orthophosphoric acid to remove any radioactivity not associated with the phosphorylated peptide. Papers were then incubated in acetone for 3 min and air-dried. Cerenkov counting of the papers was done on a scintillation counter. Kinase activity was expressed as specific activity (units of activity per mg of protein). One unit of protein kinase activity is the amount of enzyme that catalyses the incorporation of 1 nmole phosphate into the substrate in 1 min.

For IC_{50} determination active GST-ΔN-SGK1 and GST-SGK3 were purified from HEK293 cells. 1 μg of the kinase was assayed for 30 min at 30°C on 96 well plates in the presence or absence of inhibitor (0.1 nM - 30 μM) in triplicates in a 50 μL assay mixture. Reactions were terminated and the reaction products were subjected to Cerenkov counting. Results were plotted with a best-fit sigmoidal variable slope dose response curve and IC_{50} values were calculated using GraphPad Prism 5.0. The data were presented as % activity remaining in comparison to DMSO control.

2.2.30 RNA isolation, cDNA preparation and analysis of transcripts by quantitative reverse transcription-PCR (qRT-PCR)

Total RNA was isolated from cells using the RNeasy kit (Qiagen) according to manufacturer's instructions. cDNA was prepared from 1 μg of RNA using i-Script Kit (BioRad) according to manufacturer's instructions. qRT-PCR was performed in 96-well plate format using iQ5™ Real Time PCR detection system (BioRad). Each 20 μL reaction included 1% cDNA, 0.5 μM primers and 10 μL SsoFast™ EvaGreen® Supermix (BioRad). The supermix contained a heat-activated Sso7d-fusion polymerase, EvaGreen® fluorescent dye that is similar to SYBER®green, dNTPs and $MgCl_2$. The plate was subjected to the following thermal cycle: 95°C for 3 min, 40 cycles of 95°C for 20 sec and 57°C for 45 sec; then 95°C for 1 min, 55°C for 1 min followed by 80 cycles at 0.5°C increments for 10 sec up to 95°C in order to determine the melt curve. The melting curve allows the detection of non-specific products and primer dimers. A single melting peak indicates, but does not prove, that a single product is being produced. The primer sequences are shown in Table 2.6. Two independent samples were assayed with each sample assayed in duplicate. Data were normalised to an internal standard gene 18S. For the comparison of SGK isoform levels across a panel of breast cancer cell lines data were presented as relative levels in comparison to the SGK isoform mRNA levels in HEK293 cells. For all other experiments data were presented as relative levels in comparison to control treatment. The relative gene expression levels in comparison to control conditions were calculated according to the $2^{-\Delta\Delta CT}$ method (Livak and Schmittgen, 2001).

Primer name	Sequence (5' -> 3')
Human SGK1 sense	CATAGGAGTTATTGGCAAT
Human SGK1 antisense	CTTCCATCTCACTAACCA
Human SGK2 sense	CTTTGTTATTAGGGATAGTCA
Human SGK2 antisense	GAAGTGAATGGTTTGTCT
Human SGK3 sense	ATATTCTCTTGGCAGGAA
Human SGK3 antisense	AATGGCTCATTAAATCAGTT
Human 18S sense	CTAGAATTACCACAGTTATCC
Human 18S antisense	CTAGAATTACCACAGTTATCC

Table 2.6 qRT-PCR primer sequences

2.2.31 Injection of mice with IGF1

IGF1 injections were carried out by Dr K. Sakamoto and Dr L. Pearce. Mice were starved for 3 hrs before being terminally anaesthetised using pentobarbital. This was followed by an intravenous injection through the inferior vena cava of either saline or 0.5 μg per gram of body weight of IGF1. Tissues were excised after 5 min.

2.2.32 Lysis of mouse tissues

Mouse tissues were rapidly excised, frozen in liquid nitrogen and stored at -80°C until use. Tissues were weighed and homogenised in a 10-fold excess of ice-cold Tris-CHAPS or Hepes-CHAPS lysis buffer using a polytron. Lysates were clarified by centrifugation at 3,000 rpm for 15 min at 4°C and supernatants then further centrifuged at 18,000 ***g*** for 20 min at 4°C. Lysates were aliquoted, snap frozen and stored at -80°C.

2.2.33 Kidney membrane preparation

Mouse kidneys were homogenized in 10-fold excess of Tris lysis buffer lacking detergent with a Polytron. Nuclei and debris were pelleted by centrifugation at 1,500 ***g*** for 5 min. The procedure was repeated at 3,000 ***g*** for 10 min and the low-speed supernatants were next centrifuged at 100,000 ***g*** for 1 h. The pellet was washed with 1 volume of lysis buffer and centrifuged again at 100,000 ***g*** for 15 min to remove any remaining cytosolic particles. The pellet was then resuspended in lysis buffer supplemented with 1% (v/v) Nonidet P40 and centrifuged at 16,500 ***g*** for 10 min. Protein content of the membrane and cytosolic fractions was quantified and the preparations were resuspended in SDS sample buffer.

2.2.34 Mouse embryonic fibroblast (MEF) generation

Female mice at 13 days gestation were culled, the uterine horn removed and embryos placed in PBS. Embryo heads were used to confirm the genotype by PCR (performed by Mrs G. Fraser). After removing internal organs embryos were chopped and incubated with trypsin at 37°C, 5% CO_2 for 5-10 min. Cells were centrifuged at 800 rpm for 5 min and resuspended in primary MEF media (Section 2.2.6). After 24 hrs, cells were trypsinised, resuspended in primary MEF media and filtered. These cells were designated as passage 1 (P1). MEFs were immortalised by continues passaging and were considered to be immortalised once the cells were proliferating at a rate similar to primary MEFs.

2.2.35 Statistical analysis

Statistical significance was assessed by one-way analysis of variance (ANOVA) followed by Tukey's multiple comparison tests using GraphPad Prism 5.0. All the experiments presented in this thesis were performed at least two or three times with similar results obtained on each occasion. Error bars indicate the standard deviation (SD) or standard error of the mean (SEM), as indicated in figure legends.

2.2.36 Bioinformatics

Sequence alignments were undertaken using Clustal Omega (Sievers et al., 2011) and the alignments were annotated using Jalview 2 (Waterhouse et al., 2009).

3. Optimisation of the detection of endogenous SGK and study of the role of Protor in the regulation of SGK

3.1. Introduction

The major initial aim of this PhD project was to develop and characterise novel antibodies that would enable reliable and specific detection of endogenous SGK. Furthermore, when I started this project, there were no well-characterised antibodies available to monitor T-loop phosphorylation of endogenous SGKs.

Previous work carried out in our laboratory had identified Protor-1 and Protor-2 as novel constitutive components of mTORC2 (Pearce et al., 2007). Additionally, two other groups independently identified both Protor-1 and Protor-2 as mTORC2 components (Thedieck et al., 2007; Woo et al., 2007). As cell-based experiments had failed to provide any clues about the function of these proteins, Protor-1, Protor-2 and Protor-1/2 deficient mice were generated in the laboratory. Work carried out by Dr Laura Pearce indicated that mice lacking Protor-1 have a defect in the activation of SGK in kidney. In the kidney, but not in other tissues studied, loss of Protor-1 resulted in reduced phosphorylation of SGK hydrophobic motif and reduced phosphorylation of the SGK substrate NDRG1. Analysis of Protor-2 knockout mice carried out by Dr L. Pearce failed to yield any observable differences between the wild type and Protor-2 knockout animals indicating that the two Protor isoforms may have different functions. To ensure that no compensation occurred between the two Protor isoforms, I studied Protor-1/2 double knockout mice with a particular focus on the activation of SGK.

In this chapter I first describe the validation of antibody tools that allow reliable detection of endogenous SGKs. Using the improved methods to study endogenous SGK I (1) validate the compromised activation of SGK in the kidney using Protor-$1^{-/-}$Protor-$2^{-/-}$ double knockout mice as a model and (2) show that Protor is not universally required for mTORC2 mediated activation of SGK. To answer this question I describe the generation of mouse embryonic fibroblasts (MEF) lacking both Protor isoforms.

3.2. Results

3.2.1. Characterisation of SGK antibodies

In order to have state-of-the-art tools to study SGKs, antibodies designed against SGK1, SGK2 and SGK3 were raised by the DSTT (Figure 3.1). These antibodies were characterised for their ability to recognise over-expressed HA-tagged SGK isoforms by immunoblotting (Figure 3.2A-C) and to immunoprecipitate HA-SGK isoforms (Figure 3.2D-F). An anti-SGK antibody obtained from Sigma was also characterised (Figure 3.2G). Other commercial antibodies tested (appendix 1) were poorly reactive against over-expressed SGK and no further work was carried out with them (data not shown).

All DSTT antibodies tested recognised and immunoprecipitated the over-expressed isoform that they were raised against. Clear differences between the bleeds were observed in the immunoblot analysis whereas for each antibody all bleeds immunoprecipitated HA-SGKs equally well (Figure 3.2A-F). Antibodies generated against SGK2 and SGK3 (S036D and S037D, respectively) were isoform-specific whereas the anti-

SGK1 antibody (S062D) also recognised SGK2. The best bleeds were chosen for future experiments. Sigma S5188 recognised all recombinant SGK isoforms (Figure 3.2G).

A

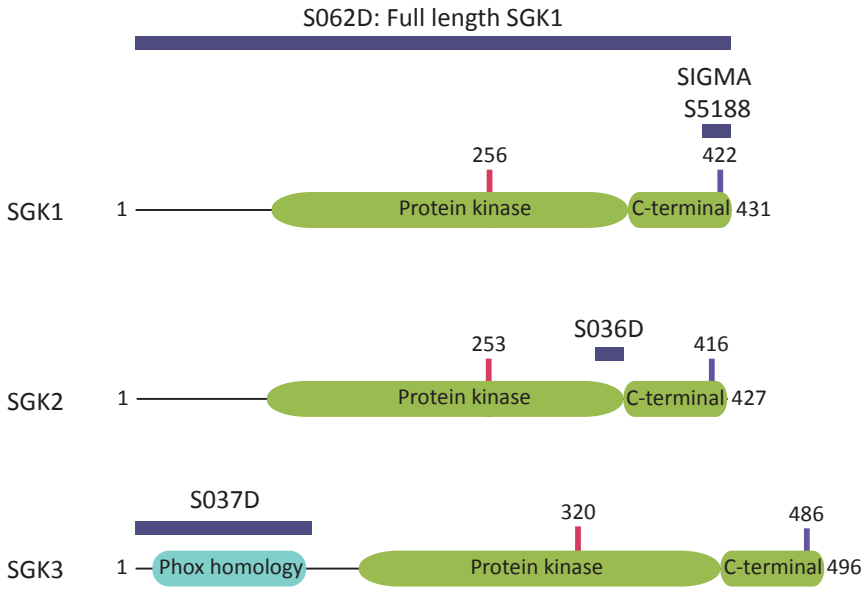

B

Antibody	Source	Species	Immunogen
S062D	DSTT	Sheep	GST-SGK1
S036D	DSTT	Sheep	GST-SGK2 333-346 (KSIGCTPDTVASSS)
S037D	DSTT	Sheep	GST-SGK3 1-130
S5188	Sigma	Rabbit	SGK1 412-431 (KEAAEAFLGFSYAPPTDSFL)

Figure 3.1 Schematic summary of SGK antibodies characterised

(**A**) Schematic representation of SGK isoforms and the regions against which the antibodies characterised were raised. (**B**) Summary of the antibodies.

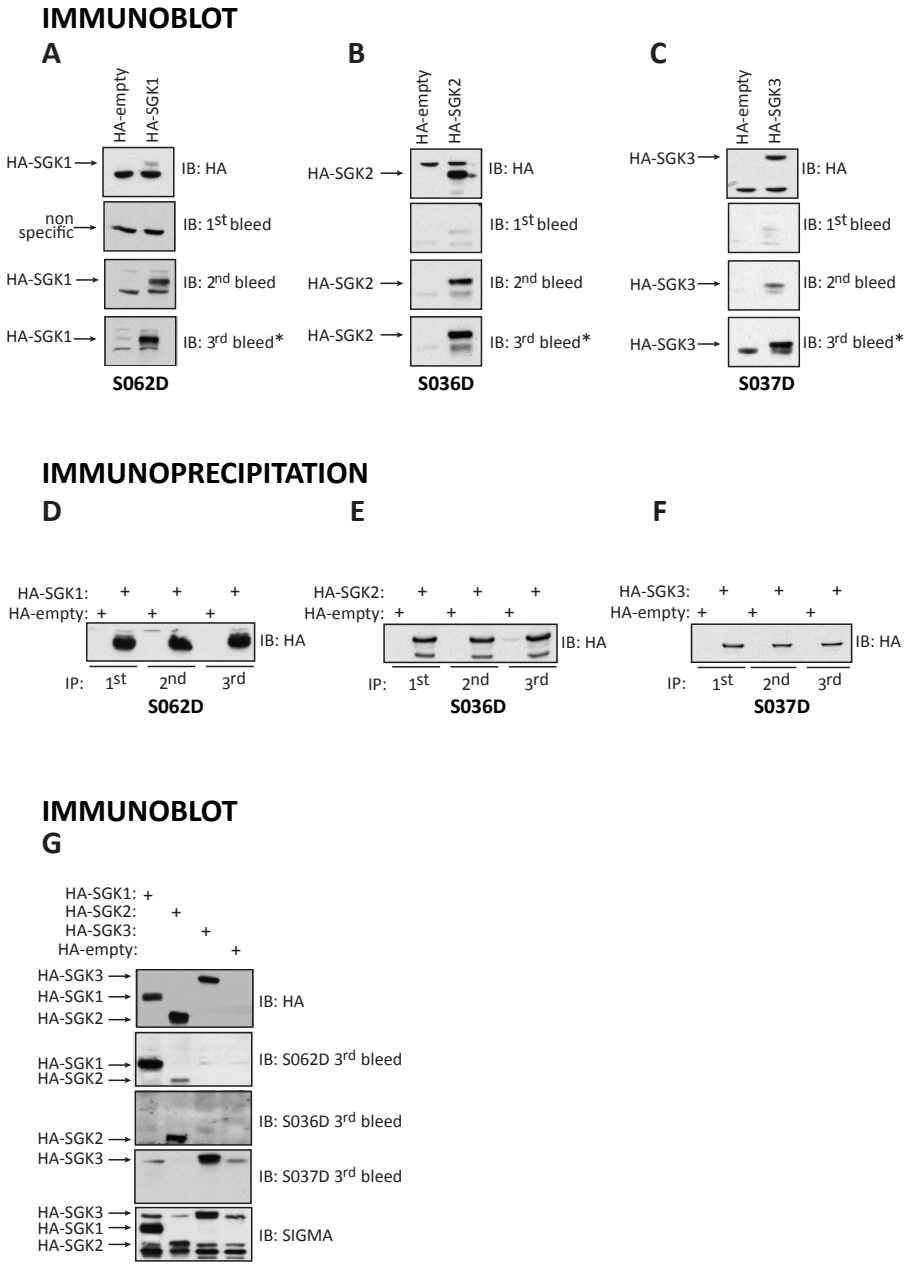

Figure 3.2 Testing of SGK antibodies in over-expression system

(**A**) HEK293 cells were transfected with indicated vectors and 10 μg of lysate was analysed by immunoblotting (IB) with indicated bleeds of S062D SGK1 or anti-HA antibodies. Asterisk indicates the best bleed. (**B**) as in (**A**) except S036D SGK2 antibody was used. (**C**) as in (**A**) except SGK3 S037D antibody was used. (**D**) as in (**A**) except 1 mg of lysate was immunoprecipitated (IP) with indicated bleeds of S062D antibody and the immunoprecipitates were analysed by immunoblotting with anti-HA antibody. (**E**) as in (**D**) except S036D was used for immunoprecipitations. (**F**) as in (**D**) except S037D was used for immunoprecipitations. (**G**) as in (**A**) except 10 μg (5 μg for HA-SGK2) of lysate was subjected to immunoblot analysis with indicated antibodies.

To test the ability of the antibodies to detect endogenous SGKs, a preliminary expression analysis of mouse tissues was undertaken. Endogenous SGK was immunoprecipitated from a range of tissues derived from wild type C57BL/6J mice with the pan-SGK antibody obtained from Sigma and the immunoprecipitates were analysed by immunoblotting with DSTT S062D antibody that based on results presented in Figure 3.2 was expected to recognise at least SGK1 and SGK2. As shown in Figure 3.3, SGK protein was detected in kidney and liver and low levels of a species that migrated higher were detected in spleen and testis. As it was unclear which isoforms were detected, next SGK immunoprecipitates from kidney, liver, spleen and testes extracts were analysed by mass spectrometry. SGK was immunoprecipitated from the four tissues with the Sigma pan-SGK antibody and the results revealed that SGK2 was the most abundant isoform in kidney and liver whereas SGK3 was the most abundant isoform in spleen and testes (Figure 3.4A and Table 3.1). To further test the DSTT SGK antibodies, immunoprecipitations with all three DSTT antibodies were performed from kidney lysates. Whilst all three SGK isoforms were detected, SGK2 was again most efficiently immunoprecipitated (Figure 3.4B, Table 3.1). The endogenous immunoprecipitations also revealed that the Sigma S5188 antibody immunoprecipitated all SGK isoforms, S062D immunoprecipitated SGK2 (based on over-expression experiments S062D would also be expected to immunoprecipitate SGK1 if SGK1 were expressed at sufficiently high levels), S036D immunoprecipitated only SGK2 and S037D immunoprecipitated only SGK3 (Figure 3.4 and Table 3.1).

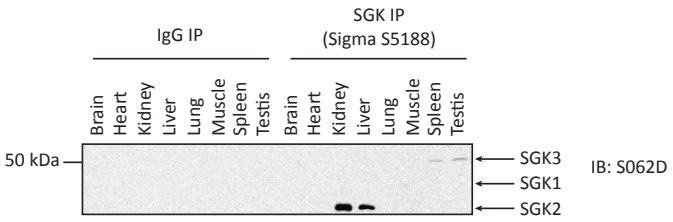

Figure 3.3 Analysis of SGK isoform expression in mouse tissues

SGK was immunoprecipitated (IP) with Sigma S5188 antibody or pre-immune IgG from 1 mg of tissue lysates and analysed by immunoblotting (IB) with S062D antibody. Arrows indicate the approximate sizes at which different isoforms are expected to run.

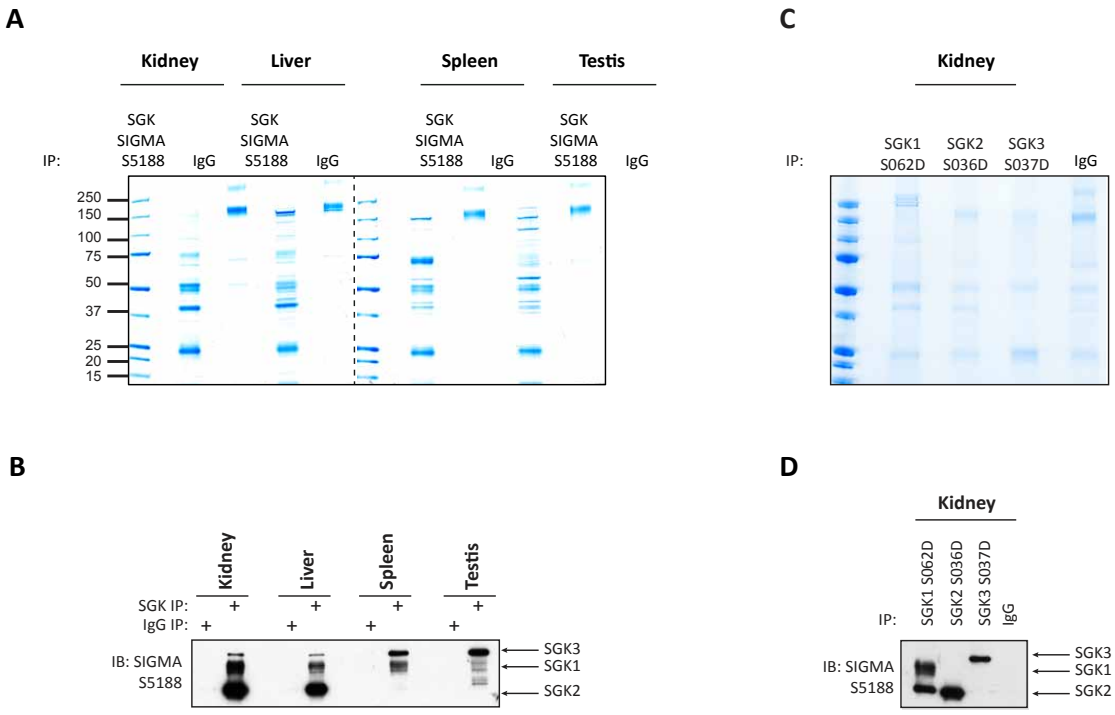

Figure 3.4 Immunoprecipitation of endogenous SGK for analysis by mass spectrometry

(**A**) Endogenous SGK isoforms were immunoprecipitated (IP) with Sigma S5188 antibody from 40 mg of the indicated tissue lysates derived from wild type C57BL/6J mice for in-gel digestion and analysis by mass spectrometry. (**B**) 5% of the immunoprecipitates were analysed by immunoblotting (IB) with Sigma S5188 anti-SGK antibody. (**C**) Endogenous SGK isoforms were immunoprecipitated with the indicated DSTT anti-SGK antibodies from 40 mg of kidney lysate for in-gel digestion and analysis by mass spectrometry. (**D**) As in (**B**). Arrows indicate approximate sizes at which different isoforms are expected to run.

Tissue	Antibody	SGK isoform identified	MASCOT Score	Sequence coverage
Kidney	Sigma S5188	SGK2	2730	61%
Kidney	Sigma S5188	SGK3	1057	51%
Kidney	Sigma S5188	SGK1	103	14%
Kidney	SGK1 S062D	SGK2	249	31 %
Kidney	SGK2 S036D	SGK2	526	41%
Kidney	SGK3 S037D	SGK3	440	31%
Liver	Sigma S5188	SGK2	1172	56%
Liver	Sigma S5188	SGK3	806	48%
Liver	Sigma S5188	SGK1	21	9%
Spleen	Sigma S5188	SGK3	1447	53%
Testis	Sigma S5188	SGK3	2474	57%
Testis	Sigma S5188	SGK1	60	5%

Table 3.1 Summary of endogenous SGK immunoprecipitations analysed by mass spectrometry

Data obtained from the large-scale mass spectrometry analysis indicated that no contaminating kinases were immunoprecipitated with endogenous SGKs under any conditions tested (appendix 2). Consequently the SGK antibodies are suitable for endogenous kinase assays. Results presented in Figure 3.4 and Table 3.1 indicate that SGK2 is the most abundant isoform in whole kidney and liver lysates. To manually confirm that all the SGK2 peptides identified in the mass spectrometry were indeed unique to SGK2, a sequence alignment of mouse SGKs was prepared and the peptides identified were matched onto the sequence alignment. As shown in Figure 3.5, the sequence alignment analysis confirmed that the peptides were indeed unique to SGK2.

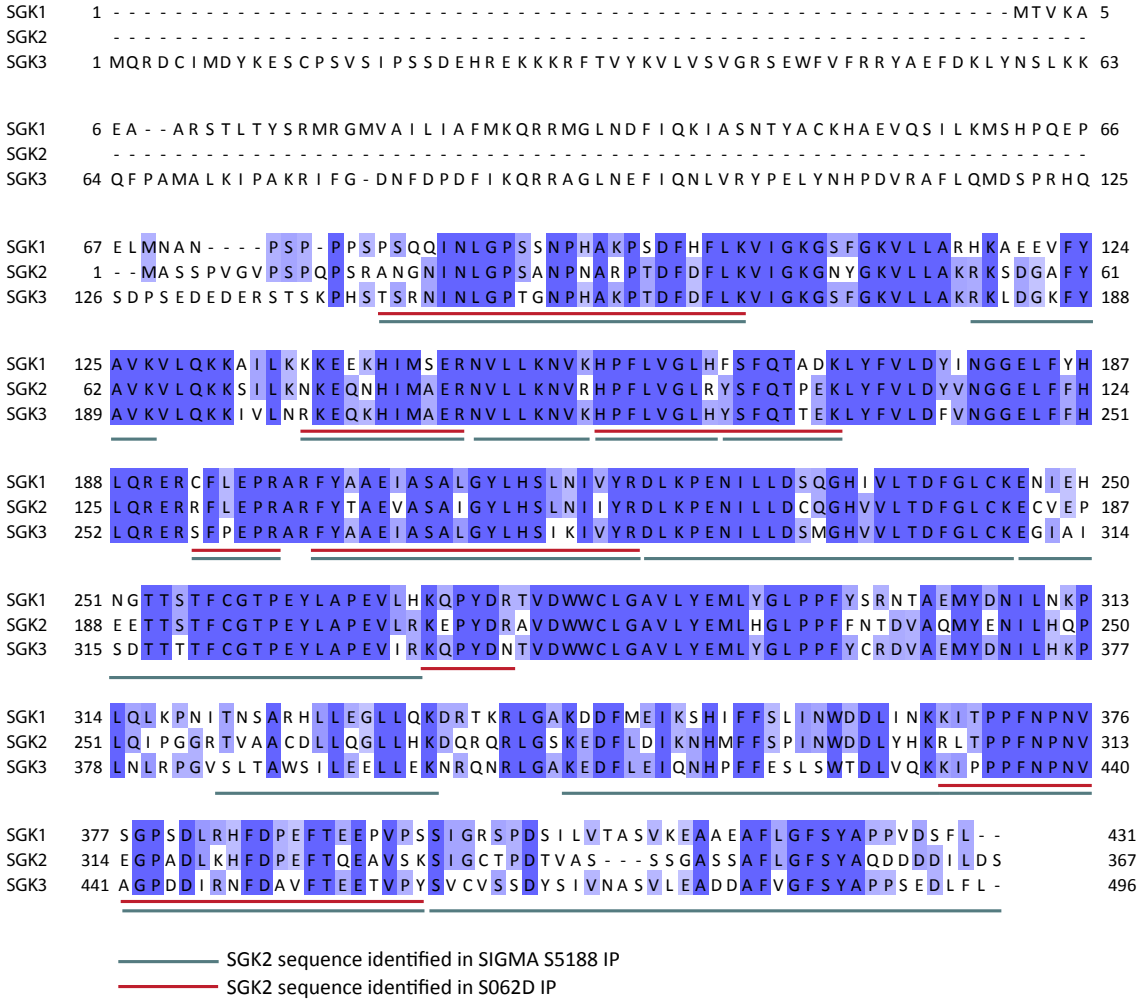

Figure 3.5 Sequence alignment of mouse SGK isoforms

Sequence alignment of mouse SGK1 (Uniprot accession number: Q9WVC6), SGK2 (Q9QZS5) and SGK3 (Q9ERE3) was undertaken using Clustal Omega (Sievers et al., 2011) and the alignment was annotated using Jalview 2 (Waterhouse et al., 2009). SGK2 peptides identified in immunoprecipitations (IP) performed with SIGMA S5188 antibody and DSTT S062D antibody are underlined in blue and red, respectively.

3.2.2. Validation of an SGK phospho-T-loop antibody

As the amino acid sequences encompassing the T-loop of S6K and SGK are very similar (Figure 3.6A), a phospho-specific pan-PDK1 site antibody, which recognises the phosphorylated T-loop of S6K (Collins et al., 2005), was tested for its ability to recognise the phosphorylated T-loop (PDK1 site) of over-expressed SGK1. The pan-PDK1 site

antibody efficiently recognised IGF1 stimulated phosphorylation of GST-ΔN-SGK1 in HEK293 cell lysates (Figure 3.6B). No immunoreactivity was observed when cells were transfected with a construct in which Thr256 was mutated into alanine. Because SGK1 is sequentially phosphorylated, first by mTORC2 at the HM-site and subsequently by PDK1 at the T-loop, mutation of the HM-site Ser422 into alanine would also be expected to inhibit Thr256 phosphorylation (Biondi et al., 2001), and this was indeed observed (Figure 3.6B).

Validation of the pan-PDK1 site antibody allowed characterisation of the effects of GSK2334470, a novel PDK1 inhibitor (Najafov et al., 2011), on T-loop phosphorylation of all SGK isoforms. HEK293 cells were transiently transfected with GST-ΔN-SGK1, GST-SGK2 or GST-SGK3 and the impact of GSK2334470 on IGF1-induced phosphorylation of the T-loop was analysed by immunoblotting (Figure 3.6C). IGF1 induced T-loop and NDRG1 phosphorylation were decreased in response to GSK2334470 in a dose-dependent manner indicating that PDK1 inhibition suppressed activation of all the three SGK isoforms (Figure 3.6C).

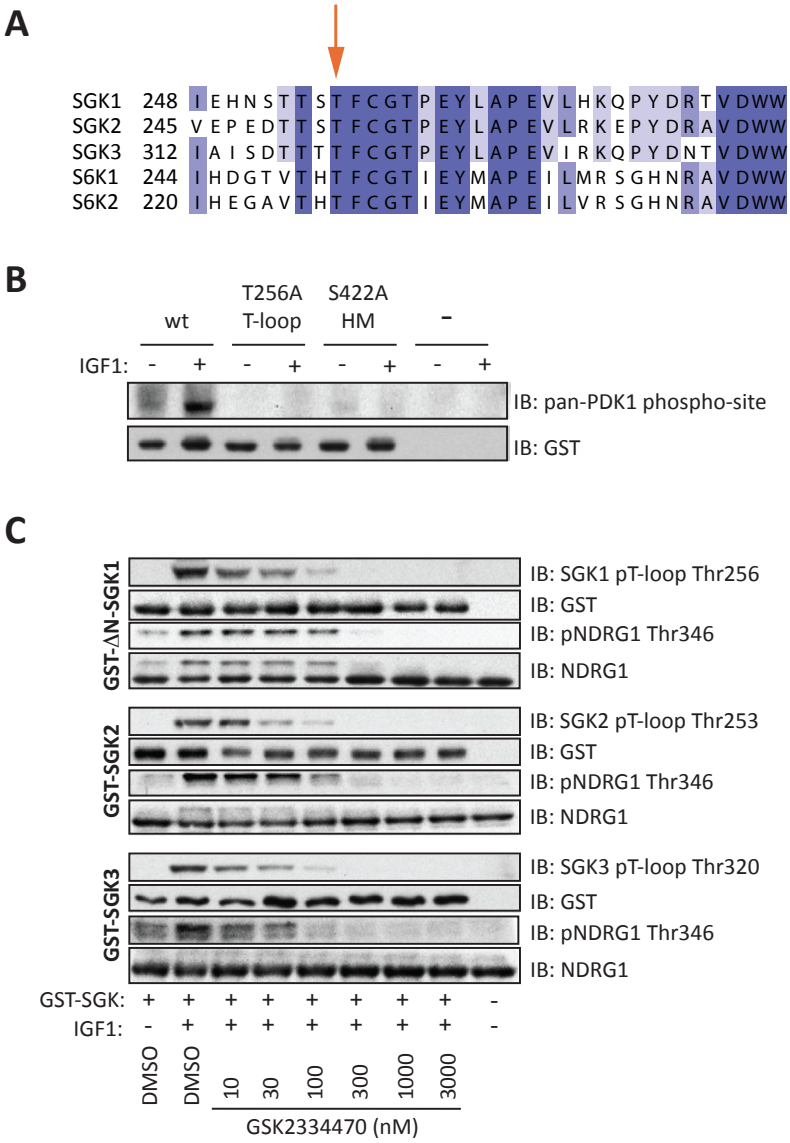

Figure 3.6 Recognition of SGK T-loop phosphorylation

(**A**) Sequences surrounding the T-loop site of human SGK1 (Uniprot accession number: O00141), SGK2 (Q9HBY8), SGK3 (Q96BR1), S6K1 (P23443) and S6K2 (Q9UBS0) were aligned using Clustal Omega (Sievers et al., 2011) and the alignment was annotated using Jalview 2 (Waterhouse et al., 2009). Arrow indicates the T-loop residue that is phosphorylated by PDK1. (**B**) 24 hours post transfection with the indicated constructs HEK293 cells were serum starved for 16 hours, stimulated with 50 ng/ml IGF1 for 30 min, lysed and analysed by immunoblotting (IB) with the indicated antibodies. Residue numbers are for full-length SGK1. (**C**) HEK293 cells were transfected with GST–ΔN-SGK1, GST–SGK2 or GST–SGK3. 24 hours post-transfection, cells were serum-starved overnight and treated with the indicated concentrations of GSK2334470 for 30 min prior to stimulation with 50 ng/mL IGF1 for 30 min. Lysates were analysed by immunoblotting with the other indicated antibodies.

3.2.3. Study of the role of Protor in SGK activation in kidney

Work carried out by Dr L. Pearce, a previous PhD student in the laboratory, suggested that activation of SGK is compromised in kidney in the absence of the mTORC2 component Protor-1. The related AGC kinases Akt, S6K and PKCα were normally activated in both fed IGF1 injected Protor-1 deficient mice. Based on further preliminary work carried out by Dr L. Pearce, loss of the closely related protein Protor-2 did not result in any noticeable defects in the activation of any of the AGC kinases tested (Pearce et al., 2011). With the aid of the development of antibodies that efficiently recognised endogenous SGK isoforms, I undertook further analysis in Protor-$1^{-/-}$Protor-$2^{-/-}$ double knockout mice that were generated in order to ensure that no compensation between the two isoforms took place. Dr L. Pearce generated and maintained the Protor-$1^{-/-}$Protor-$2^{-/-}$ double knockout mice on a pure C57BL/6J background and found that the double-knockout mice were viable, born at the expected Mendelian frequency and did not display any overt phenotype (Pearce et al., 2011).

The phosphorylation state of Akt, its substrate PRAS40, as well as of the reported SGK substrate NDRG1, was examined in kidney, liver and lung tissues obtained from fed wild type and Protor-$1^{-/-}$Protor-$2^{-/-}$mice (Figure 3.7). No significant differences were detected in Akt or PRAS40 phosphorylation between the wild type and double knockout mice in any of the tissues examined (Figure 3.7). Consistent with previous work performed in the laboratory, there was a substantial reduction in the phosphorylation of NDRG1 in the kidney, but not in the liver or lung tissues of Protor double knockout mice (Figure 3.7).

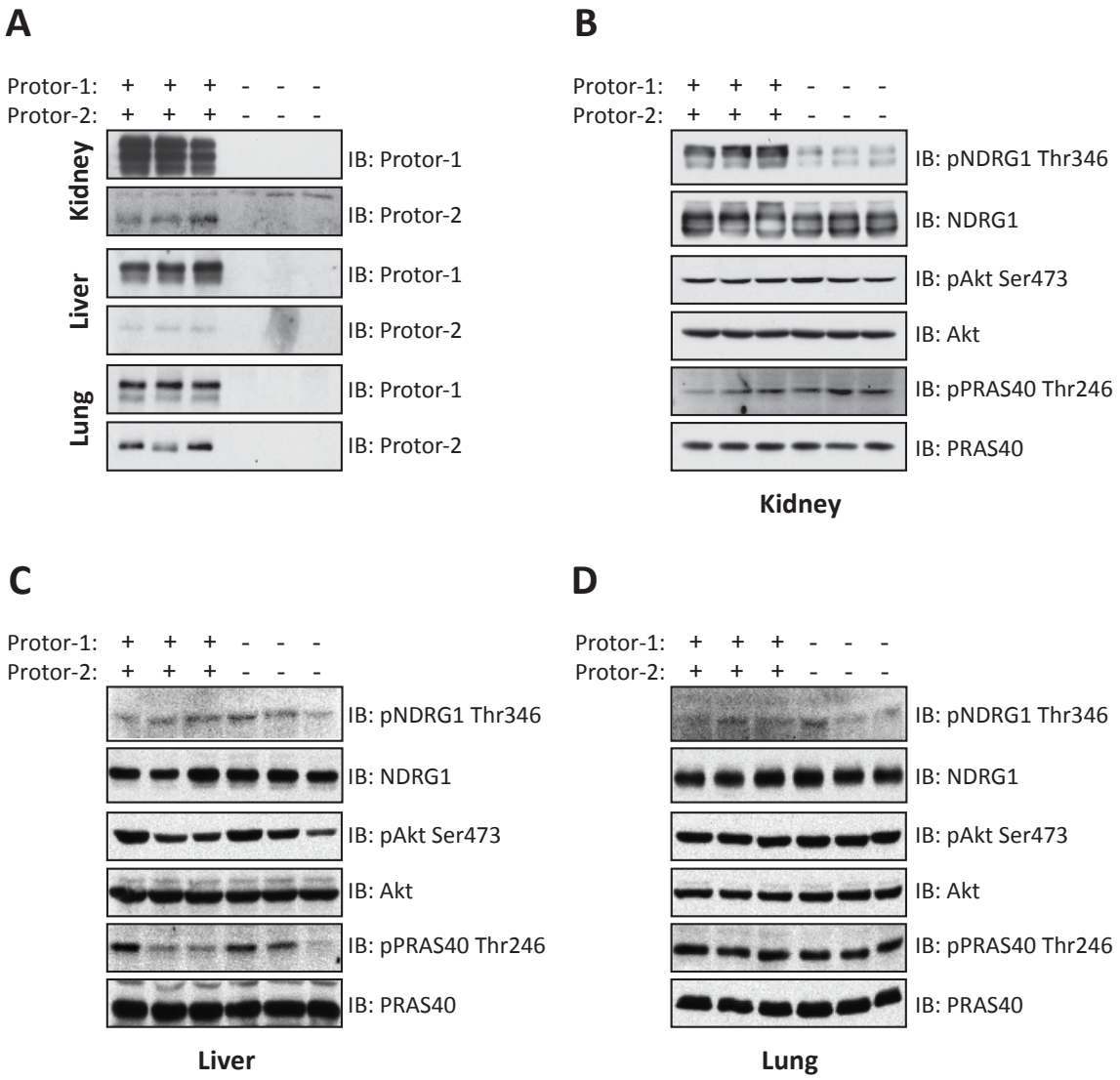

Figure 3.7 NDRG1 phosphorylation is reduced in kidney of fed Protor-1$^{-/-}$Protor-2$^{-/-}$ mice

Whole kidney, liver and lung lysates prepared from wild type and Protor-1$^{-/-}$Protor-2$^{-/-}$ mice were analysed by immunoblotting (IB) with the indicated antibodies. Dr L. Pearce prepared the samples and undertook part of the immunoblot analysis.

To further validate the importance of Protor in the regulation of SGK activation in kidney, wild type and Protor double knockout mice were injected with IGF1 to activate the PI3K pathway. Kidney and liver extracts derived from these animals were probed using antibodies that recognise SGK phosphorylated at its hydrophobic motif (Ser422 in SGK1) and validation of the T-loop antibody allowed for the detection of phosphorylated SGK T-

loop residue (Thr256 in SGK1). Although SGK1 hydrophobic motif phosphorylation was stimulated upon IGF1 treatment in wild-type mice, phosphorylation of this site was markedly reduced in the kidney of Protor-$1^{-/-}$Protor-$2^{-/-}$ mice (Figure 3.8A). Consistent with phosphorylation of Ser422 being required for the subsequent phosphorylation of Thr256 (Biondi et al., 2001; Garcia-Martinez and Alessi, 2008), there was also diminished phosphorylation of Thr256 in the double knockouts. The loss of HM-site and T-loop phosphorylation would result in a lack of SGK activation, which would account for the much-reduced phosphorylation of NDRG1. There was no significant difference in the IGF1-induced phosphorylation of Akt Ser473 or Thr308 or that of PRAS40 in the kidney of the double knockout mice (Figure 3.8A). Phosphorylation of SGK HM-site was similarly stimulated by IGF1 in liver samples derived from both wild type and Protor-1/2 double knockout mice. No T-loop phosphorylation of SGK was detected in liver and the stimulatory effect of IGF1 on NDRG1 phosphorylation was weak. As expected, loss of the two Protor isoforms did not influence IGF1 stimulated phosphorylation of Akt or its substrate PRAS40 in liver (Figure 3.8B). Total levels of SGK protein were similar in the wild type and double knockout mice in both tissues examined (Figure 3.8).

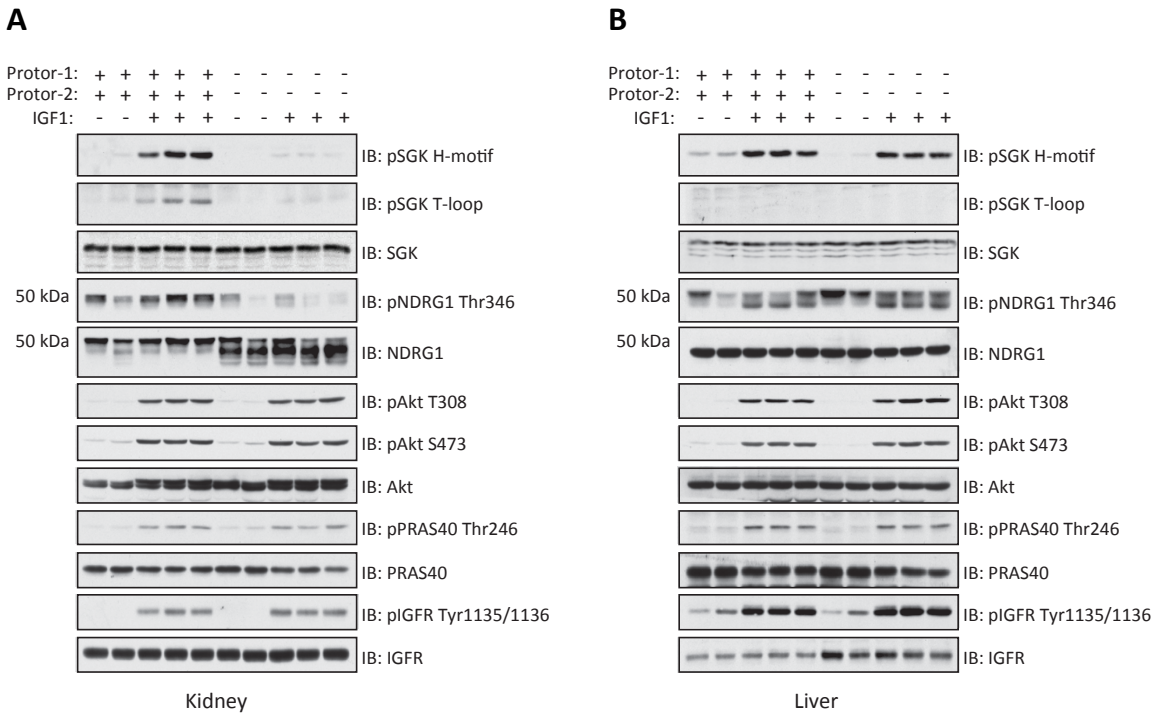

Figure 3.8 SGK phosphorylation is defective in the kidneys of Protor-1$^{-/-}$Protor-2$^{-/-}$ mice

Wild type and Protor-1$^{-/-}$Protor-2$^{-/-}$ mice deprived of food for 3 hours were injected intravenously with IGF1 (0.5 µg/g) or saline solution for 5 min. Whole kidney and liver lysates were analysed by immunoblotting (IB) with the indicated antibodies. SGK antibody used was Sigma S5188. Dr L. Pearce carried out the IGF1 injections and undertook part of the immunoblot analysis.

Given the ability of the Sigma SGK antibody to efficiently and selectively immunoprecipitate endogenous SGK from kidney, the catalytic activity of SGK immunoprecipitated from IGF1 stimulated wild type and double knockout kidney lysates was compared (Figure 3.9). IGF1 increased the activity of endogenous SGK by approximately two-fold in wild type mice. SGK immunoprecipitated from kidney of Protor-1$^{-/-}$Protor2$^{-/-}$ mice showed a significantly blunted increase in activity as a response to IGF1 stimulation confirming the defect in SGK activation in this tissue. The total levels of SGK were not altered between the two genotypes (Figure 3.9).

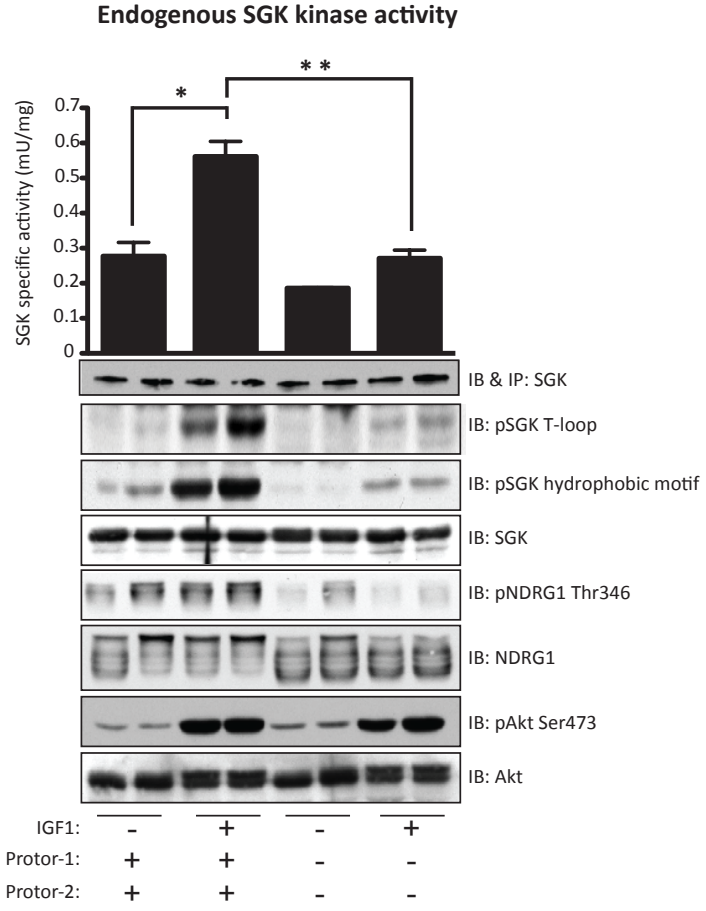

Figure 3.9 IGF1 induced SGK activation is defective in Protor-1$^{-/-}$Protor-2$^{-/-}$ kidneys

(**A**) Wild type and Protor-1$^{-/-}$Protor-2$^{-/-}$ mice deprived of food for 3 hours were intravenously injected with IGF1 (0.5 µg/g) or saline for 5 min. Endogenous SGK was immunoprecipitated (IP) from 5 mg of kidney lysate using Sigma S5188 antibody and the catalytic activity was measured using Crosstide peptide. Each bar represents the mean ± S.D. specific activity of two independent samples. Immunoprecipitates were subjected to immunoblot (IB) analysis with DSTT S062D antibody. Lysates were also subjected to immunoblot analysis with other indicated antibodies. Statistical significance was assessed by ANOVA followed by Tukey's multiple comparison tests using GraphPad Prism 5.0. *P<0.05, **P<0.01.

3.2.4. Membrane abundance of ENaC is not affected by the loss of Protor

The best-characterised role of any SGK isoform *in vivo* is that of SGK1 in the kidney. Whilst SGK1 knockout mice have no overt phenotype on a standard diet, when challenged with various solute imbalances SGK1 mice display defects in the renal handling of solutes

[reviewed in (Lang et al., 2009; Lang and Shumilina, 2013). At least in part SGK1 stimulates sodium transport into epithelial cells by enhancing the stability and plasma membrane abundance of the epithelial sodium channel ENaC. As SGK activity is reduced in kidneys of Protor-$1^{-/-}$Protor-$2^{-/-}$ mice, levels of ENaC at the membrane could also be lowered. To address this, membrane fractions were prepared from wild type and Protor double knockout kidneys. However, similar levels of ENaCα and ENaCγ subunits were observed in membrane fractions derived from wild type and Protor-$1^{-/-}$Protor-$2^{-/-}$ mice (Figure 3.10). Therefore Protor isoforms are not essential for regulating ENaC abundance at the membrane, at least in basal conditions.

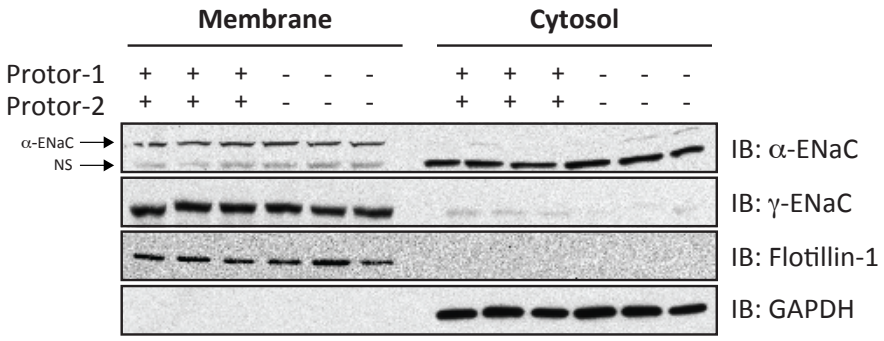

Figure 3.10 Expression of ENaC subunits in kidney membrane fractions of wild-type and Protor-$1^{-/-}$ Protor-$2^{-/-}$ mice

Membrane and cytosolic fractions were prepared from wild-type and Protor-$1^{-/-}$Protor-$2^{-/-}$ mouse kidney by ultra-centrifugation and subjected to immunoblot (IB) analysis with the specified antibodies. Flotillin-1 is a membrane and GAPDH a cytosolic protein.

3.2.5. Generation and characterisation of Protor double knockout MEFs

To study the role of Protor in the regulation of SGK activity outside of kidney, MEF cells were generated from wild type and Protor-$1^{-/-}$Protor-$2^{-/-}$ mice. Due to difficulty in detecting Protor isoforms by immunoblotting MEF lysates (data not shown), the absence

of Protor isoforms at protein level was confirmed by immunoprecipitations followed by immunoblotting (Figure 3.11).

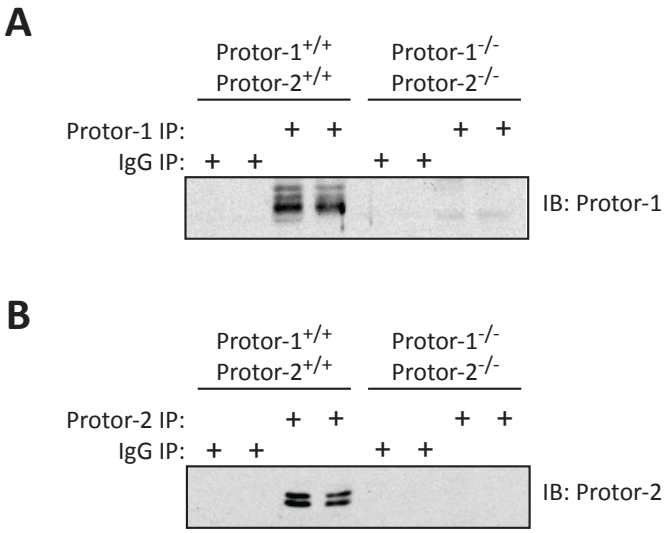

Figure 3.11 Generation of Protor-1$^{-/-}$Protor-2$^{-/-}$ double knockout MEFs

(**A**) Protor-1 was immunoprecipitated (IP) from 1 mg of wild type and Protor-1$^{-/-}$Protor-2$^{-/-}$ MEF lysate and immunoblotting (IB) was carried out using the same antibody. (**B**) Protor-2 was immunoprecipitated from 3 mg of wild type and Protor-1$^{-/-}$Protor-2$^{-/-}$ MEF lysate and immunoblotting was carried out using the same antibody.

Next the phosphorylation of NDRG1 was examined in MEF cells. Both IGF1, which activates the PI3K pathway, and the glucocorticoid dexamethasone, which induces *SGK1* expression, stimulated NDRG1 phosphorylation in wild type MEFs but failed to do so in Rictor deficient MEFs (Figure 3.12A-B) confirming the importance of the integrity of mTORC2 for SGK activation in this cell type. IGF1 and dexamethasone induced a significant phosphorylation and an electrophoretic band-shift of NDRG1 protein in both wild type and Protor-1$^{-/-}$Protor-2$^{-/-}$ MEFs indicating that SGK is normally activated in these cells in the absence of Protor isoforms (Figure 3.12C-D). IGF1 treatment leads to

activation of all SGK isoforms whereas dexamethasone is reported to induce the expression of only *SGK1* isoform (Kobayashi et al., 1999).

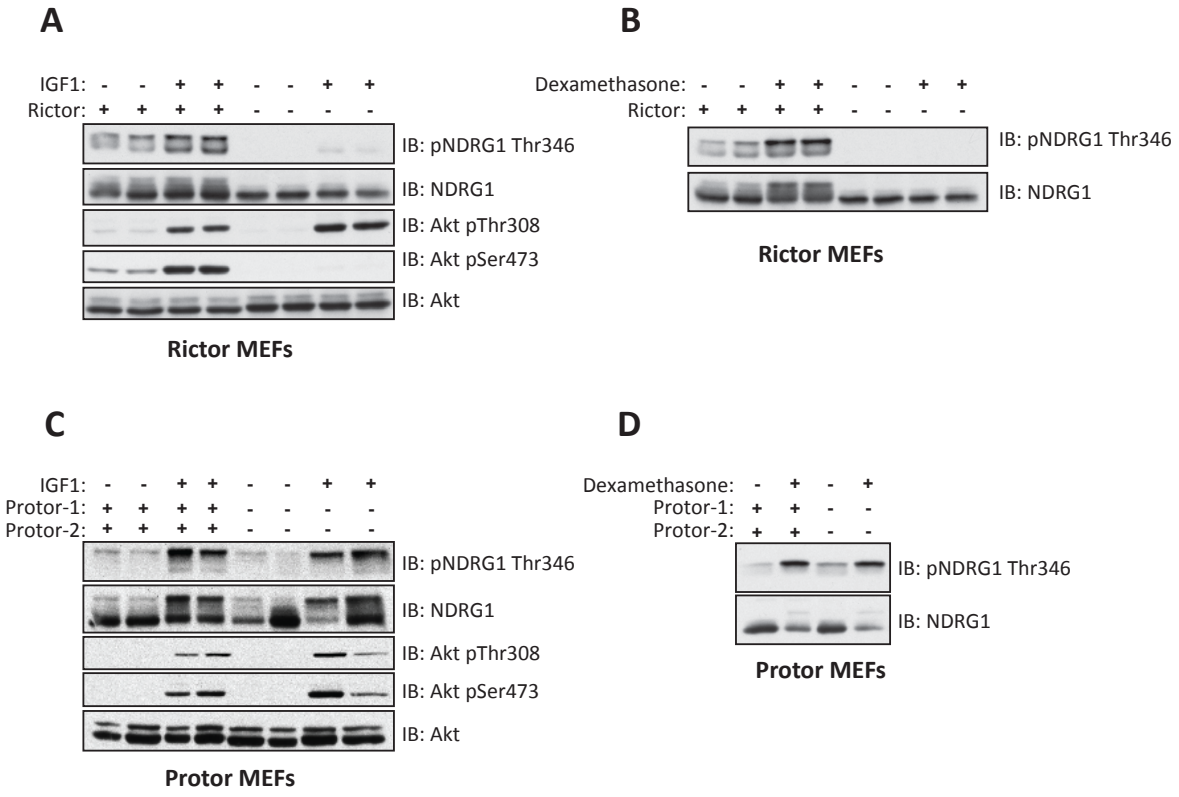

Figure 3.12 Loss of Protor does not impair mTORC2 dependent NDRG1 phosphorylation in MEFs

(**A**) Wild type and Rictor deficient MEFs were serum-starved overnight and stimulated with 50 ng/mL of IGF1 for 30 min prior to lysis and immunoblot (IB) analysis with the indicated antibodies. (**B**) Wild type and Rictor deficient MEFs were serum-starved overnight and stimulated with 0.2 μM dexamethasone for 2.5 hrs prior to lysis and immunoblot analysis. (**C**) as in (**A**) except wild type and Protor-$1^{-/-}$Protor-$2^{-/-}$ MEFs were used. (**D**) As in (**B**) except wild type and Protor-$1^{-/-}$Protor-$2^{-/-}$ MEFs were used.

3.2.6. Loss of Protor does not affect the catalytic activity of SGK in MEFs

As monitoring NDRG1 phosphorylation is an indirect measurement of SGK activity and the possibility that another kinase could be responsible for its phosphorylation cannot be excluded, a method to determine the catalytic activity of SGK in MEFs was next

developed. Wild type and Protor-1$^{-/-}$Protor-2$^{-/-}$ MEFs were transduced to stably express HA-ΔN-SGK1 using retroviral expression system based on pBABE-plasmid. Expression of full length SGK1 was undetectable (data not shown). ΔN-SGK1 lacks N-terminal residues 1-60 that target SGK1 for proteasomal degradation (Bogusz et al., 2006; Kobayashi and Cohen, 1999). HA-ΔN-SGK1 was immunoprecipitated from MEFs and its kinase activity was assayed. Neither the catalytic activity of HA-ΔN-SGK1 nor the levels of SGK1 Ser422 or Thr256 phosphorylation were affected by the absence of Protor isoforms (Figure 3.13).

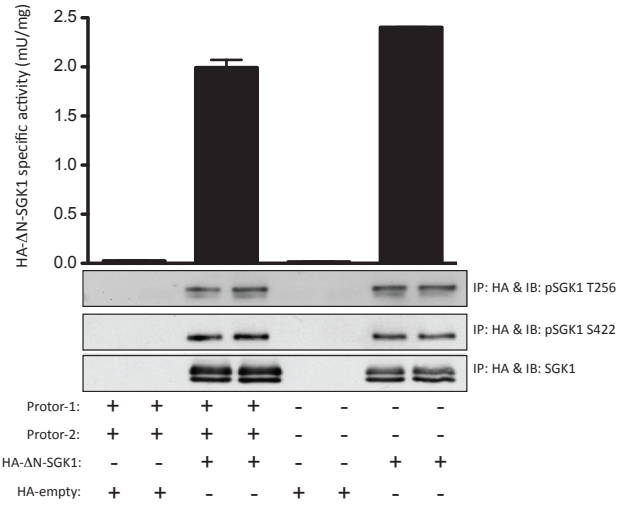

Figure 3.13 Activity of HA-ΔN-SGK1 is similar in wild type and Protor-1$^{-/-}$Protor-2$^{-/-}$ MEFs

Lysates were prepared from wild type and Protor-1$^{-/-}$Protor-2$^{-/-}$ MEFs stably expressing HA-ΔN-SGK1 or HA-empty vector. Immunoprecipitates (IP) were prepared using anti-HA-agarose from 1 mg of lysate and catalytic activity was measured against Crosstide peptide. Each bar represents the mean±S.D. activity of two separate samples. Immunoprecipitates were also subjected to immunoblot (IB) analysis with the indicated antibodies.

Since studying stably expressed HA-ΔN-SGK1 is non-physiological, the ability of different antibodies to immunoprecipitate endogenous SGK for kinase assays from MEFs was next tested. Immunoprecipitates were prepared using either DSTT S062D or Sigma S5188 antibodies from wild type and Protor-1$^{-/-}$Protor-2$^{-/-}$ MEFs. Results obtained with both antibodies indicated that the absence of Protor isoforms does not affect the activity of endogenous SGK in MEFs (Figure 3.14A-B). Immunoblot analysis revealed that SGK migrated as several species in the immunoprecipitations indicating that either several isoforms or variants were immunoprecipitated.

Next the endogenous SGK kinase assays from wild type and the Protor deficient MEFs were repeated using the DSTT S062D SGK antibody to immunoprecipitate SGK from cells treated with DMSO or 1μM PI-103 to inactivate PI3 and mTOR kinases (Fan et al., 2006b). Endogenous SGK activity was sensitive to treatment with PI-103 and again no differences were observed between wild type and Protor deficient MEFs. Moreover, levels of SGK HM-site and T-loop phosphorylation were not affected by the loss of Protor isoforms (Figure 3.14C). Immunoblot analysis of the lysates confirmed that PI-103 impaired NDRG1 phosphorylation and mTORC2 activity, as assessed by monitoring Akt Ser473 phosphorylation (Figure 3.14D).

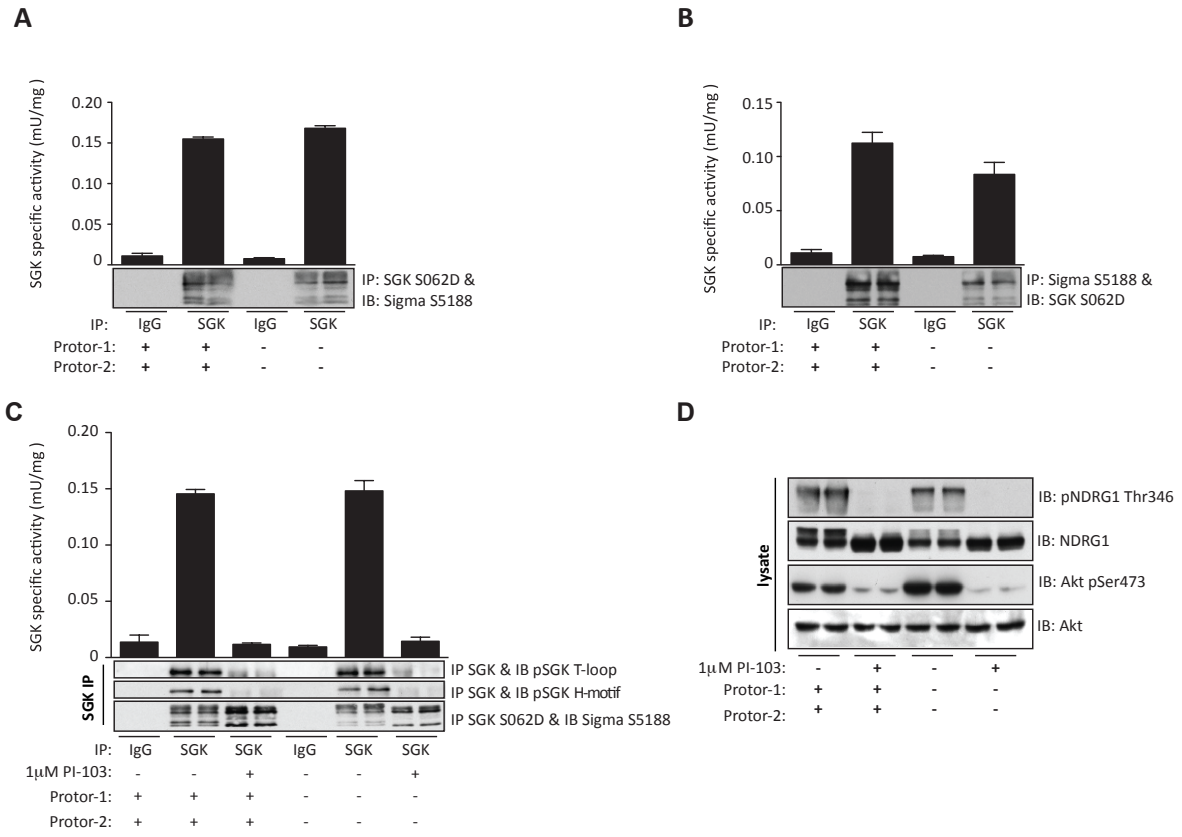

Figure 3.14 Loss of Protor does not affect the activity of endogenous SGK in MEFs

(**A**) SGK was immunoprecipitated (IP) from 3 mg of wild type and Protor-1$^{-/-}$Protor-2$^{-/-}$ MEFs lysate with DSTT S062D antibody or pre-immune IgG and catalytic activity of the immunoprecipitates was measured against Crosstide peptide. Each bar represents the mean±S.D. specific activity of two separate samples. Immunoprecipitates were also analysed by immunoblotting (IB) with the indicated antibody. (**B**) as in (**A**) except Sigma S5188 anti-SGK was used for immunoprecipitations. (**C**) as in (**A**) expect cells were treated with 1μM PI-103 or DMSO vehicle control for 1 h before lysis and immunoprecipitation with DSTT S062D SGK antibody or pre-immune IgG. Immunoprecipitates were also subjected to immunoblot analysis with indicated antibodies. (**D**) as in (**C**) except cell lysates were subjected to immunoblot analysis with indicated antibodies.

3.2.7. Protor isoforms are dispensable for the activity of mTORC2 *in vitro*

The evidence thus far implies that Protor-1 is important for the HM-site phosphorylation and activation of SGK in the kidney. Therefore, the importance of Protor for the kinase activity of mTORC2 in kidney tissue was next examined. mTORC2 was immunoprecipitated

using Sin1 antibody from either fed (Figure 3.15A-B) or IGF1-injected (Figure 3.15C-D) wild-type or Protor-1$^{-/-}$Protor-2$^{-/-}$ double knockout mouse kidney or liver lysates, and its ability to phosphorylate GST-Akt1 or GST-SGK1 *in vitro* was assessed. GST-Akt1 and GST-SGK1 used as substrates in these assays were purified from HEK293 cells that were deprived of serum overnight and incubated for a further 1 hour with 1 μM PI-103 prior to lysis to ensure that dephosphorylated forms of SGK1 and Akt1 were isolated. Dr Laura Pearce had previously optimised mTORC2 kinase assays and found them to be linear in respect to time and consequently the assays were carried out for 30 minutes which is within the linear part of these assays (personal communication). Loss of Protor isoforms did not have a significant impact on the ability of immunoprecipitated mTORC2 to phosphorylate GST–Akt1 or GST–SGK1 in cell free-assays. Similar results were observed using both kidney and liver lysates. Furthermore, similar results were also obtained when mTORC2 was immunoprecipitated from wild type or Protor-1$^{-/-}$Protor-2$^{-/-}$ MEFs (Figure 3.15). Dr L. Pearce had previous obtained similar results by comparing wild type and Protor-1 single knockouts. These findings indicate that despite the importance of Protor-1 for activation of SGK in the kidney, Protor isoforms are dispensable for regulating intrinsic mTORC2 kinase activity.

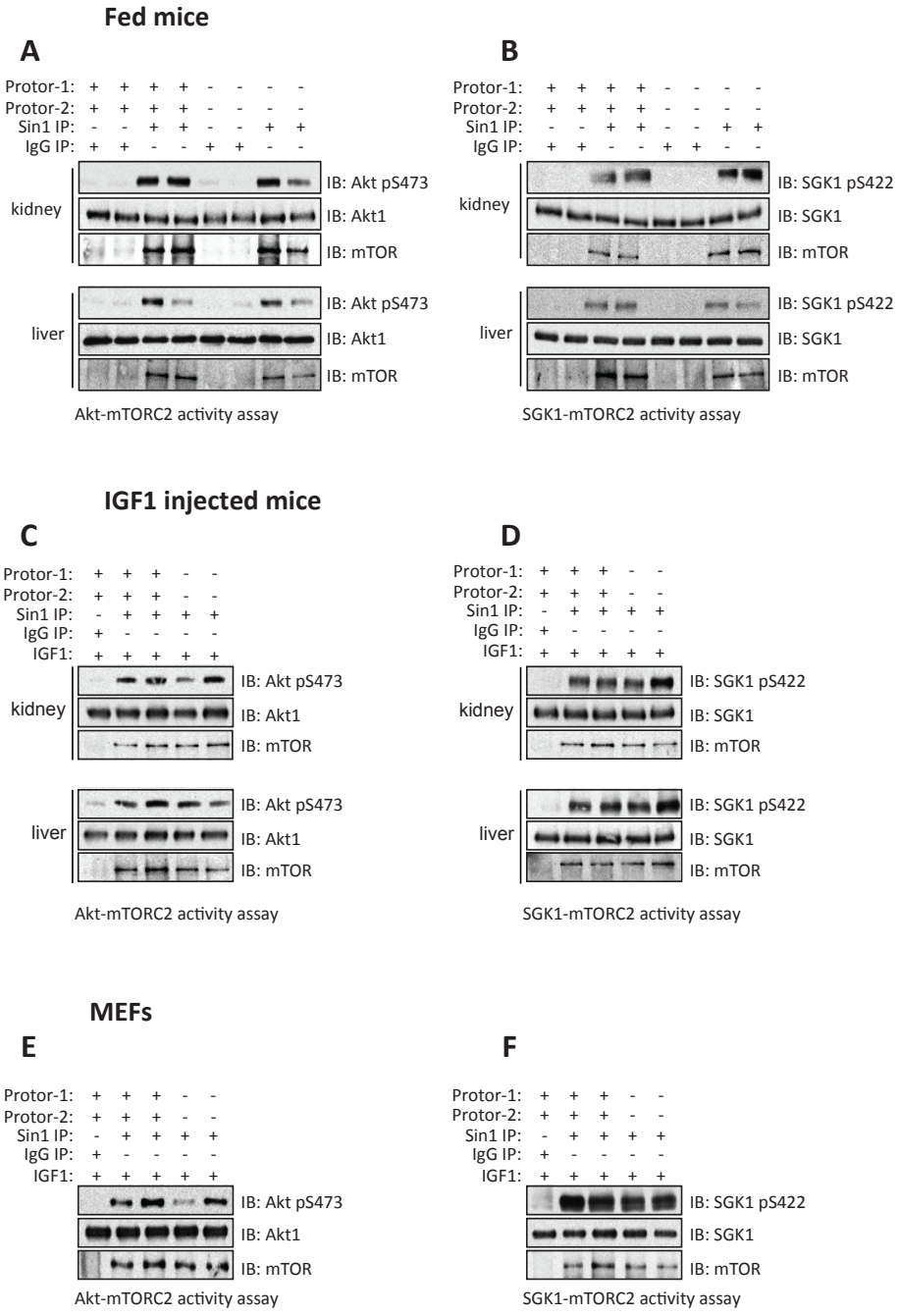

Figure 3.15 Protor isoforms are not required for mTORC2 kinase activity *in vitro*

(**A**) Immunoprecipitates (IP) were prepared using either pre-immune IgG or Sin1 antibody from fed wild-type or Protor-1$^{-/-}$Protor-2$^{-/-}$ kidney or liver lysates and their ability to phosphorylate GST-Akt1 *in vitro* was assayed. Reactions were analysed by immunoblotting (IB) with the indicated antibodies. (**B**) As in (**A**), except GST–ΔN-SGK1 was used as substrate. (**C**) As in (**A**), except immunoprecipitates were prepared from kidney or liver lysates from mice injected with IGF1 for 5 min. (**D**) As in (**C**), except GST–ΔN-SGK1 was used as substrate. (**E**) as in (**A**), except immunoprecipitates were prepared from wild-type or Protor-1$^{-/-}$Protor-2$^{-/-}$ MEFs. (**F**) as in (**E**), except GST–ΔN-SGK1 was used as substrate.

3.3. Discussion

SGK2 is the most highly expressed SGK isoform in the whole kidney

Immunoprecipitation and mass spectrometry analysis of endogenous SGKs revealed that SGK2 was the most abundant isoform detected in the whole kidney and liver lysates. Consistent with this, *SGK2* gene expression has been reported to be particularly high in epithelial tissues such as kidney and liver (Kobayashi et al., 1999). SGK2 is the least studied SGK family member and the finding that it is so robustly expressed in the kidney warrants it more careful attention in the future. In *Xenopus* oocyte co-expression studies that have compared all the three SGK isoforms, SGK2 is commonly able to perform the same functions as SGK1 (and SGK3) [reviewed in (Lang et al., 2006)]. For example, all SGK isoforms are able to stimulate the epithelial sodium channel ENaC (Friedrich et al., 2003). It is important to note that kidney is a complex organ with highly specialised tissue architecture and a weakness of the biochemical analysis presented in this chapter is the use of whole kidney lysate. One previous study has addressed the renal expression of SGK2 mainly by looking at the transcript and by immunofluorescence, which is critically dependent on highly specific antibodies. The findings indicate that SGK2 is robustly expressed in the proximal straight tubule and thick ascending limb of the loop of Henle and that SGK2 is expressed in proximal tubule cells that also express the Na^+/H^+ exchanger 3 (NHE3). Unlike *SGK1*, *SGK2* mRNA expression in renal tissue is not affected by the mineralocorticoid aldosterone. *In vitro* experiments indicate that SGK2 can regulate NHE3, suggesting that *in vivo* SGK2 could play a role in the control of sodium transport through NHE3 in the proximal tubule (Pao et al., 2010).

SGK2 knockout mice have not been characterised in peer-reviewed literature. Findings presented by Schnackenberg and colleagues in a meeting abstract suggest that SGK2 is not critical for renal homeostasis during unstressed conditions, but that SGK2 can compensate for the loss of SGK1 during salt deprivation (Schnackenberg et al., 2007). During normal diet the renal function of $SGK2^{-/-}$ mice as well as $SGK1^{-/-}SGK2^{-/-}$ double knockouts is reported to be similar to wild type mice. Unlike SGK1 knockout mice, SGK2 knockout mice do not display a salt wasting phenotype when fed a low sodium diet. $SGK1^{-/-}SGK2^{-/-}$ double knockout mice, however, are reported to display a more severe defect in renal reabsorption of water, sodium and potassium than SGK1 single knockout mice (Schnackenberg et al., 2007). Since the SGK1 single and SGK1/3 double knockout mice display near identical renal phenotypes (Grahammer et al., 2006), it appears that SGK2, which has received very little attention, may play more important roles in the kidney than SGK3.

Loss of Protor-1 impairs SGK activation in kidney

Although previous work carried out by Dr L. Pearce had not detected any obvious increase in Protor-2 expression in $Protor\text{-}1^{-/-}$ mice and no impairment of NDRG1 phosphorylation had been detected in the kidneys of $Protor\text{-}2^{-/-}$ mice, $Protor\text{-}1^{-/-}Protor\text{-}2^{-/-}$ double knockout mice were generated in order to address whether compensation occurred between the two Protor isoforms. Analysis of tissues derived from the double knockout mice emphasises that Protor-1, rather than Protor-2, is key for regulating SGK activation in the kidney. The defects in SGK and NDRG1 phosphorylation in Protor-1/2 double knockout

kidneys appeared identical to those previously seen in Protor-1 single knockouts. In both genotypes Akt was normally activated in all tissues examined. The function of NDRG1 protein and the consequence of its phosphorylation by SGK remain elusive and are further discussed in Chapter 4.

Characterisation of antibodies that allow reliable detection of endogenous SGK made crucial contributions to the study of the importance of Protor in the regulation of SGK. The measurement of endogenous SGK kinase activity in kidney lysates revealed that the stimulatory effect of IGF1 on endogenous SGK activity is significantly blunted in the absence of Protor. Furthermore, detection of the phosphorylated T-loop of endogenous SGK in the kidney confirmed the expected consequence that loss of mTORC2 mediated HM-site phosphorylation would have on SGK T-loop phosphorylation. As discussed in Section 1.6, phosphorylation of SGK HM-site creates a docking site for PDK1 leading to subsequent SGK T-loop phosphorylation and activation (Biondi et al., 2001; Collins et al., 2003; Collins et al., 2005; Garcia-Martinez and Alessi, 2008). Results presented in this chapter represent the first confirmation of this at endogenous kinase activity level. Moreover, detection of endogenous total SGK protein conclusively excluded the possibility that the defects previously observed in NDRG1 and SGK HM-site phosphorylation could be due to reduced expression of SGK protein in the kidneys of Protor-1 deficient mice. Reduced stability of SGK due to loss of Protor-1 had been a possible explanation especially given that Rictor, the direct binding partner of Protor (Pearce et al., 2007), had just been described to regulate the stability of SGK1 by forming an E3 ligase complex (Gao et al., 2010).

Protor-1/2 double knockout MEF cells were generated in order to have an additional tool to further address the importance of Protor in the regulation of SGK. Studies with MEFs clearly indicated that whilst NDRG1 phosphorylation in this cell type is critically dependent upon mTORC2 integrity following both stimulation of the PI3K pathway and dexamethasone induction of *SGK1* expression, Protor isoforms do not contribute to the activation of SGK in MEFs. Dr L. Pearce obtained similar results with Protor-1 single knockout MEFs. Furthermore, measurement of endogenous SGK kinase activity in Protor-1/2 deficient MEFs revealed no differences between the wild type and double knockout cells.

The most extensively characterised role of SGK *in vivo* is that of SGK1 in the kidney, in particularly in the aldosterone-sensitive distal nephron in the activation of ENaC. A key mechanism via which SGK1 induction in response to aldosterone is believed to stimulate Na^+ entry into the epithelial cells is via increased expression of ENaC in the luminal membrane, as discussed in Section 1.6.1. No defects were observed in the plasma membrane abundance of ENaC in the absence of Protor isoforms. This observation is, however, not entirely surprising. Firstly, the animals were fed a standard diet and the defects in Na^+ handling of SGK1 deficient mice are only seen when animals are fed a low-salt diet. Secondly, as discussed in Section 1.6.1, the defects seen in ENaC expression even in the SGK1 knockout mice are mild (Faresse et al., 2012; Fejes-Toth et al., 2008; Wulff et al., 2002). Therefore it is not unsurprising that the loss of Protor-1 did not influence ENaC abundance under the conditions studied. Furthermore, it should be noted that the mechanisms by which SGK1 deficiency lead to salt wasting remain somewhat elusive. Besides regulation of ENaC, recent findings also indicate that SGK1 dependent regulation

of the Na^+Cl^- co-transporter NCC is likely to be important for renal sodium homeostasis (Faresse et al., 2012; Fejes-Toth et al., 2008; Vallon et al., 2009).

Protor-1 may function as a scaffold protein that presents SGK to mTORC2 in the kidney

The precise mechanism by which Protor-1 regulates the efficient activation of SGK in the kidney remains unknown. Overall, little is known about the functions of Protor isoforms. Protor-1 has been proposed to control Platelet-derived growth factor receptor beta (PDGFRβ) expression via as-of-yet uncharacterised mechanisms (Woo et al., 2007). It would be interesting to analyse PDGFRβ expression levels in Protor deficient mice and MEFs. Protor-2 has been suggested to reduce apoptosis as knockdown of Protor-2 in HeLa cells modestly increased TNAα and cycloheximide induced apoptosis (Thedieck et al., 2007). A role in the de-stabilisation of certain mRNA transcripts has also been proposed for Protor-2 (Holmes et al., 2012).

Interestingly, recently Protor-2 was linked to the regulation of PKCδ activation and fibroblast migration (Gan et al., 2012). Lysophosphatidic acid (LPA) stimulates sustained PKCδ HM-site phosphorylation via the small G-protein Gα12 and mTORC2. LPA also induces the expression of E3 ubiquitin ligase RFFL leading to Protor-2 ubiquitylation and degradation and subsequently increased PKCδ HM-site phosphorylation. Consequently Protor-2 is suggested to be a suppressor of LPA and mTORC2-mediated PKCδ HM-site phosphorylation (Gan et al., 2012). This study also utilised the Protor-1/2 deficient MEFs whose generation is described in this thesis. LPA failed to induce migration of Protor-1/2 deficient MEFs but re-introduction of Protor-2 to the double knockout MEFs restored LPA

responsiveness of cell migration by suppressing basal migration (Gan et al., 2012). These observations together with the data presented in this chapter and in (Pearce et al., 2011) indicate that the roles of Protor-1 and Protor-2 are different but that both may be involved in the regulation of phosphorylation of a specific subset of mTORC2 substrates.

SGK activation and downstream signalling were markedly reduced in kidneys derived from Protor double knockouts and similar observations had previously been made in the Protor-1 single knockouts. However, it is clear that mTORC2 isolated from Protor deficient tissues and MEFs phosphorylated GST-Akt1 and GST-ΔN-SGK1 normally *in vitro*. Therefore it is unlikely that Protor-1 is required for the intrinsic kinase activity of mTORC2 towards SGK.

Neither Protor isoform possesses obviously recognisable functional domains nor do they have any obvious orthologues in lower eukaryotic species such as *Drosophila* and yeast (Pearce et al., 2007). Protor isoforms are non-essential for the overall function of mTORC2 as highlighted by the fact that in mice whole-body loss of the critical mTORC2 components mTOR, Rictor, mLST8 or Sin1 causes embryonic lethality (Gangloff et al., 2004; Guertin et al., 2006; Murakami et al., 2004; Shiota et al., 2006; Yang et al., 2006). *S. Cerevisiae* TORC2 contains two proteins termed Avo2 and Bit61 that are non-essential components of TORC2 (Loewith et al., 2002; Wullschleger et al., 2006). Avo2 and Bit61 appear to act as adaptors that bind the yeast TORC2 substrates Slm1 and Sl2m (Audhya et al., 2004; Fadri et al., 2005). Avo2 and Bit61, however, do not share any detectable identity with the two Protor isoforms (Pearce et al., 2007).

Recently, a substrate binding adaptor role was described for the mTORC2 subunit Sin1 that was found to interact with PKC isoforms and Akt (Cameron et al., 2011). HM-site phosphorylation of SGK was not addressed in this study. Furthermore, the mTORC1 component Raptor binds mTORC1 substrates such as S6K1 and 4EBP1 (Nojima et al., 2003). Association of Raptor with S6K and 4EBP1, however, is necessary for the capacity of isolated mTORC1 to phosphorylate these substrates *in vitro* as a point mutation within the substrate proteins significantly reduces their phosphorylation by mTORC1 in cell free assays (Nojima et al., 2003). Given that loss of Protor isoforms did not have any impact on the ability of immunoprecipitated mTORC2 to phosphorylate SGK1 or Akt in cell free assays, one possibility is that Protor-1 may act as a scaffolding component that presents SGK to mTORC2 in the kidney perhaps by ensuring their co-localisation.

Both the kinase activity measurements and analysis of SGK and NDRG1 phosphorylation revealed that SGK activity is not completely lost in the absence of Protor in the kidney thereby suggesting that Protor contributes towards the efficient activation of SGK but that in its absence some SGK activity does remain. This observation is consistent with the lack of effect that Protor deficiency had on isolated mTORC2 kinase assays and further strengthens the hypothesis that Protor may be crucial for distributing SGK and mTORC2 to a specific subcellular localisation rather than for the ability of mTORC2 to phosphorylate SGK. In the absence of Protor-1 SGK and mTORC2 would still come to proximity by passive diffusion allowing the HM-site phosphorylation of SGK to take place albeit at a reduced efficiency. Co-localisation of mTORC2 with its substrate would be analogous for the function of the *S. Cerevisiae* TORC2 subunits Avo2 and Bit61 which bring mTORC2 to the

plasma membrane where the substrates Slm1 and Slm2 exist (Audhya et al., 2004; Fadri et al., 2005).

Preliminary immunoprecipitations studies performed by Dr L. Pearce using over-expressed SGK isoforms in HEK293 cells suggested that Protor-1 could interact with SGKs. I, however, failed to detect either Protor isoform in large-scale endogenous SGK immunoprecipitations undertaken from mouse tissues lysed with the mild detergent CHAPS. Many kinase-substrate interactions are transient and it is entirely plausible that Protor and/or other mTORC2 components could be lost from SGK during the immunoprecipitations process.

Why should a scaffolding role for Protor-1 only be critical for efficient SGK activation in the kidney remains unsolved. One possibility is that SGK variants expressed in the kidney are particularly dependent on Protor-1 for the efficient activation. For example, for SGK1 differentially regulated transcriptional variants that alter the SGK1 N-terminus, which is particularly important for controlling the localisation of SGK1, have been described (Pao et al., 2007; Simon et al., 2007) and SGK1 has indeed been suggested to localise to various subcellular compartments including mitochondria, endoplasmic reticulum, plasma membrane, nucleus and cytoplasm (Arteaga et al., 2006; Bogusz et al., 2006; Brickley et al., 2002; Engelsberg et al., 2006; Lang et al., 2009; Pao et al., 2007). Protor-1 is most highly expressed in the kidney at both the mRNA and protein level (Johnstone et al., 2005; Pearce et al., 2007; Shan et al., 2003) highlighting that a key role for the protein may have evolved specifically in this tissue. It would certainly be interesting to study the subcellular distribution of SGK and Protor-1 proteins within different regions of the kidney. Ideally

such studies would be done utilising the knockout mice available in order to demonstrate the specificity of the antibodies used.

Whilst differences in SGK isoform expression might be important for their regulation by Protor-1, it is important to note that the endogenous mass spectrometry analysis found both kidney and liver to possess a very similar distribution of SGK isoforms with SGK2 being most abundant in whole tissue lysates derived from both sources, whereas an important role for Protor-1 was only seen in the kidney. The effect of Protor-1 on SGK1 was addressed by analysing the dexamethasone induced NDRG1 phosphorylation in Protor deficient MEFs and by measuring the kinase activity of over-expressed SGK1 in MEFs. By contrast, the endogenous kinase activity studies in MEFs were likely to measure the contribution of a range of SGK isoforms/variants as the immunoprecipitated SGK protein was seen to migrate as several bands. These notions suggest that the difference between kidney and other organs and MEFs is likely to be due to more complex reasons than just differential expression of SGK isoforms.

It is also worthwhile to note that whilst IGF1 induced SGK HM-site phosphorylation was detected in the liver, and was found to be normal in Protor deficient mice, endogenous T-loop phosphorylation was not detected in this tissue and the stimulatory effects of IGF1 on NDRG1 phosphorylation were weak in the both kidney and liver. Overall kidney is the only tissue in which most significant NDRG1 phosphorylation was seen (Pearce et al., 2011). It would be valuable to study the phosphorylation status of wider range of SGK substrates in the absence of Protor isoforms and to study the phosphorylation of SGK substrates following stimulation with dexamethasone and aldosterone. In conclusion,

Protor-1 is important for the efficient mTORC2-mediated activation of SGK in the kidney and it is clear that further work is required to understand the tissue-specific nature of the role of Protor-1 for efficient SGK activation.

4. Elevated SGK1 predicts resistance of breast cancer cells to Akt inhibitors

4.1. Introduction

Over 70% of breast cancers possess mutations that trigger activation of the PI3K pathway (Miller et al., 2011). Given the pivotal role of PI3K signalling in controlling cell growth, survival and proliferation, key components of this pathway, PI3K, mTOR and Akt, are promising targets for cancer drug discovery (Engelman, 2009; Liu et al., 2009). Although most work has focused on Akt as being the major mediator of cell proliferation induced by activation of PI3K, the closely related SGK isoforms have, by comparison, received little attention. Although there are subtle differences in the optimal substrate specificity requirements of SGK and Akt kinases, both enzymes phosphorylate substrates within a similar Arg-Xaa-Arg-Xaa-Xaa-Ser/Thr (Xaa is any amino acid) consensus sequence (Alessi et al., 1996; Murray et al., 2005). Moreover, Akt and SGK also share the same upstream activators, mTORC2 and PDK1. Consequently it is likely that Akt and SGK could possess similar functions such as promoting proliferation and survival of cancer cells. There are currently 223 clinical trials to evaluate the efficacy of Akt inhibitors for the treatment of cancer (http://www.clinicaltrials.gov/). The ability to predict which tumours will be most responsive to Akt inhibitors is an important question. Owing to the similarity of SGK and Akt isoforms and the potential that these enzymes possess analogous functions, I decided

to investigate whether tumour cells displaying high levels of SGK would be more resistant to Akt inhibitors than tumours lacking SGK.

Work carried out at AstraZeneca had identified a correlation between the sensitivity of breast cancer cells to Akt inhibition and *SGK1* mRNA levels. In this chapter I describe the verification that a number of Akt inhibitor resistant breast cancer cell lines possess elevated levels of SGK1 at both mRNA and protein levels. I present evidence that SGK1 represents a major driver of proliferation in these cells and that in contrast, the Akt inhibitor sensitive cells analysed display low or undetectable levels of SGK1 protein. I also demonstrate that in the absence of significant SGK1 activity, Akt can mediate the phosphorylation of NDRG1, which has previously been reported to be an SGK1-specific substrate (Murray et al., 2004). The findings presented in this chapter indicate that monitoring SGK1 levels as well the effect that administration of Akt inhibitors has on NDRG1 phosphorylation could have utility in predicting the sensitivity of tumours to Akt inhibitors. The results also suggest that SGK inhibitors or dual Akt-SGK inhibitors might have utility for treating cancers displaying elevated SGK activity.

4.2. Results

4.2.1. Identification of Akt inhibitor sensitive and resistant cell lines

Two structurally and mechanistically distinct Akt inhibitors that are both currently in clinical trials were utilised to study the role of Akt and SGK in breast cancer cells. MK-2206 is an allosteric inhibitor of Akt (Hirai et al., 2010). The mechanism of action of MK-2206 is

not entirely understood. Inhibition of Akt by MK-2206 and related compounds is dependent on the presence of the PtdIns(3,4,5)P_3 binding PH-domain and is not competitive with ATP (Barnett et al., 2005). These compounds disrupt the membrane localisation of Akt and are believed to induce a closed conformation of Akt that occludes the binding sites of, PDK1, mTORC2 and substrates (Cherrin et al., 2010). As expected for a non-ATP competitive compound, MK-2206 does not significantly inhibit any kinases in an *in vitro* selectivity screen (Figure 4.1). AZD5363 is an ATP-competitive Akt inhibitor that does not inhibit the related kinase SGK1 *in vitro* [(Davies et al., 2012) and (Figure 4.2)].

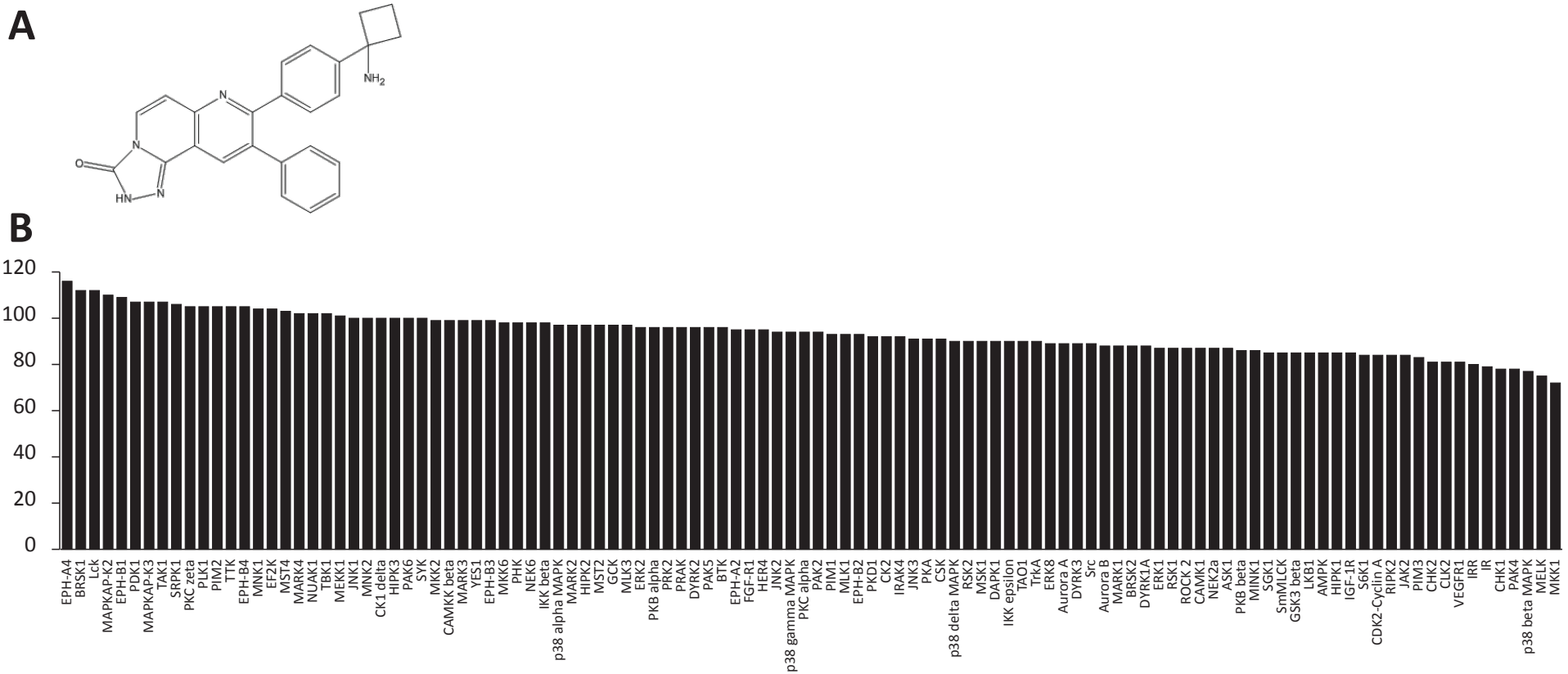

Figure 4.1 Structure and *in vitro* selectivity screening of MK-2206

(**A**) The published structure of MK-2206. (**B**) The Kinase selectivity profile was established by The National Centre for Protein Kinase Profiling (http://www.kinase-screen.mrc.ac.uk/). Data are presented as mean (n=3) % kinase activity remaining in the presence of 1 μM MK-2206. DMSO control reaction was set to 100%.

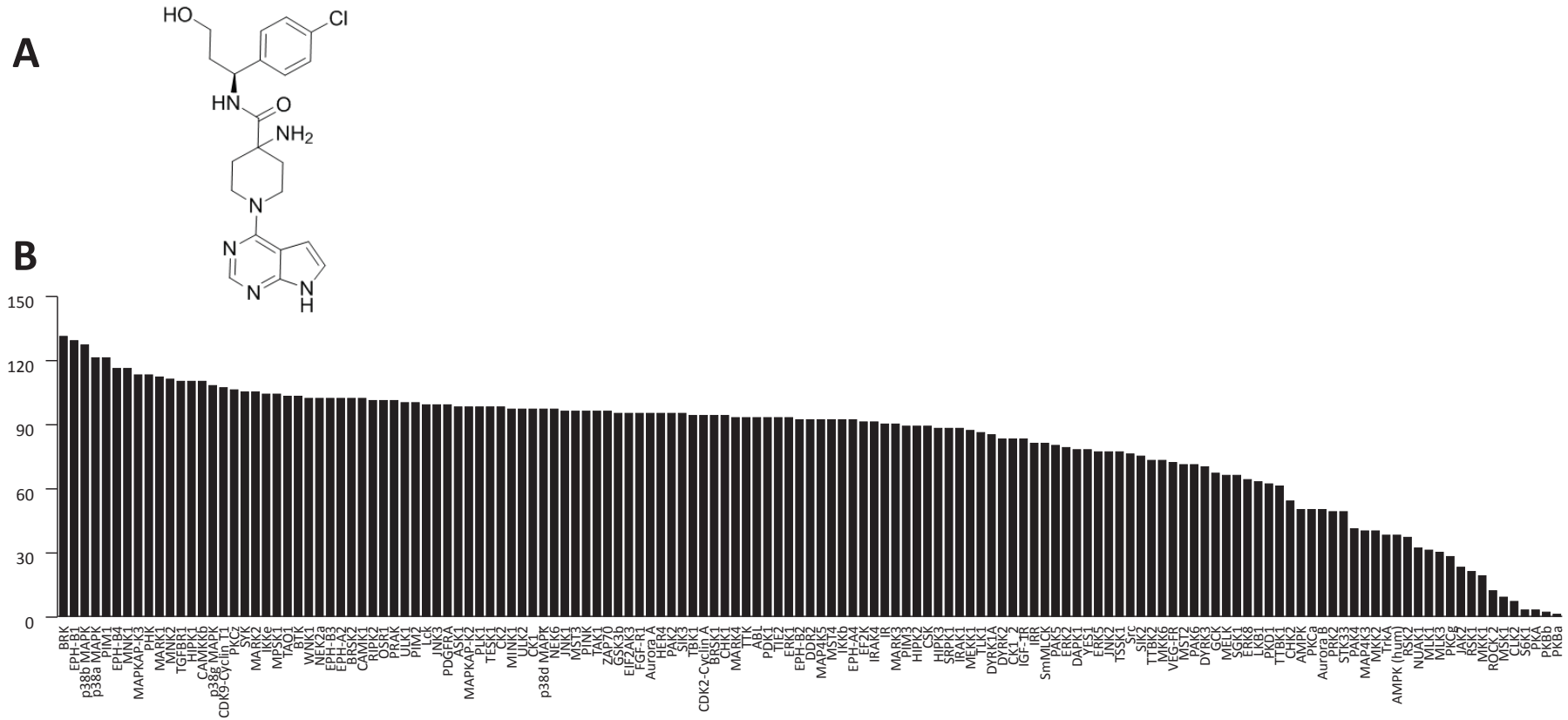

Figure 4.2 Structure and *in vitro* selectivity screening of AZD5363

(**A**) The published structure of AZD5363. (**B**) The Kinase selectivity profile was established by The National Centre for Protein Kinase Profiling (http://www.kinase-screen.mrc.ac.uk/). Data are presented as mean (n=3) % kinase activity remaining in the presence of 1 μM AZD5363. DMSO control reaction was set to 100%.

Whole transcriptome analysis performed at AstraZeneca indicated that there is a correlation between AZD5363 sensitivity and *SGK1* mRNA levels (Figure 4.3). This analysis revealed that there was a group of AZD5363-sensitive cell lines with low *SGK1* mRNA (BT-474, CAMA-1, ZR-75-1, T47D, HCC-1187 and HCC-1569) and a group of resistant cell lines with high *SGK1* mRNA (HCC-1937, MDA-MB-436, BT-549, MDA-MB-157, MDA-MB-231, HCC-1806 and JIMT-1). There were eight cell lines that displayed intermediate sensitivity towards AZD5363, six having low SGK1 mRNA (SUM-52-PE, MDA-MB-453, SK-BR-3, MCF-7, MDA-MB-468 and HCC-1419) and two with elevated SGK1 mRNA (BT-20 and HCC-1954).

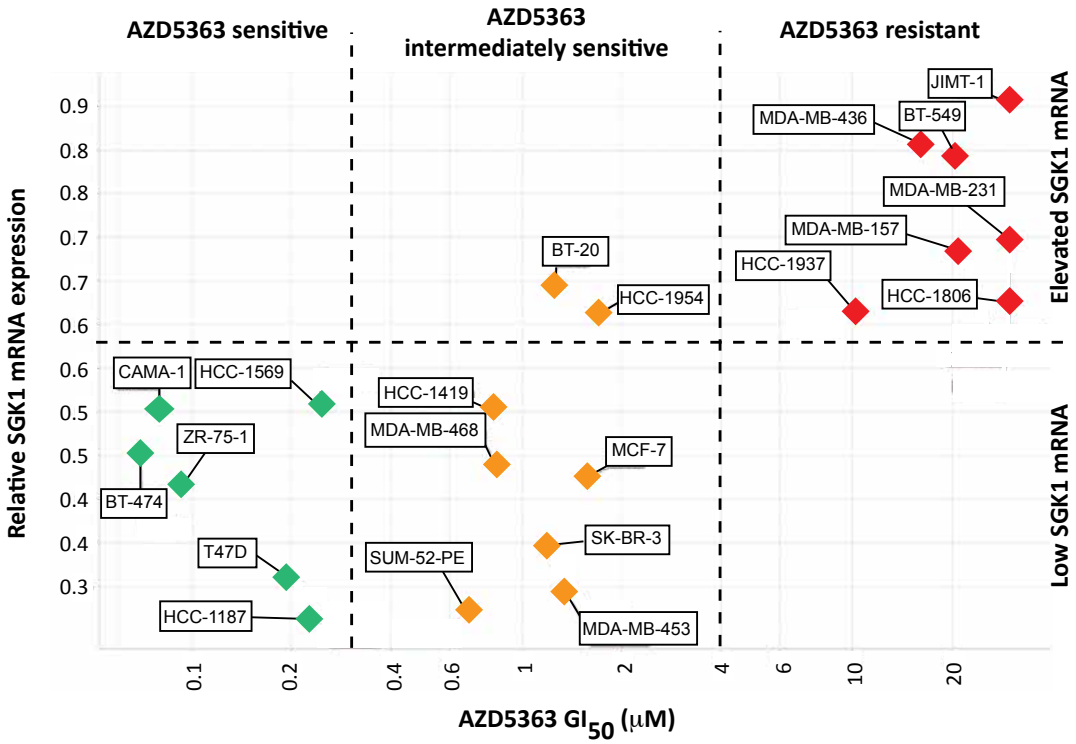

Figure 4.3 Correlation of breast cancer cell sensitivity to AZD5363 with *SGK1* expression

21 breast cancer cell lines were screened in a 72 h MTS proliferation assay. Cell lines with a GI_{50} value of <0.4 μM were classified as sensitive (green), with a GI_{50} value of 0.4 – 4 μM as intermediately sensitive (orange) and with GI_{50} value of >4 μM as resistant (red). SGK1 gene expression from whole transcriptome analysis (Affymetrix U133) was scaled relative to the expression range across a panel of 500 cell lines where 0=minimum and 1=maximum. Data was generated by H. Dry and Dr B. Davies, AstraZeneca.

Five sensitive (BT-474, CAMA-1, ZR-75-1, T47D and HCC-1187), one intermediate (SUM-52-PE) and the seven resistant (HCC-1937, MDA-MB-436, BT-549, MDA-MB-157, MDA-MB-231, HCC-1806 and JIMT-1) cell lines were chosen for further analysis. The known mutations in these cells are listed in Appendix 3. As shown in Figure 4.4, sensitivity of these cells to AZD5363 was confirmed by exposing the cells to increasing concentrations (1 nM – 10 μM) of AZD5363 for 72 hours followed by MTS assay. Data presented in Figure 4.5 and Table 4.1 also confirms that the cell lines studied displayed similar sensitivity towards the structurally and mechanistically distinct allosteric Akt inhibitor MK-2206. Interestingly, the resistant cell lines are all triple negative and all of the sensitive cell lines with the exception of HCC-1187 cells, which are triple negative, are hormone receptor positive (Appendix 3) . As discussed in the Chapter 1, currently no targeted therapies exist against the triple negative breast cancers and these breast cancers have the worst prognosis.

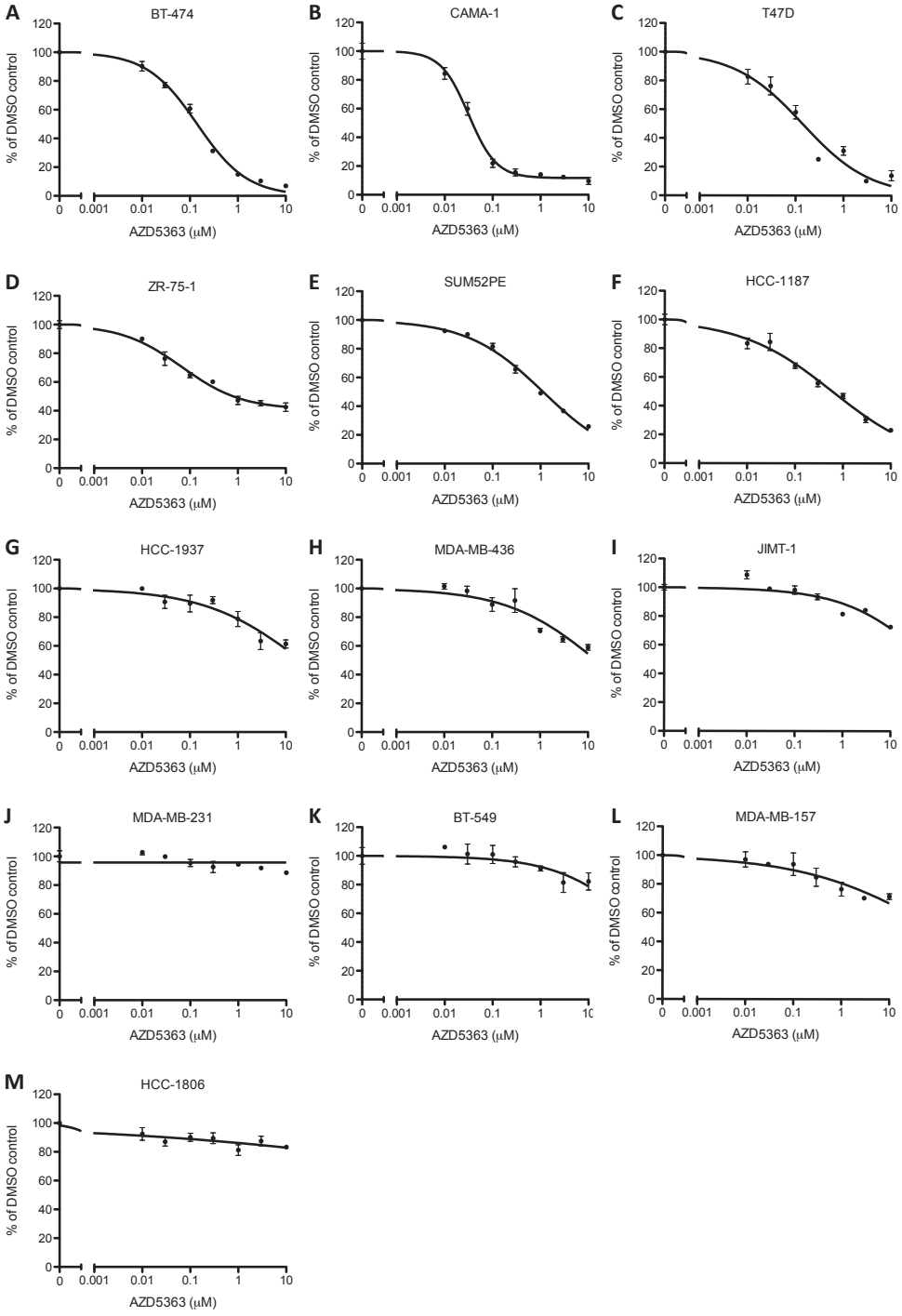

Figure 4.4 Dose response curves of breast cancer cell lines to AZD5363

Cells were exposed to DMSO or 1 nM – 10 μM AZD5363 for 72 hrs and cell viability was determined using MTS assay. Data were fitted to sigmoidal dose response curves using GraphPad Prism 5.0.

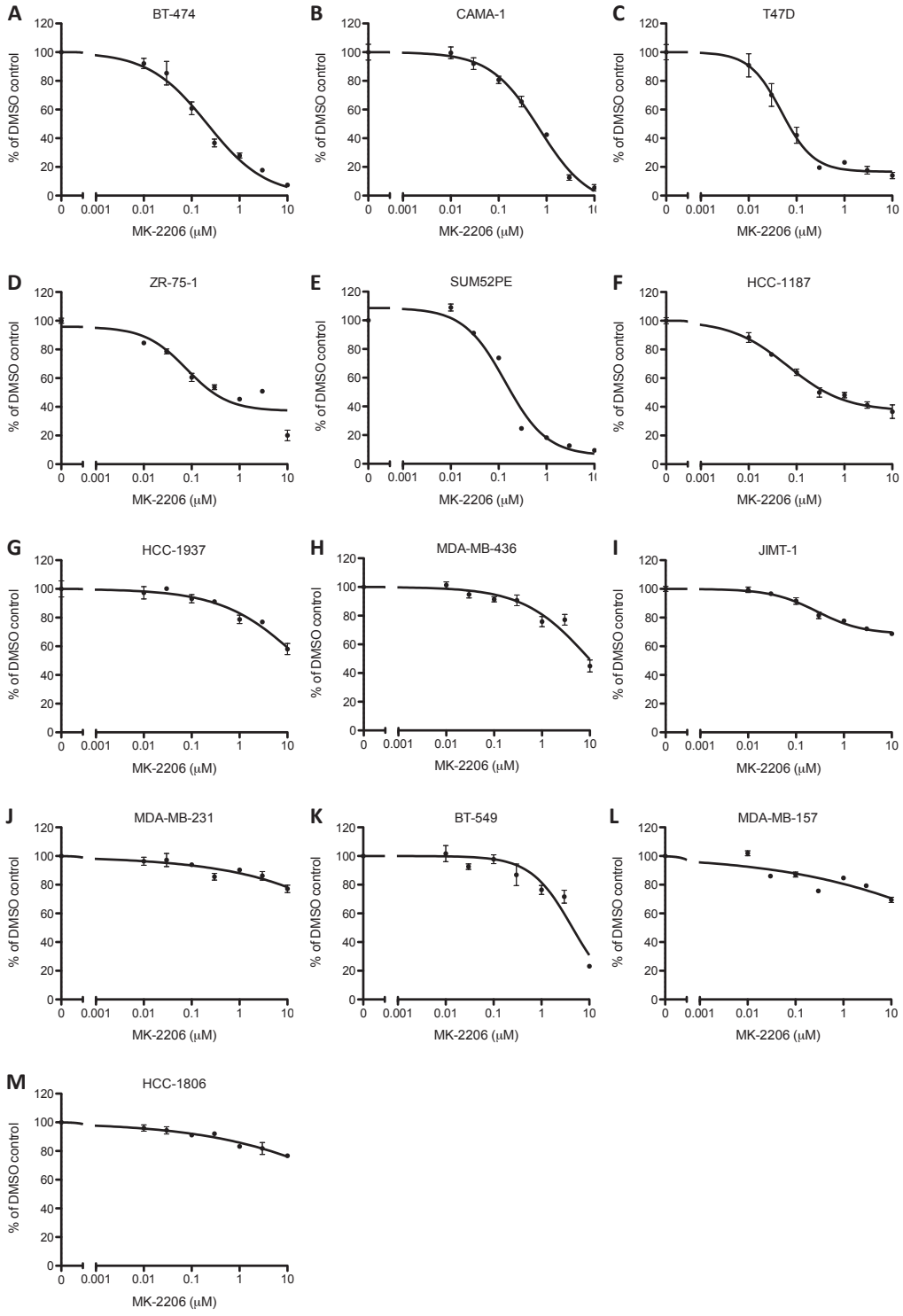

Figure 4.5 Dose response curves of breast cancer cells to MK-2206

Cells were exposed to DMSO or 1 nM – 10 μM MK-2206 for 72 hrs and cell viability was determined using MTS assay. Data were fitted to sigmoidal dose–response curves using GraphPad Prism 5.0.

Cell line	MK-2206 GI_{50}	MK-2206 GI_{50} 95% CI	AZD5363 GI_{50}	AZD5363 GI_{50} 95% CI
BT-474	0.20	0.15 - 0.25	0.14	0.12 - 0.16
CAMA-1	0.58	0.48 - 0.70	0.04	0.03 - 0.06
ZR-75-1	0.69	0.45 - 1.1	1.5	0.94 - 2.4
T47D	0.09	0.06 - 0.14	0.14	0.1 - 0.2
HCC-1187	0.88	0.57 - 1.4	0.61	0.46 - 0.8
SUM52PE	0.18	0.15 - 0.23	1.1	0.93 - 1.2
HCC-1937	> 20	-	> 20	-
MDA-MD-436	9.7	6.3- 14.9	14.9	7.2 - 31
BT-549	4.5	3.3 - 6.1	> 20	-
MDA-MB-157	> 20	-	> 20	-
HCC-1806	> 20	-	> 20	-
MDA-MB-231	> 20	-	> 20	-
JIMT-1	> 20	-	> 20	-

Table 4.1 GI_{50} values of Akt inhibitors

Cells were exposed to DMSO or 1 nM - 10 µM AZD5363 or MK-2206 for 72 hours and cell viability was determined using MTS assay. Data were fitted to sigmoidal dose response curves and GI_{50} values and 95% confidence intervals (CI) were calculated using GraphPad Prism 5.0. Where GI_{50} values exceeded 20 µM, data fitted poorly to dose response curves, and therefore no exact GI_{50} values or 95% CIs are stated for these samples.

4.2.2. Analysis of Akt inhibitor sensitive and resistant cell lines

Next the relative mRNA expression levels of all three SGK isoforms in the Akt inhibitor sensitive and resistant cell lines were determined using quantitative reverse transcription PCR (qRT-PCR) (Figure 4.6). This revealed that the Akt inhibitor resistant cell lines displayed higher levels of SGK1 mRNA than the sensitive cell lines. Levels of SGK2 mRNA were variable between sensitive and resistant cells and SGK3 mRNA levels were present at more similar levels across the resistant and sensitive cell lines (Figure 4.6).

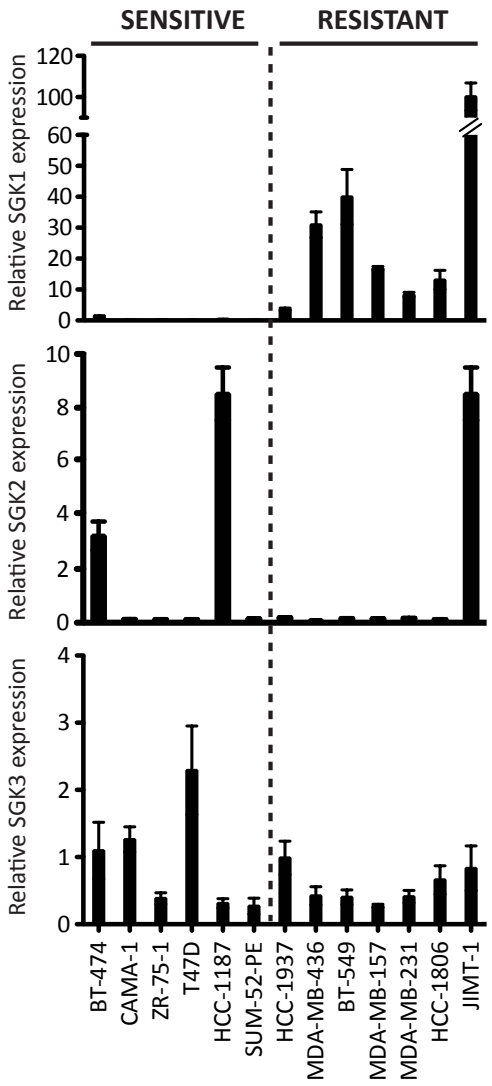

Figure 4.6 Comparison of SGK mRNA levels in Akt inhibitor sensitive and resistant cells

Total mRNA was isolated from cells and SGK isoform mRNA levels were determined by qRT-PCR. The data were normalised to an internal 18S control and are presented as relative levels in comparison with control cells (HEK293). Results represent the means ± S.E.M. of two independent samples each assayed in duplicate.

Next an immunoblot analysis was carried out to compare the relative expression levels of SGK1 and SGK3 protein as well as phosphorylation levels of NDRG1 across the cell lines. Four of the Akt inhibitor resistant cell lines (HCC-1937, MDA-MB-436, BT-549 and JIMT-1) possessed readily detectable SGK1 protein expression and also displayed high levels of

NDRG1 phosphorylation. All of these cell lines possess mutations that activate PI3K. HCC-1937, MDA-MB-436 and BT-549 cells were null for PTEN expression whereas JIMT-1 cells have an activating mutation in the catalytic subunit of PI3K (C420R) (Koninki et al., 2010). Two of the remaining Akt inhibitor resistant cell lines (HCC-1806 and MDA-MB-231), although not displaying obvious elevation of SGK1 protein, nevertheless exhibited significant phosphorylation of NDRG1. The final Akt inhibitor resistant cell line investigated (MDA-MB-157) showed low levels of NDRG1 phosphorylation and no detectable SGK1 protein suggesting that SGK signalling is not activated in these cells. Consistent with the mRNA expression data, SGK3 protein levels were more variable across the sensitive and resistant cell lines (Figure 4.7).

In addition, Akt expression and activity was monitored by assessing Akt Thr308 and Ser473 phosphorylation as well as phosphorylation of the Akt substrates PRAS40, GSK3 and FoxO1/3. All Akt inhibitor sensitive and five out of the seven resistant cell lines (HCC-1937, MDA-MB-436, BT-459, HCC-1806 and JIMT-1) displayed significant Akt Thr308/Ser473 and PRAS40 phosphorylation, confirming that Akt signalling is active in these cells. In contrast, resistant MDA-MB-157 and HCC-1806 cells had very low levels of Akt Thr308/Ser473 and undetectable PRAS40 phosphorylation suggesting that Akt signalling is weak in these cells. Levels of GSK3 and FoxO1/3 phosphorylation were more variable across all the cell lines examined. Levels of mTORC1 activity were estimated by monitoring phosphorylation of S6 protein. Similar levels of S6 phosphorylation were detected in all cell lines, except HCC-1187 and MDA-MB-436 cells that possessed lower S6 phosphorylation (Figure 4.7).

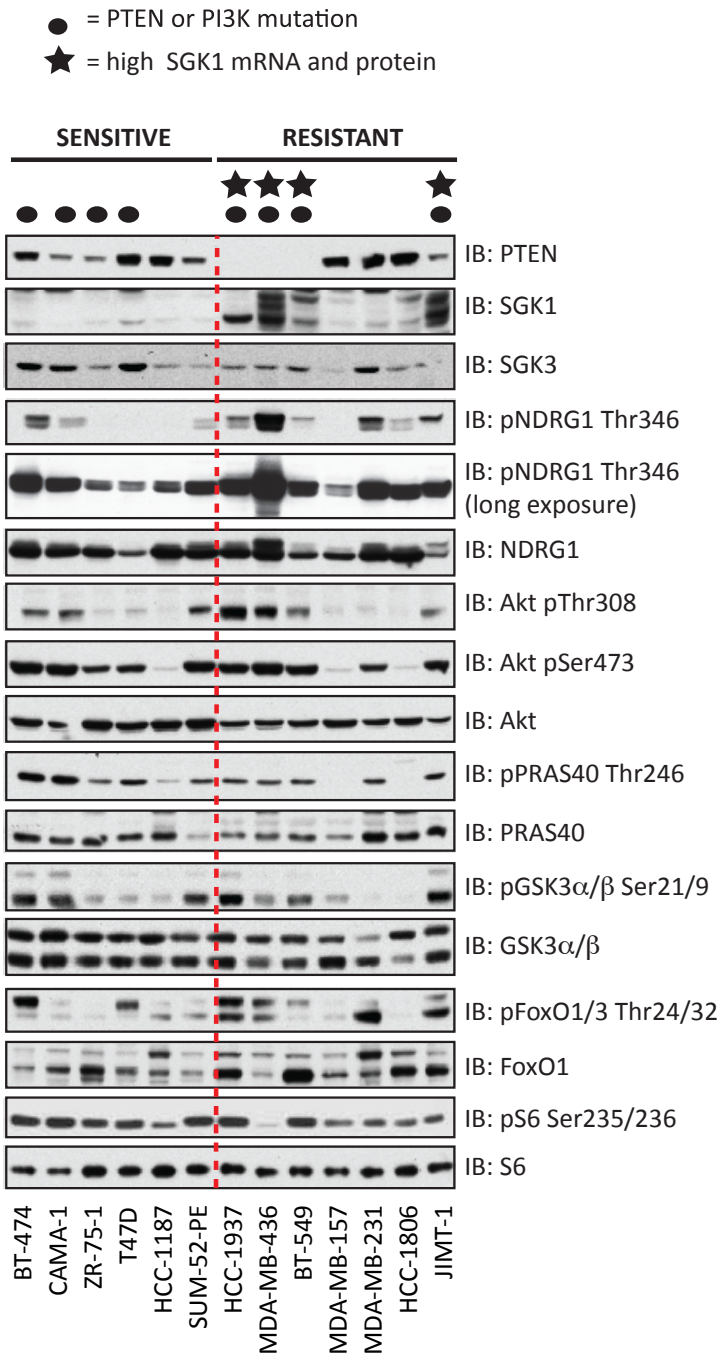

Figure 4.7 Immunoblot analysis of Akt inhibitor sensitive and resistant cells

Total protein was isolated from cells and analysed by immunoblotting (IB) with the indicated antibodies.

4.2.3. SGK1 knockdown impairs proliferation of Akt inhibitor resistant cells

SGK1 has a short half-life (Brickley et al., 2002), making it straightforward to knockdown SGK1 protein expression using RNA interference. Five independent lentiviral shRNAs reduced the expression of SGK1 protein to near undetectable levels in the Akt inhibitor resistant cell lines displaying high levels of SGK1 protein (BT-549, MDA-MB-436, JIMT-1 and HCC-1937 (Figure 4.8A). Consistent with the efficient knockdown of SGK1 protein, all shRNAs also markedly reduced NDRG1 phosphorylation in the resistant cell lines (Figure 4.8A). Strikingly, knockdown of SGK1 protein markedly impaired proliferation of all Akt inhibitor resistant cell lines examined (Figure 4.8B). In contrast, transduction of Akt inhibitor sensitive cells (BT-474, T47D and ZR-75-1) with SGK1 shRNAs had no effect on NDRG1 phosphorylation or proliferation (Figure 4.9).

To confirm that inhibition of proliferation following SGK1 knockdown in Akt inhibitor resistant cells was indeed mediated by a SGK1 deficiency, a rescue experiment was carried out. Endogenous SGK1 expression was knocked down in BT-549 cells stably over-expressing wild type or kinase inactive SGK1. This experiment revealed that in BT-549 cells lacking endogenous SGK1, proliferation and NDRG1 phosphorylation can be rescued by over-expression of wild type, but not kinase inactive SGK1 (Figure 4.10).

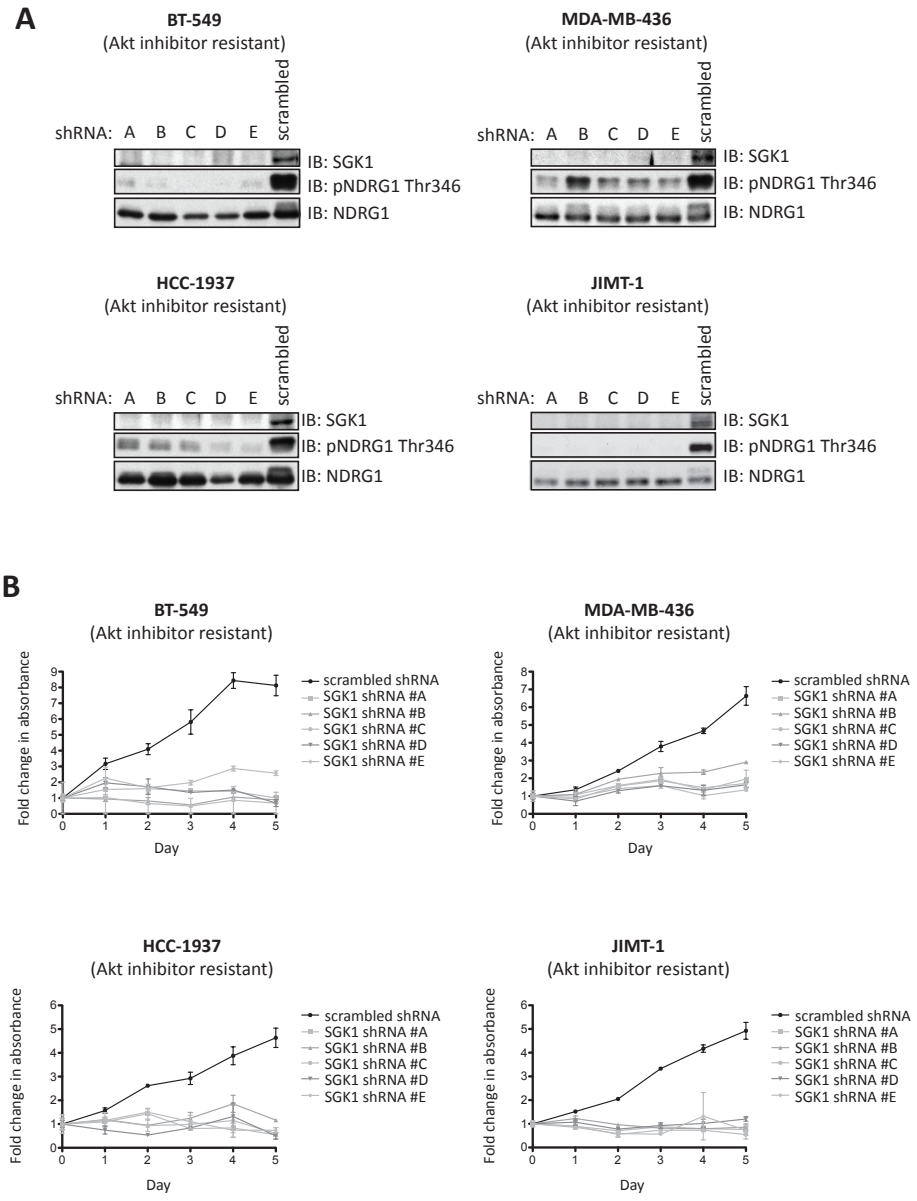

Figure 4.8 SGK1 knockdown impairs proliferation of Akt inhibitor resistant cells

(A) The indicated Akt inhibitor resistant cells were transduced with SGK1 and scrambled shRNAs. Cells were lysed 72 hours post infection and the lysates were analysed with the indicated antibodies by immunoblotting (IB). (**B**) Akt inhibitor resistant cells were transduced with lentiviral SGK1 and scrambled shRNAs. Equal numbers of cells were seeded onto 96-well plates 48 hours post infection and allowed to adhere overnight. Cell proliferation was then determined over a 5-day period by carrying out MTS assay at 24 hour intervals. Each data point is the average MTS assay of samples assayed in triplicate±S.D. The data are presented as fold change relative to day 0 values (day 0 equals 24 h post-seeding).

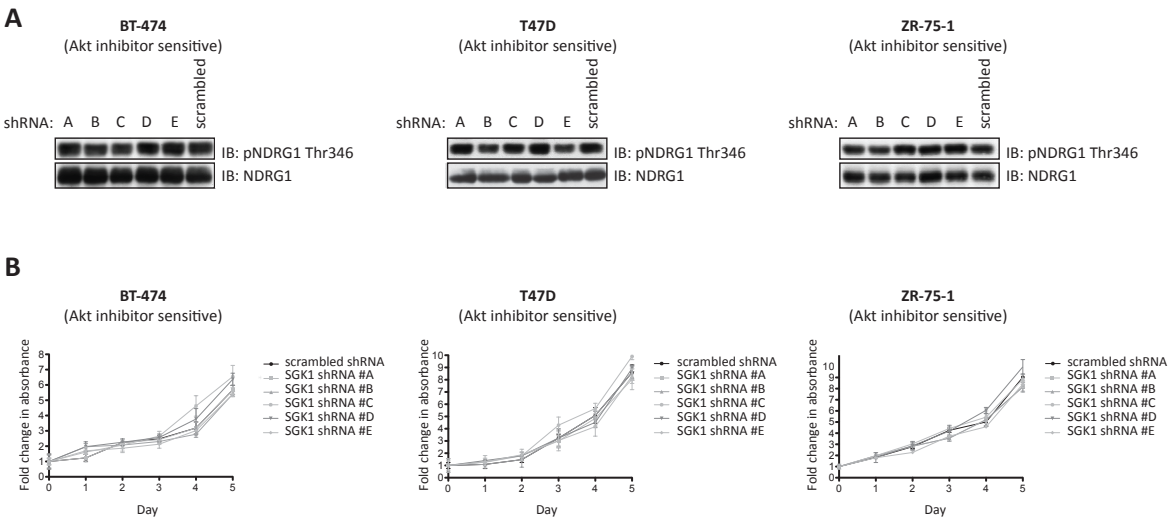

Figure 4.9 SGK1 knockdown does not affect proliferation of Akt inhibitor sensitive cells

(**A**) Akt inhibitor sensitive cells were transduced with SGK1 and scrambled shRNAs. Cells were lysed 72 hours post infection and the lysates were analysed with the indicated antibodies by immunoblotting (IB). (**B**) Akt inhibitor sensitive cells were transduced with SGK1 and scrambled shRNAs. Equal numbers of cells were seeded onto 96-well plates 48 hours post infection and allowed to adhere overnight. Cell proliferation was then determined over a 5-day period by carrying out MTS assay at 24 hour intervals. Each data point is the average MTS assay of samples assayed in triplicate±S.D. The data are presented as fold change relative to day 0 values (day 0 equals 24 h post-seeding).

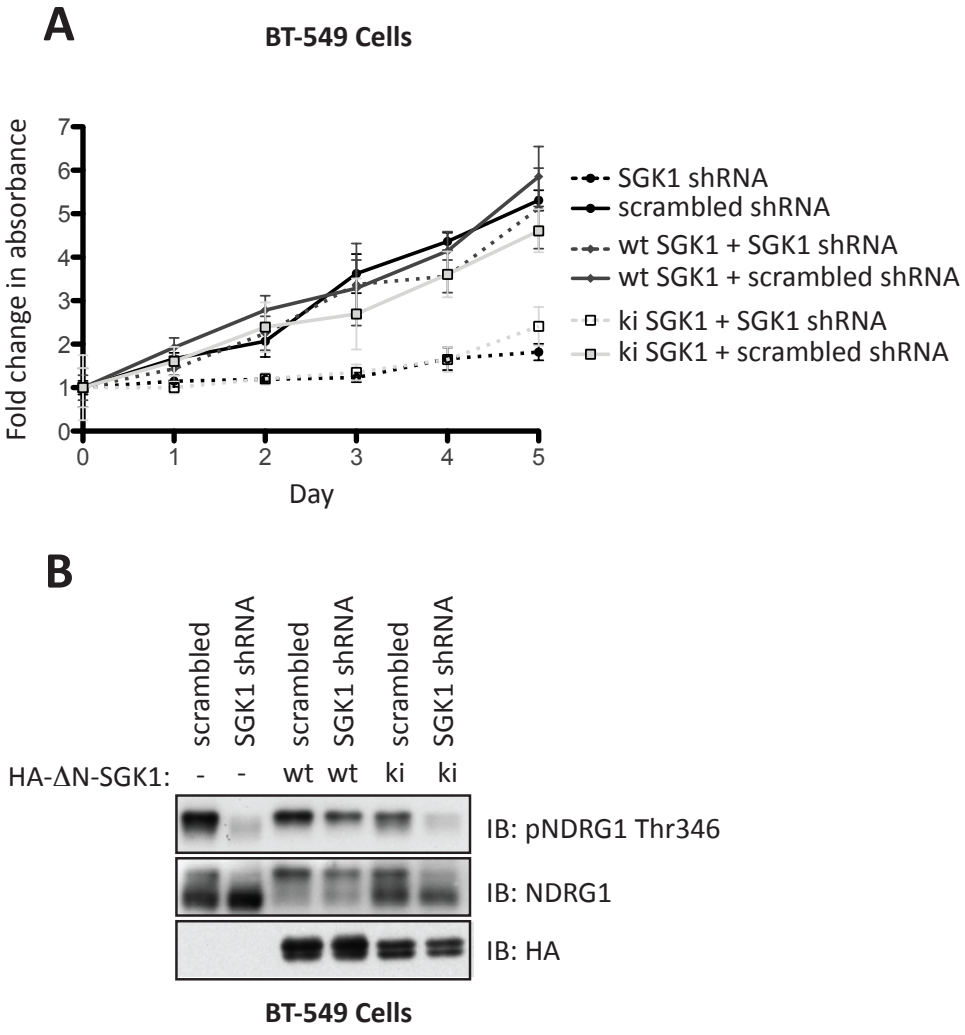

Figure 4.10 Rescue of SGK1 knockdown induced proliferation defect

BT-549 cells stably expressing HA–ΔN-SGK1 wild type (wt) or kinase-inactive (ki) constructs were transduced with SGK1 shRNA #D or scrambled shRNA. (**A**) Equal numbers of cells were seeded 48 hours post shRNA infection onto 96-well plates and allowed to adhere overnight. Cell proliferation was then determined by carrying out the MTS assay over a 5-day period with cells assayed at 24 hour intervals. Each data point is the average MTS assay of samples assayed in triplicate ± S.D. The data are presented as fold change relative to day 0 values (day 0 equals 24 h post-seeding). (**B**) Cells were lysed 72 h post infection with shRNAs and analysed by immunoblotting (IB) with the indicated antibodies.

4.2.4. SGK1 knockdown reduces the invasive ability of BT-549 cells

SGK1 has previously been reported to be important for the ability of various cell types to migrate (Eylenstein et al., 2011; Schmidt et al., 2012a; Schmidt et al., 2012b). Therefore, the effect of SGK1 knockdown on the ability of highly invasive BT-549 cells to invade into three-dimensional Matrigel matrix in a transwell invasion assay was next determined. Knockdown of SGK1 by two independent shRNAs markedly reduced the invasiveness of BT-549 cells in this assay (Figure 4.11A). To confirm that the impaired invasion was due to SGK1 knockdown, a rescue experiment was performed. Over-expression of wild type, but not kinase inactive SGK1, restored invasiveness of SGK1 shRNA-infected cells back to control levels (Figure 4.11B).

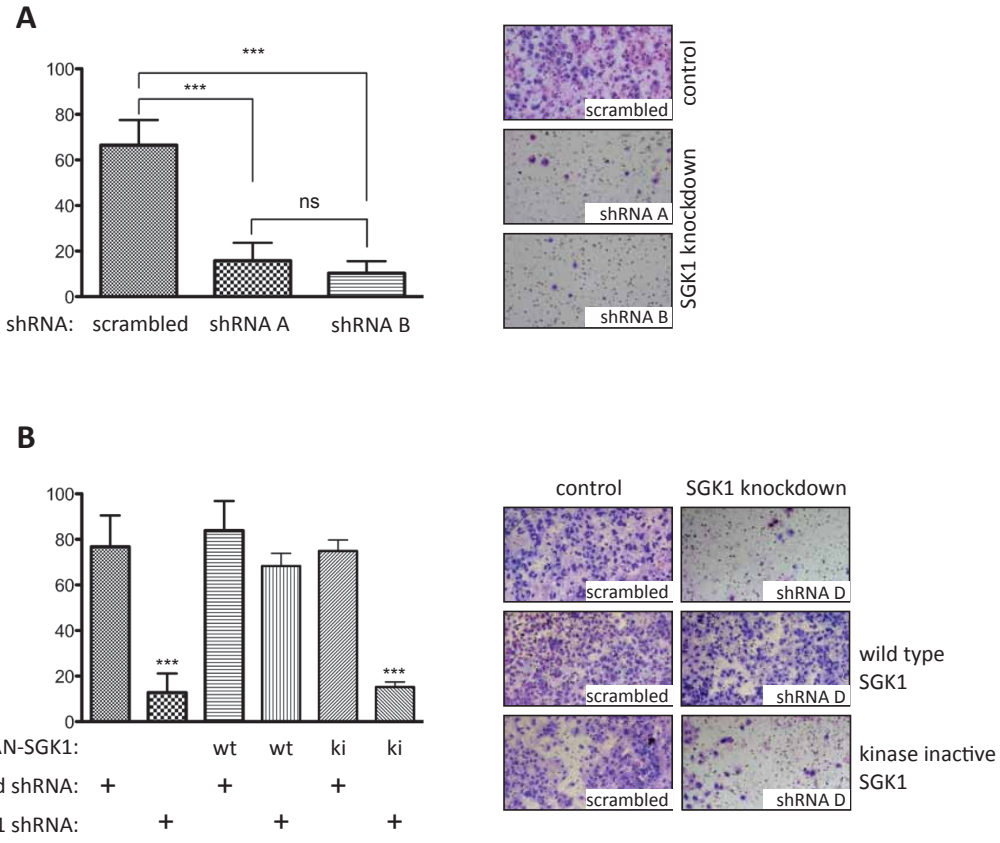

Figure 4.11 SGK1 knockdown reduces the invasive ability of BT-549 cells

(**A**) BT-549 cells were transduced with SGK1 or scrambled shRNAs. Cells were plated for a transwell invasion assay 48 hours post infection in triplicates using 10% FBS as a chemoattractant. Cells that had invaded through to the lower face of the filters were fixed and photographed (×10 magnification). Invasive cells were counted and the data are presented as the mean number of migrated cells ± S.D. (**B**) BT-549 cells stably expressing HA–ΔN-SGK1 wild type (wt) or kinase-inactive (ki) constructs were transduced with SGK1 shRNA #D or scrambled shRNA and 48 h post infection cells were plated for a transwell invasion assay as in (**A**). Statistical significance was assessed by ANOVA followed by Tukey's multiple comparison test using GraphPad Prism 5.0. ***P<0.001 compared with the scrambled control; ns, not significant.

4.2.5. SGK1 knockdown does not affect Akt signalling

To assess whether SGK1 depletion influences Akt signalling, phosphorylation status of PRAS40 and Akt Thr308 and Ser573 was assessed at 48 and 72 hours post-infection with SGK1 shRNAs in BT-549 cells. SGK1 knockdown did not influence Akt or PRAS40

phosphorylation (Figure 4.12). Furthermore, the effect of SGK1 knockdown on phosphorylation of other key Akt substrates, FoxO1/3, GSK3 and TSC2 was also assessed. Although SGK1 has been suggested to phosphorylate GSK3 (Sakoda et al., 2003) and FoxOs (Brunet et al., 2001), SGK1 knockdown in BT-549 cells had no effect on the phosphorylation of these proteins (Figure 4.12).

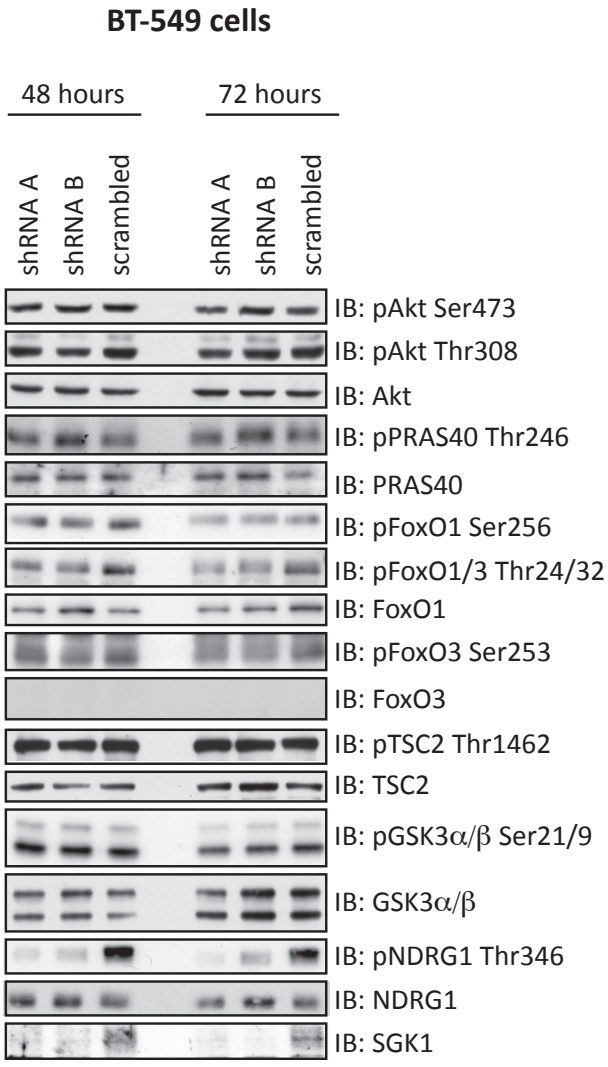

Figure 4.12 Knockdown of SGK1 does not affect Akt signalling

BT-549 cells were transduced with SGK1 and scrambled shRNAs. Cells were lysed at 48 and 72 hours post infection and the lysates were analysed with the indicated antibodies by immunoblotting (IB).

4.2.6. Akt inhibitor resistant cells are sensitive to mTOR inhibition

mTOR is a critical activator of SGK1. Therefore the sensitivity of the Akt inhibitor resistant cells to the mTOR kinase inhibitor AZD8055 (Chresta et al., 2010) was next investigated. BT-549, JIMT-1 and MDA-MB-436 were treated with increasing doses (1 nM – 10 μM) of AZD8055 for 72 hours. AZD8055 suppressed the proliferation of the three Akt inhibitor resistant cell lines tested (Figure 4.13). The GI_{50} values determined were approximately ~0.2 μM for BT-549, ~0.1 μM for JIMT-1, and ~0.2 μM for MDA-MB-436. Moreover, AZD8055 also suppressed phosphorylation of the T-loop (Thr256) and hydrophobic motif (Ser422) of endogenous SGK1 and phosphorylation of NDRG1 in the three Akt inhibitor resistant cells tested (Figure 4.14).

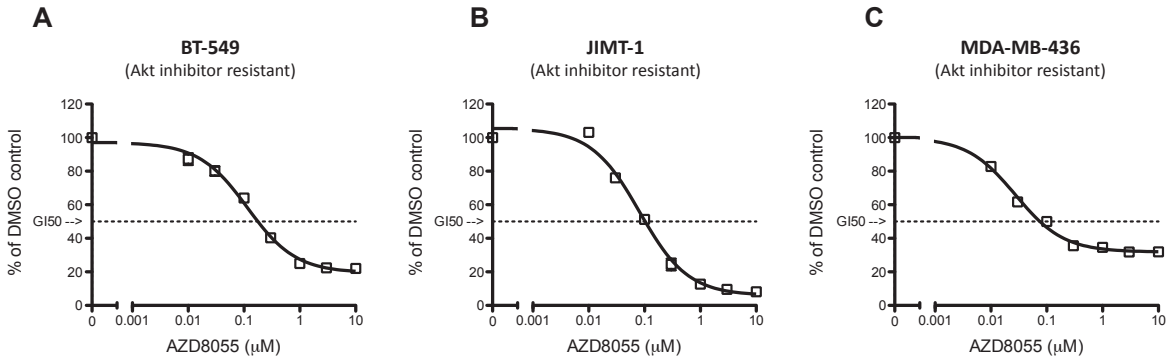

Figure 4.13 Cells with elevated SGK1 levels are sensitive to mTOR inhibitor AZD8055

The indicated Akt inhibitor resistant cells were exposed to DMSO or increasing concentrations (1 nM – 10 μM) of AZD8055 and 72 hours post inhibitor treatment cell viability was determined using MTS assay. Data were fitted to sigmoidal dose response curves using GraphPad Prism 5.0. The results are the means ± S.D. of a triplicate assay and are normalized to the DMSO control that was set to 100%.

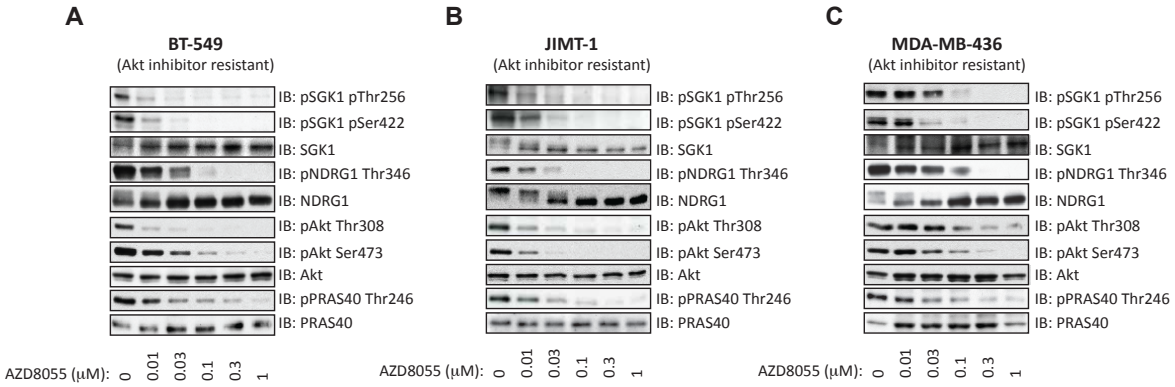

Figure 4.14 mTOR inhibitor AZD8055 inhibits the activation of SGK1

Cells were treated with the indicated doses of the AZD8055 mTOR inhibitor for 1 hour followed by lysis and immunoblot (IB) analysis with the indicated antibodies.

4.2.7. Akt can mediate NDRG1 phosphorylation in the absence of SGK

Interestingly, two Akt inhibitor sensitive cell lines examined (BT-474 and CAMA-1) and one cell line displaying high sensitivity to MK-2206 and intermediate sensitivity towards AZD5363 (SUM-52-PE) despite possessing low SGK1 mRNA/protein displayed significant phosphorylation of NDRG1 (Figure 4.7). On a long exposure, several other Akt inhibitor sensitive cells displayed observable phosphorylation of NDRG1 (Figure 4.7). One possibility to account for this would be if NDRG1 were phosphorylated by Akt rather than by SGK in the Akt inhibitor sensitive cells.

To test this, Akt inhibitor sensitive cell lines (BT-474, CAMA-1, T47D, SUM-52-PE, ZR-75-1 and HCC-1187) were treated with DMSO or 10 nM - 1 μM MK-2206 for 1 hour and analysed by immunoblotting. As expected, Akt inhibition decreased PRAS40 and FoxO1/3 phosphorylation in all cell lines examined. MK-2206 also suppressed phosphorylation of NDRG1 in a dose-dependent manner in five out of the six cell lines (Figure 4.15). NDRG1

phosphorylation was insensitive to MK-2206 only in HCC-1187 cells. To confirm the effect that Akt inhibition has on NDRG1 phosphorylation in Akt inhibitor sensitive cells, BT-474, CAMA-1 and T47D cells were also treated with the distinct AZD5363 Akt inhibitor and identical results were obtained (Figure 4.16). These results indicate that phosphorylation of NDRG1 is mediated by Akt in the absence of significant SGK levels. In HCC-1187 cells either SGK or another kinase would be expected to mediate NDRG1 phosphorylation.

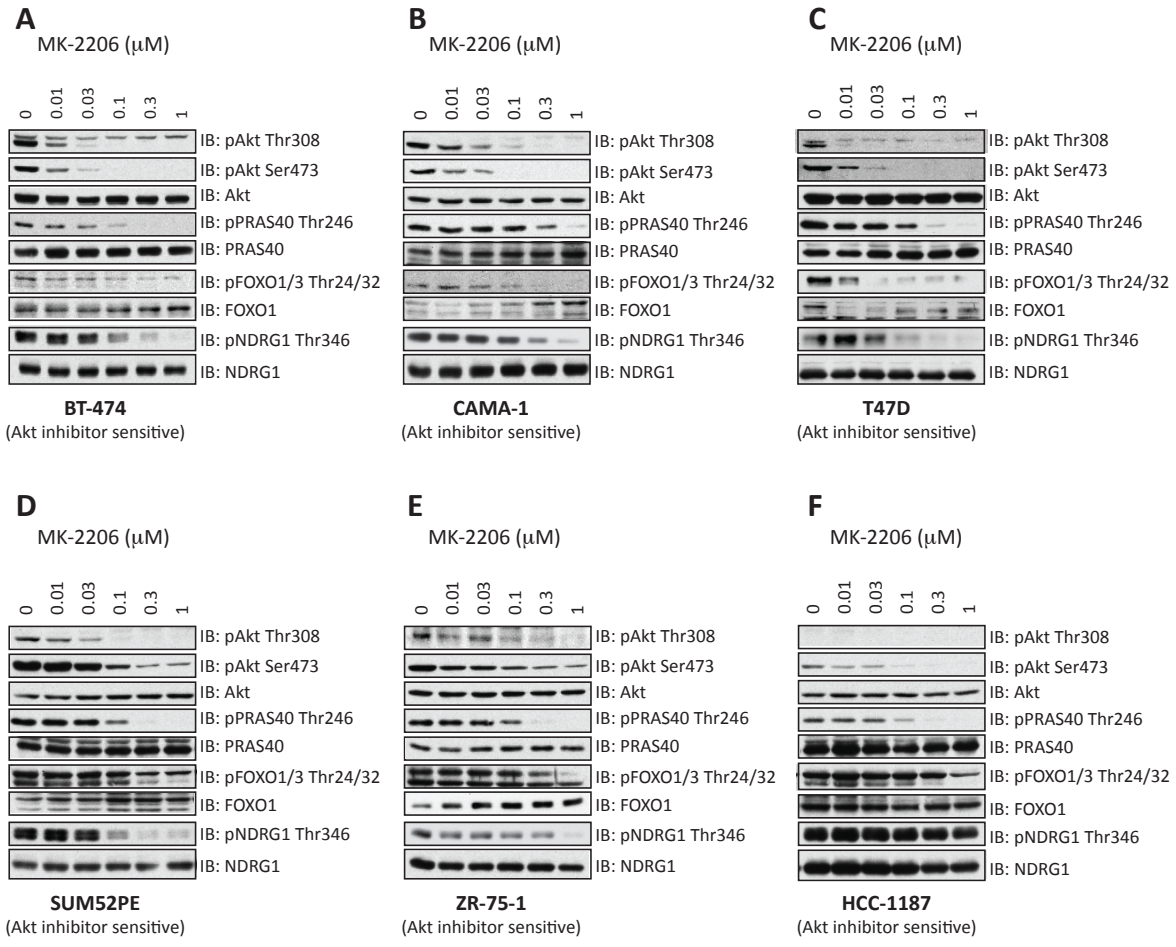

Figure 4.15 MK-2206 inhibits NDRG1 phosphorylation in Akt inhibitor sensitive cells

Cells were treated with the indicated doses of MK-2206 for 1 hour prior to lysis and immunoblot (IB) analysis with the indicated antibodies.

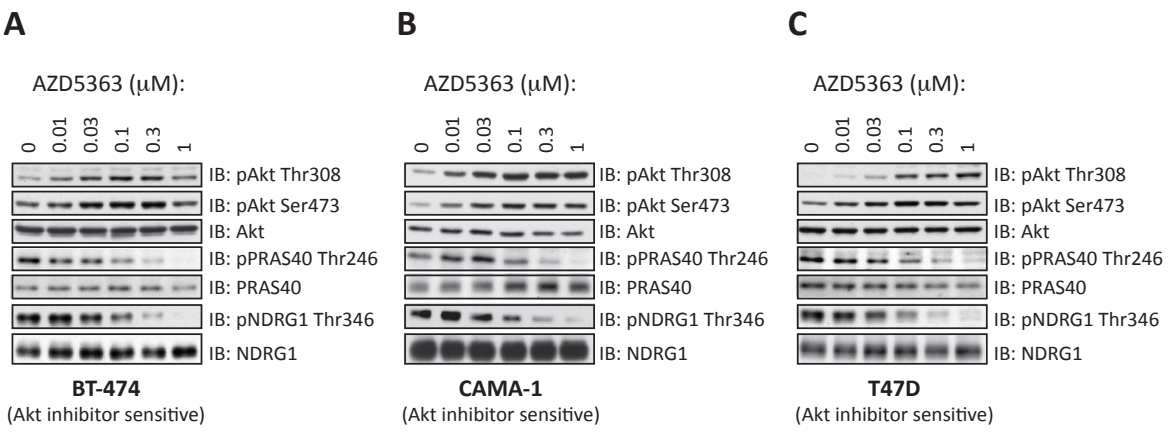

Figure 4.16 AZD5363 inhibits NDRG1 phosphorylation in Akt inhibitor sensitive cells

Cells were treated with the indicated doses of AZD5363 for 1 hour followed by lysis and immunoblot (IB) analysis with the indicated antibodies.

The effect of MK-2206 on PRAS40 and NDRG1 phosphorylation was also tested in six Akt inhibitor resistant cell lines (MDA-MB-436, JIMT-1, BT-549, HCC-1937, HCC-1806, MDA-MB-231) (Figure 4.17). As expected, Akt inhibition with MK-2206 induced dephosphorylation of PRAS40 in all cell lines tested. Phosphorylation of FoxO1/3 was also sensitive to MK-2206 in these cells. In contrast, NDRG1 phosphorylation was insensitive to MK-2206 in the Akt inhibitor resistant cells. Only in HCC-1937 cells a minor decrease in NDRG1 phosphorylation was seen in response to high (1 μM) concentration of MK-2206 indicating that in these cells Akt may contribute towards NDRG1 phosphorylation (Figure 4.17). These results were confirmed by treating two of the Akt inhibitor resistant cell lines (BT-549 and MDA-MB-436) also with the distinct Akt inhibitor AZD5363. As expected, AZD5363 also had no effect on NDRG1 phosphorylation in the cells tested (Figure 4.18). Notably, AZD5363 induced hyper-phosphorylation of Akt in all cell lines, as previously reported for ATP-competitive Akt inhibitors (Davies et al., 2012; Okuzumi et al., 2009).

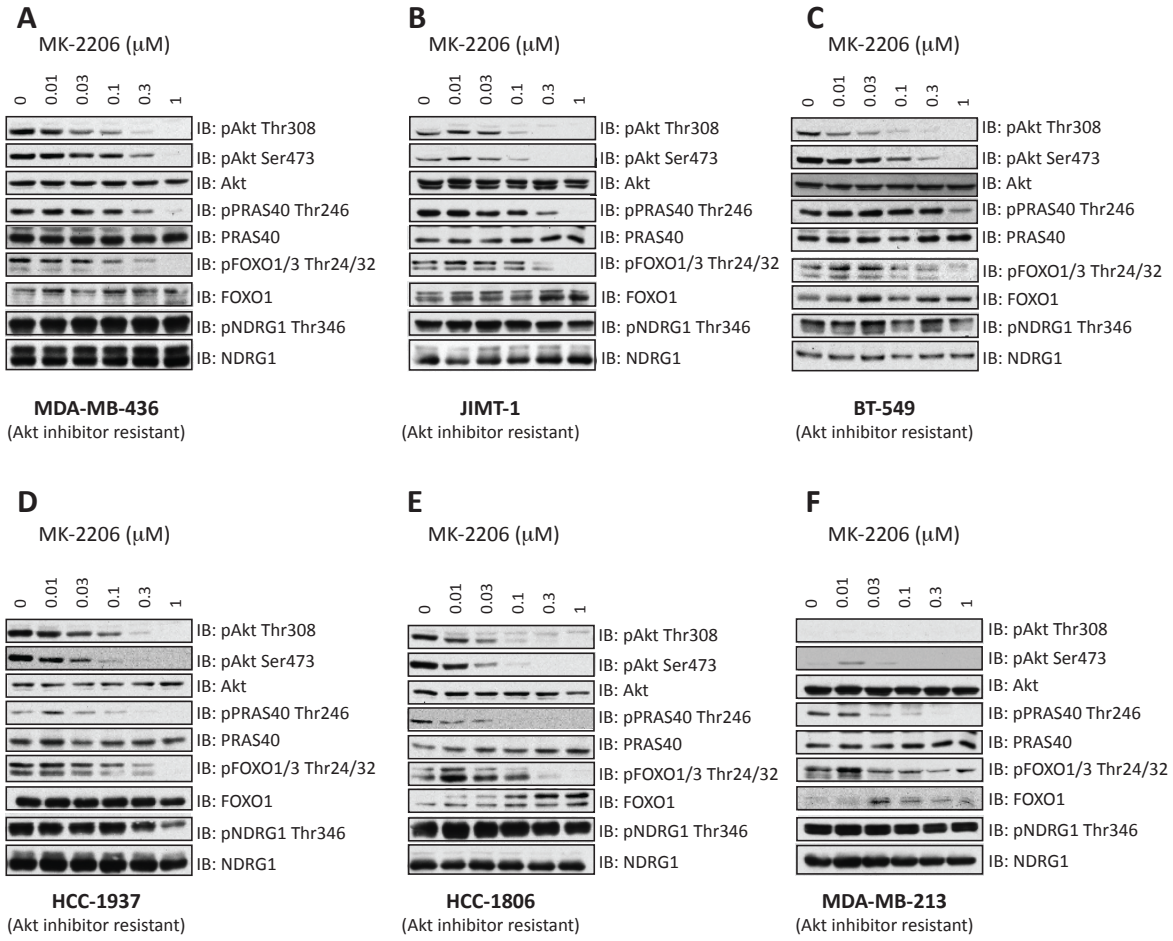

Figure 4.17 NDRG1 phosphorylation is resistant to MK-2206 in Akt inhibitor resistant cells

Cells were treated with the indicated doses of the MK-2206 for 1 hour followed by lysis and immunoblot (IB) analysis with the indicated antibodies.

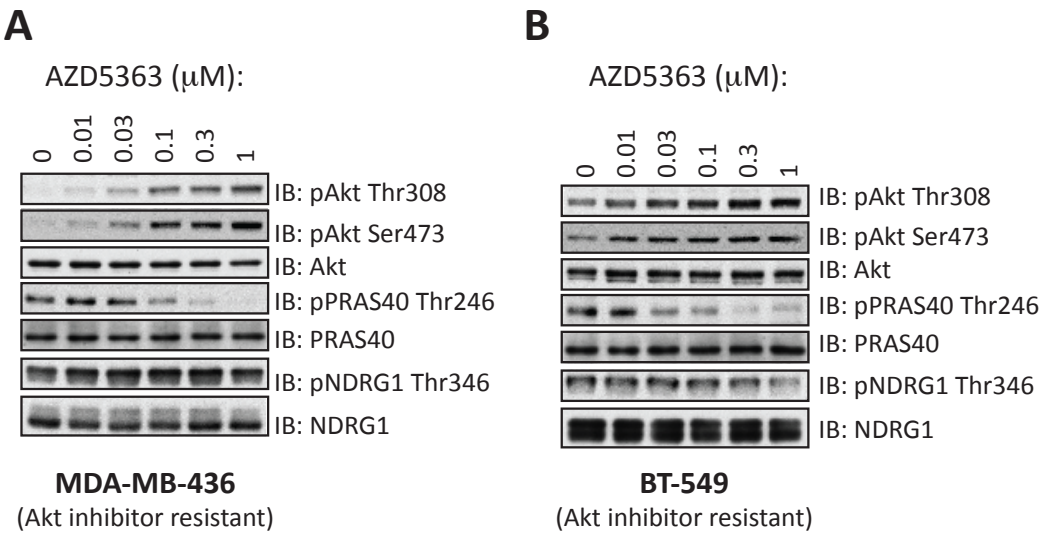

Figure 4.18 NDRG1 phosphorylation is resistant to AZD5363 in Akt inhibitor resistant cells

Cells were treated with the indicated doses of the AZD5363 for 1 hour followed by lysis and immunoblot (IB) analysis with the indicated antibodies.

To further study the regulation of NDRG1 phosphorylation outside of breast cancer cells, the effect of MK-2206 on IGF1 induced NDRG1 phosphorylation was assessed in HeLa (Figure 4.19) and HEK293 (Figure 4.20) cells. HeLa cells are reported to display detectable levels of SGK1 protein and to possess SGK1 knockdown sensitive NDRG1 phosphorylation (Murray et al., 2004). Consistent with this, NDRG1 phosphorylation was resistant to treatment with the Akt inhibitor MK-2206 in HeLa cells (Figure 4.19). In contrast, in HEK293 cells NDRG1 phosphorylation was sensitive to MK-2006 treatment (Figure 4.20A). Transfection of GST-ΔN-SGK1 into HEK293 cells induced MK-2206 resistant NDRG1 phosphorylation (Figure 4.20B). These observations indicate that SGK1 mediated NDRG1 phosphorylation is, as expected resistant to Akt inhibition. Furthermore, HEK293 cells are likely to possess low basal levels of SGK activity and in these cells basal NDRG1

phosphorylation is mediated by Akt or possibly by a combination of Akt and SGK. Notably, in both HeLa and HEK293 cells IGF1 induced PRAS40 phosphorylation was only modestly inhibited by MK-2206. As shown in Figure 4.19 and Figure 4.20, monitoring Akt Thr308/Ser473 phosphorylation and assessing S6K activity by blotting for phospho-S6K and phospho-S6 confirmed that Akt was efficiently inhibited in these cells.

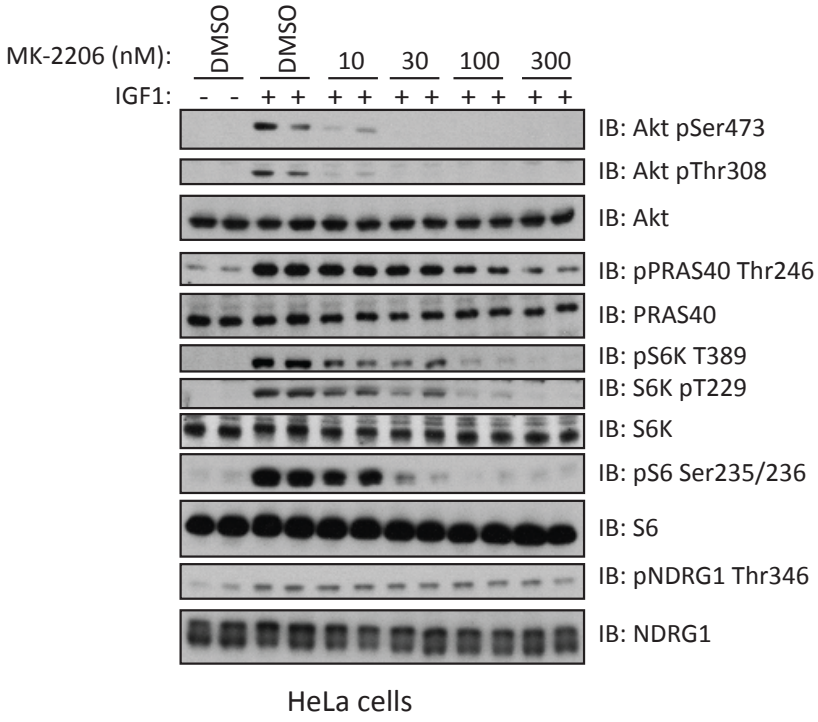

Figure 4.19 NDRG1 phosphorylation is resistant to MK-2206 in HeLa cells

HeLa cells were serum starved overnight and treated with the indicated doses of MK-2206 for 30 minutes prior to stimulation with 50 ng/ml IGF1 for 30 min. Cell lysates were analysed by immunoblotting (IB) with the indicated antibodies.

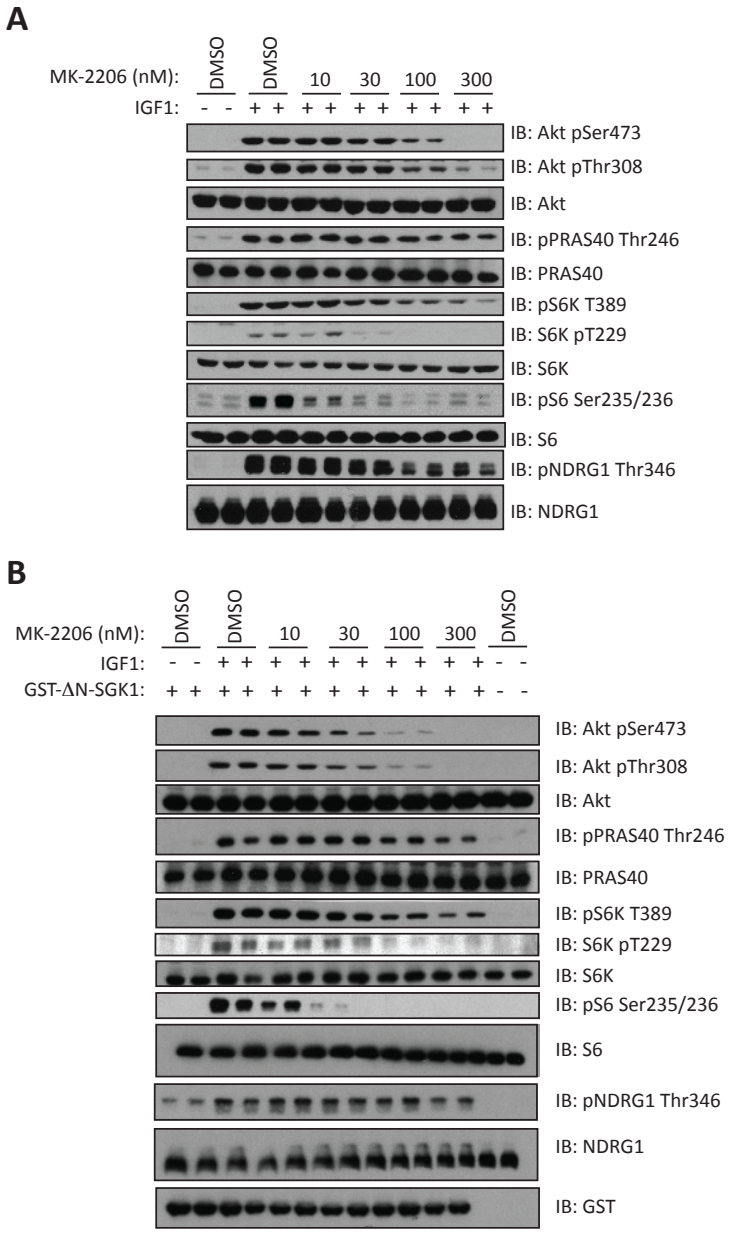

Figure 4.20 NDRG1 phosphorylation is resistant to MK-2206 in HEK293 cells over-expressing SGK1

(**A**) HEK293 cells were serum starved overnight and treated with the indicated doses of MK-2206 for 30 minutes prior to stimulation with 50 ng/ml IGF1 for 30 min. Cell lysates were analysed by immunoblotting (IB) with the indicated antibodies. (**B**) 24 hours post transfection with GST-ΔN-SGK1, HEK293 cells were serum starved for 16 hours and treated with the indicated doses of MK-2206 for 30 minutes followed by stimulation with 50 ng/ml IGF1 for 30 min. Cell lysates were analysed by immunoblotting with the indicated antibodies.

Akt has been reported to phosphorylate NDRG1 *in vitro*, albeit much less efficiently than SGK1 (Murray et al., 2004). To confirm this, the abilities of ΔN-SGK1 and Akt1 purified from HEK293 cells to phosphorylate NDRG1 *in vitro* were compared in parallel using equal activities of each kinase. As previously reported, both kinases phosphorylated NDRG1 *in vitro*, but SGK1 did this more efficiently than Akt (Figure 4.21). Similar results were observed with phosphorylation of Nedd4.2 that was also included in the experiment.

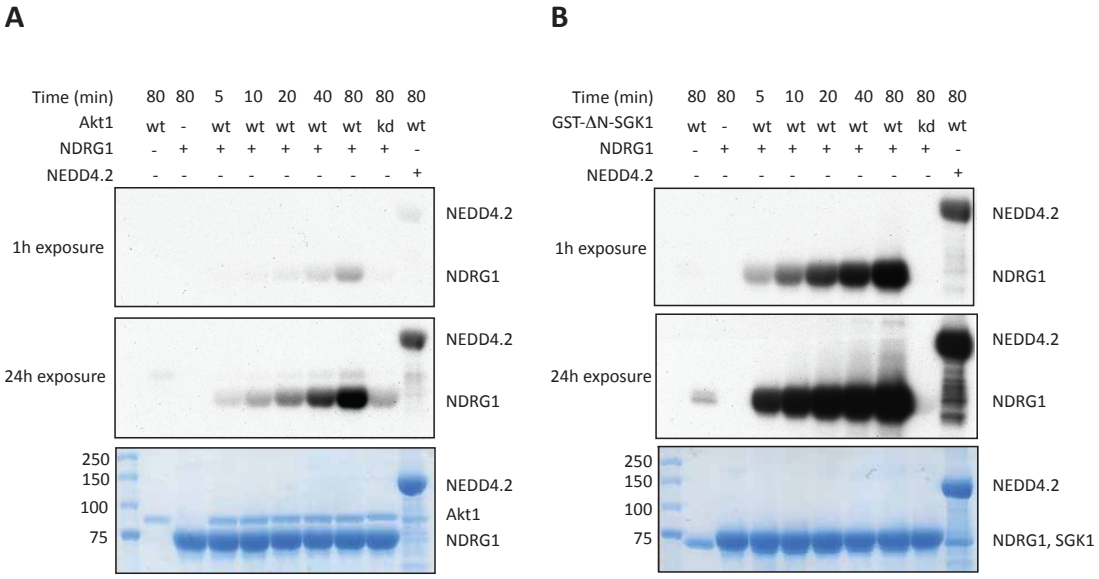

Figure 4.21 Phosphorylation of NDRG1 *in vitro by* SGK and Akt

5 μg of NDRG1 or Nedd4.2 purified from *E.coli* was incubated with equal activity of either wild type (wt) or kinase dead (kd) full length GST-Akt1 (245 ng) (**A**) or GST-ΔN-SGK1 (175 ng) (**B**) purified from HEK293 cells in the presence of 0.1 mM [γ^{32}P]-ATP and 10 mM magnesium acetate for the indicated times. Assays were terminated by addition of SDS sample buffer. Proteins were detected by Coomassie staining (lower panel) and incorporation of [γ^{32}P]-ATP was detected by autoradiography (upper panels).

4.3. Discussion

Elevated SGK1 expression in breast cancer cells correlates with SGK1- rather than Akt-driven proliferation

Results presented in this chapter demonstrate that SGK1 can mediate innate resistance of breast cancer cells to Akt inhibitors and therefore elevation of SGK1 expression represents one mechanism predicting Akt inhibitor resistance. In the Akt inhibitor resistant breast cancer cell lines displaying elevated SGK1 (BT-549, JIMT-1, MDA-MB-436 and HCC-1937), knockdown of SGK1 markedly suppressed cell proliferation. Rescue experiment performed in BT-549 cells demonstrated that the impaired proliferation was due to SGK1 deficiency and not due to off-target effects. SGK1 expression is induced by the glucocorticoid dexamethasone that is routinely used to reduce inflammation and to mitigate chemotherapy associated nausea in cancer patients (Volden and Conzen, 2013). This raises the possibility that administration of steroid hormones to cancer patients receiving Akt inhibitors might have the potential to induce SGK1 in tumour cells and thereby induce resistance to Akt inhibitors. Glucocorticoid receptor (GR) activation has different effects depending on cell type. For example in lymphocytes glucocorticoids induce apoptosis (Distelhorst, 2002) whereas in mammary epithelial cells (MEC) glucocorticoids are anti-apoptotic (Moran et al., 2000; Schorr and Furth, 2000) and in a xenograft model of lung cancer glucocorticoids induce resistance to apoptosis caused by cisplatin (Herr et al., 2003). Based on over-expression studies, glucocorticoid associated apoptosis resistance is suggested to be mediated by SGK1 in MECs (Mikosz et al., 2001). Moreover, SGK1 knockdown has been shown to blunt dexamethasone induced resistance to apoptosis

caused by chemotherapy in breast cancer cells (Wu et al., 2004). These observations and data presented in this chapter emphasise the key role that SGK1 activity can play in driving the expansion and survival of tumour cells. Indeed, by promoting induction of SGK1, steroid treatment could have the potential to promote many cancers.

Pro-proliferative and pro-survival roles have been described for SGK1 also outside of breast cancers. Most notably, SGK1 knockout mice are resistant to chemically induced colonic carcinogenesis (Nasir et al., 2009) and spontaneous intestinal tumour development in the APC deficient *apc*$^{min/+}$ mice (Wang et al., 2010). Additionally, SGK1 has been suggested to mediate interleukin 6 (IL6) dependent survival in cholangiocarcinoma cells in which SGK1 knockdown sensitises cells to chemotherapy and similar observations have been demonstrated for IL2 mediated survival of renal cancer cells (Amato et al., 2007; Meng et al., 2005). Further evidence for SGK1 acting as a cytokine responsive pro-survival gene comes from studies with multiple myeloma cells. In these cells *SGK1* is induced as a response to IL6, IL21 and tumour necrosis factor α and SGK1 knockdown inhibits proliferation and is associated with reduced expression of cell cycle promoting genes suggesting that SGK1 can influence cell cycle progression (Fagerli et al., 2011). Additionally, androgen stimulates *SGK1* expression and based on over-expression and knockdown studies SGK1 is reported to promote androgen mediated survival of prostate cancer cells (Shanmugam et al., 2007). SGK1 expression has been proposed to be down-regulated in some cancer types, such as prostate (Rauhala et al., 2005), ovarian (Chu et al., 2002) and hepatocellular carcinoma (Chung et al., 2002). It should be noted that without further functional characterisation correlating expression levels with physiological significance should be interpreted conservatively.

SGK1 appears to promote proliferation via mechanisms that are distinct from Akt

The Akt inhibitor resistant cell lines that possess elevated SGK1 displayed similar Akt signalling to Akt inhibitor sensitive cells and in all cell lines examined Akt inhibitors similarly reduced phosphorylation of the Akt substrates examined (PRAS40, FoxO1/3). Therefore resistance of the cells displaying elevated SGK1 to Akt inhibitors cannot simply be explained by lack of Akt activity. SGK1 knockdown impaired the capacity of Akt inhibitor resistant breast cancer cells to proliferate and SGK1 carrying out functions commonly attributed to Akt could account for this. Assessing the phosphorylation status of Akt and a subset of its substrates that are linked to pro-survival and proliferative functions, namely FoxO1/3, GSK3, PRAS40 and TSC2, revealed no differences between SGK1 and scrambled shRNA infected BT-549 cells. Therefore it appears unlikely that SGK1 supports cell proliferation via phosphorylating these substrates, at least in BT-549 cells.

The first report to identify FoxO3 as a target of SGK1 utilised *in vitro* phosphorylation assays and over-expression studies and reported that both SGK1 and Akt phosphorylate Thr32 and SGK1 additionally preferentially phosphorylates Ser315 whereas Akt favours Ser253 (Brunet et al., 2001). I did not examine FoxO3 Ser315 phosphorylation and failed to reliably detect total FoxO3 protein. It would of course be valuable to monitor Ser315 phosphorylation and total FoxO3 levels in the cells studied. Since the initial report of SGK1 mediated phosphorylation of FoxOs, a number of studies have reported similar observations. For instance, over-expression of SGK1 has been reported to prevent de-attachment induced de-phosphorylation of FoxO3 Thr32 (Shelly and Herrera, 2002) and SGK1 knockdown has been reported to cause a moderate decrease in stress induced

FoxO3 Thr32 phosphorylation (You et al., 2004). Also, dexamethasone induced FoxO3 Thr32 phosphorylation in breast epithelial cells has been shown to be partially blunted by siRNA-mediated knockdown of SGK1 (Wu et al., 2006) and based on immunofluorescence and reporter expression assays combined with SGK1 knockdown, SGK1 has been suggested to regulate FoxO3 in colon cancer cells (Dehner et al., 2008). In chemically induced colon tumours isolated from wild type and SGK1 knockout mice, tumours isolated from the knockouts displayed higher total levels of FoxO3. The knockouts also were more resistant to chemically induced carcinogenesis (Nasir et al., 2009).

Over-expressed SGK1 can also phosphorylate GSK3 (Sakoda et al., 2003). Notably, embryonic stem (ES) cells, in which activation of SGK, but not of Akt, is blunted due to a PIF-binding pocket mutation of PDK1, display normal phosphorylation of GSK3 and FoxO1 indicating that Akt is likely to be the predominant kinase regulating the phosphorylation of these substrates, at least in the absence of SGK activity (Collins et al., 2003). Based on results presented in this chapter, Akt appears to be the key kinase for FoxO1/3 Thr24/32 phosphorylation in the breast cancer cell lines examined. Further work is required to address to which extinct SGKs might contribute to FoxO phosphorylation in various cell types.

Given that SGK1 did not appear to simply replace Akt in the Akt inhibitor resistant cells, the mechanisms via which SGK1 promotes proliferation of these cells remain unknown. Many proposed SGK1 substrates, some of which are discussed below, could contribute to cell proliferation. Currently for many potential substrates validation at the endogenous

level is lacking. Nevertheless, a number of studies, as outlined above, have identified SGK1 as a promoter of survival and proliferation.

Over-expressed SGK1 phosphorylates mitogen-activated protein kinase kinase 4 (MAP2K4) (also known as JNKK1, MKK4 SEK1) at Ser80 (Kim et al., 2007). siRNA-mediated knockdown of SGK1 in breast cancer cells impairs stress induced phosphorylation of SEK1 and SEK1-JNK signalling, indicating that MAP2K4 may be a *bona fide* substrate of SGK1 (Kim et al., 2007). The same site also phosphorylated by Akt (Park et al., 2002). SGK1 or Akt mediated phosphorylation of MAP2K4 inhibits JNK activation thereby down-regulating stress activated MAPK signalling that promotes apoptosis (Kim et al., 2007; Park et al., 2002). Inhibition of MAP2K4 through SGK1 may be one of the cytoprotective effects of SGK1 and it would be interesting to examine MAP2K4 Ser80 phosphorylation status in the cell lines studied in this chapter.

SGK1 has been linked to activation of the Nuclear factor-κB (NF-κB) transcription factor via phosphorylation of the IκB kinase (IKK) complex that is important for the activation of NF-κB. NF-κB regulates transcription of many pro-proliferative and –survival genes (Karin, 2006). SGK1 has been shown to phosphorylate the IκB kinase α (IKKα) *in vitro* and SGK1 knockdown reduces IGF1 induced IKKα phosphorylation (Tai et al., 2009). Furthermore, aldosterone stimulated IKKα/β dependent NF-κB transcriptional activity in renal collecting duct principal cells is partially sensitive to SGK1 knockdown (Leroy et al., 2009) and NF-κB activation in response to mineralocorticoids is blunted in SGK1 knockout lung fibroblasts (Vallon et al., 2006). SGK1 has also been suggested to mediate glucocorticoid induced breast cancer cell survival via the activation of NF-κB pathway (Zhang et al., 2005).

Recently the physiological importance of SGK1-NF-κB signalling for cell survival was demonstrated in *Xenopus* embryos (Endo et al., 2011). SGK1 knockdown in the embryos caused defective development due to excessive apoptosis, a phenotype rescued by re-expression of SGK1. SGK1 knockdown in the embryos was associated with decreased expression of NF-κB targets and increased expression of death-inducing signalling complex (DISC) components. Mechanistically SGK1 is suggested to induce NF-κB targets that cause a subsequent decrease of DISC gene expression (Endo et al., 2011).

As previously discussed, SGK1 regulates a large number of channels and transporters [reviewed in (Lang and Shumilina, 2013)]. For instance, stimulation glucose and amino acid transporters by SGK1 may aid cancer cells to meet their energy demands. SGK1 also stimulates the potassium channel Kv1.3 and growth factor stimulated activity of potassium channels is correlated with cell proliferation in multiple cell lines, including breast cancer cells and Kv1.3 blockers have been reported to disrupt IGF1 induced proliferation (Gamper et al., 2002; Lang et al., 2006). K^+ channels are also critical for the maintenance of negative membrane potential that is necessary for Ca^{2+} entry into cells. Ca^{2+} is critical for many cellular functions such as progression through the cell cycle. Intracellular Ca^{2+} levels can be raised either through mobilisation from intracellular stores or entry across the cell membrane (Roderick and Cook, 2008). Release of Ca^{2+} from intracellular stores activates the Ca^{2+} release-activated Ca^{2+} channel (CRAC) leading to store operated Ca^{2+} entry (SOCE). CRAC is composed of Orai pore forming subunits that are activated by Ca^{2+} sensing STIM1/2 proteins upon depletion of Ca^{2+} from the endoplasmic reticulum (ER) (Feske, 2010). Ora1 is critical for cell proliferation [reviewed in

(Lang et al., 2012)] and additionally Ora1 and STIM1 have been shown to be critical for breast cancer cell migration and metastasis (Yang et al., 2009). SGK1 stimulates SOCE at least partially via inhibition of Nedd4-2 and via NF-κB activation mediated transcriptional up-regulation of *Ora1* and *STIM1* expression (Eylenstein et al., 2011; Eylenstein et al., 2012). SGK1 knockout bone marrow derived mast cells (BMMC) express decreased levels of Ora1 and STIM1 and only in wild type BMMCs stimulation of the PI3K pathway induces nuclear translocation of the NF-κB p65 subunit and *STIM1* and *Ora1* gene expression (Eylenstein et al., 2012).

SGK1 is critical for the invasive ability of BT-549 cells

Metastasis represents the major cause of cancer-related mortality and the ability to migrate and invade is critical for metastasis. Cell migration and invasion are multistep processes that involve the formation of F-actin rich protrusions at the leading edge followed by contraction of the trailing edge. Invasive protrusions (invadopodia) have the capacity to degrade matrix and to thus overcome barriers of migration. Invadiopodia are also involved in direction sensing and chemotaxis [reviewed in (Bravo-Cordero et al., 2012)].

Breast cancer cell migration *in vitro* and breast cancer metastasis *in vivo* are dependent upon Ca^{2+} signalling and in particular on Orai and STIM1 that regulate focal adhesion turnover in migrating cells (Yang et al., 2009). As discussed above, Ora1 and STIM1 are regulated by SGK1 (Eylenstein et al., 2011; Eylenstein et al., 2012). SGK1 dependent stimulation of SOCE is important for cell migration as SGK1 deficient BMMCs display a reduced ability to migrate, especially following stimulation with thapsigargin, a

sarcoplasmic/endoplasmic reticulum Ca^{2+}-ATPase inhibitor that stimulates SOCE by causing Ca^{2+} release from intracellular stores (Eylenstein et al., 2011). Therefore it is possible that the impaired ability of BT-549 breast cancer cells to invade following SGK1 depletion could be at least partially accounted for by disturbances to Ca^{2+} uptake. SGK1 dependent migration and invasion have also recently also been linked to control of vinculin phosphorylation and membrane androgen receptors (Schmidt et al., 2012a).

Akt can mediate NDRG1 phosphorylation in the absence of significant SGK activity

Results presented in this chapter emphasise that caution is required when employing NDRG1 as a surrogate marker for SGK1 activity. In the cell lines displaying high levels of SGK1, NDRG1 phosphorylation is insensitive to Akt inhibitors and knockdown of SGK1 inhibits NDRG1 phosphorylation. By contrast, NDRG1 phosphorylation is suppressed by Akt inhibitors, but not by SGK1 knockdown, in several cell lines displaying high Akt activity and low SGK1 indicating that, at least in these cells, Akt, rather than SGK1, phosphorylates NDRG1. In agreement with previous studies (Murray et al., 2004), Akt can phosphorylate NDRG1 *in vitro*, albeit less efficiently than SGK1. SGK1 has been reported to phosphorylate NDRG1 at three C-terminal residues (Thr328, Ser330 and Thr346) and NDRG2 in the corresponding residues. Phosphorylation of NDRG1 by SGK1 primes NDRG1 for further phosphorylation by GSK3 at another three residues (Ser342, Ser352 and Ser362) (Murray et al., 2004). The precise molecular function of NDRG1 is unknown and consequently the role of its phosphorylation by SGK1/Akt and GSK3 remains uncharacterised.

NDRG1 expression is regulated via multiple mechanisms including up-regulation by stress signals such as changes to redox potential (Kokame et al., 1996), nickel toxicity (Zhou et

al., 1998), DNA damage, elevated p53 (Kurdistani et al., 1998), and hypoxia (Le and Richardson, 2004; Park et al., 2000) and down-regulation by the proto-oncogene N-myc (Shimono et al., 1999). Both oncogenic and tumour suppressive roles have been proposed for NDRG1. Whilst decreased NDRG1 expression has been described in a number of tumour types, including breast cancer, increased NDRG1 expression has also been described in a number of cancers (Melotte et al., 2010). It is unclear whether these contrasting observations could be due to tissue-specific functions of NDRG1. Furthermore, as the precise molecular function(s) of NDRG1 remain poorly characterised, it is difficult to correlate expression levels with cellular and physiological outcomes.

Several studies have correlated the levels of NDRG1 expression with invasiveness and proliferation (Melotte et al., 2010). For example, ectopic over-expression of NDRG1 in MDA-MB-468 breast cancer cells is reported to suppress *in vitro* invasiveness (Bandyopadhyay et al., 2004) and ectopic over-expression of NDRG1 in cultured MCF-7 breast cancer cells is reported to suppress proliferation rate (Kurdistani et al., 1998). The effect of SGK1 knockdown on reducing the proliferation rate of Akt inhibitor resistant cell lines and the invasive ability of BT-549 cells could therefore be also at least partially mediated via altered function of NDRG1 due to its de-phosphorylation. In future it would be of interest to dissect the precise molecular role(s) that phosphorylation of NDRG1 by SGK1/Akt and GSK3 plays. NDRG1 has additionally been linked to regulation of NF-κB (Hosoi et al., 2009) and therefore the effects that accumulating evidence shows that SGK1 has on NF-κB could at least in theory be also partially mediated via NDRG1.

Overall conclusion

Elevated SGK1 might be deployed to predict resistance of breast-cancer-derived cells to Akt inhibitors. This finding will be of relevance to the numerous clinical trials evaluating the therapeutic potential of Akt inhibitors for the treatment of cancer. In future work it would be important to gauge whether the cancers most responsive to Akt inhibitors do indeed possess low levels of SGK1 protein/mRNA.

It would also be important to establish whether potent and selective inhibitors of SGK1 would inhibit proliferation of tumour cells displaying elevated SGK1 activity. Moreover, as Akt and SGK1 are related kinases, it might be feasible to develop inhibitors that target both enzymes. It should be noted that mechanisms other than enhanced SGK1 activity are also likely to contribute to the resistance to Akt inhibitors. Indeed, one of the Akt-inhibitor-resistant cell lines analysed (MDA-MB-157) displayed both low SGK1 levels and NDRG1 phosphorylation. This emphasises the importance of future work to profile a much larger number of breast and other types of cancer cells to establish the proportion of different tumours that are resistant to Akt inhibitors and also display elevated SGK1 as well as elevated NDRG1 phosphorylation that is not suppressed by Akt inhibitors. Monitoring NDRG1 phosphorylation responses following administration of Akt inhibitors could represent an effective general biomarker to assess SGK1 activity in tumour cells. As illustrated in Figure 4.22, results presented in this chapter indicate that breast cancers most likely to be sensitive to Akt inhibitors would be those displaying high Akt, low SGK1 mRNA/protein and in which phosphorylation of NDRG1 is suppressed by Akt inhibitors. In contrast, tumours displaying elevated SGK1 mRNA/protein in which NDRG1

phosphorylation is not suppressed by Akt inhibitors are likely to be more resistant to Akt inhibitors. Such tumours might be better treated with signal transduction suppressors that reduce SGK1 activity, such as mTOR inhibitors. Finally, more work is also needed to determine whether administration of steroids to patients has the potential to induce SGK1 expression and cause resistance to Akt inhibitors.

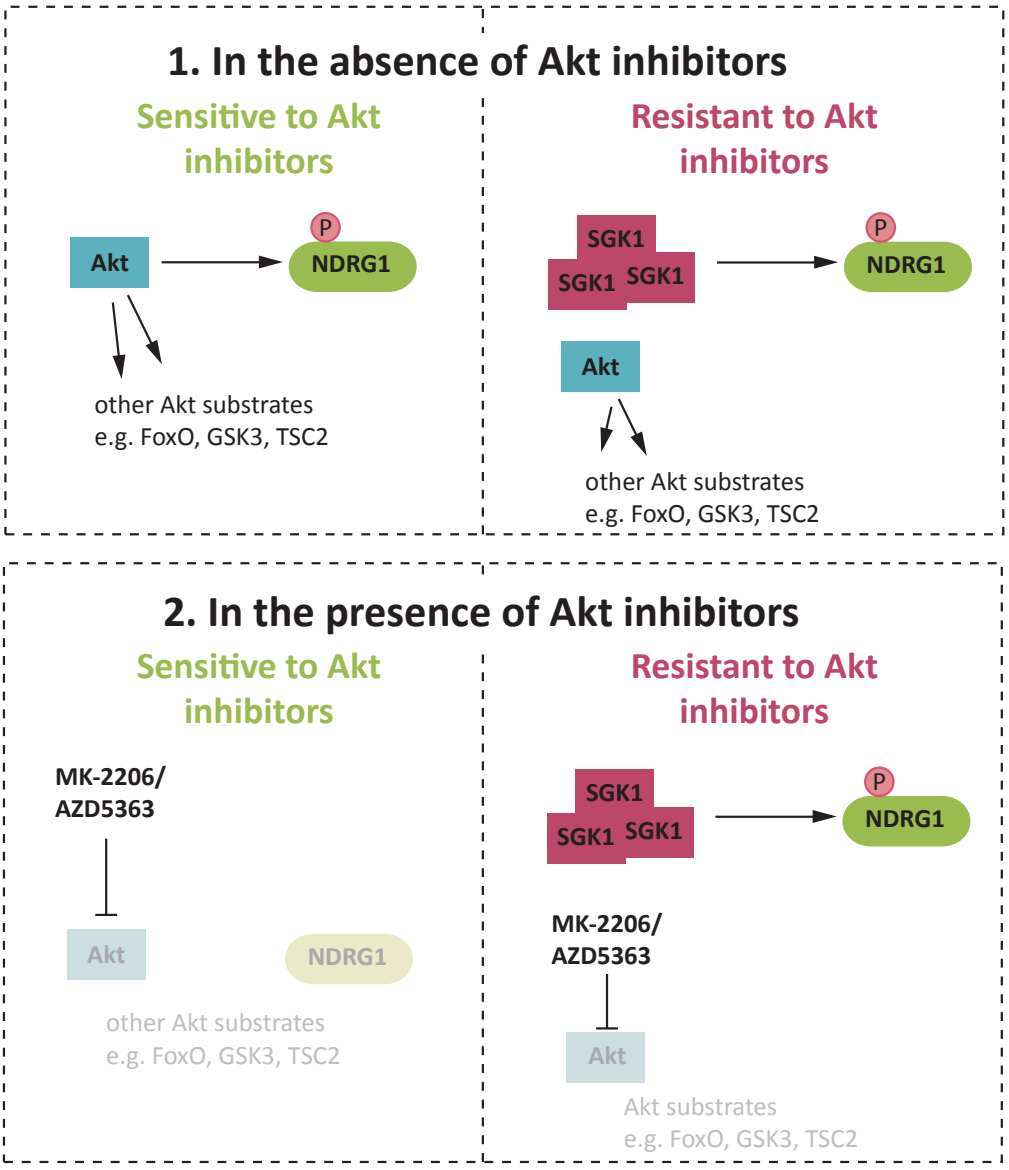

Figure 4.22 Differential sensitivity of NDRG1 phosphorylation to Akt inhibitors in Akt inhibitor sensitive and resistant cells

5. Sustained Akt inhibition leads to bi-phasic up-regulation of SGK3

5.1. Introduction

Results presented in Chapter 4 demonstrate that breast cancer cells expressing elevated levels of SGK1 protein and mRNA are intrinsically resistant to Akt inhibitors and that in these cells SGK1 is a key proliferation driver. Moreover, results presented in Chapter 4 also indicate that Akt can mediate NDRG1 phosphorylation in the absence of significant SGK activity. Careful consideration of feedback regulation that governs signal transduction cascades is emerging as a critical area of cancer drug discovery. Comprehensive understanding of the long-term consequences of inhibiting components of the PI3K pathway will aid in rational development of therapies that effectively turn off this signalling network and minimise the up-regulation of intrinsic resistance mechanisms. Due to their similarities, SGK family members are obvious candidates for kinases that could compensate for the loss of Akt. Therefore I decided to study whether chronic Akt inhibition could lead to emergence of compensatory signalling mediated by SGKs.

In this chapter I describe a novel method of feedback regulation that operates within the PI3K pathway. I show that in Akt inhibitor sensitive cells sustained Akt inhibition leads to recovery of NDRG1 phosphorylation, which is due to an elevation in the levels and the catalytic activity of SGK3. I present evidence indicating that downstream of Akt the regulation of SGK3 levels is dependent on mTORC1. I furthermore also demonstrate that

exposure to sustained Akt inhibition reduces the efficiency of Akt inhibitors in cells and present data that implies that the induction of SGK3 is responsible for the reduction in cells' sensitivity to Akt inhibitors.

Finally, I also present preliminary data implying that the model of activation of endogenous SGK3 by PI3K, PDK1 and mTORC2, as outlined in the introduction, may need to be re-evaluated. mTORC2 mediated HM-site phosphorylation is not necessary for the activation of Akt and accordingly Akt is insensitive to chronic mTORC1/2 inhibition. In contrast, several studies have demonstrated that for SGK and S6K HM-site phosphorylation is required for subsequent T-loop phosphorylation and activation (Pearce et al., 2010b). This model is based upon studies that have analysed SGK1 isoform. Unlike SGK1, SGK3, however, contains a phosphoinositide binding PX domain. Interestingly, data that I present in this Chapter suggests that SGK3 is insensitive to long term mTORC1/2 inhibition. This suggests that the PX domain of SGK3 may render activation of SGK3 analogous to that of the PH domain containing Akt.

5.2. Results

5.2.1. Sustained Akt inhibition causes recovery of NDRG1 phosphorylation and elevation of SGK3

In order to investigate whether treatment of Akt inhibitor sensitive cells with Akt inhibitors for a long period of time could induce activation of SGK isoforms, BT-474, CAMA-1 and ZR-75-1 cells were challenged with sustained Akt inhibition (up to 5 and 10

days) (Figure 5.1). Long-term treatment of the three cell lines with the two structurally and mechanistically distinct Akt inhibitors, MK-2206 and AZD5363, strikingly revealed that whilst Akt remained inhibited throughout the experiment, as assessed by sustained de-phosphorylation of the Akt substrate PRAS40, phosphorylation of NDRG1 protein was sensitive to an acute one hour treatment with both Akt inhibitors but was largely restored by 24 hours and was completely insensitive to five and ten days of Akt inhibition (Figure 5.1). Furthermore, as expected, MK-2206 induced sustained de-phosphorylation of Akt Thr308 and Ser473, whilst AZD5363 induced sustained hyper-phosphorylation at both sites (Figure 5.1). Strikingly, monitoring levels of SGK isoforms throughout the time-course revealed a clear increase in the levels of SGK3 following five and ten days of Akt inhibition. Levels of SGK1 and SGK2 isoforms remained undetectable throughout the time-course (Figure 5.1).

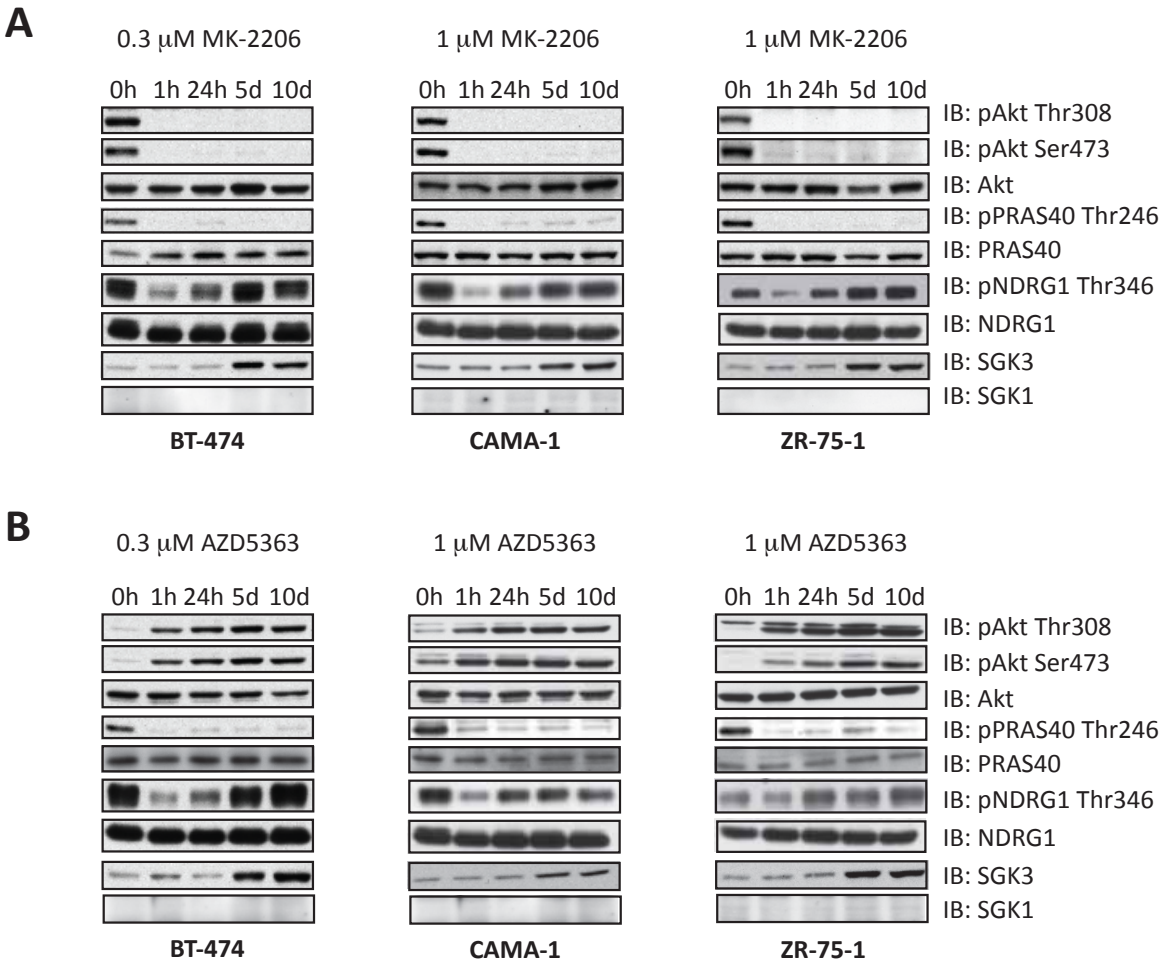

Figure 5.1 Sustained Akt inhibition leads to recovery of NDRG1 phosphorylation and is associated with elevation of SGK3 levels in Akt inhibitor sensitive cell lines

(**A**) The indicated Akt inhibitor sensitive cells were treated with MK-2206 (0.3 μM for BT-474 and 1 μM for CAMA-1 and ZR-75-1 cells) for the indicated time points or for 10 days with DMSO. All cells were seeded at the same time and treatment commenced in a staggered fashion. For DMSO control, 24 hour and 1 hour samples approximately $1x10^4$, for 5 day treatment approximately $1x10^5$ and for 10 day treatment approximately $1x10^6$ cells were seeded per well of a 6-well plate. Growth medium was replaced with fresh medium containing either DMSO or inhibitor on days 3, 6 and 8. Cells were harvested all at the same time at approximately 80% confluency and the lysates were analysed by immunoblotting (IB) with the indicated antibodies. (**B**) As in (**A**) except cells were treated with the indicated concentrations of AZD5363.

5.2.2. Akt inhibition up-regulates SGK3 protein and mRNA levels

In order to further analyse the increase in SGK3 protein levels, ZR-75-1 cells were treated with the two distinct Akt inhibitors for 0, 2, 4, 6, 8 and 10 days and the levels of SGK3 protein were monitored by quantitative immunoblotting using Li-Cor system. This time-course analysis confirmed the initial observation that NDRG1 phosphorylation is resistant to chronic Akt inhibition and that sustained Akt inhibition is associated with increased SGK3 levels (Figure 5.2A-B). Throughout the time-course Akt remained inhibited, as assessed by sustained de-phosphorylation of the Akt substrates PRAS40 and FoxO1/3, and sustained down-regulation of mTORC1 signalling, as monitored by following S6 phosphorylation (Figure 5.2A-B). Both Akt inhibitors led to approximately two-fold up-regulation of SGK3 protein levels after two days of Akt inhibition and by four/six days of Akt inhibition SGK3 protein up-regulation was around four-fold and it plateaued at these levels. Levels of both SGK1 and SGK2 remained unaltered throughout the experiment (Figure 5.2A-B).

In parallel, qRT-PCR analysis was undertaken to assess the levels of SGK isoform mRNA levels following sustained Akt inhibition. Following two days of Akt inhibition SGK3 mRNA levels were elevated by approximately two-to-three-fold. At later time-points approximately five-to-eight-fold up-regulation in comparison to basal (DMSO control) levels was detected. mRNA levels of the related SGK1 and SGK2 isoforms were not altered by sustained Akt inhibition (Figure 5.2C-D).

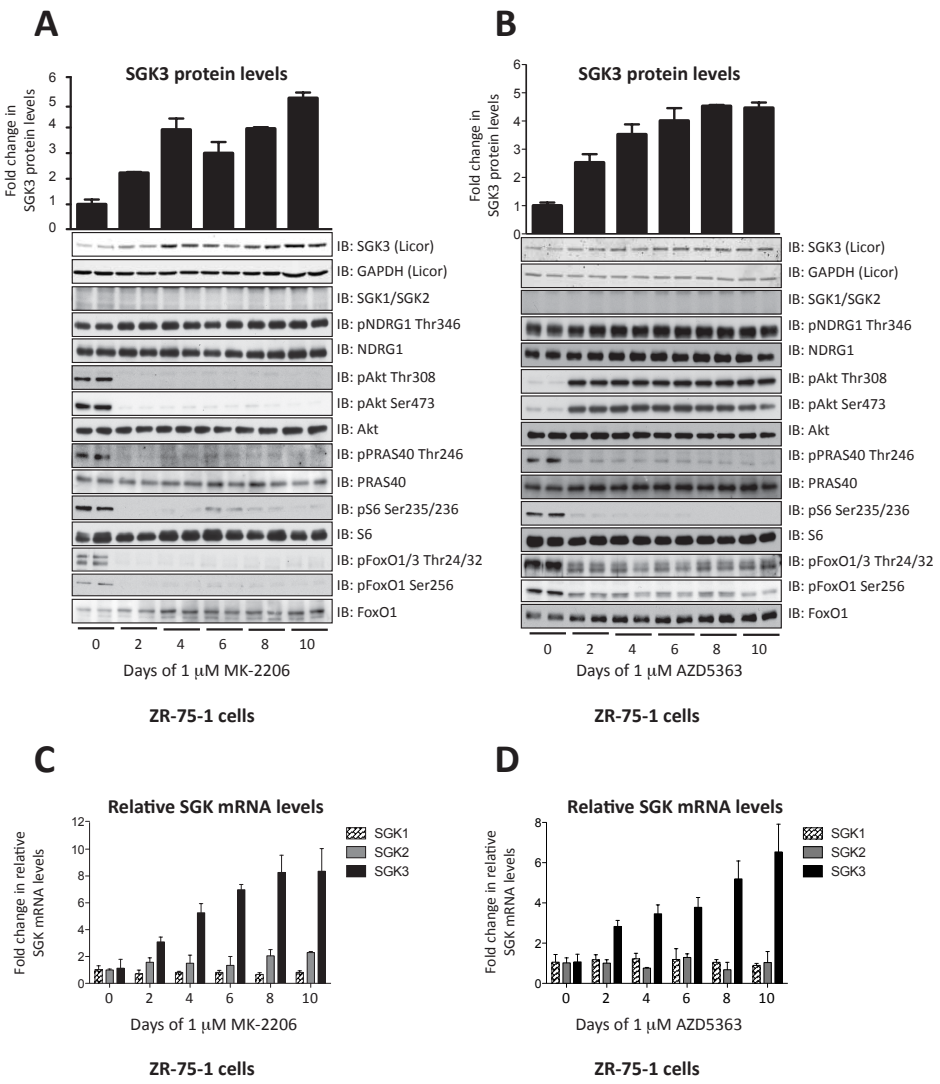

Figure 5.2 Chronic Akt inhibition up-regulates SGK3 protein levels approximately 4-fold

(**A**) ZR-75-1 cells seeded onto 6-well plates in duplicates were treated with 1 μM MK-2206 for 2, 4, 6, 8 or 10 days or with DMSO for 10 days. All cells were seeded at the same time and treatment commenced in a staggered fashion. Growth medium was replaced with fresh inhibitor or DMSO containing medium on days 3 and 8. On day 5 all cells were re-plated in the presence of MK-2206 or DMSO. All samples (approximately 80% confluent) were harvested at the same time. For SGK3 and GAPDH quantitative Li-Cor immunoblot (IB) analysis was undertaken and the data are presented as relative SGK3 levels over GAPDH levels ± S.D. Basal levels were set to 1. (**B**) as in (**A**) except 1 μM AZD5363 was used. (**C**) as in (**A**) except total mRNA was isolated and SGK mRNA levels were determined by qRT-PCR. The data were normalised to an internal 18S control and are presented as relative levels in comparison with control cells (DMSO). Results represent the means ± S.D of two independent samples each assayed in duplicate. (**D**) as in (**C**) except 1 μM AZD5363 was used.

5.2.3. SGK3 levels return to basal following re-activation of Akt

Next an inhibitor washout experiment was performed in order to assess the effect of re-activating Akt on SGK3 levels. ZR-75-1 cells were first treated with the ATP-competitive Akt inhibitor AZD5363 for four days in order to up-regulate SGK3. The inhibitor was then washed out and fresh growth medium lacking the inhibitor was added for 2 – 72 hours (Figure 5.3). This revealed that Akt was rapidly re-activated as phosphorylation of the Akt substrate PRAS40 reached normal levels already two hours after the inhibitor was removed. Recovery of mTORC1 activity, however, took longer and, as assessed by S6 phosphorylation, was apparent 12 hours after the inhibitor was removed. SGK3 levels were partially decreased 12 hours after the inhibitor washout and had returned to approximately basal levels (similar to DMSO control) 24 hours after the washout. Notably, AZD5363 induced Akt hyper-phosphorylation returned to basal levels only 48 hours after the washout (Figure 5.3). As SGK3 levels return to basal following Akt re-activation, the data suggest that Akt activity dynamically regulates SGK3 levels.

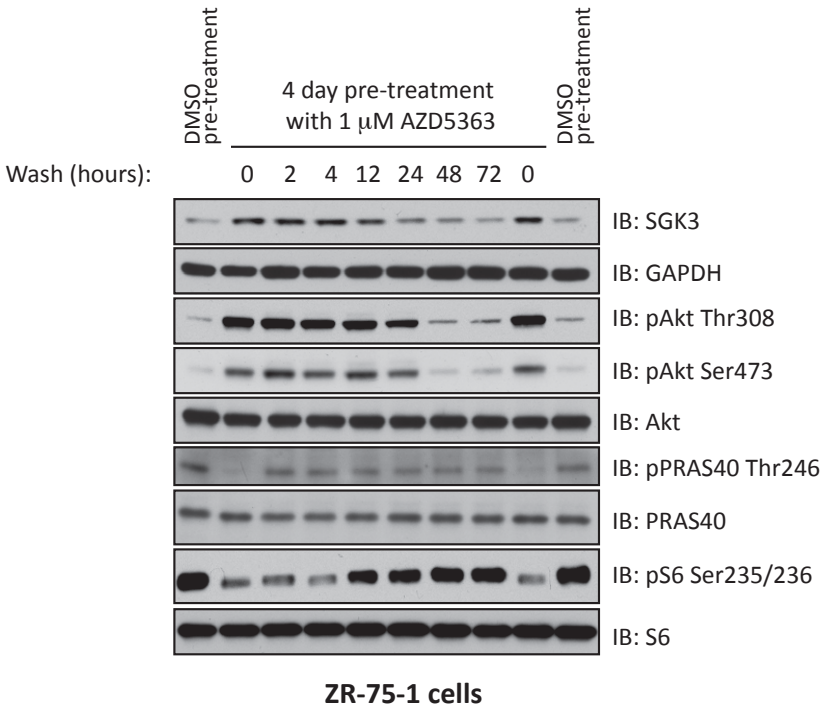

Figure 5.3 SGK3 up-regulation by Akt inhibition is reversible

ZR-75-1 cells grown on 6-well plates were pre-treated with 1 μM AZD5363 for 4 days to up-regulate SGK3 levels. In parallel control cells were maintained in the presence of DMSO. For inhibitor pre-treated wells approximately $5x10^5$ and for DMSO pre-treated wells approximately $1x10^5$ cells were seeded per well. Inhibitor containing medium was replaced with fresh growth medium lacking the inhibitor for 2, 4, 12, 24, 48 or 72 hours. For cells with 0 hour washout growth medium was replaced with fresh growth medium containing 1 μM AZD5363 for 72 hours. All cells were lysed at the same time and the lysates were analysed with the indicated antibodies by immunoblotting (IB).

5.2.4. Chronic Akt inhibition leads to increased SGK3 catalytic activity

As shown in Figure 5.1, whilst in Akt inhibitor sensitive cells NDRG1 phosphorylation was sensitive to an acute one-hour treatment with Akt inhibitors, it had started recovering by 24 hours of Akt inhibition. Elevated SGK3 protein levels were, however, only detected following five and ten days of Akt inhibition (Figure 5.1) and more careful analysis of SGK3 up-regulation revealed that maximum levels of SGK3 protein were reached following four-

to-six days of Akt inhibition (Figure 5.2). To determine whether Akt inhibition modulated SGK3 in a biphasic manner by 1) first leading to elevated SGK3 activity and 2) secondly leading to elevated SGK3 levels, the catalytic activity of endogenous SGK3 was monitored following Akt inhibition for 1, 12, 24, 48 and 96 hours (Figure 5.4). Immunoprecipitation of endogenous SGK3 also enabled the detection of phospho-SGK3. The two key phosphorylation sites on SGK3 are the HM-site Ser486, which is phosphorylated by mTORC2, and the T-loop site Thr320, which is phosphorylated by PDK1.

Acute (one hour) Akt inhibition with MK-2206 did not alter SGK3 kinase activity, phosphorylation or protein levels but inhibited NDRG1 phosphorylation (Figure 5.4). Following 12 and 24 hours of Akt inhibition a moderate, approximately two-fold, increase in SGK3 kinase activity was observed and the increase in SGK3 activity was accompanied with a moderate increase in both HM-site and T-loop phosphorylation of SGK3 without marked effects on total SGK3 levels (Figure 5.4). Furthermore, as previously shown for the 24-hour treatment (Figure 5.1), at these time points a partial recovery of NDRG1 phosphorylation was also observed. Following 48 and 96 hours of Akt inhibition a more substantial increase in SGK3 kinase activity was detected (approximately three-to-four-fold) accompanied by markedly increased levels of SGK3 total protein as well as SGK3 HM-site and T-loop phosphorylation. Moreover, following 48 and 96 hours of Akt inhibition levels of NDRG1 phosphorylation had fully recovered. Phosphorylation of Akt itself and of the Akt substrate PRAS40 remained suppressed throughout the time-course (Figure 5.4).

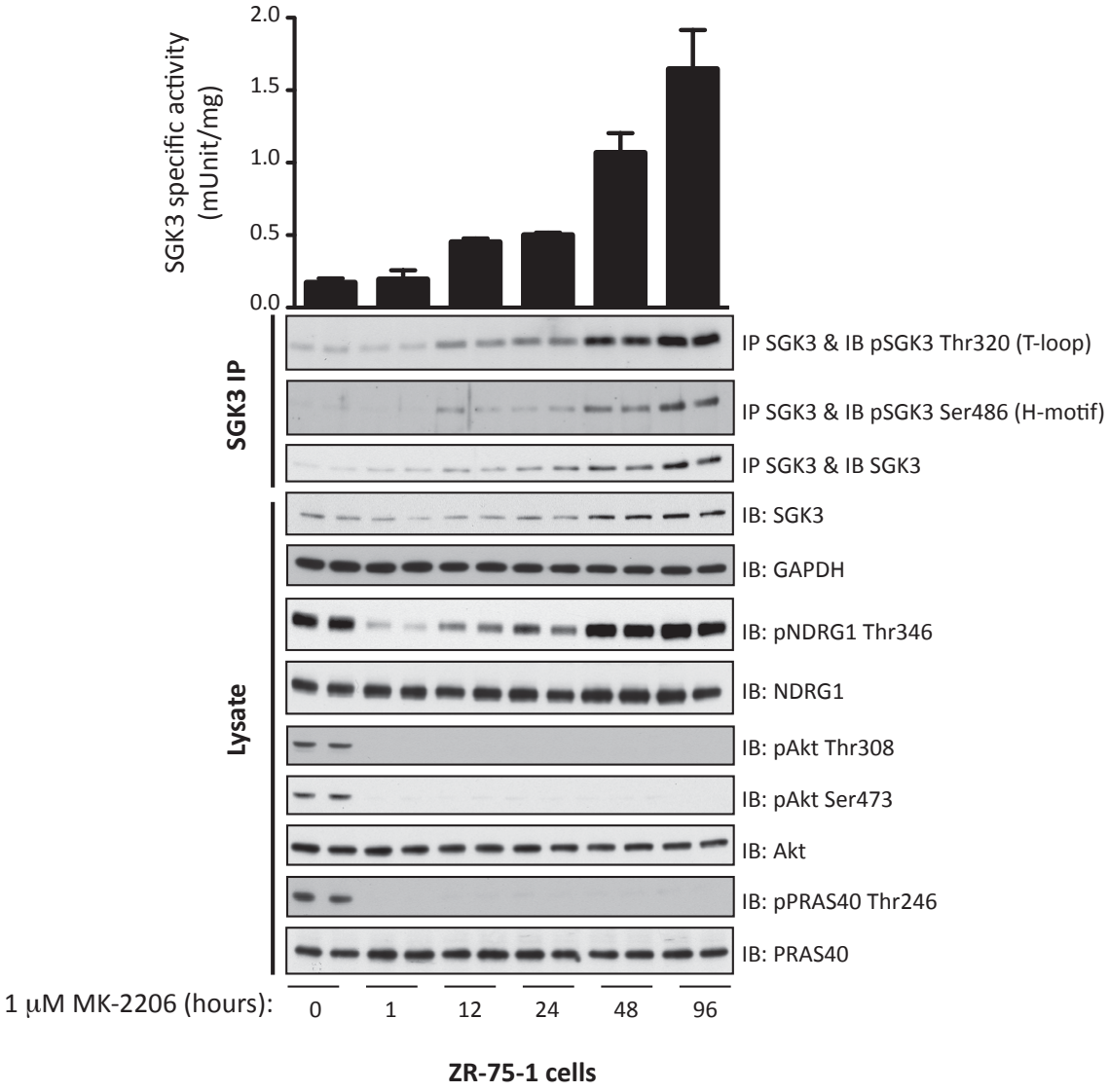

Figure 5.4 Sustained Akt inhibition stimulates SGK3 catalytic activity

ZR-75-1 cells were seeded onto 15-cm dishes, allowed to adhere overnight and treated with 1 μM MK-2206 for the indicated time points or with DMSO for 96 hours. For DMSO control, 1, 12 and 24 hour samples approximately $1x10^6$ and for 48 hour and 96 hour samples approximately $1x10^7$ and $2x10^7$,respectively cells were seeded per dish. All cells were approximately 80% confluent at the time of lysis. Endogenous SGK3 was immunoprecipitated (IP) from 2 mg of fresh lysate and SGK3 catalytic activity was measured using Crosstide substrate peptide. Results represent the means ± S.E.M. of two independent samples each assayed in duplicates. Lysates and immunoprecipitates were analysed by immunoblotting (IB) with the indicated antibodies.

mTORC2 inhibition is expected to suppress SGK3 HM-site phosphorylation leading to subsequent loss of also SGK3 T-loop phosphorylation and SGK3 activity (Biondi et al., 2001; Garcia-Martinez and Alessi, 2008; Kobayashi and Cohen, 1999). To test this, SGK3 activity and levels were stimulated by chronic Akt inhibition and the sensitivity of SGK3 to 1-hour treatment with mTOR inhibitor AZD8055 was assessed (Figure 5.5). 96 hours of Akt inhibition in ZR-75-1 cells with MK-2206 markedly increased SGK3 activity, T-loop and HM-site phosphorylation and total levels as well as induced Akt inhibitor resistant NDRG1 phosphorylation (Figure 5.5). Acute treatment with AZD8055 reduced SGK3 kinase activity to below basal levels and induced SGK3 and NDRG1 de-phosphorylation (Figure 5.5).

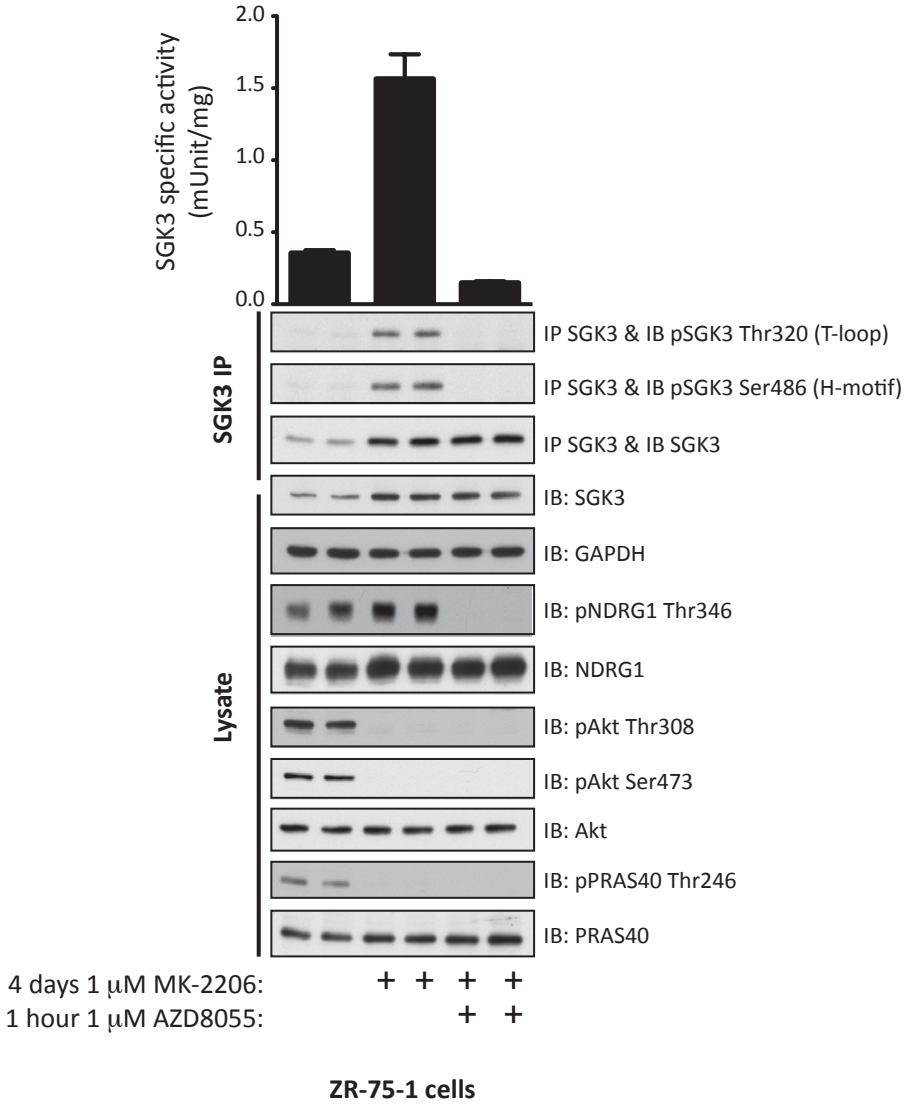

Figure 5.5 Increase in kinase activity is sensitive to acute mTOR kinase inhibition

ZR-75-1 cells were seeded onto 15-cm dishes, allowed to adhere overnight and treated with 1 μM MK-2206 or DMSO for 96 hours. Prior to lysis MK-2206 pre-treated cells were exposed to 1 μM AZD8055 or DMSO for 1 hour. Endogenous SGK3 was immunoprecipitated (IP) from 2 mg of fresh lysate and SGK3 catalytic activity was measured using Crosstide substrate peptide. Results represent the means ± S.E.M. of two independent samples each assayed in duplicate. Lysates and immunoprecipitates were analysed by immunoblotting (IB) with the indicated antibodies.

5.2.5. Akt inhibitor resistant NDRG1 phosphorylation is sensitive to inhibition of the up-stream regulators of SGKs

In Akt inhibitor sensitive cells a striking correlation between the increase in SGK3 activity and the emergence of Akt inhibitor resistant phosphorylation of NDRG1 was observed (Figure 5.1; Figure 5.4) suggesting that in these cells SGK3 could be the kinase that phosphorylates NDRG1 in the absence of Akt activity. To address this possibility, the sensitivity of Akt inhibitor resistant NDRG1 phosphorylation to inhibition of the PI3K pathway at different nodes was assessed (Figure 5.6). Akt inhibitor resistant NDRG1 phosphorylation, as well as SGK3 activation, was induced by 10 days of treatment with MK-2206 in CAMA-1 and ZR-75-1 cells. Akt inhibitor resistant NDRG1 phosphorylation was in both cell lines sensitive to one-hour treatment with the PDK1 inhibitor GSK2334470 and mTOR inhibitor AZD8055 but not to the mTORC1 selective inhibitor rapamycin (Figure 5.6). These results are consistent with an SGK isoform being responsible for mediating phosphorylation of NDRG1 in these cells in the absence of Akt activity. In contrast to the PDK1 and mTOR inhibitors, the Class I PI3K inhibitor GDC-0941 caused only a partial decrease in Akt inhibitor resistant NDRG1 phosphorylation.

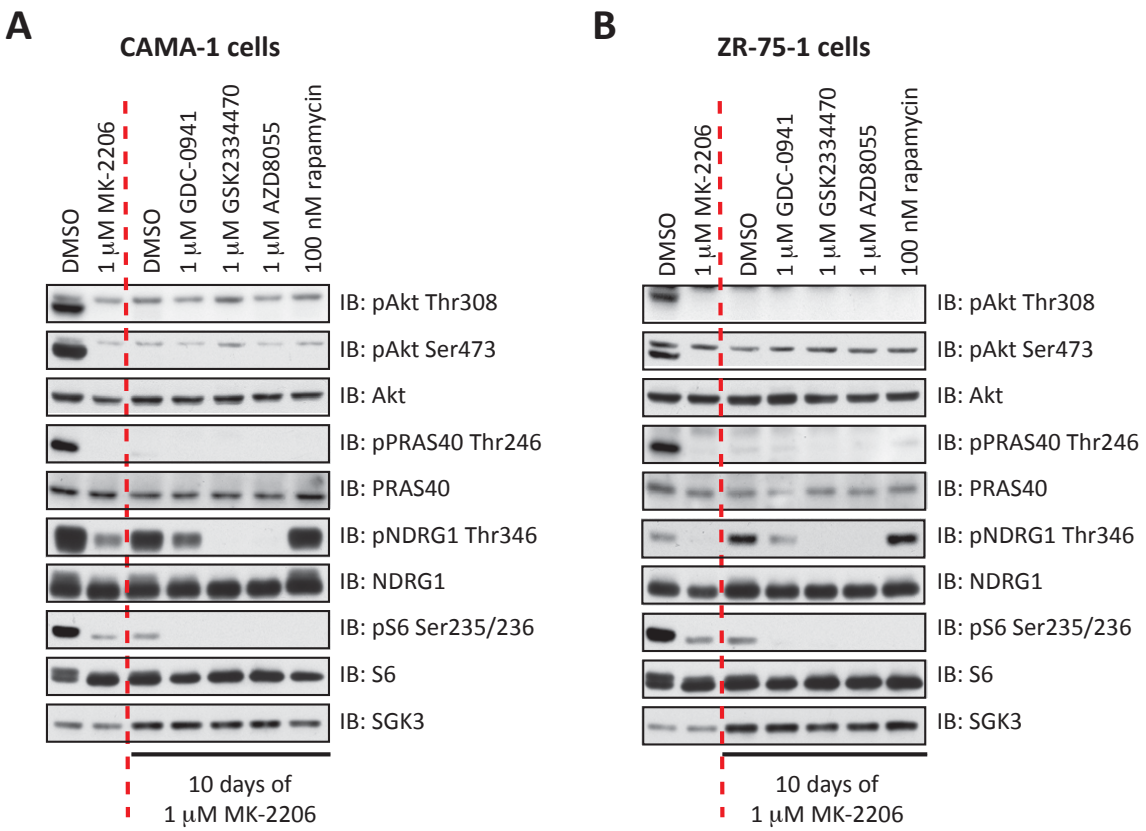

Figure 5.6 Akt inhibitor resistant NDRG1 phosphorylation is sensitive to inhibition of the upstream regulators of SGK

CAMA-1 and ZR-75-1 cells were maintained in the presence of 1 μM MK-2206 or DMSO for 10 days prior to seeding onto 6-well plates in the presence of 1 μM MK-2206 or DMSO. 48 hours later DMSO pre-treated cells were exposed to 1 μM MK-2206 or DMSO for 1 hour and MK-2206 pre-treated cells were exposed to 1 μM GDC-0941, 1 μM GSK-233470, 1 μM AZD8055, 100 nM Rapamycin or DMSO for 1 hour. Lysates were analysed by immunoblotting (IB) with the indicated antibodies.

5.2.6. Akt inhibitor resistant NDRG1 phosphorylation is mediated by SGK3

The sensitivity of Akt inhibitor resistant NDRG1 phosphorylation to the mTOR catalytic inhibitor AZD8055 and to the PDK1 inhibitor GSK2334470, but not to the mTORC1 inhibitor rapamycin, is consistent with NDRG1 phosphorylation being mediated by SGK, rather than by S6K. In order to further analyse the correlation between the emergence of

Akt inhibitor resistant NDRG1 phosphorylation and up-regulation of SGK3 and to determine whether SGK3 is the SGK isoform responsible for phosphorylation of NDRG1 in the absence of Akt activity, a number of SGK3 shRNAs were tested. SGK3 shRNAs #B, #D and #E were most efficient in reducing the levels of SGK3 protein in both CAMA-1 and ZR-75-1 cells (Figure 5.7) and these shRNAs were selected for further experiments.

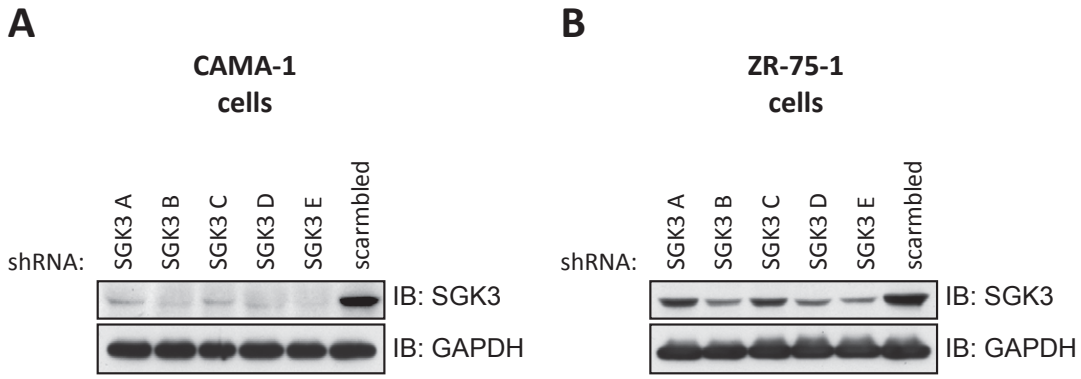

Figure 5.7 Evaluation of SGK3 shRNAs

CAMA-1 and ZR-75-1 cells were infected with SGK3 or scrambled shRNAs. 72 hours post infection cell lysates were analysed by immunoblotting (IB) with the indicated antibodies.

To test whether SGK3 mediated phosphorylation of NDRG1 in the absence of Akt activity, SGK3 was up-regulated in CAMA-1 and ZR-75-1 cells by chronic Akt inhibition with either MK-2206 (Figure 5.8A,C) or AZD5363 (Figure 5.8B,D) and the cells were then infected with either scrambled or SGK3 shRNAs. The elevated SGK3 protein was efficiently knocked down to undetectable levels with each of the three independent SGK3 shRNAs and SGK3 knockdown was accompanied by complete loss of Akt inhibitor resistant NDRG1 phosphorylation (Figure 5.8).

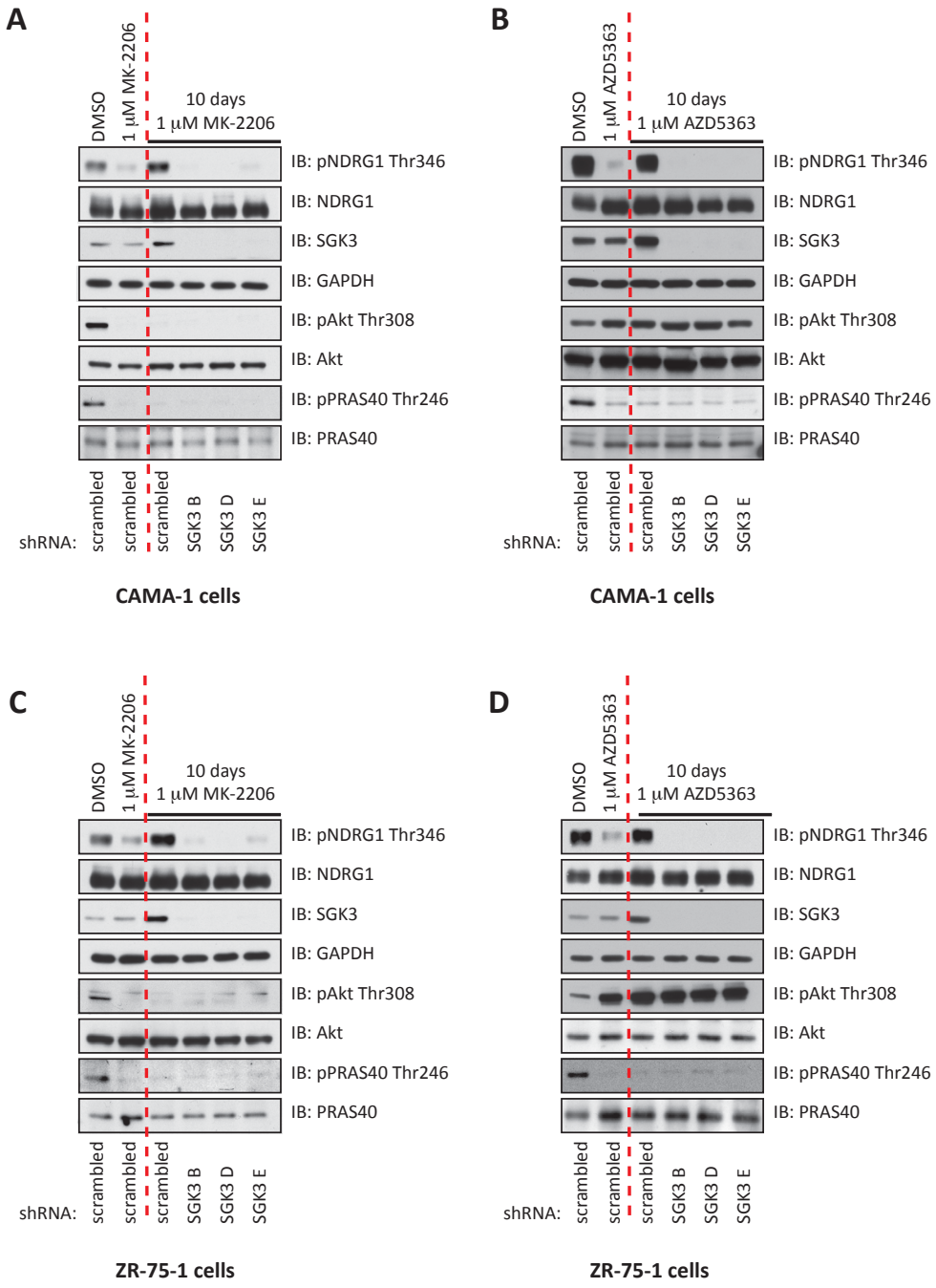

Figure 5.8 Akt inhibitor resistant NDRG1 phosphorylation is mediated by SGK3

(**A, C**) CAMA-1 and ZR-75-1 cells were maintained in the presence of 1 μM MK-2206 or DMSO for 10 days prior to infection with scrambled or SGK3 shRNAs in the sustained presence of either 1 μM MK-2206 or DMSO. 72 hours post infection DMSO pre-treated cells were exposed to 1 μM MK-2206 or DMSO for 1 hour and MK-2206 pre-treated cells were exposed to DMSO for 1 hour. Lysates were analysed by immunoblotting (IB) with the indicated antibodies. (**B, D**) as in (**A, C**) except 1 μM AZD5363 was used.

Next the effect of SGK3 knockdown on basal NDRG1 phosphorylation in CAMA-1 and ZR-75-1 cells was assessed. SGK3 was knocked down with the three independent shRNAs in cells pre-treated for 48 hours with either DMSO (active Akt) or MK-2206 (in-active Akt). In the presence of Akt activity SGK3 knockdown did not affect NDRG1 phosphorylation in CAMA-1 cells, in contrast Akt inhibitor resistant NDRG1 phosphorylation was sensitive to SGK3 knockdown (Figure 5.9A). In ZR-75-1 cells SGK3 knockdown had a partial effect on basal NDRG1 phosphorylation and induced complete loss of NDRG1 phosphorylation in cells treated with MK-2206 for 48 hours (Figure 5.9B). This observation indicates that in ZR-75-1 cells basal NDRG1 phosphorylation is likely to be mediated by a combination of Akt and SGK3. SGK3 knockdown did not affect phosphorylation of Akt or the Akt substrate PRAS40 in either of the cell lines studied (Figure 5.9).

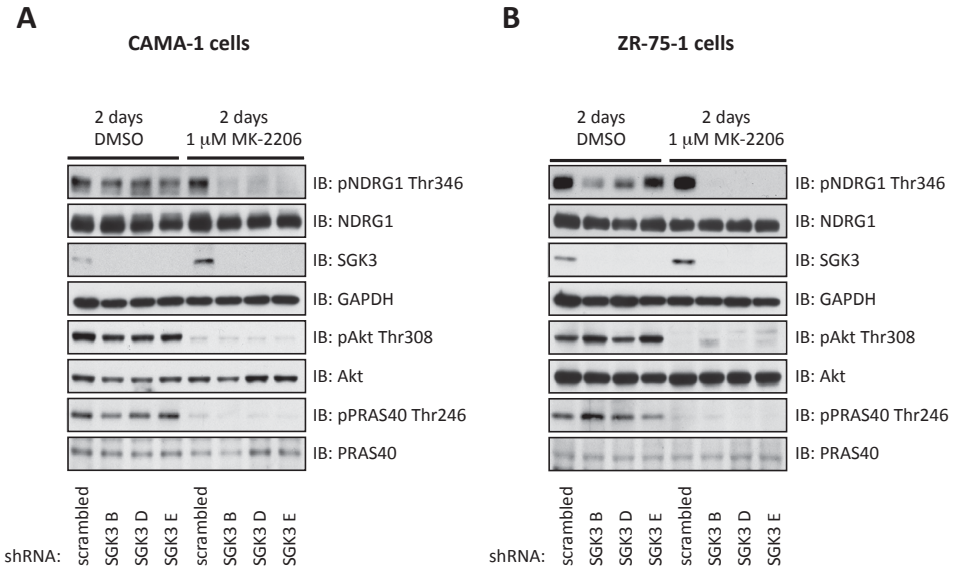

Figure 5.9 Effect of SGK3 knockdown on basal NDRG1 phosphorylation

48 hours post infection with scrambled or SGK3 shRNAs the indicated cells were seeded onto 6-well plates and allowed to adhere overnight prior to exposure to 1 μM MK-2206 or DMSO for 48 hrs. Lysates were analysed by immunoblotting (IB) with the indicated antibodies.

To verify that the loss of Akt inhibitor resistant NDRG1 phosphorylation was due to SGK3 knockdown, a rescue experiment was carried out. ZR-75-1 cells were transduced to stably express HA-tagged wild type (wt) and kinase inactive (ki) SGK3 that was engineered to be resistant to SGK3 shRNA #D. The resistant construct possesses three silent mutations that alter the nucleotide but not the expressed amino acid sequence thus making the construct resistant to RNA interference. In ZR-75-1 cells stably expressing wild type but not kinase inactive shRNA resistant SGK3, Akt inhibitor resistant NDRG1 phosphorylation was not affected by SGK3 knockdown (Figure 5.10). This result confirmed that the effect of SGK3 knockdown on Akt inhibitor resistant NDRG1 phosphorylation was specific.

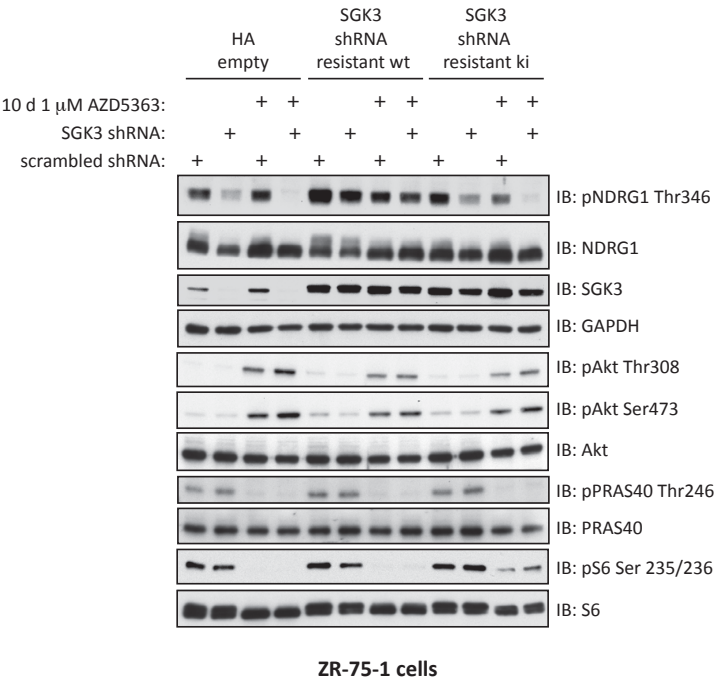

Figure 5.10 Rescue of SGK3 knockdown induced loss of Akt inhibitor resistant NDRG1 phosphorylation

ZR-75-1 cells stably expressing SGK3 shRNA #D resistant HA-SGK3 wild-type (wt) or kinase inactive (ki) were maintained in the presence of either 1 μM AZD5363 or DMSO for 10 days prior to infection with SGK3 shRNA #D or scrambled shRNA in the sustained presence of either 1 μM AZD5363 or DMSO. 72 hours post infection cells were lysed and analysed by immunoblotting (IB) with the indicated antibodies.

5.2.7. *In vitro* characterization of SGK inhibitors

Results obtained from SGK3 knockdown studies demonstrate that in CAMA-1 and ZR-75-1 cells SGK3 mediates NDRG1 phosphorylation in the absence of Akt. Therefore the effects of potential SGK3 inhibitors in cultured cells can be determined by monitoring Akt inhibitor resistant NDRG1 phosphorylation. Three SGK inhibitors were obtained and initially characterised *in vitro*. One of the inhibitors, EMD638683, has been published (Ackermann et al., 2011). Two of the inhibitors, DSTT SGKi1 and DSTT SGKi2, were obtained from the DSTT collaboration with pharmaceutical companies. The structures of these compounds are not disclosed. DSTT SGKi1 was expected to be an SGK specific inhibitor and DSTT SGKi2 was expected to be a dual Akt/SGK inhibitor. In order to test the specificities of these inhibitors, the effects of 1 μM of these compounds upon the activities of 141 protein kinases *in vitro* were tested (Figure 5.11-13).

EMD638683 did not inhibit any kinases other than SGK1 by more than 50% being the most specific compound. 1 μM EMD638683, however, only inhibited SGK1 by 86% (Figure 5.11). In contrast, 1 μM DSTT SGKi1 inhibited SGK1 by 95% but was less selective. 1 μM DSTT SGKi1 inhibited 31 kinases by more than 50% and 15 kinases by more than 75%. Amongst the most inhibited kinases were (in decreasing order of inhibition): GSK3β, DYRK1A, CLK2, PIM1 and SGK1 (Figure 5.12). DSTT SGKi2 was the least selective compound as 1 μM DSTT SGKi2 inhibited 49 kinases by more than 50% and 32 kinases by more than 75%. Amongst the most inhibited kinases were (in decreasing order of inhibition): Akt1, S6K1, MSK1, Akt2, PKA and SGK1. Akt1 was inhibited by 100%, Akt2 by 99% and SGK1 by 97% (Figure 5.13).

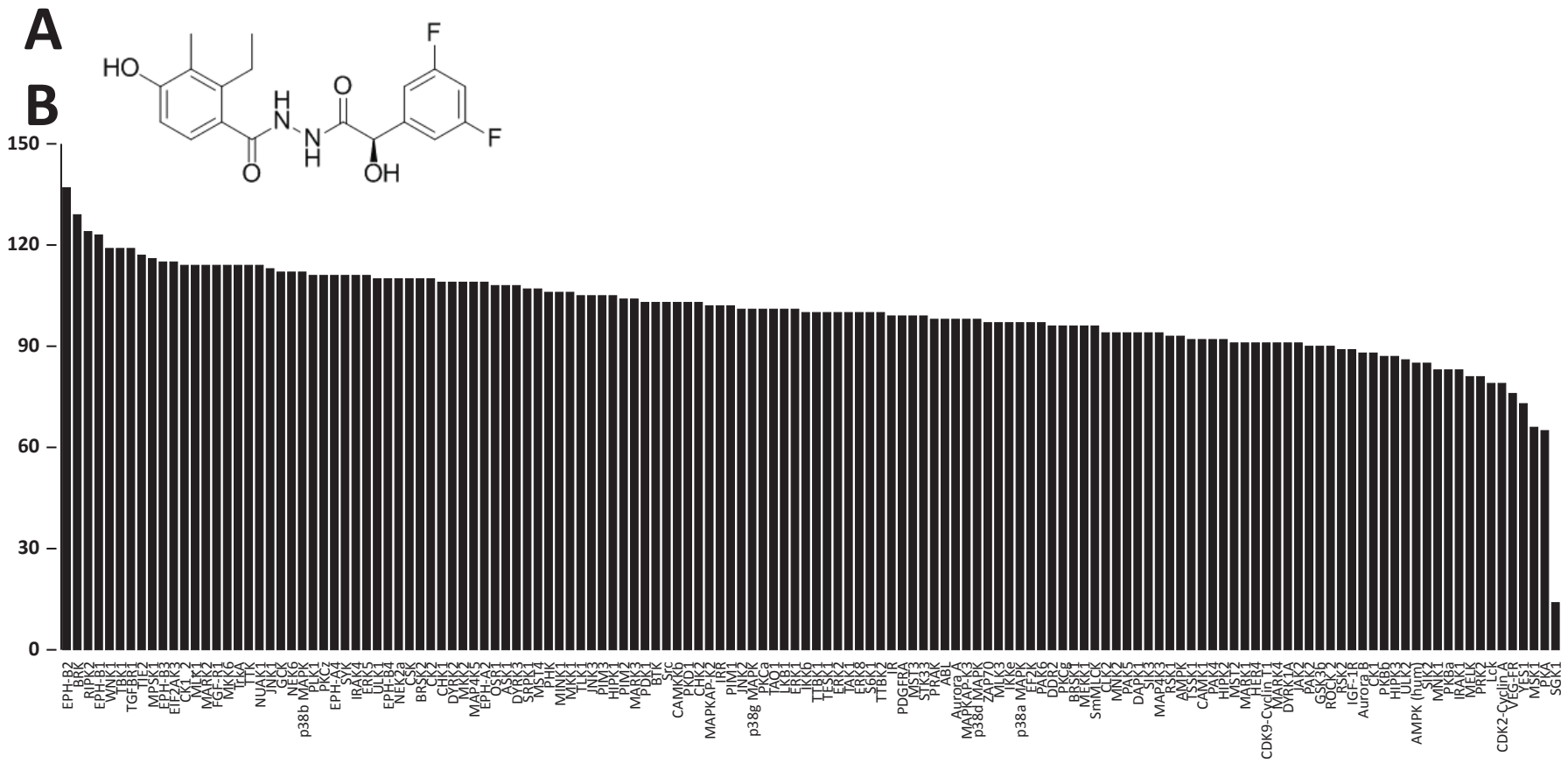

Figure 5.11 Effect of 1 μM EMD638683 upon the activity of 141 protein kinases *in vitro*

(**A**) The published structure of EMD638683. (**B**) The Kinase selectivity profile was established by The International Centre for Protein Kinase Profiling (http://www.kinase-screen.mrc.ac.uk/). Data are presented as mean (n=3) % kinase activity remaining in the presence of 1 μM EMD638683. DMSO control reaction was set to 100%.

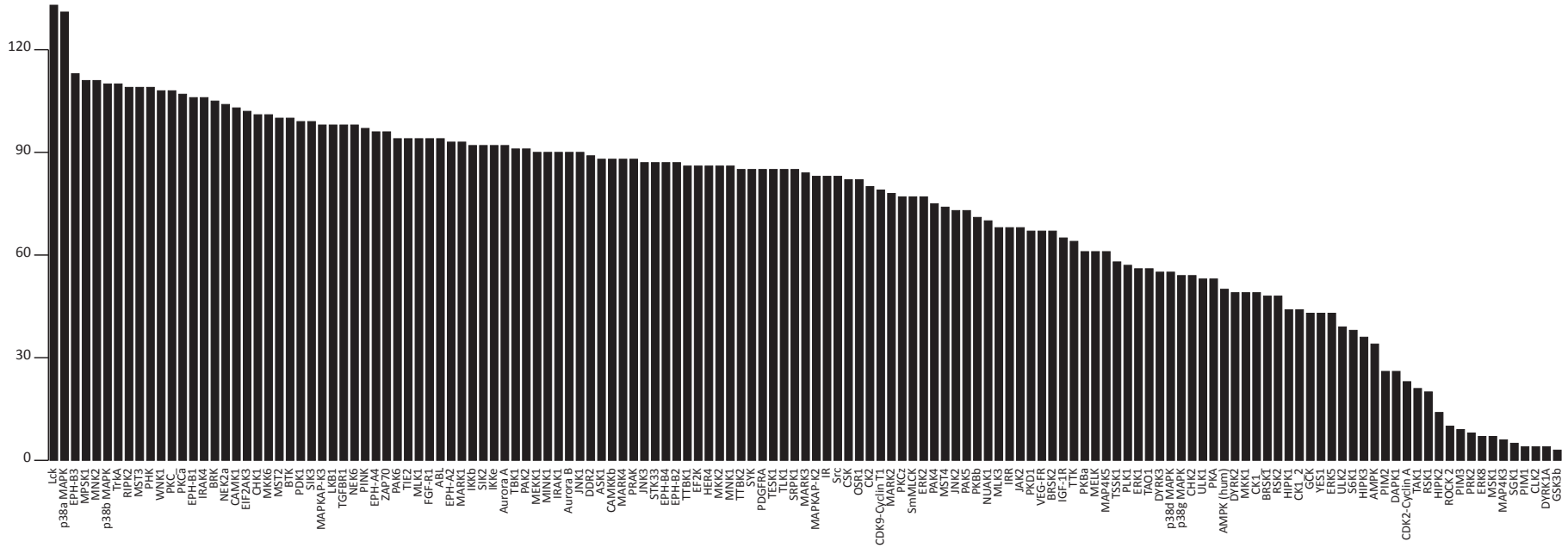

Figure 5.12 Effect of 1 μM DSTT SGKi1 upon the activity of 141 protein kinases *in vitro*

The Kinase selectivity profile was established by The International Centre for Protein Kinase Profiling (http://www.kinase-screen.mrc.ac.uk/). Data are presented as mean (n=3) % kinase activity remaining in the presence of 1 μM DSTT SGKi1. DMSO control reaction was set to 100%.

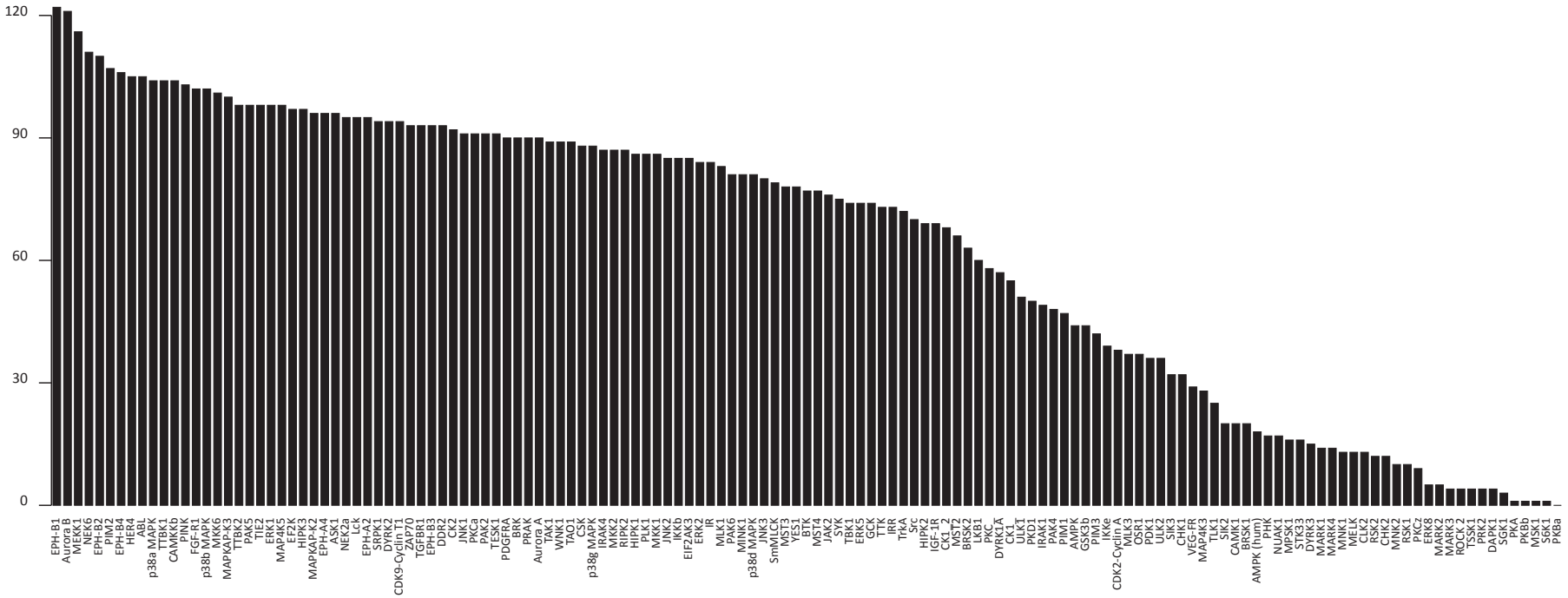

Figure 5.13 Effect of 1 μM DSTT SGKi2 upon the activity of 141 protein kinases *in vitro*

The Kinase selectivity profile was established by The International Centre for Protein Kinase Profiling (http://www.kinase-screen.mrc.ac.uk/). Data are presented as mean (n=3) % kinase activity remaining in the presence of 1 μM DSTT SGKi2. DMSO control reaction was set to 100%.

The kinase selectivity screen lacked SGK3. In order to determine the *in vitro* potencies of the compounds against the two SGK isoforms of particular interest, SGK1 and SGK3, active GST-ΔN-SGK1 and GST-SGK3 were purified from IGF1 stimulated HEK293 cells and their catalytic activities were assayed in the presence of increasing concentrations (0.1 nM – 30 μM) of the inhibitors (Figure 5.14). All three inhibitors inhibited both SGK1 and SGK3 and each inhibitor was approximately equally potent against both SGK isoforms. IC_{50} values of EMD638683 against SGK1 and SGK3 were 230 and 280 nM, respectively, IC_{50} values of DSTT SGKi1 against SGK1 and SGK3 were 12 and 23 nM, respectively and IC_{50} values of DSTT SGKi2 against SGK1 and SGK3 were 90 and 68 nM, respectively. DSTT SGKi1 was the most potent *in vitro*. EMD638683, which was very selective (Figure 5.11), was approximately 20-fold less potent than DSTT SGKi1 against SGK1 and 13-fold less potent against SGK3 (Figure 5.14). DSTT SGKi2 displayed intermediate potency *in vitro* (Figure 5.14) but was very non-selective (Figure 5.13).

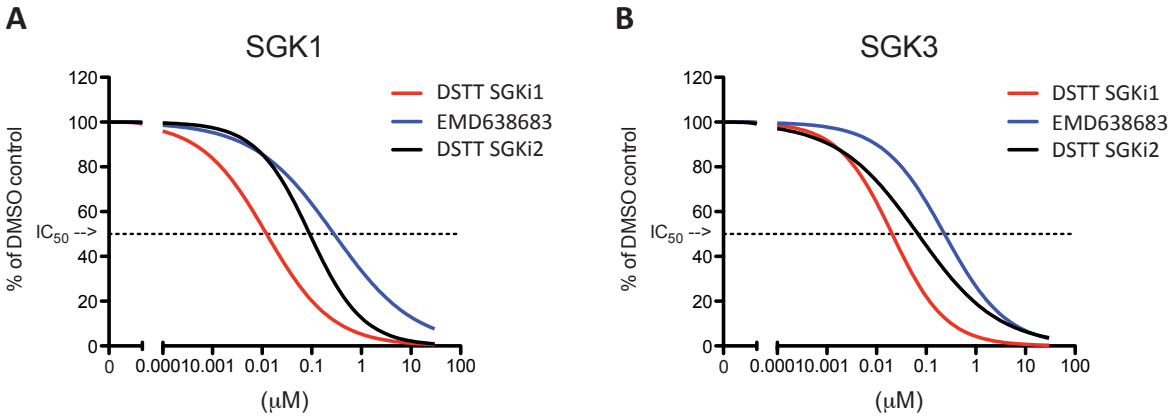

C

IC_{50} values

	SGK1	SGK3
DSTT SGKi1	12 nM	21 nM
DSTT SGKi2	90 nM	68 nM
EMD638683	230 nM	280 nM

Figure 5.14 *In vitro* potencies of EMD638683, DSTT SGKi1 and DSTT SGKi2 against SGK1 and SGK3

GST-ΔN-SGK1 (**A**) and GST-SGK3 (**B**) purified from HEK293 cells were assayed in the presence of increasing concentrations (0.1 nM – 30 μM) of EMD638683 (blue line), DSTT SGKi1 (red line) or DSTT SGKi2 (black line) against Crosstide substrate peptide. Data are represented as percentage of kinase activity relative to the control (DMSO) and are the average of triplicate reactions. Sigmoidal dose response curves were fitted using GraphPad Prism 5.0. (**C**) IC_{50} values were calculated using GraphPad Prism 5.0.

5.2.8. *In vivo* characterisation of SGK inhibitors in cell based assays

Next the three compounds that all inhibited SGK1 and SGK3 *in vitro* were analysed in cell-based assays. EMD638683 and DSTT SGKi1, which were more selective in vitro than DSTT SGKi2, were first tested for their ability to inhibit SGK1 in cells. These experiments were performed in BT-549 and MDA-MB-436 cells because results presented in Chapter 4 demonstrate that in these cells SGK1 phosphorylates NDRG1. BT-549 and MDA-MB-436

cells were treated with increasing concentrations (0.3 – 30 μM) of the inhibitors for one hour. As mTOR kinase inhibition induces complete loss of NDRG1 phosphorylation in these cells (Chapter 4), AZD8055 was used as a positive control (Figure 5.15). As expected, 1 μM AZD8055 completely diminished NDRG1 phosphorylation in BT-549 and MDA-MB-436 cells. However, the cellular potencies of both EMD638683 and DSTT SGKi1 were fairly poor. In both cell lines 1 – 3 μM DSTT SGKi1 had a partial effect on NDRG1 phosphorylation and more substantial effects were seen at 10 - 30 μM DSTT SGKi1 (Figure 5.15A,C). EMD638683 was moderately less potent than DSTT SGKi1 as EMD638683 had partial effects on NDRG1 phosphorylation at around 3 - 10 μM and stronger effects at 30 μM (Figure 5.15B,D).

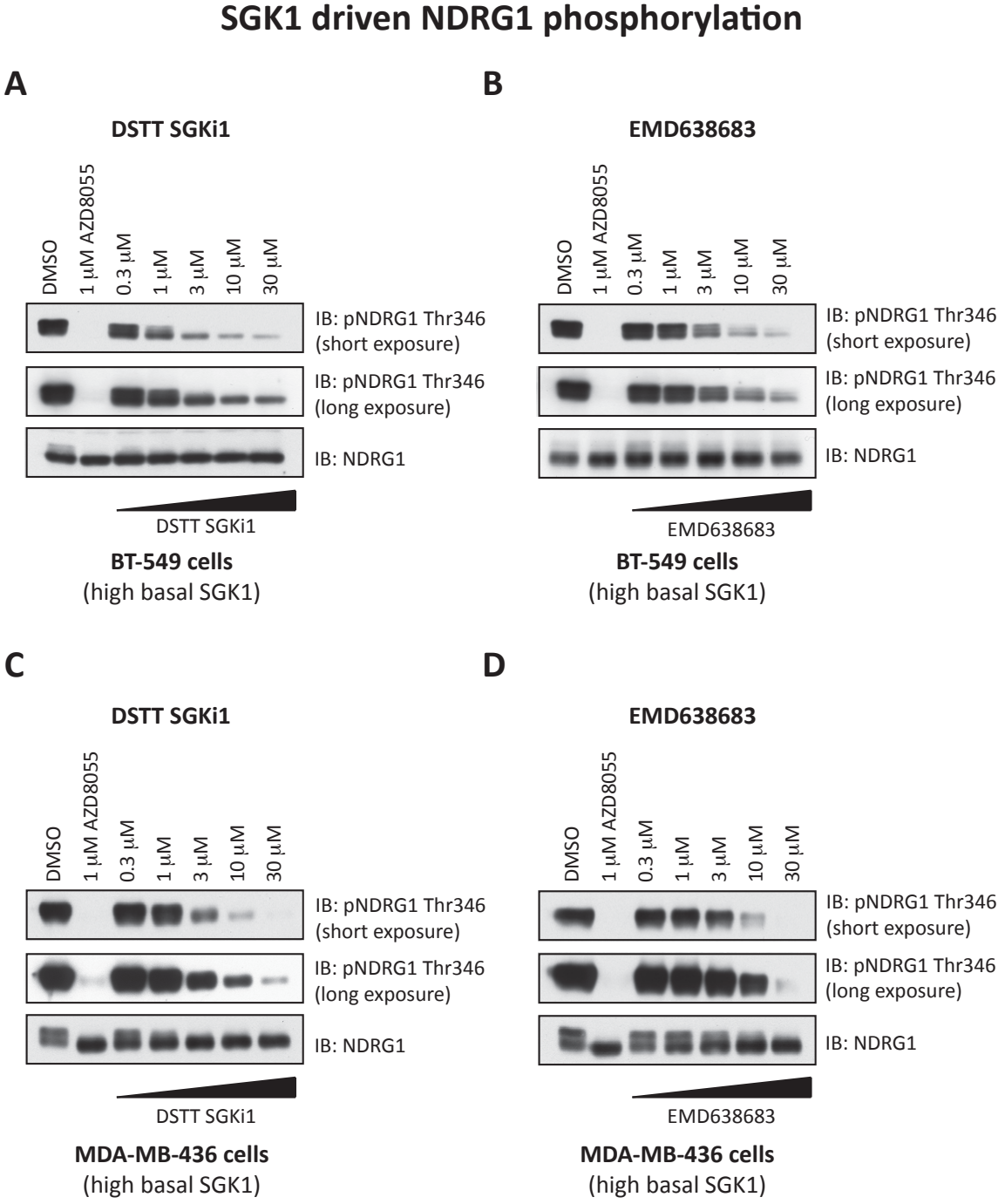

Figure 5.15 Effect of EMD638683 and DSTT SGKi1 on SGK1 dependent NDRG1 phosphorylation

(**A**) BT-549 cells were treated with increasing concentrations (0.3 – 30 μM) of DSTT SGKi1 or 1 μM AZD8055 for 1 hour prior to lysis and immunoblot (IB) analysis with the indicated antibodies. (**B**) As in (**A**) except EMD638683 was used. (**C**) as in (**A**) except MDA-MD-436 cells were used. (**D**) as in (**B**) except MDA-MB-436 cells were used.

Next EMD638683 and DSTT SGKi1 were tested for their ability to inhibit SGK3 in cells. ZR-75-1 and CAMA-1 cells were treated with MK-2206 for 120 hours in order to induce SGK3 mediated NDRG1 phosphorylation and the cells were then treated with increasing concentrations (0.3 – 30 μM) of the inhibitors for one hour. 1 μM AZD8055 that was used as a positive control caused complete loss of NDRG1 phosphorylation (Figure 5.16). In both cell lines 3 – 10 μM DSTT SGKi1 had partial effects on NDRG1 phosphorylation and more substantial effects were seen at 30 μM DSTT SGKi1 (Figure 5.16A,C). Consistent with the *in vitro* potency data presented in Figure 5.14, EMD638683 was less potent than DSTT SGKi1 in cells only inhibiting SGK3 driven NDRG1 phosphorylation at around 30 μM (Figure 5.16B,D).

Because shRNA-mediated knockdown of SGK3 had no effect on basal NDRG1 phosphorylation in CAMA-1 but partially affected basal NDRG1 phosphorylation in ZR-75-1 cells, the effect of the more potent SGK inhibitor, DSTT SGKi1, on NDRG1 phosphorylation in the presence of normal Akt activity was next tested in these cells (Figure 5.17). In CAMA-1 cells NDRG1 phosphorylation was sensitive to treatment with 1 μM MK-2206 and 1 μM AZD8055 but was insensitive to SGK inhibition under conditions in which Akt is active (Figure 5.17A). In contrast whilst in ZR-75-1 cells 1 μM AZD8055 induced a complete loss of NDRG1 phosphorylation, 1 μM MK-2206 had a partial effect and at around and above 3 μM concentrations DSTT SGKi1 also caused a reduction in NDRG1 phosphorylation (Figure 5.17B). Taken together the results obtained using SGK3 knockdowns and DSTT SGKi1 suggest that under normal growth conditions NDRG1 phosphorylation is differentially regulated in CAMA-1 and in ZR-75-1 cells. In CAMA-1 cells

it is nearly exclusively mediated by Akt whereas in ZR-75-1 cells it is co-operatively mediated by Akt and SGK3.

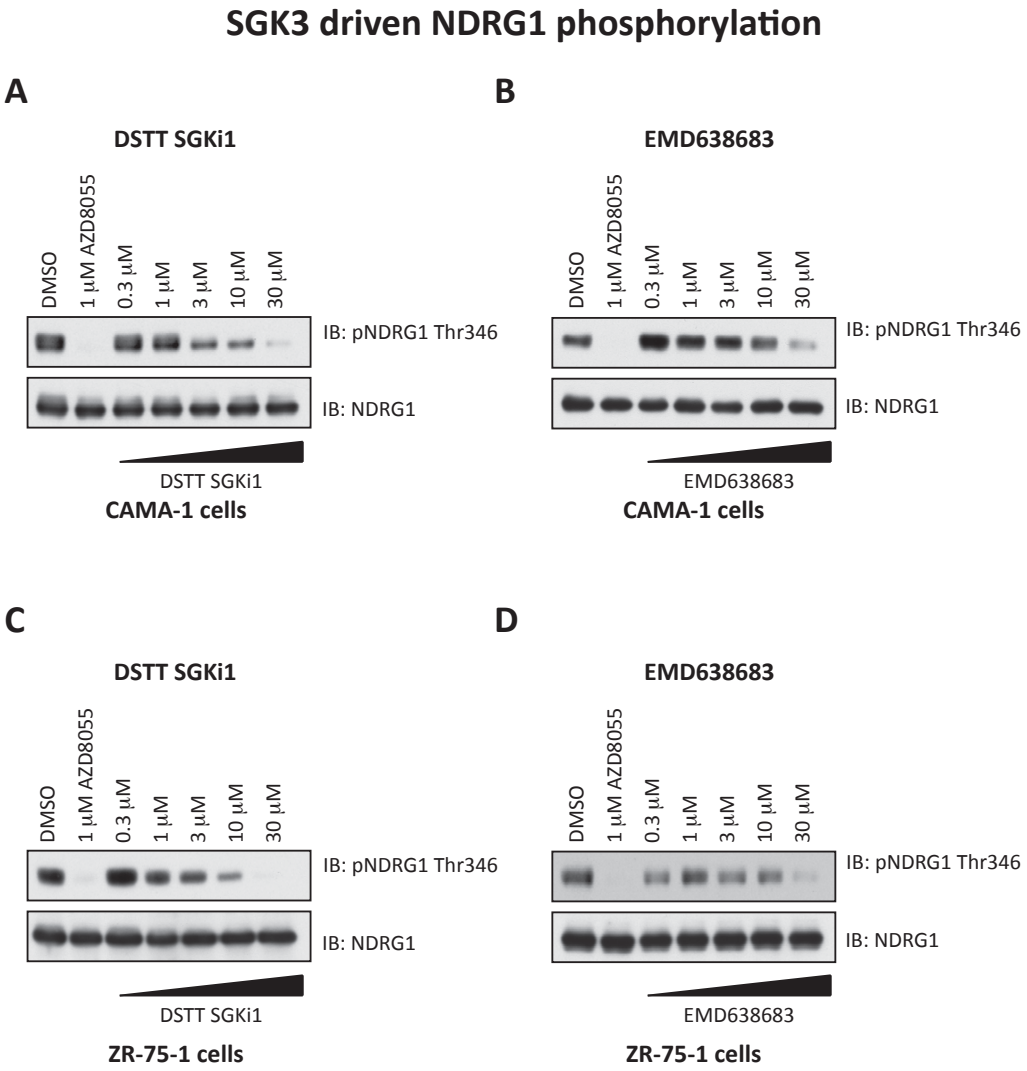

Figure 5.16 Effect of EMD638683 and DSTT SGKi1 on SGK3 mediated NDRG1 phosphorylation

(**A**) CAMA-1 cells pre-treated with 1 μM MK-2206 for 120 hrs to induce SGK3 driven NDRG1 phosphorylation, were treated with increasing concentrations (0.3 – 30 μM) of DSTT SGKi1 or 1 μM AZD8055 for 1 hour prior to lysis and immunoblot (IB) analysis with the indicated antibodies. (**B**) As in (**A**) except EMD638683 was used. (**C**) as in (**A**) except ZR-75-1 cells were used. (**D**) as in (**B**) except ZR-75-1 cells were used.

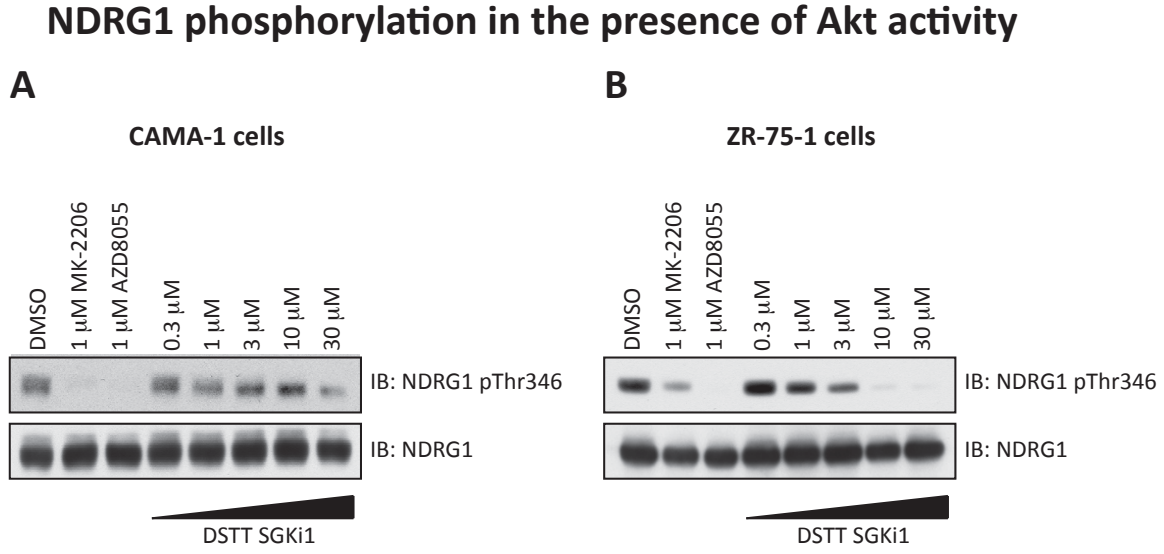

Figure 5.17 Effect of DSTT SGKi1 on NDRG1 phosphorylation in Akt inhibitor sensitive cells under basal conditions

(**A**) CAMA-1 and (**B**) ZR-75-1 cells were treated with 1 μM MK-2206, 1 μM AZD8055 or 0.3 – 30 μM DSTT SGKi1 for 1 hour followed by immunoblot (IB) analysis with the indicated antibodies.

DSTT SGKi2, despite being non-selective *in vitro*, efficiently inhibited both SGK isoforms and Akt *in vitro* (Figure 5.13, Figure 5.14). Therefore treatment of ZR-75-1 cells with DSTT SGKi2 under normal growth conditions would be expected to induce complete loss of NDRG1 phosphorylation. DSTT SGKi2 was compared directly side-by-side with the Akt-selective inhibitor AZD5363 in ZR-75-1 cells and in also MDA-MB-436 cells that possess elevated SGK1 levels. The cells were treated with 1 - 10 μM DSTT SGKi2 and AZD5363 for one hour. 1 μM AZD8055 was used as a positive control. Both inhibitors led to efficient inhibition of Akt as determined by a dose-dependent reduction in PRAS40 phosphorylation and hyper-phosphorylation of Akt itself (Figure 5.18). As demonstrated in Chapter 4, the Akt-selective compound AZD5363 had no influence on NDRG1

phosphorylation in MDA-MB-436 cells. In contrast DSTT SGKi2 led to a dose-dependent decrease in NDRG1 phosphorylation in MDA-MB-436 cells indicating that at around 3 – 10 μM concentrations it inhibited SGK1. In ZR-75-1 cells, however, both AZD5363 and DSTT SGKi2 caused a dose-dependent reduction in NDRG1 phosphorylation (Figure 5.18). Consistent with SGK3 phosphorylation being mediated by both Akt and SGK3 in ZR-75-1 cells under basal conditions, the dual Akt/SGK inhibitor, DSTT SGKi2, was slightly more potent in inhibiting NDRG1 phosphorylation than the Akt-selective AZD5363 compound.

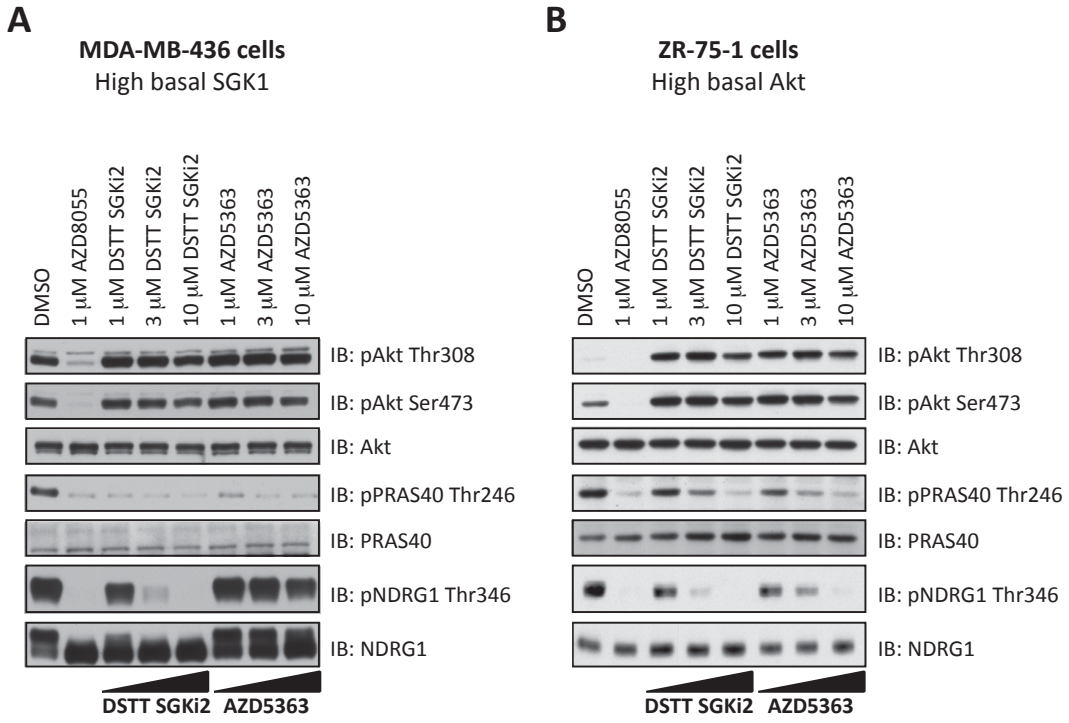

Figure 5.18 Comparison of Akt-selective inhibitor AZD5363 and dual Akt/SGK inhibitor DSTT SGKi2

(**A**) MDA-MB-436 and (**B**) ZR-75-1 cells were treated with the indicated concentrations of AZD8055, DSTT SGKi2 and AZD5363 and lysates were analysed by immunoblotting (IB) with the indicated antibodies.

5.2.9. SGK3 knockdown does not markedly affect how CAMA-1 and ZR-75-1 cells respond to Akt inhibitors

SGK3 and Akt are related kinases regulated by the same upstream activators and sustained Akt inhibition causes up-regulation of SGK3 levels and activity. Therefore the ability of SGK3 to compensate for Akt-driven cellular proliferation was next examined in the Akt inhibitor sensitive CAMA-1 and ZR-75-1 cells. Cells were transduced with two independent SGK3 shRNAs or with scrambled shRNA and the effect of SGK3 knockdown on the sensitivity of CAMA-1 and ZR-75-1 cells to both MK-2206 and AZD5363 was assessed in a 96-hour dose response assay (Figure 5.19). SGK3 knockdown did not have marked effects on the cells' dose responses to the two Akt inhibitors. Some subtle increases in sensitivity to the two Akt inhibitors were observed. It must be noted that by 96 hours of Akt inhibition SGK3 levels will only just have reached their maximum levels.

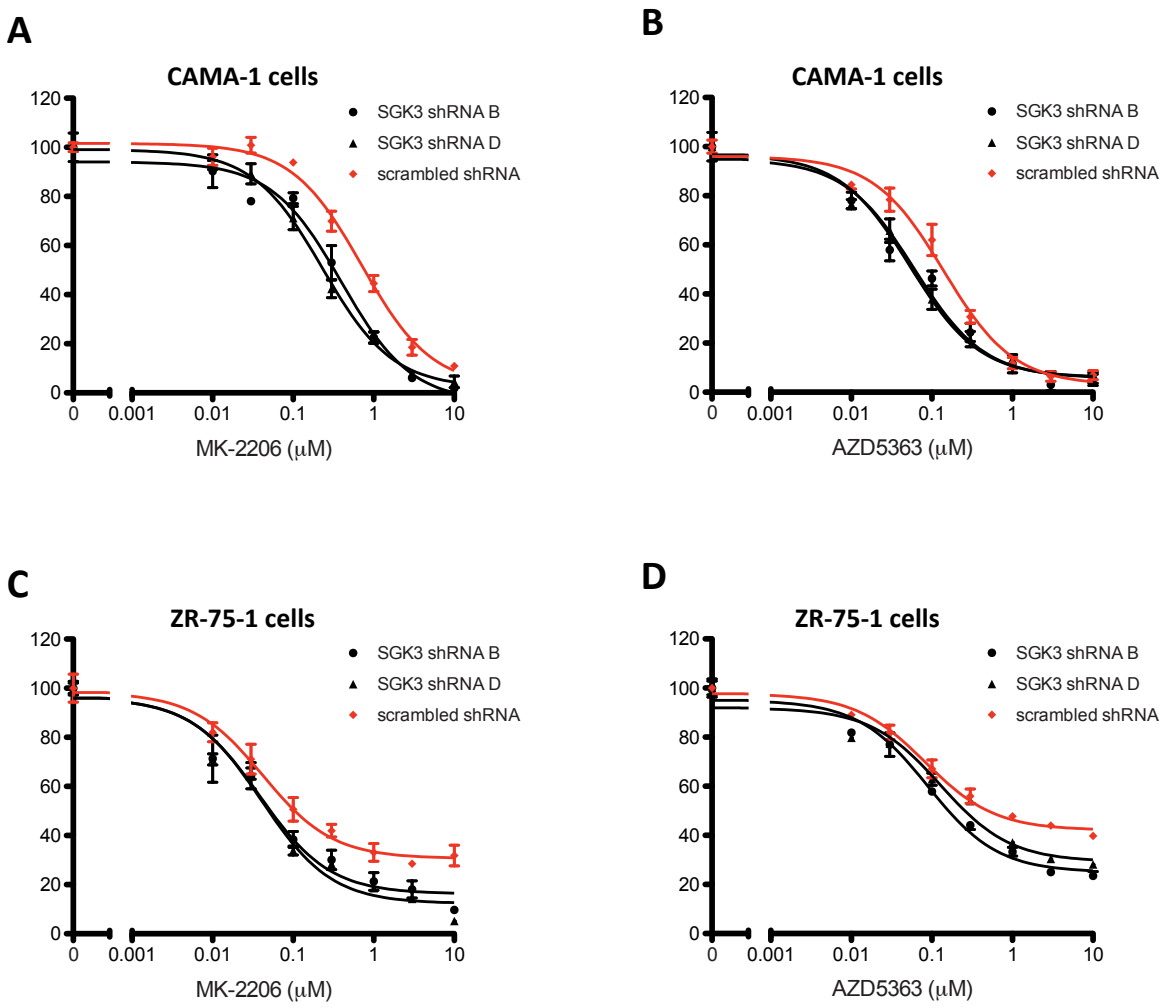

Figure 5.19 Effect of SGK3 knockdown on the ability of MK-2206 and AZD5363 to inhibit proliferation of CAMA-1 and ZR-75-1 cells

(**A**) CAMA-1 cells were transduced with SGK3 or scrambled shRNAs. 72 hours post infection cells were seeded onto 96-well plates and allowed to adhere overnight prior to exposure to 1 nM – 10 μM of MK-2206. 96 hours later cell viability was determined using MTS assay. Data were fitted to dose–response curves using GraphPad Prism 5.0. The results are the means ± S.D. of a triplicate assay and are normalised to the DMSO control that was set to 100%. (**B**) as in (**A**) except AZD5363 was used. (**C**) as in (**A**) except ZR-75-1 cells were used. (**D**) as in (**B**) except ZR-75-1 cells were used.

5.2.10. Sustained Akt inhibition reduces the sensitivity of CAMA-1 and ZR-75-1 cells to subsequent challenge with Akt inhibitors

To further examine whether SGK3 could compensate for Akt, the effect that sustained Akt inhibition had on the capacity of Akt inhibitors to inhibit proliferation was next examined. CAMA-1 and ZR-75-1 cells were subjected to 10 days Akt inhibition with the ATP-competitive inhibitor AZD5363 in order to up-regulate SGK3. AZD5363 was then washed out and cells were treated with DMSO or increasing concentrations of the two Akt inhibitors, AZD5363 and MK-2206. 96 hours later MTS assay was carried out (Figure 5.19). Pre-treatment with AZD5363 induced a decrease in the sensitivity of both CAMA-1 and ZR-75-1 cells to both Akt inhibitors. In order to determine whether the shift in sensitivity was specific to Akt inhibitors, CAMA-1 and ZR-75-1 cells pre-treated with AZD5363 were also subjected to a 96-hour proliferation assay with increasing concentrations of the PI3K inhibitor GDC-0941 and the mTOR inhibitor AZD8055. Pre-treatment with AZD5363 had no influence on the ability of either PI3K or mTOR inhibition to reduce proliferation of CAMA-1 or ZR-75-1 cells (Figure 5.21).

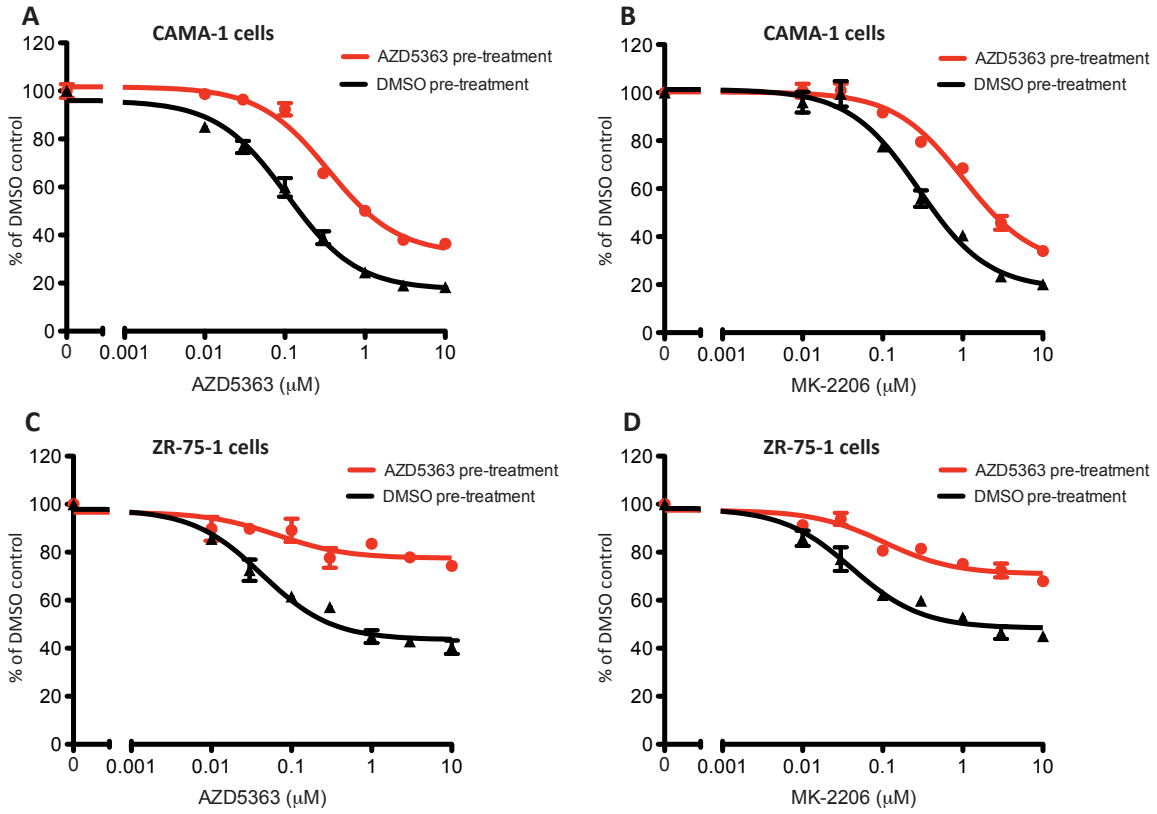

Figure 5.20 Pre-treatment with the Akt inhibitor AZD5363 induces cell culture derived resistance to Akt inhibitors

(**A**) CAMA-1 cells were maintained in the presence of 1 μM AZD5363 or DMSO for 10 days. The inhibitor was washed out, cells were seeded onto 96-well plates and allowed to adhere overnight prior to exposure to increasing concentrations (1 nM – 10 μM) of AZD5363. 96 hours later cell viability was assessed using MTS assay. Data were fitted to dose–response curves using GraphPad Prism 5.0. The results are the means ± S.D. of a triplicate assay and are normalised to the DMSO control that was set to 100%. (**B**) As in (**A**) except MK-2206 was used. (**C**) as in (**A**) except ZR-75-1 cells were used. (**D**) as in (**B**) except ZR-75-1 cells were used.

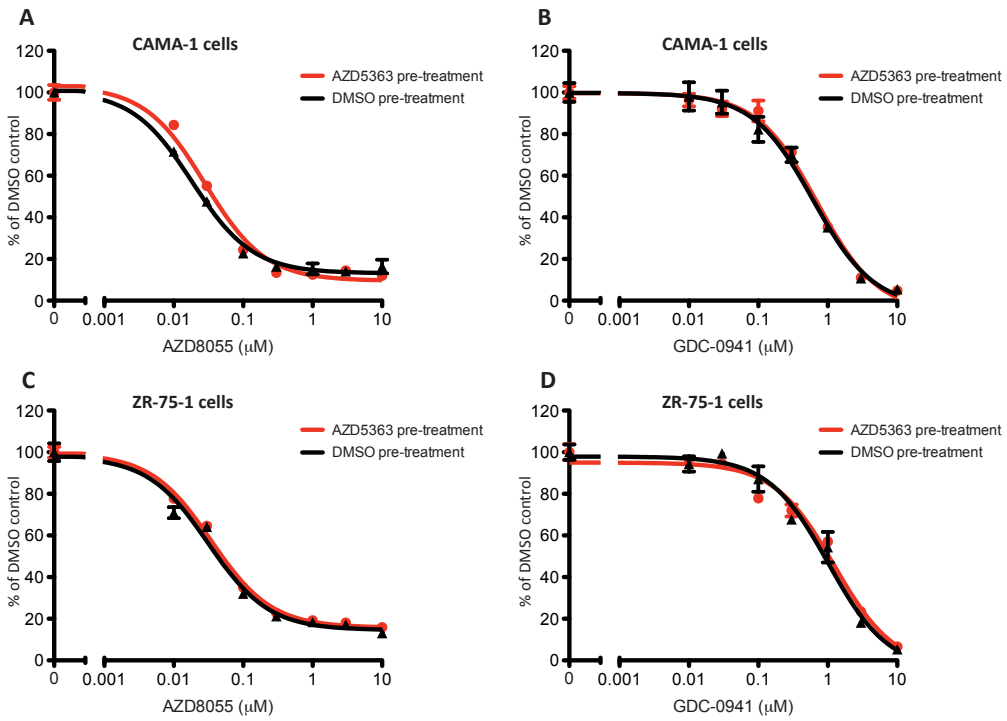

Figure 5.21 Pre-treatment with AZD5363 does not alter how PI3K or mTOR inhibition affects cell proliferation

(**A**) CAMA-1 cells were maintained in the presence of 1 μM AZD5363 or DMSO for 10 days. AZD5363 was washed out and cells were seeded onto 96-well plates and allowed to adhere overnight prior to exposure to increasing concentrations (1 nM – 10 μM) of mTOR inhibitor AZD8055. 96 hours later cell viability was assessed using MTS assay. Data were fitted to dose–response curves using GraphPad Prism 5.0. The results are the means ± S.D. of a triplicate assay and are normalised to the DMSO control that was set to 100%. (**B**) As in (**A**) except PI3K inhibitor GDC-0941 was used. (**C**) as in (**A**) except ZR-75-1 cells were used. (**D**) as in (**B**) except ZR-75-1 cells were used.

5.2.11. SGK3 depletion reverses cell culture derived Akt inhibitor resistance

To study whether the resistance to Akt inhibitors that chronic AZD5363 treatment caused was due to up-regulation of SGK3, SGK3 was knocked down in AZD5363 pre-treated cells. CAMA-1 and ZR-75-1 cells were subjected to 10 days of treatment with AZD5363 followed by infection with SGK3 or scrambled shRNAs whilst maintained in the presence of

AZD5363. AZD5363 was washed out 72 hours post infection and the cells were exposed to increasing concentrations of both MK-2206 and AZD5363 in a 96-hour proliferation assay. Decrease in sensitivity to Akt inhibitors caused by AZD5363 pre-treatment was indeed blunted by SGK3 knockdown (Figure 5.22).

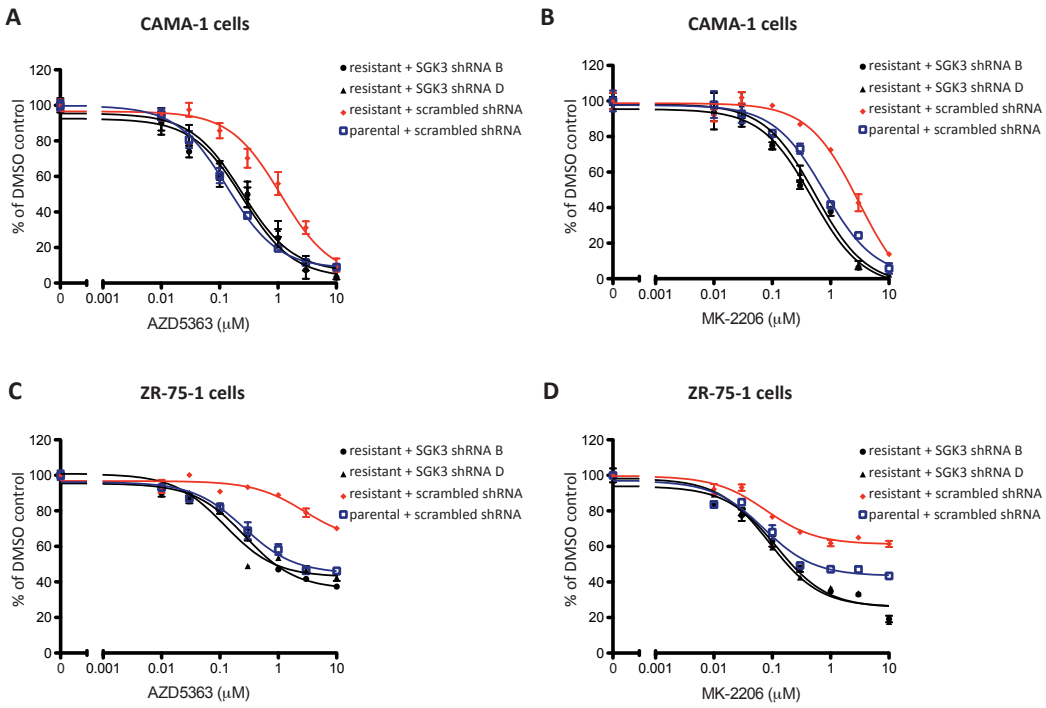

Figure 5.22 SGK3 knockdown reverses cell culture-derived resistance to Akt inhibitors

(**A**) CAMA-1 cells were maintained in the presence of 1 μM AZD5363 (to create resistant population) or DMSO (parental population) for 10 days prior to infection with indicated shRNAs in the sustained presence of either 1 μM AZD5363 or DMSO. 72 hours post infection AZD5363 was washed out and cells were seeded onto 96-well plates and allowed to adhere overnight prior to exposure to 1 nM – 10 μM AZD5363. 96 hours later cell viability was assessed using MTS assay. Data were fitted to dose–response curves using GraphPad Prism 5.0. The results are the means ± S.D. of a triplicate assay and are normalised to the DMSO control that was set to 100%. (**B**) As in (**A**) except MK-2206 was used. (**C**) as in (**A**) except ZR-75-1 cells were used. (**D**) as in (**B**) except ZR-75-1 cells were used.

The data thus far implied that up-regulation of SGK3 as a response to chronic Akt inhibition decreases cells' sensitivity to anti-proliferative effects of Akt inhibitors. To ensure that the effects seen with SGK3 knockdown were indeed due loss of SGK3 protein, a rescue experiment was next performed. ZR-75-1 cells were transduced to stably express HA-tagged wild type (wt) and kinase inactive (ki) SGK3 that was engineered to be resistant to SGK3 shRNA #D. The cells were pre-treated with AZD5363 and, as previously, the inhibitor was washed off and the cells were subjected to a 96-hour dose response experiment with the two Akt inhibitors. Expression of wild type but not kinase inactive shRNA resistant SGK3 prevented the ability of SGK3 knockdown to re-sensitise ZR-75-1 cells to both AZD5363 and MK-2206 (Figure 5.23).

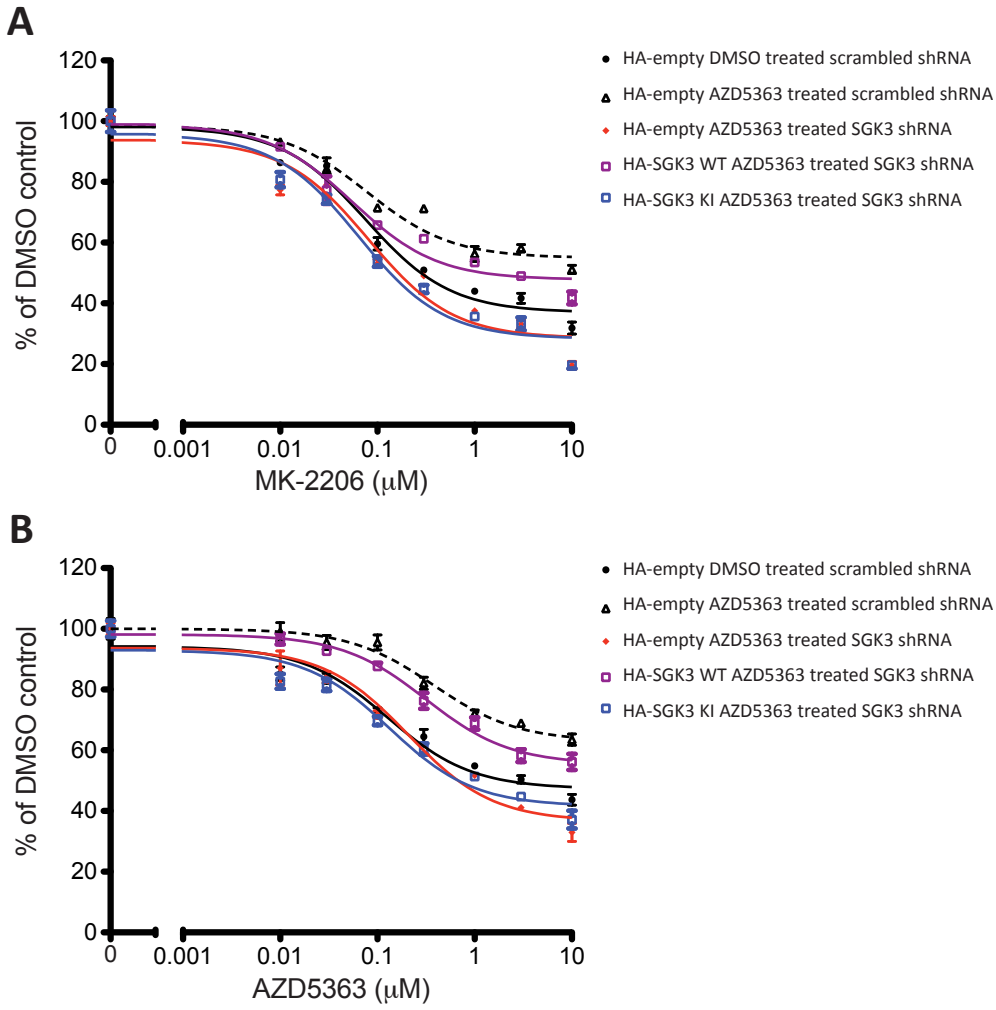

Figure 5.23 Expression of shRNA resistant SGK3 prevents the ability of SGK3 knockdown to re-sensitise ZR-75-1 cells to Akt inhibitors following cell culture derived resistance

ZR-75-1 cells stably expressing HA–SGK3 wild-type (wt) or kinase-inactive (ki) constructs designed to be resistant to SGK3 shRNA #D were maintained in the presence of either 1 μM AZD5363 or DMSO for 10 days prior to infection with lentiviral SGK3 shRNA #D or scrambled shRNA in the sustained presence of either 1 mM AZD5363 or DMSO. 72 hours post infection the cells were seeded onto 96-well plates and allowed to adhere overnight prior to exposure to increasing concentrations (1 nM – 10 μM) of the Akt inhibitors (MK-2206 or AZD5363). 96 hours later cell viability was assessed using MTS assay. Data were fitted to dose–response curves using GraphPad Prism 5.0. The results are the means ± S.D. of a triplicate assay and are normalised to the DMSO control that was set to 100%.

5.2.12. Evidence that Akt regulates SGK3 levels via mTORC1

The data thus far presented implies that Akt activity down-regulates SGK3 levels and activity. In order to gain insights into the molecular mechanisms via which Akt activity influences SGK3 levels and activity, ZR-75-1 cells were treated for five days with a range of inhibitors that target the PI3K pathway at different nodes. Besides the Akt inhibitors, MK-2206 and AZD5363, also PI3K inhibitor GDC-0941, PDK1 inhibitor GSK-2334470, mTOR inhibitor AZD8055 and mTORC1 inhibitor Rapamycin induced an increase in SGK3 protein levels whereas neither S6K inhibitor PF-4708671 nor SGK inhibitor EMD638683 led to an increase in SGK3 levels (Figure 5.24B). Strikingly, the inhibitors that induced increased SGK3 protein levels converged on mTORC1 inhibition. As EMD638683 is not very potent in cells (Figure 5.16), a high 30 μM concentration was used. Likewise, because the S6K inhibitor PF-4708671 only affects S6 phosphorylation in HEK-293 cells at around 3 – 10 μM (Pearce et al., 2010a), 10 μM of PF-4708671 was used.

Long-term treatment of ZR-75-1 cells with Akt inhibitors induced Akt inhibitor resistant NDRG1 phosphorylation whilst control one-hour treatments inhibited NDRG1 phosphorylation. As expected, acute treatment with PI3K inhibitor GDC-041 inhibited phosphorylation of Akt, PRAS40, S6 and NDRG1. Surprisingly, NDRG1 phosphorylation was not sensitive to sustained 120-hour treatment with GDC-0941 even though the treatment inhibited phosphorylation of Akt, PRAS40 and S6. PDK1 inhibitor GSK2334470 inhibited Akt T-loop (Thr308), PRAS40, S6 and NDRG1 phosphorylation following both 1 and 120 hours. The use of mTOR kinase inhibitor AZD8055 revealed a previously described bi-phasic regulation of Akt (Rodrik-Outmezguine et al., 2011). Acute treatment with

AZD8055 inhibited phosphorylation of Akt at both the HM-site and the T-loop and also inhibited phosphorylation of the Akt substrate PRAS40. Sustained AZD8055, however, caused de-phosphorylation of Akt HM-site (Ser473) but led to hyper-phosphorylation of Akt T-loop, a partial recovery of PRAS40 phosphorylation and high levels of NDRG1 phosphorylation. The elevated NDRG1 phosphorylation may be due to AZD8055 induced hyper-activation of Akt. Rapamycin is an mTORC1 selective inhibitor but long-term rapamycin treatment leads to mTORC2 inhibition due to disruption of the integrity of mTORC2 complex (Sarbassov et al., 2005). As expected, acute treatment with rapamycin only affected S6 phosphorylation. Long-term rapamycin treatment also inhibited S6 phosphorylation and modestly elevated phosphorylation of Akt T-loop. Surprisingly, acute treatment with S6K inhibitor PF-4708671 only revealed a minor effect on S6 phosphorylation but sustained 120 hour PF-4708671 treatment efficiently suppressed S6 phosphorylation. PF-4708671 had no effect on Akt, PRAS40 or NDRG1 phosphorylation. Both acute and long-term treatments with SGK inhibitor EMD638683 had partial effects on NDRG1 phosphorylation and did not affect Akt, PRAS40 or S6 phosphorylation (Figure 5.24).

In order to test whether the various inhibitors of the PI3K pathway would suppress Akt inhibitor resistant NDRG1 phosphorylation, the long-term experiment was also performed in the sustained presence of either MK-2206 or AZD5363 (Figure 5.25). Surprisingly, Akt inhibitor resistant NDRG1 phosphorylation was only sensitive to sustained treatment with the PDK1 inhibitor GSK2334470 and, as previously observed (Figure 5.16), to the SGK inhibitor EMD638683 (Figure 5.25). Strong levels of Akt inhibitor resistant phosphorylation

were detected despite sustained PI3K inhibition with GDC-0941 or mTOR inhibition with AZD8055.

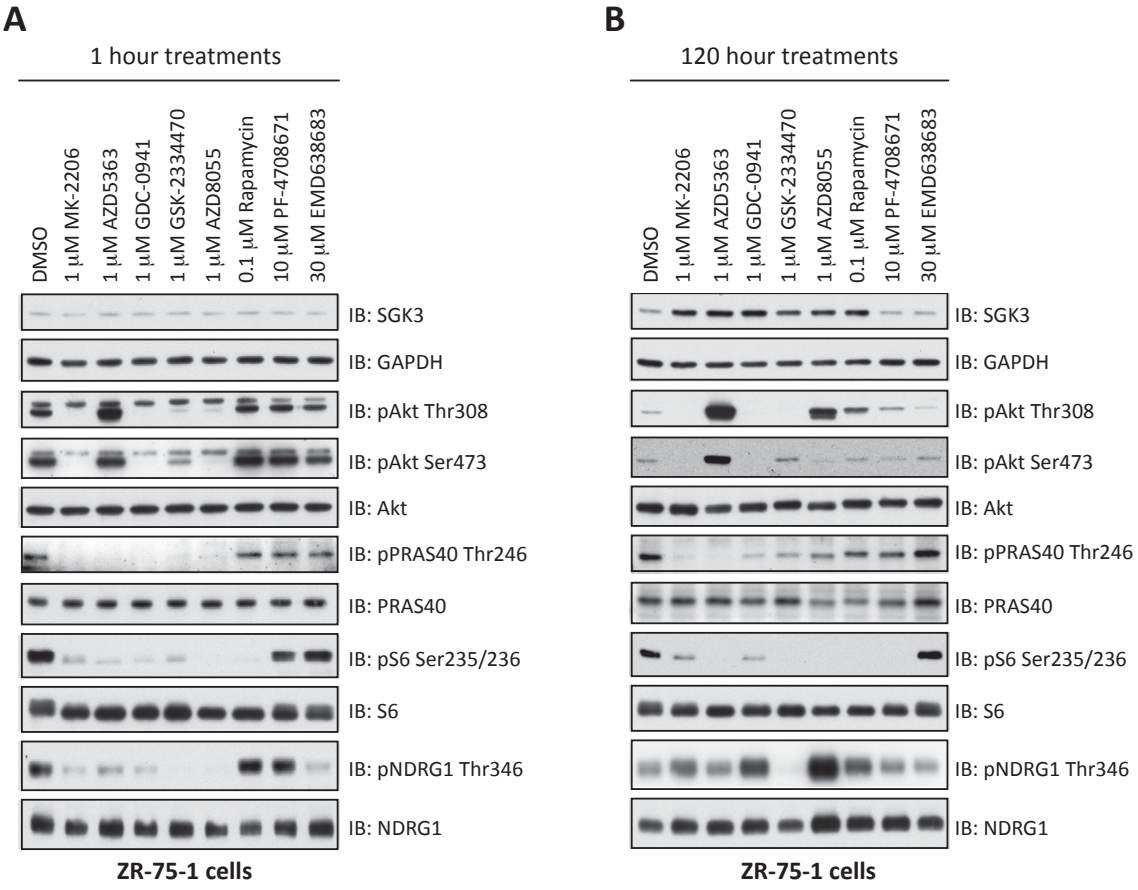

Figure 5.24 Chronic mTORC1 inhibition is associated with elevation of SGK3 levels

(**A**) ZR-75-1 cells were exposed to DMSO or the indicated concentrations of the indicated PI3K pathway inhibitors for 1 hour prior to lysis and immunoblot (IB) analysis with the indicated antibodies. (**B**) as in (**A**) except cells were exposed to the indicated compounds for 5 days.

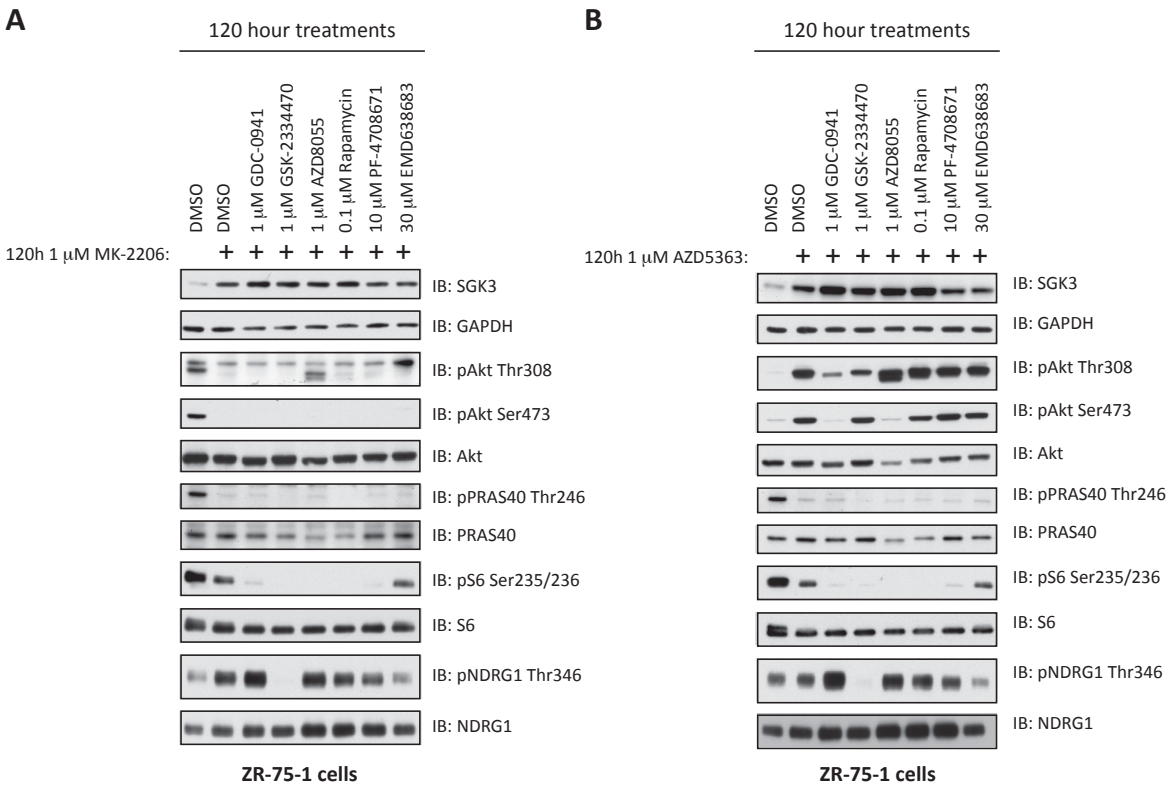

Figure 5.25 SGK3 mediated NDRG1 phosphorylation is insensitive to chronic mTORC1/2 and PI3K Class I inhibition

(**A**) ZR-75-1 cells were exposed to DMSO, 1 μM MK-2206 alone or 1 μM MK-2206 in combination with the indicated PI3K pathway inhibitors for 5 days prior to lysis and immunoblot (IB) analysis with the indicated antibodies. (**B**) as in (**A**) except 1 μM AZD5363 was used instead of MK-2206.

5.2.13. SGK3 is resistant to long term mTOR inhibition

Strikingly, SGK3-mediated NDRG1 phosphorylation was resistant to chronic mTORC1/2 inhibition. To address this observation further, a kinase assay was next undertaken in order to measure the catalytic activity of SGK3 following chronic Akt/mTOR inhibition (Figure 5.26). ZR-75-1 cells were treated with DMSO, 1 μM Akt inhibitor MK-2206, 1 μM mTORC1/2 inhibitor AZD8055 or a combination of MK-2206 and AZD8055 for 120 hours. Similar to a previous experiment (See Figure 5.5), cells exposed to sustained MK-2206

treatment were also subjected to an acute 1 hour AZD8055 treatment in order to differentiate between the effects that chronic and acute mTOR inhibition have on SGK3 activity. As previously shown (Figure 5.5), sustained Akt inhibition led to elevated SGK3 activity and HM-site and T-loop phosphorylation as well as NDRG1 phosphorylation that were all sensitive to acute 1 hour treatment with AZD8055 (Figure 5.26). In agreement with the detection of NDRG1 phosphorylation under conditions in which both Akt and mTOR are inhibited (Figure 5.25), SGK3 possessed high levels of catalytic activity despite the combination of sustained Akt and mTOR inhibition (Figure 5.26). Under these conditions, T-loop phosphorylation of SGK3 was at similar levels as with Akt inhibition alone, but HM-site phosphorylation was significantly inhibited indicating that the T-loop of SGK3 can be phosphorylated independently of the HM-site. Sustained mTOR inhibition alone led to elevated total levels of SGK3 protein without influencing SGK3 kinase activity or phosphorylation. As a control, the T-loop and HM-site phosphorylation of S6K were also monitored. HM-site phosphorylation is a pre-requisite for T-loop phosphorylation and activation of S6K [reviewed in (Pearce et al., 2010b). Sustained Akt inhibition modestly inhibited S6K HM-site phosphorylation and T-loop phosphorylation reflecting the effect that Akt inhibitors have on inhibiting mTORC1. As expected, sustained mTOR inhibition alone and in combination with sustained Akt inhibition led to complete loss of S6K HM-site and T-loop phosphorylation. Notably, a strong band that migrated lower than S6K was detected in S6K T-loop immunoblot analysis. This band might represent T-loop phosphorylated Akt isoforms, since long-term mTOR inhibition leads to elevated Akt T-loop phosphorylation.

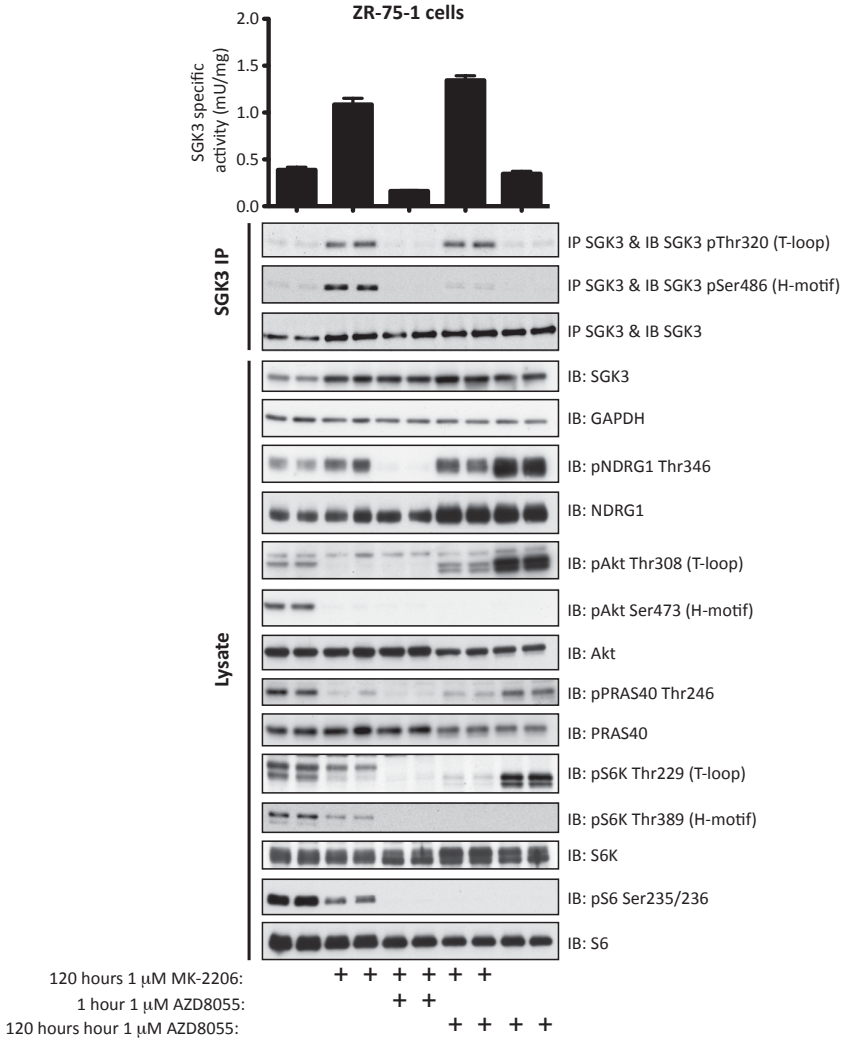

Figure 5.26 SGK3 is resistant to chronic mTORC1/2 inhibition

ZR-75-1 cells were seeded onto 15-cm dishes, allowed to adhere overnight and treated with DMSO, 1 μM MK-2206, 1 μM AZD8055 or a combination of 1 μM MK-2206 and 1 μM AZD8055 for 120 hours. For DMSO control approximately $1x10^7$, MK-2206 treatment $2x10^7$, AZD8055 treatment $4x10^7$ and MK-2206/AZD8055 treatment $8x10^7$ cells were seeded per dish. At the time of lysis all cells were approximately 60-80% confluent. Prior to lysis MK-2206 pre-treated cells were exposed to 1 μM AZD8055 or DMSO for 1 hour. Endogenous SGK3 was immunoprecipitated (IP) from 2 mg of fresh lysate and SGK3 catalytic activity was measured using Crosstide substrate peptide. Results represent the means ± S.E.M. of two independent samples each assayed in duplicate. Lysates and immunoprecipitates were also analysed by immunoblotting (IB) with the indicated antibodies.

5.3. Discussion

Results presented in the present Chapter reveal a novel mechanism of feedback regulation within the PI3K pathway. In Chapter 4 I showed that depending on the levels of SGK within a cell, NDRG1 could be phosphorylated by either SGK or Akt. Therefore I decided to use phospho-NDRG1 as readout for monitoring whether Akt inhibitor sensitive cells would display compensatory SGK activity following prolonged Akt inhibition. Strikingly, sustained Akt inhibition led to recovery of NDRG1 phosphorylation and revealed a bi-fold up-regulation of SGK3. As determined by monitoring recovery of NDRG1 phosphorylation and induction of SGK3 kinase activity, Akt inhibition first induced SGK3 activation. Following the initial activation phase, levels of both SGK3 levels were increased. Potential molecular mechanisms that could account for this are discussed below. As demonstrated by SGK3 knockdown, accompanied by a rescue experiment, and by pharmacological inhibition of SGKs, SGK3 mediated NDRG1 phosphorylation in the absence of Akt activity.

These results indicate that the effect of Akt inhibitors on NDRG1 phosphorylation is dependent upon the length of Akt inhibition. Therefore, in contrast to the model proposed in Chapter 4, following the effects that Akt inhibitors have on NDRG1 phosphorylation, may not represent a straightforward tool for predicting the long-term sensitivity of tumour cells to Akt inhibitors.

Characterisation of SGK inhibitors

The ability of SGK inhibitors to suppress both SGK1 and SGK3 mediated NDRG1 phosphorylation was determined. Common to all the three inhibitors was a considerable *in vitro – in vivo* potency drop off. Because of the low cellular potencies no further work was carried out with these inhibitors. Development of specific and highly potent SGK inhibitors would certainly be beneficial for the study of SGKs. Of the inhibitors EMD638683 was remarkably specific but only inhibited SGK1 and SGK3 mediated NDRG1 phosphorylation at high (around 10 μM) concentrations thereby lacking potency. EMD638683 has been previously published and has indeed been reported to be highly specific and capable of inhibiting all SGK isoforms *in vitro*, to inhibit NDRG1 phosphorylation at high (~10 μM) concentrations in cells and to lower fructose/saline induced blood pressure *in vivo* (Ackermann et al., 2011).

Akt inhibition up-regulates SGK3 levels via inhibition of mTORC1

As SGK3 levels were increased following sustained Akt inhibition, Akt activity appears to negatively regulate SGK3 levels. All inhibitors, namely Akt, PDK1, mTORC1/2 and mTORC1 inhibitors, that up-regulated SGK3 levels converged on the inhibition of mTORC1. To validate the importance of mTORC1 for the regulation of SGK3 levels, it would be interesting to see if Raptor knockdown mimicked the results observed with mTORC1 inhibition. Because the S6K inhibitor PF-4708671 failed to induce SGK3, mTORC1 outputs other than S6K are likely to mediate the regulation of SGK3 levels.

Chronic Akt inhibition increased SGK3 transcript levels and consistent with this, recent work carried out by Dr R. Bago in our laboratory has revealed that sustained treatment with AZD8055 or rapamycin also increases SGK3 transcripts. Transcriptional up-regulation of *SGK3* could represent the primary mechanism via which SGK3 levels are elevated following inhibition of Akt-mTORC1 signalling. If that were the case, the elevation in *SGK3* expression would be caused by direct or indirect modulation of transcription factors by mTORC1. Transcription factors that mTORC1 is thought to directly regulate are summarised in Table 5.1. Interestingly, a recent study identified *SGK3* as a gene whose expression was increased following over-expression of TFEB, which mTORC1 inhibits by direct phosphorylation (Martina et al., 2012; Roczniak-Ferguson et al., 2012; Settembre et al., 2013; Settembre et al., 2012). Another study identified *SGK3* as a gene whose expression negatively correlated with PPARγ, which is though to be activated by mTORC1 (Cipolletta et al., 2012; Laplante and Sabatini, 2013). In future work it would be interesting to investigate whether TFEB or PPARγ controlled *SGK3* expression by using for example knockdown studies and PPAR agonists. Because the increases in *SGK3* transcript levels are seen at relatively late time points indirect mechanisms could operate to increase SGK3 transcripts. mTORC1 inhibition has been described to, for example, cause PI3K dependent activation of MAPK signalling (Carracedo et al., 2008). Alternatively, Akt/mTORC1 inhibition could stabilise SGK3 protein levels and the increase in SGK3 transcripts could be a secondary observation potentially caused by positive feedback from SGK3 itself. Clearly more work is required to elucidate the mechanism(s) via which the Akt-mTORC1 signalling axis regulates SGK3 levels.

Transcription factor	mTORC1 regulation	Regulated process
HIF1α	mTORC1 activates via multiple mechanisms	Glucosemetabolism, proliferation
PPARα	mTORC1 inhibits (may be via S6K2)	Hepatic ketogenesis
PPARγ	mTORC1 activates (poorly defined mechanisms)	Adipogenesis
SREBP1/2	mTORC1 activates via multiple mechanisms	Lipid synthesis
STAT3	mTORC1 activates by direct phosphorylation	Survival, proliferation, migration, angiogenesis, immune tolerance
TFEB	mTORC1 inhibits by direct phosphorylation	Lysosomal function
YY1–PGC1α	mTORC1 activates via poorly defined mechanisms	Mitochondrial biogenesis, oxidative metabolism

Table 5.1 Transcription factors that mTORC1 directly regulates

Adapted from (Laplante and Sabatini, 2013). Abbreviations not defined in text: signal transducer and activator of transcription 3 (STAT3); sterol-regulatory-element-binding protein (SREBP); transcription factor EB (TFEB); Hypoxia-inducible factor (HIF1); peroxisome proliferator-activated receptor (PPAR).

Like Akt, SGK3 is resistant to sustained mTORC1/2 inhibition

Activity of SGK3 following its induction by Akt inhibition was clearly sensitive to acute mTORC1/2 inhibition as assessed by monitoring the effects of 1 hour AZD8055 treatment on SGK3 activity and NDRG1 phosphorylation. Surprisingly, however, NDRG1 was phosphorylated following 120 hours of concurrent Akt and mTORC1/2 inhibition to similar levels seen following Akt inhibition alone. These observations resemble the behaviour of Akt following long-term mTORC1/2 inhibition. PRAS40 phosphorylation was sensitive to acute AZD8055 treatment but recovered following 120 hours of mTORC1/2 inhibition and this was accompanied by a substantial increase in Akt T-loop (Thr308) phosphorylation. Similar results have previously been described in studies using AZD8055 for up to 24 hours (Rodrik-Outmezguine et al., 2011). Sustained AZD8055 treatment was also accompanied with high levels of NDRG1 phosphorylation, which would be expected to due to up-regulation of Akt activity. Recent work carried out by Dr R. Bago in our laboratory indeed

confirmed that following sustained exposure to AZD8055, NDRG1 phosphorylation is sensitive to acute Akt inhibition. Notably, total levels of PRAS40 were reduced following chronic AZD8055 or rapamycin treatment indicating that prolonged mTORC1 inhibition may lead to reduced stability or expression of its negative regulator, PRAS40. mTORC1 regulates PRAS40 by direct phosphorylation that causes loss of PRAS40 binding to mTORC1 (Oshiro et al., 2007). It is entire possible that mTORC1 could also regulate the stability and/or expression of PRAS40. Interestingly, chronic rapamycin treatment did not induce Akt activity as strongly as AZD8055 did. Why this should be the case is unclear and could reflect either more potent inhibition of mTORC1 by AZD8055 or could also be due to mTORC2 mediated outputs. Further work is required to address these observations.

A few possibilities could explain why NDRG1 phosphorylation was resistant to sustained Akt/mTOR inhibition. Firstly, SGK3 activation may resemble the mechanism of Akt activation more closely than the mechanism of SGK1/S6K activation. Secondly, another kinase could phosphorylate NDRG1 in the absence of Akt and SGK3 activities. Thirdly, in the absence of mTORC2 activity another kinase could phosphorylate SGK3 HM-site. To address these possibilities, kinase activity of endogenous SGK3 was measured following sustained Akt/mTOR inhibition. Despite complete loss of HM-site phosphorylation, SGK3 T-loop was strongly phosphorylated indicating that the T-loop site can be phosphorylated independently of the HM-site thereby suggesting that SGK3 activation resembles that of Akt. Consistent with this, immunoprecipitated SGK3 was also highly active following sustained Akt/mTOR inhibition. Interestingly, chronic mTOR kinase inhibition alone, despite elevating SGK3 levels, did not induce SGK3 T-loop phosphorylation or activation.

This observation is discussed in more detail below. T-loop Thr320 phosphorylation is critical for SGK3 activity as under all conditions tested the PDK1 inhibitor GSK2334470 fully suppressed SGK3 mediated NDRG1 phosphorylation.

Multiple lines of evidence exist for the differential importance of mTOR mediated HM-site phosphorylation of SGK/S6K and Akt. Knock in mutations that prevent PDK1 from interacting with phosphorylated HM-site residue by disrupting the PIF-binding pocket of PDK1 prevent the activation of SGK and S6K but not of Akt (Collins et al., 2003; Collins et al., 2005). Consistent with this, in MEFs knockout of mTORC2 components Rictor, mLST8 or Sin1 prevents activation of SGK but whilst Akt Ser473 phosphorylation is ablated in these cells, phosphorylation of Akt Thr308 and of Akt substrates is not affected (Garcia-Martinez and Alessi, 2008; Guertin et al., 2006; Jacinto et al., 2006; Shiota et al., 2006). In contrast, a point mutation within PDK1 PH domain that impairs PtdIns(3,4,5)P_3 binding, prevents activation of Akt, but not of S6K/SGK (Bayascas et al., 2008; Komander et al., 2004). Finally, Akt Ser473Ala mutation does not affect the ability of PDK1 to phosphorylate and activate Akt *in vitro* in the presence of PtdIns(3,4,5)P_3 containing vesicles (Biondi et al., 2001). It is important to note that recent work has indicated that the HM-site phosphorylation of Akt does nevertheless contribute towards efficient activation of Akt (Najafov et al., 2012).

The studies described above have analysed activation of the SGK1 isoform that lacks a phosphoinositide-binding domain. Thus far the role of SGK3 PX domain has been studied utilising over-expression and *in vitro* techniques. Accumulating evidence suggests that SGK3 localises to early endosomal antigen-1 (EEA1) positive endosomes and/or recycling

endosomes (He et al., 2011; Tessier and Woodgett, 2006; Virbasius et al., 2001; Xu et al., 2001). Based on lipid overlay assays SGK3 has been suggested to primarily interact with PtdIns(3)P (Tessier and Woodgett, 2006; Virbasius et al., 2001) or with PtdIns(3,4,5)P_3 , PtdIns(4,5)P_2 and PtdIns(3,5)P_2 (Xu et al., 2001). Introducing either Arg90Ala (Tessier and Woodgett, 2006; Xu et al., 2001) or Tyr51Ala (Virbasius et al., 2001) mutations into the PX domain abrogates lipid binding and endosomal localisation. In over-expression systems Tyr51Ala inhibits the kinase activity of HA-SGK3 (Virbasius et al., 2001) and Arg90Ala blunts the ability of PDK1 to phosphorylate SGK3 whereas the phospho-mimetic HM-site Ser468Asp mutation makes SGK3 T-loop phosphorylation independent of endosomal localisation (Tessier and Woodgett, 2006) indicating that in the absence of co-localisation at the membrane the PIF-binding pocket mechanism promotes phosphorylation of SGK3 by PDK1. Another study reported co-localisation of SGK3 and PDK1 in recycling endosomes where SGK3 activated the Na^+/H^+ exchanger 3 (NHE3). Arg90Ala mutation disrupted the endosomal localisation of SGK3 and the regulation of NHE3 by SGK3 (He et al., 2011). Taken together, these observations indicate that membrane localisation of SGK3 is likely to be important for its activation.

Based on over-expression studies deletion of SGK3 PX-domain increases SGK3 activity whereas Arg90Ala (Xu et al., 2001) and Tyr51Ala (Virbasius et al., 2001) mutations inhibit SGK3 suggesting that *in vivo* lipid binding is important for proper activation of SGK3 and that in the absence of lipid binding the PX domain may adopt a conformation that suppresses SGK3 activity. This is analogous to the regulation of Akt by its PH domain. Inactive Akt adopts a conformation in which the PH domain folds in and prevents the

phosphorylation of Akt T-loop by PDK1. Association of Akt PH domain with PtdIns(3,4,5)P_3 causes a conformation change that makes the T-loop site available for phosphorylation by PDK1 (Calleja et al., 2007; Milburn et al., 2003). Removal of the PX domain from SGK3 would be expected to make SGK3 behave like SGK1 and SGK2 isoforms by decoupling its regulation from the endosomal membrane.

SGK3 activity is insensitive to long-term PI3K Class I inhibition

Sustained treatment with the Class I selective PI3K inhibitor GDC-0941 (Folkes et al., 2008) failed to inhibit NDRG1 phosphorylation whilst phosphorylation of S6, Akt and the Akt substrate PRAS40 was efficiently suppressed and moreover, combined Akt/GDC-0941 treatment was also associated with high levels of NDRG1 phosphorylation. Consistent with this, acute GDC-0941 treatment only partially suppressed SGK3 mediated NDRG1 phosphorylation. Recent work carried out by Dr R. Bago in our laboratory confirmed that endogenous SGK3 kinase activity is insensitive to long-term GDC-0941 treatment. Taken together, these observations indicate that, at least in the prolonged absence of Class I PI3K activity, SGK3 can be activated via another mechanism. This could be achieved by the creation of phosphoinositides by Class II or Class III phosphoinositide 3-kinases that, like SGK3, are associated with intracellular membranes (Vanhaesebroeck et al., 2010). The functional roles of PI3K Class II enzymes are still poorly characterised but interestingly they possess a PX domain and the PX domain of Class II Cα isoform has been shown to bind PtdIns(4,5)P_2. Class II PI3Ks can be activated by growth factors and hormones and are thought preferentially generate PtdIns(3)P and to a lesser extinct PtdIns(3,4)P_2. Class II PI3Ks have been linked to for instance endocytosis, cell growth, survival and migration

[reviewed in (Falasca and Maffucci, 2012). Vps34, which generates PtdIns(3)P, is the sole Class III PI3K and is part of a constitutive Vps34:Vps15 heterodimer that is tethered to intracellular membranes via myristoylated Vps15. Other proteins associate with the heterodimeric complex to dictate different functions, including autophagy and endosomal trafficking. Clearly extensive further work is required to fully understand which PI3K family members are most critical for the activation of SGK3. It would be important to compare to effects of GDC-0941 to pan-PI3K inhibitors, such as wortmannin and LY294002, although these compounds do not potently inhibit PI3K Class II (Vanhaesebroeck et al., 2010). Additionally, two Vps34 inhibitors that do not inhibit Class I PI3Ks have recently been reported. One of these is an ataxia telangiectasia mutated (ATM) inhibitor KU55933 that also inhibits Vps34 (Farkas et al., 2011) and Novartis recently filed a patent for Vps34 specific inhibitors (Cornella Taracido et al., 2013). In future work it would be important to delineate the roles that these inhibitors have on SGK3 activation. Figure 5.27 illustrates a model for the activation of SGK3 at the endosome.

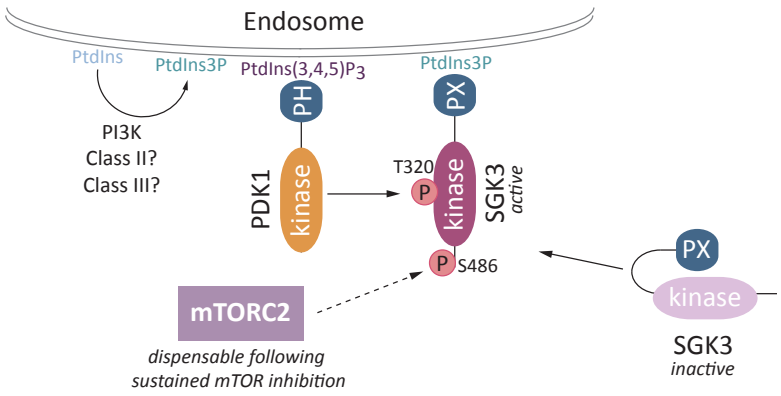

Figure 5.27 Model for PX-domain dependent activation of SGK3

PDK1 and SGK3 co-localise at the endosomal membrane by virtue of their PtdIns-binding domains. PtdIns3P generation by Class II and/or III PI3Ks recruits SGK3 to the membrane.

Sustained mTOR inhibition, despite elevating SGK3 levels, did not induce SGK3 T-loop phosphorylation or activation indicating that Akt activity negatively regulates SGK3 T-loop phosphorylation via an mTORC1 independent mechanism. Dr R. Bago recently confirmed this result by using rapamycin, which too caused up-regulation of SGK3 levels but did not induce SGK3 T-loop phosphorylation or activation. The notion that Akt negatively controls SGK3 activity is also highlighted by results demonstrating that Akt inhibition causes bi-phasic regulation of SGK3 consisting of an initial activation phase followed by elevation of SGK3 levels. Further work is required to address the mechanism via which Akt negatively controls SGK3 activity. For example, inhibition of either Class II or Class III PI3Ks by Akt could explain why Akt inhibition causes SGK3 activation. Excitingly, Akt has been reported to phosphorylate Beclin 1, which is a binding partner of Vps34, and to inhibit activity of Beclin 1 associated Vps34 (Wang et al., 2012). Alternatively, following Akt inhibition, FoxO activation associated increase in receptor tyrosine kinase expression (Chandarlapaty et al., 2011) could promote downstream activation of SGK3.

SGK3 contributes to cell culture acquired decrease in sensitivity to Akt inhibitors

Sustained Akt inhibition followed by inhibitor wash out induced a shift in cells' sensitivity towards a subsequent challenge with the two structurally and mechanistically distinct Akt inhibitors. Responses to PI3K or mTOR inhibitors were not altered indicating that the decreased sensitivity was specific to Akt inhibitors. Importantly, Akt was effectively inhibited following long-term treatments; for example PRAS40 phosphorylation was suppressed to a similar degree throughout the time courses studied. Therefore the most likely explanation for the cells' reduced sensitivity to Akt inhibitors would be alterations to

signal transduction. SGK3 knockdown re-sensitised AZD5363 pre-treated cells to Akt inhibitors, an effect rescued by expression of shRNA resistant wild type SGK3, indicating that the induction and activation of SGK3 following Akt inhibition contributes to the reduced ability of Akt inhibitors to suppress proliferation. Figure 5.28 summarises how the induction of SGK3 activity and levels by Akt-mTORC1 inhibition leads to reduced efficacy of Akt inhibitors.

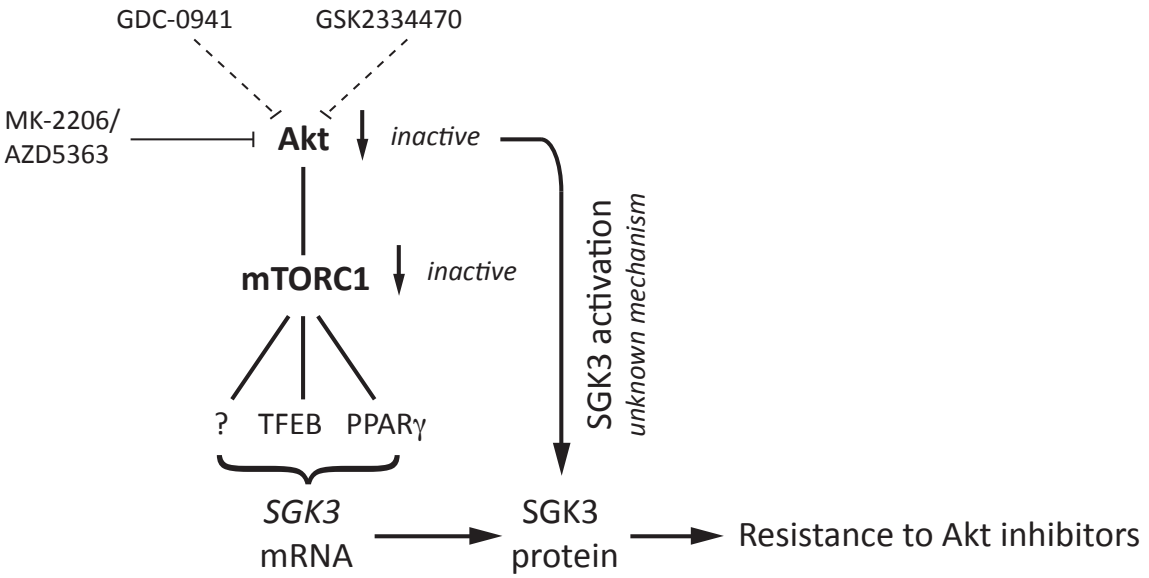

Figure 5.28 Up-regulation of SGK3 activity and levels as a response to Akt-mTORC1 inhibition

Proliferation driving roles have been previously described for SGK3 and as discussed in Chapter 4 also for the closely related SGK1. In 2000 a screen utilising enhanced retroviral mutagenesis identified *SGK3* as a gene required for IL3-mediated survival of hematopoietic cells in which SGK3 over-expression protects from IL3-withdrawal induced

apoptosis (Liu et al., 2000). More recently a comparison of PI3K and PTEN mutant breast cancer cell lines revealed that many PI3K mutant lines display surprisingly low levels of Akt signalling and are not dependent on Akt for anchorage independent growth whereas they remain dependent on PI3K ad PDK1. An shRNA screen revealed that SGK3 is important for the viability of these cells (Vasudevan et al., 2009). *SGK3* is also an oestrogen receptor (ER) responsive gene (Wang et al., 2011; Xu et al., 2012) and ER mediated induction of *SGK3* expression promotes breast cancer cell survival based on knockdown studies (Wang et al., 2011). Additionally, SGK3 over-expression has recently been shown to correlate with poor survival of hepatocellular carcinoma patients (Liu et al., 2012). Over-expression of SGK3 increases the proliferation and survival of human liver cancer cells in culture and tumourigenesis in xenograft models, whereas SGK3 knockdown reduces proliferation and survival in culture and *in vivo* (Liu et al., 2012). Studies with SGK3 knockout mice provide further evidence for proliferation supporting roles of SGK3 as *SGK3*$^{-/-}$ mice display reduced keratinocyte proliferation (Alonso et al., 2005; McCormick et al., 2004).

The mechanisms via which SGK3 promotes proliferation remain poorly characterised. Given that SGK1 and SGK3 are closely related, these two kinases are likely to phosphorylate an overlapping set of substrates and perform many similar functions. This is indeed evidenced by results demonstrating that SGK3 too can phosphorylate NDRG1. Furthermore, SGK3 can also regulate many of the channels and transporters that SGK1 regulates [reviewed in (Lang et al., 2006). Therefore it is likely that SGK1 and SGK3 could promote proliferation and survival via similar mechanisms (discussed in Chapter 4). Some unique SGK3 substrates, including E3-ubiquiting ligase AIP4 that controls the levels of

chemokine receptor CXCR4 (Slagsvold et al., 2006) and Flightless-1 (Xu et al., 2009), have been reported but the physiological relevance of these remains to be elucidated. As discussed in Chapter 4, SGKs have been reported to phosphorylate FoxOs. Chronic AZD5363 or MK-2206 treatments caused sustained de-phosphorylation of FoxO1/3. This was accompanied with increased total levels of FoxO1 reflecting reduced phosphorylation induced degradation of FoxOs. Activation and up-regulation of SGK3 was accompanied with recovery of NDRG1 phosphorylation but not with FoxO1/3 phosphorylation (at least at Thr24/32 and Thr253). Therefore SGK3 does not appear to contribute towards the phosphorylation of these sites, at least in ZR-75-1 cells.

Feedback mechanisms operating within the PI3K-Akt-mTOR pathway

As discussed in the introduction (Section 1.5.1), mTORC1 inhibition leads to activation of PI3K pathway via removal of negative feedback to IRS1 and Grb10. The best-characterised mTORC1 mediated negative feedback is that of mTORC1-S6K-IRS1 [reviewed in (Laplante and Sabatini, 2012)]. However, the S6K inhibitor PF-4708671 does not induce hyper activation of PI3K signalling [(Pearce et al., 2010b) and personal communication]. Consistent with this, results presented in this Chapter do not reveal any up-regulation of Akt activity following chronic PF-4708671 treatment. Moreover, inhibition of mTORC1 via loss of Raptor still leads to activation of Akt in $S6K1^{-/-}S6K2^{-/-}$ cells and mTORC1 inhibits PI3K also by directly phosphorylating IRS1 (Hsu et al., 2011; Tzatsos, 2009; Tzatsos and Kandror, 2006). Therefore the mTORC1-S6K-IRS1 axis is not the sole mechanism by which mTORC1 inhibition leads to hyper-activation of PI3K signalling. Work presented in this Chapter reveals a novel feedback mechanism comprising of bi-phasic up-regulation of SGK3

following inhibition of the Akt-mTORC1 signalling axis. A model of feedback-regulation operating within the PI3K pathway is presented in Figure 5.29. SGK3 can compensate for the loss of Akt activity and therefore SGK3 activation may represent a resistance mechanism to Akt inhibitors. In future work it will be important to extend the studies to a wider range of cancer types.

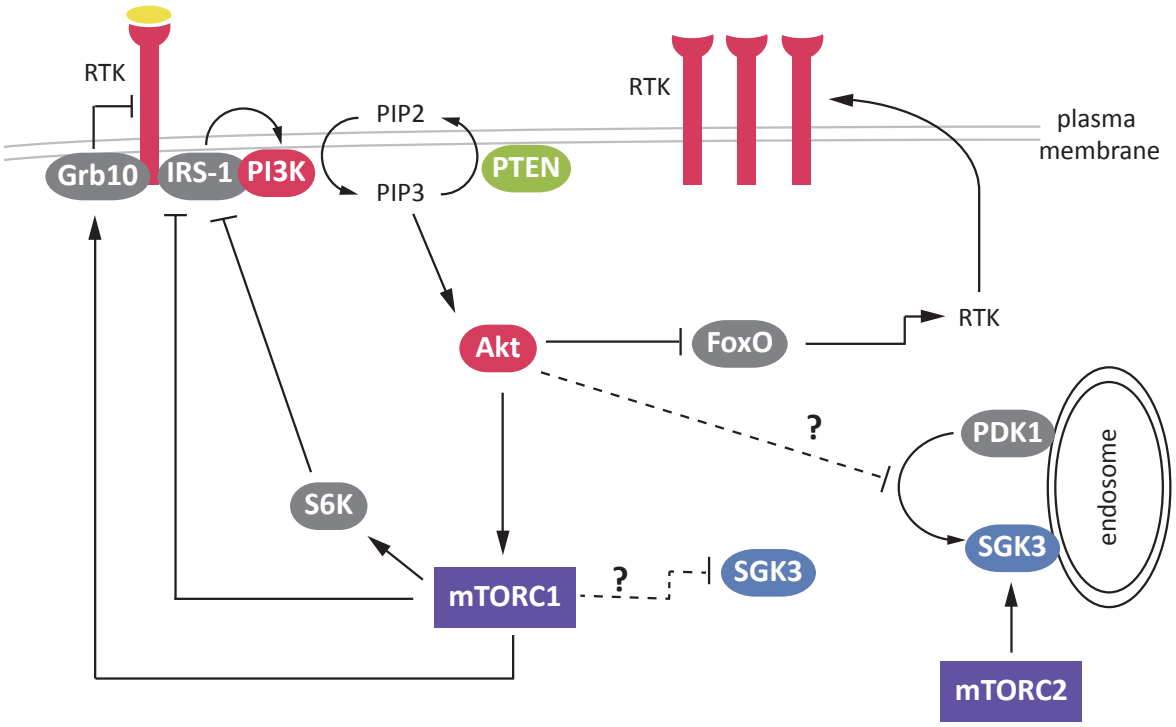

Figure 5.29 Akt-mTORC1 signalling negatively regulates SGK3 levels and activity

Receptor tyrosine kinase (RTK) activation stimulates PI3K-Akt activity causing inhibition of FoxO-mediated RTK transcription. Akt activation also stimulates mTORC1, which directs inhibitory feedback to PI3K via IRS1 and Grb10. Via as-of-yet unknown mechanisms Akt negatively regulates SGK3 activity and mTORC1 negatively regulates SGK3 levels.

6. Final summary and future perspectives

My work demonstrates that high levels of SGK1 in breast cancer cells can be utilised to predict resistance to Akt inhibitors. I also show that induction of SGK3 as a response to sustained Akt inhibition represents a resistance mechanism that reduces the ability of Akt inhibitors to suppress proliferation. Taken together my results highlight that SGK isoforms, which in comparison to Akt have received little attention, can promote survival and proliferation of cancer cells. Therefore future work should be carried out to address whether inhibition of SGK isoforms either alone or in combination with Akt or other inhibitors would be clinically beneficial for the treatment of cancer. It would also be important to extend these studies into other cell types.

My research into the roles of SGK isoforms in cancer cells reveals a number questions which remain to be addressed. Most importantly, the mechanisms via which SGKs promote proliferation and survival remain elusive. In future work it would be interesting to identify novel SGK substrates and to evaluate the importance of such substrates for disease relevant processes. It would be valuable to carry out non-biased phospho-proteomics screens and to take advantage of novel genome engineering techniques such as the TALEN or CRISPR/Cas technologies that enable editing of the endogenous gene sequence (Gaj et al., 2013). Introducing catalytically inactive mutation into the endogenous gene sequence would create a stringent control for substrate screens. In future it would certainly also be of interest to dissect the precise molecular role(s) that phosphorylation of NDRG1 by SGK/Akt and GSK3 plays.

In Chapter 4 I describe a novel method of feedback regulation that operates within the PI3K pathway. I demonstrate that Akt negatively regulates the levels and activity of SGK3 and that the induction of SGK3 as a response to sustained Akt inhibition reduces the ability of Akt inhibitors to suppress proliferation. I present data suggesting that the Akt-mTORC1 signalling axis negatively regulates SGK3 at transcriptional levels but further work is required to elucidate the mechanisms via which SGK3 levels are regulated. My results imply that sustained Akt inhibition first increases SGK3 activity followed by elevation of SGK3 expression. Therefore further work is also required to address the mechanisms via which Akt negatively regulates SGK3 activity. Moreover, I also present preliminary data implying that SGK3 is insensitive to long term Class I PI3K and mTORC1/2 inhibition. These observations indicate that the creation of phosphatidylinositols by either Class II or III PI3Ks is likely to be key for the ability of PDK1 to phosphorylate the T-loop residue of SGK3 and that PDK1 can phosphorylate the T-loop of SGK3 independently of SGK3 HM-site phosphorylation. I feel that further work is required to elaborate the role that the PX domain of SGK3 plays in the regulation SGK3 activation.

In addition, in collaboration with Dr L. Pearce, I studied the role that Protor isoforms, which are mTORC2 subunits, play in the activation of SGK. My studies utilising Protor-$1^{-/-}$ Protor-$2^{-/-}$ double knockout mice revealed that these mice do not significantly differ from Protor-1 single knockout mice, which had previously been characterised, implying that Protor-1, but not Protor-2, is important for efficient activation of SGK in the kidney. The tissue specific nature of for the requirement of Protor-1 for maximal activation of SGK remains unsolved.

7. Appendix

Antibody	Source	Catalog #
SGK1	Epitomics	S1493
SGK	Epitomics	1617-1
SGK1	Assay Designs	KAP-PKO15

Appendix 1 Additional commercial antibodies tested

Access #	Score	Coverage	Gene	Protein Name
DSTT S062D, Kidney				
Q8VDN2	1053	24%	Atp1a1	Sodium/potassium-transporting ATPase subunit alpha-1
P38647	1030	37%	Hspa9	Stress-70 protein, mitochondrial
Q9DBS9	822	18%	Osbpl3	Oxysterol-binding protein-related protein 3
Q9QZS5	**249**	**31%**	**Sgk2**	**Serine/threonine-protein kinase Sgk2**
P62270	153	36%	Rps18	40S ribosomal protein S18
Q64676	143	15%	Ugt8	2-hydroxyacylsphingosine 1-beta-galactosyltransferase
Q68FD5	133	2%	Cltc	Clathrin heavy chain 1
P97817	129	16%	Cdr2	Cerebellar degeneration-related protein 2
P55014	84	1%	Slc12a1	Solute carrier family 12 member 1
Q9Z2I9	71	5%	Sucla2	Succinyl-CoA ligase [ADP-forming] subunit beta, mitochondrial
DSTT S036D, Kidney				
Q9QZS5	**526**	**41%**	**Sgk2**	**Serine/threonine-protein kinase Sgk2**
Q3UNZ8	350	45%	At1g23740	Quinone oxidoreductase-like protein 2
P17563	188	12%	Selenbp1	Selenium-binding protein 1
Q3UNZ8	156	14%	At1g23740	Quinone oxidoreductase-like protein 2
P48962	114	11%	Slc25a4	ADP/ATP translocase 1
DSTT S037D, Kidney				
P38647	1025	39%	Hspa9	Stress-70 protein, mitochondrial
Q9ERE3	**440**	**31%**	**Sgk3**	**Serine/threonine-protein kinase Sgk3**
P16858	248	18%	Gapdh	Glyceraldehyde-3-phosphate dehydrogenase
Q61235	90	15%	Sntb2	Beta-2-syntrophin
Sigma S5188, Kidney				
Q9QZS5	**2730**	**61%**	**Sgk2**	**Serine/threonine-protein kinase Sgk2**
Q6P9Q6	2550	37%	Fkbp15	FK506-binding protein 15
Q8VDN2	1447	32%	Atp1a1	Sodium/potassium-transporting ATPase subunit alpha-1
Q9DBN5	1160	48%	Lonp2	Lon protease homolog 2, peroxisomal
Q9ERE3	**1057**	**51%**	**Sgk3**	**Serine/threonine-protein kinase Sgk3**
O35488	1024	41%	Slc27a2	Very long-chain acyl-CoA synthetase
Q60668	886	43%	Hnrnpd	Heterogeneous nuclear ribonucleoprotein D0
Q8K2B3	601	33%	Sdha	Succinate dehydrogenase [ubiquinone] flavoprotein subunit, mitochondrial
Q8C1B7	528	25%	Sep-11	Septin-11
O55131	528	44%	Sep-07	Septin-7
Q3ULD5	376	25%	Mccc2	Methylcrotonoyl-CoA carboxylase beta chain, mitochondrial
Q9D394	354	26%	Rufy3	Protein RUFY3
P50516	317	18%	Atp6v1a	V-type proton ATPase catalytic subunit A
P56480	311	24%	Atp5b	ATP synthase subunit beta, mitochondrial
P05622	305	21%**	Pdgfrb	Beta-type platelet-derived growth factor receptor
P50544	294	14%	Acadvl	Very long-chain specific acyl-CoA dehydrogenase, mitochondrial
P39054	289	15%	Dnm2	Dynamin-2
Q9QZS5	**260**	**32%**	**Sgk2**	**Serine/threonine-protein kinase Sgk2**
P83940	258	39%	Tceb1	Transcription elongation factor B polypeptide 1
P24270	225	22%	Cat	Catalase
P26618	223	14%	Pdgfra	Alpha-type platelet-derived growth factor receptor
Q8BMS1	222	12%	Hadha	Trifunctional enzyme subunit alpha, mitochondrial
P62715	198	27%	Ppp2cb	Serine/threonine-protein phosphatase 2A catalytic subunit beta isoform
P41216	192	8%	Acsl1	Long-chain-fatty-acid--CoA ligase 1
Q04646	185	21%	Fxyd2	Sodium/potassium-transporting ATPase subunit gamma
Q9WV27	162	8%	Atp1a4	Sodium/potassium-transporting ATPase subunit alpha-4
Q9QWK4	161	22%	Cd5l	CD5 antigen-like
P28661	159	12%	Sep-04	Septin-4
Q91VR2	144	14%	Atp5c1	ATP synthase subunit gamma, mitochondrial
P52760	140	26%	Hrsp12	Ribonuclease UK114
Q8VEM8	130	6%	Slc25a3	Phosphate carrier protein, mitochondrial
Q8C650	130	8%	Sep-10	Septin-10
Q8CHH9	130	12%	Sep-08	Septin-8
Q8BUV3	120	18%	Gphn	Gephyrin
Q60668	116	3%	Hnrnpd	Heterogeneous nuclear ribonucleoprotein D0
P51881	113	19%	Slc25a5	ADP/ATP translocase 2
A2ARV4	113	2%	Lrp2	Low-density lipoprotein receptor-related protein 2
Q99LC5	106	19%	Etfa	Electron transfer flavoprotein subunit alpha, mitochondrial
Q9WVC6	**103**	**14%**	**Sgk1**	**Serine/threonine-protein kinase Sgk1**
Q9DA97	102	5%	Sep-14	Septin-14
Q99MR8	98	6%	Mccc1	Methylcrotonoyl-CoA carboxylase subunit alpha, mitochondrial
Q9R112	98	3%	Sqrdl	Sulfide:quinone oxidoreductase, mitochondrial
Q9DCZ4	96	5%	Apoo	Apolipoprotein O
Q05920	95	4%	Pc	Pyruvate carboxylase, mitochondrial
P51660	88	8%	Hsd17b4	Peroxisomal multifunctional enzyme type 2
P62869	88	21%	Tceb2	Transcription elongation factor B polypeptide 2
Q8CHT0	87	5%	Aldh4a1	Delta-1-pyrroline-5-carboxylate dehydrogenase, mitochondrial

P10639	87	20%	Txn	Thioredoxin
Q9Z1W8	86	2%	Atp12a	Potassium-transporting ATPase alpha chain 2
Q80UG5	85	9%	Sep-09	Septin-9
Q9D394	84	2%	Rufy3	Protein RUFY3
Q9JMA7	82	1%	Cyp3a41a	Cytochrome P450 3A41
Q9Z130	81	5%	Hnrpdl	Heterogeneous nuclear ribonucleoprotein D-like
P80316	81	1%	Cct5	T-complex protein 1 subunit epsilon
Q68FD5	76	3%	Cltc	Clathrin heavy chain 1
O88338	75	6%	Cdh16	Cadherin-16
P01027	74	1%	C3	Complement C3
P53395	74	8%	Dbt	Lipoamide acyltransferase component of branched-chain alpha-keto acid dehydrogenase complex,
Sigma S5188, Liver				
Q6P9Q6	5395	47%	Fkbp15	FK506-binding protein 15
Q8C196	2754	52%	Cps1	Carbamoyl-phosphate synthase [ammonia], mitochondrial
Q9DBN5	1388	50%	Lonp2	Lon protease homolog 2, peroxisomal
P16460	1371	67%	Ass1	Argininosuccinate synthase
O55131	1180	54%	Sep-07	Septin-7
Q9QZS5	**1172**	**56%**	**Sgk2**	**Serine/threonine-protein kinase Sgk2**
Q8BUV3	1149	48%	Gphn	Gephyrin
O35490	1063	70%	Bhmt	Betaine--homocysteine S-methyltransferase 1
Q03265	1003	40%	Atp5a1	ATP synthase subunit alpha, mitochondrial
Q8C1B7	972	42%	Sep-11	Septin-11
Q9ERE3	**806**	**48%**	**Sgk3**	**Serine/threonine-protein kinase Sgk3**
Q9QXE0	656	26%	Hacl1	2-hydroxyacyl-CoA lyase 1
P41216	639	26%	Acsl1	Long-chain-fatty-acid--CoA ligase 1
Q91VS7	628	45%	Mgst1	Microsomal glutathione S-transferase 1
P54869	605	32%	Hmgcs2	Hydroxymethylglutaryl-CoA synthase, mitochondrial
P39054	586	19%	Dnm2	Dynamin-2
P56480	581	36%	Atp5b	ATP synthase subunit beta, mitochondrial
Q6NZC7	567	29%	Sec23ip	SEC23-interacting protein
Q60668	534	38%	Hnrnpd	Heterogeneous nuclear ribonucleoprotein D0
P47738	461	29%	Aldh2	Aldehyde dehydrogenase, mitochondrial
P24270	452	33%	Cat	Catalase
Q9QXF8	430	34%	Gnmt	Glycine N-methyltransferase
O70570	427	17%	Pigr	Polymeric immunoglobulin receptor
P10126	413	32%	Eef1a1	Elongation factor 1-alpha 1
P55096	397	23%	Abcd3	ATP-binding cassette sub-family D member 3
Q8R0Y6	365	23%	Aldh1l1	Aldehyde dehydrogenase family 1 member L1
Q9QWK4	360	34%	Cd5l	CD5 antigen-like
P62869	344	53%	Tceb2	Transcription elongation factor B polypeptide 2
Q8BMS1	341	14%	Hadha	Trifunctional enzyme subunit alpha, mitochondrial
P83940	340	58%	Tceb1	Transcription elongation factor B polypeptide 1
Q91YQ5	339	17%	Rpn1	Dolichyl-diphosphooligosaccharide--protein glycosyltransferase subunit 1
P50544	313	18%	Acadvl	Very long-chain specific acyl-CoA dehydrogenase, mitochondrial
Q9DB77	281	15%	Uqcrc2	Cytochrome b-c1 complex subunit 2, mitochondrial
Q9CWS1	280	24%	Rnf135	E3 ubiquitin-protein ligase RNF135
P62715	279	8%	Ppp2cb	Serine/threonine-protein phosphatase 2A catalytic subunit beta isoform
Q9QZS5	**269**	**26%**	**Sgk2**	**Serine/threonine-protein kinase Sgk2**
Q8CHH9	259	39%	Sep-08	Septin-8
Q80UG5	258	20%	Sep-09	Septin-9
P51660	256	17%	Hsd17b4	Peroxisomal multifunctional enzyme type 2
P28661	255	19%	Sep-04	Septin-4
Q9DBG6	228	16%	Rpn2	Dolichyl-diphosphooligosaccharide--protein glycosyltransferase subunit 2
Q8K2B3	223	25%	Sdha	Succinate dehydrogenase [ubiquinone] flavoprotein subunit, mitochondrial
Q62191	221	14%	Trim21	E3 ubiquitin-protein ligase TRIM21
P17563	219	25%	Selenbp1	Selenium-binding protein 1
P53395	214	32%	Dbt	Lipoamide acyltransferase component of branched-chain alpha-keto acid dehydrogenase complex,
P07310	212	13%	Ckm	Creatine kinase M-type
Q91X83	204	19%	Mat1a	S-adenosylmethionine synthase isoform type-1
Q60668	191	22%	Hnrnpd	Heterogeneous nuclear ribonucleoprotein D0
P50247	188	18%	Ahcy	Adenosylhomocysteinase
Q9R1T4	176	15%	Sep-06	Septin-6
P11725	175	18%	Otc	Ornithine carbamoyltransferase, mitochondrial
Q9D394	171	10%	Rufy3	Protein RUFY3
Q8C650	161	8%	Sep-10	Septin-10
P35700	155	33%	Prdx1	Peroxiredoxin-1
Q63886	137	23%	Ugt1a1	UDP-glucuronosyltransferase 1-1
P80316	132	4%	Cct5	T-complex protein 1 subunit epsilon
P25688	129	12%	Uox	Uricase
P21981	125	15%	Tgm2	Protein-glutamine gamma-glutamyltransferase 2
Q9D394	124	5%	Rufy3	Protein RUFY3
Q9CQS8	124	37%	Sec61b	Protein transport protein Sec61 subunit beta
P24549	123	26%	Aldh1a1	Retinal dehydrogenase 1
Q8BFY9	123	9%	Tnpo1	Transportin-1
Q68FD5	122	4%	Cltc	Clathrin heavy chain 1
Q64458	121	18%	Cyp2c29	Cytochrome P450 2C29
Q9ERE3	**121**	**3%**	**Sgk3**	**Serine/threonine-protein kinase Sgk3**
P62270	117	27%	Rps18	40S ribosomal protein S18
Q8K268	114	8%	Abcf3	ATP-binding cassette sub-family F member 3
O54734	114	11%	Ddost	Dolichyl-diphosphooligosaccharide--protein glycosyltransferase 48 kDa subunit
Q9CY58	114	6%	Serbp1	Plasminogen activator inhibitor 1 RNA-binding protein
P50136	112	16%	Bckdha	2-oxoisovalerate dehydrogenase subunit alpha, mitochondrial
Q6ZQM8	105	12%	Ugt1a7c	UDP-glucuronosyltransferase 1-7C
Q91XE8	104	12%	Tmem205	Transmembrane protein 205
P34914	103	15%	Ephx2	Epoxide hydrolase 2
O88451	100	8%	Rdh7	Retinol dehydrogenase 7
Q9Z130	99	5%	Hnrpdl	Heterogeneous nuclear ribonucleoprotein D-like
P19096	98	3%	Fasn	Fatty acid synthase
P56654	96	11%	Cyp2c37	Cytochrome P450 2C37
Q99LC5	93	10%	Etfa	Electron transfer flavoprotein subunit alpha, mitochondrial
Q9EP89	89	12%	Lactb	Serine beta-lactamase-like protein LACTB, mitochondrial
O88844	80	21%	Idh1	Isocitrate dehydrogenase [NADP] cytoplasmic
O35945	79	17%	Aldh1a7	Aldehyde dehydrogenase, cytosolic 1

P06151	79	6%	Ldha	L-lactate dehydrogenase A chain
Q9QZS5	**79**	**14%**	**Sgk2**	**Serine/threonine-protein kinase Sgk2**
Q8BZ98	78	7%	Dnm3	Dynamin-3
P03995	78	4%	Gfap	Glial fibrillary acidic protein
P16331	76	11%	Pah	Phenylalanine-4-hydroxylase
Q4LDG0	75	4%	Slc27a5	Bile acyl-CoA synthetase
Q91XD4	75	14%	Ftcd	Formimidoyltransferase-cyclodeaminase
Q05421	73	10%	Cyp2e1	Cytochrome P450 2E1
Sigma S5188,Spleen				
Q6P9Q6	8018	52%	Fkbp15	FK506-binding protein 15
Q60668	1811	43%	Hnrnpd	Heterogeneous nuclear ribonucleoprotein D0
Q9ERE3	**1447**	**53%**	**Sgk3**	**Serine/threonine-protein kinase Sgk3**
Q8C1B7	908	44%	Sep-11	Septin-11
O55131	879	52%	Sep-07	Septin-7
P28661	632	31%	Sep-04	Septin-4
Q6NZC7	563	26%	Sec23ip	SEC23-interacting protein
P39054	544	20%	Dnm2	Dynamin-2
Q5SVL6	532	41%	Rap1gap2	Rap1 GTPase-activating protein 2
P05622	490	46%**	Pdgfrb	Beta-type platelet-derived growth factor receptor
P63330	479	43%	Ppp2ca	Serine/threonine-protein phosphatase 2A catalytic subunit alpha isoform
Q8BG05	443	17%	Hnrnpa3	Heterogeneous nuclear ribonucleoprotein A3
Q8CHH9	413	47%	Sep-08	Septin-8
Q8BTM8	388	6%	Flna	Filamin-A
Q9QWK4	348	33%	Cd5l	CD5 antigen-like
P42208	343	49%	Sep-02	Septin-2
Q8BFY9	325	21%	Tnpo1	Transportin-1
P26618	324	19%	Pdgfra	Alpha-type platelet-derived growth factor receptor
P10126	252	25%	Eef1a1	Elongation factor 1-alpha 1
Q9R1T4	234	34%	Sep-06	Septin-6
Q9Z130	227	5%	Hnrpdl	Heterogeneous nuclear ribonucleoprotein D-like
Q68FD5	218	6%	Cltc	Clathrin heavy chain 1
P53395	191	26%	Dbt	Lipoamide acyltransferase component of branched-chain alpha-keto acid dehydrogenase complex,
Q8C650	191	17%	Sep-10	Septin-10
P49312	185	5%	Hnrnpa1	Heterogeneous nuclear ribonucleoprotein A1
P11911	174	12%	Cd79a	B-cell antigen receptor complex-associated protein alpha chain
Q9Z2X1	163	22%	Hnrnpf	Heterogeneous nuclear ribonucleoprotein F
Q9CWS1	162	17%	Rnf135	E3 ubiquitin-protein ligase RNF135
P15530	143	7%	Cd79b	B-cell antigen receptor complex-associated protein beta chain
Q8BUV3	138	21%	Gphn	Gephyrin
Q8VEK3	128	9%	Hnrnpu	Heterogeneous nuclear ribonucleoprotein U
P62631	122	16%	Eef1a2	Elongation factor 1-alpha 2
P62869	118	44%	Tceb2	Transcription elongation factor B polypeptide 2
P14131	108	26%	Rps16	40S ribosomal protein S16
Q62191	105	9%	Trim21	E3 ubiquitin-protein ligase TRIM21
O89053	103	10%	Coro1a	Coronin-1A
P83940	85	39%	Tceb1	Transcription elongation factor B polypeptide 1
O35737	84	9%	Hnrnph1	Heterogeneous nuclear ribonucleoprotein H
Q9CQS8	83	27%	Sec61b	Protein transport protein Sec61 subunit beta
P28867	81	4%	Prkcd	Protein kinase C delta type
P61979	79	9%	Hnrnpk	Heterogeneous nuclear ribonucleoprotein K
Q62351	79	6%	Tfrc	Transferrin receptor protein 1
Q921F2	72	4%	Tardbp	TAR DNA-binding protein 43
Q8BZ98	71	5%	Dnm3	Dynamin-3
Sigma S5188,Testis				
Q6P9Q6	6869	56%	Fkbp15	FK506-binding protein 15
Q6NZC7	2630	49%	Sec23ip	SEC23-interacting protein
Q9ERE3	**2474**	**57%**	**Sgk3**	**Serine/threonine-protein kinase Sgk3**
P39054	1767	44%	Dnm2	Dynamin-2
Q3V0F0	1562	35%	Rimbp3	RIMS-binding protein 3
P42208	1207	51%	Sep-02	Septin-2
P62715	1086	58%	Ppp2cb	Serine/threonine-protein phosphatase 2A catalytic subunit beta isoform
P63330	1029	52%	Ppp2ca	Serine/threonine-protein phosphatase 2A catalytic subunit alpha isoform
O55131	985	52%	Sep-07	Septin-7
P26618	927	29%	Pdgfra	Alpha-type platelet-derived growth factor receptor
Q8BFY9	859	37%	Tnpo1	Transportin-1
Q8K268	689	26%	Abcf3	ATP-binding cassette sub-family F member 3
Q8BUV3	519	49%	Gphn	Gephyrin
Q99LG2	433	16%	Tnpo2	Transportin-2
Q80U93	423	19%	Nup214	Nuclear pore complex protein Nup214
P00342	406	43%	Ldhc	L-lactate dehydrogenase C chain
Q80UG5	387	24%	Sep-09	Septin-9
Q9D394	366	25%	Rufy3	Protein RUFY3
Q8C1B7	357	17%	Sep-11	Septin-11
P97470	351	28%	Ppp4c	Serine/threonine-protein phosphatase 4 catalytic subunit
Q8BZ98	341	10%	Dnm3	Dynamin-3
Q9CWS1	337	30%	Rnf135	E3 ubiquitin-protein ligase RNF135
Q8C650	297	13%	Sep-10	Septin-10
P10126	289	24%	Eef1a1	Elongation factor 1-alpha 1
P39053	287	11%	Dnm1	Dynamin-1
Q8BIL5	279	22%	Hook1	Protein Hook homolog 1
Q9DA97	205	18%	Sep-14	Septin-14
Q8CHH9	200	19%	Sep-08	Septin-8
P83940	189	47%	Tceb1	Transcription elongation factor B polypeptide 1
O70325	164	42%	Gpx4	Phospholipid hydroperoxide glutathione peroxidase, mitochondrial
P62908	157	19%	Rps3	40S ribosomal protein S3
Q03265	157	11%	Atp5a1	ATP synthase subunit alpha, mitochondrial
Q8C2Q3	157	10%	Rbm14	RNA-binding protein 14
P70168	155	9%	Kpnb1	Importin subunit beta-1
P62264	128	15%	Rps14	40S ribosomal protein S14
P03995	127	4%	Gfap	Glial fibrillary acidic protein
Q9Z1R2	125	7%	Bag6	Large proline-rich protein BAG6
P06151	124	12%	Ldha	L-lactate dehydrogenase A chain

Q9ERE3	122	15%	Sgk3	Serine/threonine-protein kinase Sgk3
Q9DBN5	119	17%	Lonp2	Lon protease homolog 2, peroxisomal
Q8BMS1	119	7%	Hadha	Trifunctional enzyme subunit alpha, mitochondrial
P28661	111	15%	Sep-04	Septin-4
Q9JIF0	110	11%	Prmt1	Protein arginine N-methyltransferase 1
Q8BMF4	109	11%	Dlat	Dihydrolipoyllysine-residue acetyltransferase component of pyruvate dehydrogenase complex,
Q9Z2Q6	106	15%	Sep-05	Septin-5
P32037	104	5%	Slc2a3	Solute carrier family 2, facilitated glucose transporter member 3
P62869	102	38%	Tceb2	Transcription elongation factor B polypeptide 2
Q7TNK1	100	7%	Rfx4	Transcription factor RFX4
Q5ND19	98	7%		Uncharacterized protein C17orf47 homolog
Q99PU5	96	1%	Acsbg1	Long-chain-fatty-acid--CoA ligase ACSBG1
P53395	95	14%	Dbt	Lipoamide acyltransferase component of branched-chain alpha-keto acid dehydrogenase complex,
Q68FD5	94	4%	Cltc	Clathrin heavy chain 1
P49025	83	4%	Cit	Citron Rho-interacting kinase
Q8CEC0	81	10%	Nup88	Nuclear pore complex protein Nup88
Q8VDM4	78	1%	Psmd2	26S proteasome non-ATPase regulatory subunit 2
Q68FD5	78	5%	Cltc	Clathrin heavy chain 1
P14106	72	9%	C1qb	Complement C1q subcomponent subunit B

Appendix 2 Proteins identified in immunoprecipitations by mass spectrometry

Proteins with MASCOT scores greater than 70 are included and actin, tubulin and heat shock protein isoforms are excluded.

Cell line	Subtype	Gene	Mutation (amino acid)	Reference
BT-474	Luminal B	PIK3CA	K111N	
		P53	E285K	
CAMA-1	Luminal A	CDH1	?	
		PTEN	T277 -> frameshift	
		PTEN	D29H	
		P53	R280T	
ZR-75-1	Luminal A	PTEN	L108R	
T47D	Luminal A	PI3KCA	H1047R	
		P53	L194F	
HCC-1187	Triple negative	P53	G108 -> deletion	
SUM52PE	Luminal B	CDKN2A	A68V	
HCC-1937	Triple negative	BRCA1	Q1756 -> frameshift	
		P53	R306 -> stop	
		PTEN	Deletion of exons 1-9	(Hollestelle et al., 2007)
MDA-MD-436	Triple negative	BRCA1	?	
		RB1	G203 -> frameshift	
BT-549	Triple negative	PTEN	V275 -> frameshift	
		RB1	?	
		P53	R249S	
MDA-MB-157	Triple negative	NF1	S275 -> frameshift	
		P53	A88 -> frameshift	
HCC-1806	Triple negative	LKB1	Deletion	
		P53	T256 -> frameshift	
		KDM6A	Deletion	
		CDKN2a(p14)	Deletion	
		CDKN2A	Deletion	
MDA-MB-231	Triple negative	BRAF	G464V	
		CDKN2A	Deletion	
		CDKN2a(p14)	Deletion	
		KRAS	G13D	
		NF2	E231 -> stop	
		P53	R280K	
JIMT-1	Triple negative	HER-2	Amplification	(Tanner et al., 2004)
		PIK3CA	C420R (T1258C)	(Koninki et al., 2010)

Appendix 3 Summary of known mutations in breast cancer cell lines studied

Unless othetwise stated, obtained from the Cosmic database available online at: http://cancer.sanger.ac.uk/cancergenome/projects/cosmic/. HCC-1187 and HCC-1937 have been sequenced for a larger number of genes than the other cell lines. Only cancer gene relevant mutations have been listed here. Full list of mutations for these two cell lines is available online at the Cosmic database.

8. References

Ackermann, T.F., Boini, K.M., Beier, N., Scholz, W., Fuchss, T., and Lang, F. (2011). EMD638683, a Novel SGK Inhibitor with Antihypertensive Potency. Cellular Physiology and Biochemistry *28*, 137-146.

Ahmed, N.N., Franke, T.F., Bellacosa, A., Datta, K., Gonzalez-Portal, M.E., Taguchi, T., Testa, J.R., and Tsichlis, P.N. (1993). The proteins encoded by c-akt and v-akt differ in post-translational modification, subcellular localization and oncogenic potential. Oncogene *8*, 1957-1963.

Alessi, D.R., Caudwell, F.B., Andjelkovic, M., Hemmings, B.A., and Cohen, P. (1996). Molecular basis for the substrate specificity of protein kinase B; Comparison with MAPKAP kinase-1 and p70 S6 kinase. Febs Letters *399*.

Alessi, D.R., Deak, M., Casamayor, A., Caudwell, F.B., Morrice, N., Norman, D.G., Gaffney, P., Reese, C.B., MacDougall, C.N., Harbison, D*., et al.* (1997a). 3-Phosphoinositide-dependent protein kinase-1 (PDK1): structural and functional homology with the Drosophila DSTPK61 kinase. Curr Biol *7*, 776-789.

Alessi, D.R., James, S.R., Downes, C.P., Holmes, A.B., Gaffney, P.R., Reese, C.B., and Cohen, P. (1997b). Characterization of a 3-phosphoinositide-dependent protein kinase which phosphorylates and activates protein kinase Balpha. Curr Biol *7*, 261-269.

Alonso, L., Okada, H., Pasolli, H.A., Wakeham, A., You- Ten, A.I., Mak, T.W., and Fuchs, E. (2005). Sgk3 links growth factor signaling to maintenance of progenitor cells in the hair follicle. J Cell Biol *170*, 559-570.

Alvarez de la Rosa, D., Zhang, P., Náray-Fejes-Tóth, A., Fejes-Tóth, G., and Canessa, C.M. (1999). The serum and glucocorticoid kinase sgk increases the abundance of epithelial sodium channels in the plasma membrane of Xenopus oocytes. J Biol Chem *274*, 37834-37839.

Amato, R., Menniti, M., Agosti, V., Boito, R., Costa, N., Bond, H.M., Barbieri, V., Tagliaferri, P., Venuta, S., and Perrotti, N. (2007). IL-2 signals through Sgkl and inhibits proliferation and apoptosis in kidney cancer cells. Journal of Molecular Medicine-Jmm *85*, 707-721.

Andersson, S., Davis, D.L., Dahlback, H., Jornvall, H., and Russell, D.W. (1989). CLONING, STRUCTURE, AND EXPRESSION OF THE MITOCHONDRIAL CYTOCHROME-P-450 STEROL 26-HYDROXYLASE, A BILE-ACID BIOSYNTHETIC ENZYME. J Biol Chem *264*.

Aoki, M., Hao, J., and Vogt, P.K. (2004). Proteasomal degradation of the Fox01 transcriptional regulator in cells transformed by the P3k and Akt oncoproteins. P Natl Acad Sci USA *101*, 13613-13617.

Arteaga, C.L., Sliwkowski, M.X., Osborne, C.K., Perez, E.A., Puglisi, F., and Gianni, L. (2012). Treatment of HER2-positive breast cancer: current status and future perspectives. Nature Reviews Clinical Oncology *9*.

Arteaga, M.F., Wang, L., Ravid, T., Hochstrasser, M., and Canessa, C.M. (2006). An amphipathic helix targets serum and glucocorticoid-induced kinase 1 to the endoplasmic reticulum-associated ubiquitin-conjugation machinery. P Natl Acad Sci USA *103*, 11178-11183.

Audhya, A., Loewith, R., Parsons, A.B., Gao, L., Tabuchi, M., Zhou, H.L., Boone, C., Hall, M.N., and Emr, S.D. (2004). Genome-wide lethality screen identifies new PI4,5P2 effectors that regulate the actin cytoskeleton. Embo J *23*, 3747-3757.

Baldwin, A., Grueneberg, D.A., Hellner, K., Sawyer, J., Grace, M., Li, W., Harlow, E., and Munger, K. (2010). Kinase requirements in human cells: V. Synthetic lethal interactions between p53 and the protein kinases SGK2 and PAK3. Proc Natl Acad Sci U S A *107*, 12463-12468.

Bandyopadhyay, S., Pai, S.K., Hirota, S., Hosobe, S., Takano, Y., Saito, K., Piquemal, D., Commes, T., Watabe, M., Gross, S.C*., et al.* (2004). Role of the putative tumor metastasis suppressor gene Drg-1 in breast cancer progression. Oncogene *23*, 5675-5681.

Banerji, S., Cibulskis, K., Rangel-Escareno, C., Brown, K.K., Carter, S.L., Frederick, A.M., Lawrence, M.S., Sivachenko, A.Y., Sougnez, C., Zou, L*., et al.* (2012). Sequence analysis of mutations and translocations across breast cancer subtypes. Nature *486*, 405-409.

Bar-Peled, L., Schweitzer, L.D., Zoncu, R., and Sabatini, D.M. (2012). Ragulator Is a GEF for the Rag GTPases that Signal Amino Acid Levels tomTORC1. Cell *150*, 1196-1208.

Barnett, S.F., Defeo-Jones, D., Fu, S., Hancock, P.J., Haskell, K.M., Jones, R.E., Kahana, J.A., Kral, A.M., Leander, K., Lee, L.L*., et al.* (2005). Identification and characterization of pleckstrin-homology-domain-dependent and isoenzyme-specific Akt inhibitors. Biochem J *385*, 399-408.

Baselga, J., and Swain, S.M. (2009). Novel anticancer targets: revisiting ERBB2 and discovering ERBB3. Nat Rev Cancer *9*, 463-475.

Bayascas, J.R., Leslie, N.R., Parsons, R., Fleming, S., and Alessi, D.R. (2005). Hypomorphic mutation of PDK1 suppresses tumorigenesis in PTEN+/- mice. Current Biology *15*.

Bayascas, J.R., Wullschleger, S., Sakamoto, K., García-Martínez, J.M., Clacher, C., Komander, D., van Aalten, D.M., Boini, K.M., Lang, F., Lipina, C*., et al.* (2008). Mutation of the PDK1 PH domain inhibits protein kinase B/Akt, leading to small size and insulin resistance. Mol Cell Biol *28*, 3258-3272.

Belova, L., Sharma, S., Brickley, D.R., Nicolarsen, J.R., Patterson, C., and Conzen, S.D. (2006). Ubiquitin-proteasome degradation of serum- and glucocorticoid-regulated kinase-1 (SGK-1) is mediated by the chaperone-dependent E3 ligase CHIP. Biochem J *400*, 235-244.

Bendell, J.C., Ervin, T.J., Senzer, N.N., Richards, D.A., Firdaus, I., Lockhart, A.C., Cohn, A.L., Saleh, M.N., Gardner, L.R., Sportelli, P*., et al.* (2012). Results of the X-PECT study: A phase III randomized double-blind, placebo-controlled study of perifosine plus capecitabine (P-CAP) versus placebo plus capecitabine (CAP) in patients (pts) with refractory metastatic colorectal cancer (mCRC). J Clin Oncol *30*.

Bhalla, V., Daidie, D., Li, H.Y., Pao, A.C., LaGrange, L.P., Wang, J., Vandewalle, A., Stockand, J.D., Staub, O., and Pearce, D. (2005). Serum- and glucocorticoid-regulated kinase 1 regulates ubiquitin

ligase neural precursor cell-expressed, developmentally down-regulated protein 4-2 by inducing interaction with 14-3-3. Molecular Endocrinology *19*, 3073-3084.

Biggs, W.H., Meisenhelder, J., Hunter, T., Cavenee, W.K., and Arden, K.C. (1999). Protein kinase B/Akt-mediated phosphorylation promotes nuclear exclusion of the winged helix transcription factor FKHR1. P Natl Acad Sci USA *96*, 7421-7426.

Biondi, R.M., Kieloch, A., Currie, R.A., Deak, M., and Alessi, D.R. (2001). The PIF-binding pocket in PDK1 is essential for activation of S6K and SGK, but not PKB. Embo J *20*, 4380-4390.

Bogusz, A.M., Brickley, D.R., Pew, T., and Conzen, S.D. (2006). A novel N-terminal hydrophobic motif mediates constitutive degradation of serum- and glucocorticoid-induced kinase-1 by the ubiquitin-proteasome pathway. Febs Journal *273*.

Boini, K.M., Nammi, S., Grahammer, F., Osswald, H., Kuhl, D., and Lang, F. (2008). Role of serum- and glucocorticoid-inducible kinase SGK1 in glucocorticoid regulation of renal electrolyte excretion and blood pressure. Kidney & Blood Pressure Research *31*, 280-289.

Boyd, C., and Toth, A.N.F. (2005). Gene regulation of ENaC subunits by serum- and glucocorticoid-inducible kinase-1. American Journal of Physiology-Renal Physiology *288*, F505-F512.

Bravo-Cordero, J.J., Hodgson, L., and Condeelis, J. (2012). Directed cell invasion and migration during metastasis. Current Opinion in Cell Biology *24*, 277-283.

Brickley, D.R., Mikosz, C.A., Hagan, C.R., and Conzen, S.D. (2002). Ubiquitin modification of serum and glucocorticoid-induced protein kinase-1 (SGK-1). J Biol Chem *277*, 43064-43070.

Brown, E.J., Albers, M.W., Shin, T.B., Ichikawa, K., Keith, C.T., Lane, W.S., and Schreiber, S.L. (1994). A mammalian protein targeted by G1-arresting rapamycin-receptor complex. Nature *369*, 756-758.

Brunet, A., Bonni, A., Zigmond, M.J., Lin, M.Z., Juo, P., Hu, L.S., Anderson, M.J., Arden, K.C., Blenis, J., and Greenberg, M.E. (1999). Akt promotes cell survival by phosphorylating and inhibiting a forkhead transcription factor. Cell *96*, 857-868.

Brunet, A., Park, J., Tran, H., Hu, L.S., Hemmings, B.A., and Greenberg, M.E. (2001). Protein kinase SGK mediates survival signals by phosphorylating the forkhead transcription factor FKHRL1 (FOXO3a). Mol Cell Biol *21*, 952-965.

Busjahn, A., Aydin, A., Uhlmann, R., Krasko, C., Bahring, S., Szelestei, T., Feng, Y.X., Dahm, S., Sharma, A.M., Luft, F.C*., et al.* (2002). Serum- and glucocorticoid-regulated kinase (SGK1) gene and blood pressure. Hypertension *40*, 256-260.

Cahill, C.M., Tzivion, G., Nasrin, N., Ogg, S., Dore, J., Ruvkun, G., and Alexander-Bridges, M. (2001). Phosphatidylinositol 3-kinase signaling inhibits DAF-16 DNA binding and function via 14-3-3-dependent and 14-3-3-independent pathways. J Biol Chem *276*, 13402-13410.

Calleja, V., Alcor, D., Laguerre, M., Park, J., Vojnovic, B., Hemmings, B.A., Downward, J., Parker, P.J., and Larijani, B. (2007). Intramolecular and intermolecular interactions of protein kinase B define its activation in vivo. Plos Biol *5*, 780-791.

Cameron, A.J.M., Linch, M.D., Saurin, A.T., Escribano, C., and Parker, P.J. (2011). mTORC2 targets AGC kinases through Sin1-dependent recruitment. Biochem J *439*, 287-297.

Carey, L.A., Perou, C.M., Livasy, C.A., Dressler, L.G., Cowan, D., Conway, K., Karaca, G., Troester, M.A., Tse, C.K., Edmiston, S.*, et al.* (2006). Race, breast cancer subtypes, and survival in the Carolina Breast Cancer Study. JAMA *295*, 2492-2502.

Carpten, J.D., Faber, A.L., Horn, C., Donoho, G.P., Briggs, S.L., Robbins, C.M., Hostetter, G., Boguslawski, S., Moses, T.Y., Savage, S.*, et al.* (2007). A transforming mutation in the pleckstrin homology domain of AKT1 in cancer. Nature *448*, 439-444.

Carracedo, A., Ma, L., Teruya-Feldstein, J., Rojo, F., Salmena, L., Alimonti, A., Egia, A., Sasaki, A.T., Thomas, G., Kozma, S.C.*, et al.* (2008). Inhibition of mTORC1 leads to MAPK pathway activation through a PI3K-dependent feedback loop in human cancer. Journal of Clinical Investigation *118*.

Carter, P., Presta, L., Gorman, C.M., Ridgway, J.B., Henner, D., Wong, W.L., Rowland, A.M., Kotts, C., Carver, M.E., and Shepard, H.M. (1992). Humanization of an anti-p185HER2 antibody for human cancer therapy. Proc Natl Acad Sci U S A *89*, 4285-4289.

Casamayor, A., Torrance, P.D., Kobayashi, T., Thorner, J., and Alessi, D.R. (1999). Functional counterparts of mammalian protein kinases PDK1 and SGK in budding yeast. Current Biology *9*, 186-197.

Catela, C., Kratsios, P., Hede, M., Lang, F., and Rosenthal, N. (2010). Serum and Glucocorticoid-Inducible Kinase 1 (SGK1) Is Necessary for Vascular Remodeling During Angiogenesis. Developmental Dynamics *239*, 2149-2160.

Chandarlapaty, S., Sawai, A., Scaltriti, M., Rodrik-Outmezguine, V., Grbovic-Huezo, O., Serra, V., Majumder, P.K., Baselga, J., and Rosen, N. (2011). AKT Inhibition Relieves Feedback Suppression of Receptor Tyrosine Kinase Expression and Activity. Cancer Cell *19*.

Chen, S.Y., Bhargava, A., Mastroberardino, L., Meijer, O.C., Wang, J., Buse, P., Firestone, G.L., Verrey, F., and Pearce, D. (1999). Epithelial sodium channel regulated by aldosterone-induced protein sgk. P Natl Acad Sci USA *96*, 2514-2519.

Chen, W.S., Xu, P.Z., Gottlob, K., Chen, M.L., Sokol, K., Shiyanova, T., Roninson, I., Weng, W., Suzuki, R., Tobe, K.*, et al.* (2001). Growth retardation and increased apoptosis in mice with homozygous disruption of the Akt1 gene. Genes Dev *15*, 2203-2208.

Cherrin, C., Haskell, K., Howell, B., Jones, R., Leander, K., Robinson, R., Watkins, A., Bilodeau, M., Hoffman, J., Sanderson, P.*, et al.* (2010). An allosteric Akt inhibitor effectively blocks Akt signaling and tumor growth with only transient effects on glucose and insulin levels in vivo. Cancer Biology & Therapy *9*, 493-503.

Cho, H., Mu, J., Kim, J.K., Thorvaldsen, J.L., Chu, Q., Crenshaw, E.B., Kaestner, K.H., Bartolomei, M.S., Shulman, G.I., and Birnbaum, M.J. (2001a). Insulin resistance and a diabetes mellitus-like syndrome in mice lacking the protein kinase Akt2 (PKB beta). Science *292*, 1728-1731.

Cho, H., Thorvaldsen, J.L., Chu, Q., Feng, F., and Birnbaum, M.J. (2001b). Akt1/PKBalpha is required for normal growth but dispensable for maintenance of glucose homeostasis in mice. J Biol Chem *276*, 38349-38352.

Chresta, C.M., Davies, B.R., Hickson, I., Harding, T., Cosulich, S., Critchlow, S.E., Vincent, J.P., Ellston, R., Jones, D., Sini, P.*, et al.* (2010). AZD8055 is a potent, selective, and orally bioavailable ATP-competitive mammalian target of rapamycin kinase inhibitor with in vitro and in vivo antitumor activity. Cancer Research *70*, 288-298.

Chu, S., Rushdi, S., Zumpe, E.T., Mamers, P., Healy, D.L., Jobling, T., Burger, H.G., and Fuller, P.J. (2002). FSH-regulated gene expression profiles in ovarian tumours and normal ovaries. Molecular Human Reproduction *8*, 426-433.

Chung, E.J., Sung, Y.K., Farooq, M., Kim, Y., Im, S., Tak, W.Y., Hwang, Y.J., Kim, Y.I., Han, H.S., Kim, J.C.*, et al.* (2002). Gene expression profile analysis in human hepatocellular carcinoma by cDNA microarray. Molecules and Cells *14*, 382-387.

Cipolletta, D., Feuerer, M., Li, A., Kamei, N., Lee, J., Shoelson, S.E., Benoist, C., and Mathis, D. (2012). PPAR-gamma is a major driver of the accumulation and phenotype of adipose tissue T-reg cells. Nature *486*, 549-U151.

Cohen, P., and Alessi, D.R. (2013). Kinase Drug Discovery - What's Next in the Field? Acs Chemical Biology *8*, 96-104.

Collins, B.J., Deak, M., Arthur, J.S.C., Armit, L.J., and Alessi, D.R. (2003). In vivo role of the PIF-binding docking site of PDK1 defined by knock-in mutation. Embo J *22*, 4202-4211.

Collins, B.J., Deak, M., Murray-Tait, V., Storey, K.G., and Alessi, D.R. (2005). In vivo role of the phosphate groove of PDK1 defined by knockin mutation. J Cell Sci *118*, 5023-5034.

Cornella Taracido, I., Harrington, E.M., Honda, A., and Keaney, E. New bi-hetereoaryl compound useful in pharmaceutical composition and for treating disease, disorder, or syndrome associated with vacuolar protein sorting 34 inhibitions which is selected form cancer or inflammation in a subject.

Cross, D.A., Alessi, D.R., Cohen, P., Andjelkovich, M., and Hemmings, B.A. (1995). Inhibition of glycogen synthase kinase-3 by insulin mediated by protein kinase B. Nature *378*, 785-789.

Currie, R.A., Walker, K.S., Gray, A., Deak, M., Casamayor, A., Downes, C.P., Cohen, P., Alessi, D.R., and Lucocq, J. (1999). Role of phosphatidylinositol 3,4,5-trisphosphate in regulating the activity and localization of 3-phosphoinositide-dependent protein kinase-1. Biochem J *337 (Pt 3)*, 575-583.

Dahlberg, J., Smith, G., Norrving, B., Nilsson, P., Hedblad, B., Engstrom, G., Lovkvist, H., Carlson, J., Lindgren, A., and Melander, O. (2011). Genetic variants in serum and glucocortocoid regulated kinase 1, a regulator of the epithelial sodium channel, are associated with ischaemic stroke. Journal of Hypertension *29*, 884-889.

Datta, S.R., Dudek, H., Tao, X., Masters, S., Fu, H., Gotoh, Y., and Greenberg, M.E. (1997). Akt phosphorylation of BAD couples survival signals to the cell-intrinsic death machinery. Cell *91*, 231-241.

Davies, B.R., Greenwood, H., Dudley, P., Crafter, C., Yu, D.-H., Zhang, J., Li, J., Gao, B., Ji, Q., Maynard, J.*, et al.* (2012). Preclinical Pharmacology of AZD5363, an Inhibitor of AKT: Pharmacodynamics, Antitumor Activity, and Correlation of Monotherapy Activity with Genetic Background. Mol Cancer Ther *11*.

Davies, M.A., Stemke-Hale, K., Tellez, C., Calderone, T.L., Deng, W., Prieto, V.G., Lazar, A.J.F., Gershenwald, J.E., and Mills, G.B. (2008). A novel AKT3 mutation in melanoma tumours and cell lines. British Journal of Cancer *99*, 1265-1268.

Debonneville, C., Flores, S., Kamynina, E., Plant, P., Tauxe, C., Thomas, M., Munster, C., Chraibi, A., Pratt, J., Horisberger, J.*, et al.* (2001). Phosphorylation of Nedd4-2 by Sgk1 regulates epithelial Na+ channel cell surface expression. Embo J *20*, 7052-7059.

deHart, A.K.A., Schnell, J.D., Allen, D.A., and Hicke, L. (2002). The conserved Pkh-Ypk kinase cascade is required for endocytosis in yeast. J Cell Biol *156*, 241-248.

Dehner, M., Hadjihannas, M., Weiske, J., Huber, O., and Behrens, J. (2008). Wnt signaling inhibits Forkhead box O3a-induced transcription and apoptosis through up-regulation of serum- and glucocorticoid-inducible kinase 1. J Biol Chem *283*, 19201-19210.

del Peso, L., Gonzalez-Garcia, M., Page, C., Herrera, R., and Nunez, G. (1997). Interleukin-3-induced phosphorylation of BAD through the protein kinase Akt. Science *278*, 687-689.

Demetri, G.D., Chawla, S.P., Ray-Coquard, I., Le Cesne, A., Staddon, A.P., Milhem, M.M., Penel, N., Riedel, R.F., Bui-Nguyen, B., Cranmer, L.D.*, et al.* (2013). Results of an International Randomized Phase III Trial of the Mammalian Target of Rapamycin Inhibitor Ridaforolimus Versus Placebo to Control Metastatic Sarcomas in Patients After Benefit From Prior Chemotherapy. J Clin Oncol *31*, 2485-2492.

Di Cristofano, A., Pesce, B., Cordon-Cardo, C., and Pandolfi, P.P. (1998). Pten is essential for embryonic development and tumour suppression. Nature Genetics *19*, 348-355.

Dieter, M., Palmada, M., Rajamanickam, J., Aydin, A., Busjahn, A., Boehmer, C., Luft, F.C., and Lang, F. (2004). Regulation of glucose transporter SGLT1 by ubiquitin ligase Nedd4-2 and kinases SGK1, SGK3, and PKB. Obesity Research *12*, 862-870.

Distelhorst, C.W. (2002). Recent insights into the mechanism of glucocorticosteroid-induced apoptosis. Cell Death and Differentiation *9*, 6-19.

Durocher, Y., Perret, S., and Kamen, A. (2002). High-level and high-throughput recombinant protein production by transient transfection of suspension-growing human 293-EBNA1 cells. Nucleic Acids Research *30*.

Easton, R.M., Cho, H., Roovers, K., Shineman, D.W., Mizrahi, M., Forman, M.S., Lee, V.M., Szabolcs, M., de Jong, R., Oltersdorf, T.*, et al.* (2005). Role for Akt3/protein kinase Bgamma in attainment of normal brain size. Mol Cell Biol *25*, 1869-1878.

Endicott, J.A., Noble, M.E.M., and Johnson, L.N. (2012). The Structural Basis for Control of Eukaryotic Protein Kinases. In Annual Review of Biochemistry, Vol 81, R.D. Kornberg, ed. (Palo Alto, Annual Reviews), pp. 587-613.

Endo, T., Kusakabe, M., Sunadome, K., Yamamoto, T., and Nishida, E. (2011). The Kinase SGK1 in the Endoderm and Mesoderm Promotes Ectodermal Survival by Down-Regulating Components of the Death-Inducing Signaling Complex. Science Signaling *4*.

Engelman, J.A. (2009). Targeting PI3K signalling in cancer: opportunities, challenges and limitations. Nature Reviews Cancer *9*.

Engelsberg, A., Kobelt, F., and Kuhl, D. (2006). The N-terminus of the serurn- and glucocorticoid-inducible kinase Sgk1 specifies mitochondrial localization and rapid turnover. Biochem J *399*, 69-76.

Escobedo, J.A., Navankasattusas, S., Kavanaugh, W.M., Milfay, D., Fried, V.A., and Williams, L.T. (1991). cDNA cloning of a novel 85 kd protein that has SH2 domains and regulates binding of PI3-kinase to the PDGF beta-receptor. Cell *65*, 75-82.

Eylenstein, A., Gehring, E.-M., Heise, N., Shumilina, E., Schmidt, S., Szteyn, K., Muenzer, P., Nurbaeva, M.K., Eichenmueller, M., Tyan, L.*, et al.* (2011). Stimulation of Ca2+-channel Orai1/STIM1 by serum- and glucocorticoid-inducible kinase 1 (SGK1). Faseb J *25*.

Eylenstein, A., Schmidt, S., Gu, S.C., Yang, W.T., Schmid, E., Schmidt, E.M., Alesutan, I., Szteyn, K., Regel, I., Shumilina, E.*, et al.* (2012). Transcription Factor NF-kappa B Regulates Expression of Pore-forming Ca2+ Channel Unit, Orai1, and Its Activator, STIM1, to Control Ca2+ Entry and Affect Cellular Functions. J Biol Chem *287*, 2719-2730.

Fadri, M., Daquinag, A., Wang, S., Xue, T., and Kunz, J. (2005). The pleckstrin homology domain proteins Slm1 and Slm2 are required for actin cytoskeleton organization in yeast and bind phosphatidylinositol-4,5-bisphosphate and TORC2. Mol Biol Cell *16*, 1883-1900.

Fagerli, U.M., Ullrich, K., Stuehmer, T., Holien, T., Koechert, K., Holt, R.U., Bruland, O., Chatterjee, M., Nogai, H., Lenz, G.*, et al.* (2011). Serum/glucocorticoid-regulated kinase 1 (SGK1) is a prominent target gene of the transcriptional response to cytokines in multiple myeloma and supports the growth of myeloma cells. Oncogene *30*.

Falasca, M., and Maffucci, T. (2012). Regulation and cellular functions of class II phosphoinositide 3-kinases. Biochem J *443*, 587-601.

Fan, C., Oh, D.S., Wessels, L., Weigelt, B., Nuyten, D.S., Nobel, A.B., van't Veer, L.J., and Perou, C.M. (2006a). Concordance among gene-expression-based predictors for breast cancer. N Engl J Med *355*, 560-569.

Fan, Q.W., Knight, Z.A., Goldenberg, D.D., Yu, W., Mostov, K.E., Stokoe, D., Shokat, K.M., and Weiss, W.A. (2006b). A dual PI3 kinase/mTOR inhibitor reveals emergent efficacy in glioma. Cancer Cell *9*, 341-349.

Faresse, N., Lagnaz, D., Debonneville, A., Ismailji, A., Maillard, M., Fejes-Toth, G., Naray-Fejes-Toth, A., and Staub, O. (2012). Inducible kidney-specific Sgk1 knockout mice show a salt-losing phenotype. American Journal of Physiology-Renal Physiology *302*, F977-F985.

Farkas, T., Daugaard, M., and Jaattela, M. (2011). Identification of Small Molecule Inhibitors of Phosphatidylinositol 3-Kinase and Autophagy. J Biol Chem *286*, 38904-38912.

Fejes-Toth, G., Frindt, G., Naray-Fejes-Toth, A., and Palmer, L.G. (2008). Epithelial Na(+) channel activation and processing in mice lacking SGK1. American Journal of Physiology-Renal Physiology *294*, F1298-F1305.

Ferlay, J., Shin, H.R., Bray, F., Forman, D., Mathers, C., and Parkin, D.M. (2010). Estimates of worldwide burden of cancer in 2008: GLOBOCAN 2008. International Journal of Cancer *127*, 2893-2917.

Feske, S. (2010). CRAC channelopathies. Pflugers Archiv-European Journal of Physiology *460*, 417-435.

Fischer, E.H., and Krebs, E.G. (1955). Conversion of phosphorylase b to phosphorylase a in muscle extracts. The Journal of biological chemistry *216*, 121-132.

Folkes, A.J., Ahmadi, K., Alderton, W.K., Alix, S., Baker, S.J., Box, G., Chuckowree, I.S., Clarke, P.A., Depledge, P., Eccles, S.A.*, et al.* (2008). The identification of 2-(1H-indazol-4-yl)-6-(4-methanesulfonyl-piperazin-1-ylmethyl)-4-morphol in-4-yl-thieno 3,2-d pyrimidine (GDC-0941) as a potent, selective, orally bioavailable inhibitor of class I PI3 kinase for the treatment of cancer. Journal of Medicinal Chemistry *51*, 5522-5532.

Forbes, S.A., Bindal, N., Bamford, S., Cole, C., Kok, C.Y., Beare, D., Jia, M., Shepherd, R., Leung, K., Menzies, A*., et al.* (2011). COSMIC: mining complete cancer genomes in the Catalogue of Somatic Mutations in Cancer. Nucleic Acids Research *39*, D945-950.

Frias, M.A., Thoreen, C.C., Jaffe, J.D., Schroder, W., Sculley, T., Carr, S.A., and Sabatini, D.M. (2006). mSin1 is necessary for Akt/PKB phosphorylation, and its isoforms define three distinct mTORC2s. Curr Biol *16*, 1865-1870.

Friedrich, B., Feng, Y., Cohen, P., Risler, T., Vandewalle, A., Broer, S., Wang, J., Pearce, D., and Lang, F. (2003). The serine/threonine kinases SGK2 and SGK3 are potent stimulators of the epithelial Na+ channel alpha,beta,gamma-ENaC. Pflugers Archiv-European Journal of Physiology *445*, 693-696.

Futreal, P.A., Coin, L., Marshall, M., Down, T., Hubbard, T., Wooster, R., Rahman, N., and Stratton, M.R. (2004). A census of human cancer genes. Nat Rev Cancer *4*, 177-183.

Gaj, T., Gersbach, C.A., and Barbas, C.F., 3rd (2013). ZFN, TALEN, and CRISPR/Cas-based methods for genome engineering. Trends Biotechnol *31*, 397-405.

Gamper, N., Fillon, S., Huber, S.M., Feng, Y., Kobayashi, T., Cohen, P., and Lang, F. (2002). IGF-1 up-regulates K+ channels via PI3-kinase, PDK1 and SGK1. Pflugers Archiv-European Journal of Physiology *443*, 625-634.

Gan, X., Wang, J., Su, B., and Wu, D. (2011). Evidence for direct activation of mTORC2 kinase activity by phosphatidylinositol 3,4,5-trisphosphate. J Biol Chem *286*, 10998-11002.

Gan, X., Wang, J., Wang, C., Sommer, E., Kozasa, T., Srinivasula, S., Alessi, D., Offermanns, S., Simon, M.I., and Wu, D. (2012). PRR5L degradation promotes mTORC2-mediated PKC-delta phosphorylation and cell migration downstream of G alpha(12). Nature Cell Biology *14*, 686-696.

Gangloff, Y.G., Mueller, M., Dann, S.G., Svoboda, P., Sticker, M., Spetz, J.F., Um, S.H., Brown, E.J., Cereghini, S., Thomas, G.*, et al.* (2004). Disruption of the mouse mTOR gene leads to early postimplantation lethality and prohibits embryonic stem cell development. Mol Cell Biol *24*, 9508-9516.

Gao, D., Wan, L., Inuzuka, H., Berg, A.H., Tseng, A., Zhai, B., Shaik, S., Bennett, E., Tron, A.E., Gasser, J.A.*, et al.* (2010). Rictor Forms a Complex with Cullin-1 to Promote SGK1 Ubiquitination and Destruction. Mol Cell *39*.

Garcia-Martinez, J.M., and Alessi, D.R. (2008). mTOR complex 2 (mTORC2) controls hydrophobic motif phosphorylation and activation of serum- and glucocorticoid-induced protein kinase 1 (SGK1). Biochem J *416*, 375-385.

Garofalo, R.S., Orena, S.J., Rafidi, K., Torchia, A.J., Stock, J.L., Hildebrandt, A.L., Coskran, T., Black, S.C., Brees, D.J., Wicks, J.R.*, et al.* (2003). Severe diabetes, age-dependent loss of adipose tissue, and mild growth deficiency in mice lacking Akt2/PKB beta. J Clin Invest *112*, 197-208.

Gewinner, C., Wang, Z.C., Richardson, A., Teruya-Feldstein, J., Etemadmoghadam, D., Bowtell, D., Barretina, J., Lin, W.M., Rameh, L., Salmena, L.*, et al.* (2009). Evidence that inositol polyphosphate 4-phosphatase type II is a tumor suppressor that inhibits PI3K signaling. Cancer Cell *16*, 115-125.

Grahammer, F., Artunc, F., Sandulache, D., Rexhepaj, R., Friedrich, B., Risler, T., McCormick, J.A., Dawson, K., Wang, J., Pearce, D.*, et al.* (2006). Renal function of gene-targeted mice lacking both SGK1 and SGK3. Am J Physiol Regul Integr Comp Physiol *290*, R945-950.

Guertin, D.A., Stevens, D.M., Thoreen, C.C., Burds, A.A., Kalaany, N.Y., Moffat, J., Brown, M., Fitzgerald, K.J., and Sabatini, D.M. (2006). Ablation in mice of the mTORC components raptor, rictor, or mLST8 reveals that mTORC2 is required for signaling to Akt-FOXO and PKC alpha but not S6K1. Developmental Cell *11*, 859-871.

Hanahan, D., and Weinberg, R.A. (2000). The hallmarks of cancer. Cell *100*, 57-70.

Hanahan, D., and Weinberg, R.A. (2011). Hallmarks of cancer: the next generation. Cell *144*, 646-674.

Hanks, S.K., and Hunter, T. (1995). Protein kinases 6. The eukaryotic protein kinase superfamily: kinase (catalytic) domain structure and classification. Faseb J *9*, 576-596.

Hanks, S.K., Quinn, A.M., and Hunter, T. (1988). The protein kinase family: conserved features and deduced phylogeny of the catalytic domains. Science *241*, 42-52.

Hara, K., Maruki, Y., Long, X., Yoshino, K., Oshiro, N., Hidayat, S., Tokunaga, C., Avruch, J., and Yonezawa, K. (2002). Raptor, a binding partner of target of rapamycin (TOR), mediates TOR action. Cell *110*, 177-189.

Harper, M.J., and Walpole, A.L. (1966). Contrasting endocrine activities of cis and trans isomers in a series of substituted triphenylethylenes. Nature *212*, 87.

Harrington, L.S., Findlay, G.M., Gray, A., Tolkacheva, T., Wigfield, S., Rebholz, H., Barnett, J., Leslie, N.R., Cheng, S., Shepherd, P.R*., et al.* (2004). The TSC1-2 tumor suppressor controls insulin-PI3K signaling via regulation of IRS proteins. J Cell Biol *166*, 213-223.

Haruta, T., Uno, T., Kawahara, J., Takano, A., Egawa, K., Sharma, P.M., Olefsky, J.M., and Kobayashi, M. (2000). A rapamycin-sensitive pathway down-regulates insulin signaling via phosphorylation and proteasomal degradation of insulin receptor substrate-1. Molecular Endocrinology *14*, 783-794.

He, P.J., Lee, S.J., Lin, S.B., Seidler, U., Lang, F., Fejes-Toth, G., Naray-Fejes-Toth, A., and Yun, C.C. (2011). Serum- and glucocorticoid-induced kinase 3 in recycling endosomes mediates acute activation of Na+/H+ exchanger NHE3 by glucocorticoids. Mol Biol Cell *22*, 3812-3825.

Heitman, J., Movva, N.R., and Hall, M.N. (1991). Targets for cell cycle arrest by the immunosuppressant rapamycin in yeast. Science *253*, 905-909.

Herr, I., Ucur, E., Herzer, K., Okouoyo, S., Ridder, R., Krammer, P.H., Doeberitz, M.V., and Debatin, K.M. (2003). Glucocorticoid cotreatment induces apoptosis resistance toward cancer therapy in carcinomas. Cancer Research *63*, 3112-3120.

Hers, I., Vincent, E.E., and Tavare, J.M. (2011). Akt signalling in health and disease. Cellular Signalling *23*, 1515-1527.

Hertweck, M., Göbel, C., and Baumeister, R. (2004). C. elegans SGK-1 is the critical component in the Akt/PKB kinase complex to control stress response and life span. Dev Cell *6*, 577-588.

Hirai, H., Sootome, H., Nakatsuru, Y., Miyama, K., Taguchi, S., Tsujioka, K., Ueno, Y., Hatch, H., Majumder, P.K., Pan, B.-S*., et al.* (2010). MK-2206, an Allosteric Akt Inhibitor, Enhances Antitumor Efficacy by Standard Chemotherapeutic Agents or Molecular Targeted Drugs In vitro and In vivo. Mol Cancer Ther *9*, 1956-1967.

Hollestelle, A., Elstrodt, F., Nagel, J.H., Kallemeijn, W.W., and Schutte, M. (2007). Phosphatidylinositol-3-OH kinase or RAS pathway mutations in human breast cancer cell lines. Mol Cancer Res *5*, 195-201.

Holmes, B., Artinian, N., Anderson, L., Martin, J., Masri, J., Cloninger, C., Bernath, A., Bashir, T., Benavides-Serrato, A., and Gera, J. (2012). Protor-2 interacts with tristetraprolin to regulate mRNA stability during stress. Cellular Signalling *24*, 309-315.

Hosoi, F., Izumi, H., Kawahara, A., Murakami, Y., Kinoshita, H., Kage, M., Nishio, K., Kohno, K., Kuwano, M., and Ono, M. (2009). N-myc Downstream Regulated Gene 1/Cap43 Suppresses Tumor Growth and Angiogenesis of Pancreatic Cancer through Attenuation of Inhibitor of kappa B Kinase beta Expression. Cancer Research *69*, 4983-4991.

Hsu, P.P., Kang, S.A., Rameseder, J., Zhang, Y., Ottina, K.A., Lim, D., Peterson, T.R., Choi, Y., Gray, N.S., Yaffe, M.B*., et al.* (2011). The mTOR-Regulated Phosphoproteome Reveals a Mechanism of mTORC1-Mediated Inhibition of Growth Factor Signaling. Science *332*, 1317-1322.

Huang, D.Y., Boini, K.M., Friedrich, B., Metzger, M., Just, L., Osswald, H., Wulff, P., Kuhl, D., Vallon, V., and Lang, F. (2006a). Blunted hypertensive effect of combined fructose and high-salt diet in

gene-targeted mice lacking functional serum- and glucocorticoid-inducible kinase SGK1. American Journal of Physiology-Regulatory Integrative and Comparative Physiology *290*, R935-R944.

Huang, D.Y., Boini, K.M., Osswald, H., Friedrich, B., Artunc, F., Ullrich, S., Rajamanickam, J., Palmada, M., Wulff, P., Kuhl, D*., et al.* (2006b). Resistance of mice lacking the serum- and glucocorticoid-inducible kinase SGK1 against salt-sensitive hypertension induced by a high-fat diet. American Journal of Physiology-Renal Physiology *291*, F1264-F1273.

Hunter, T., and Sefton, B.M. (1980). Transforming gene product of Rous sarcoma virus phosphorylates tyrosine. Proc Natl Acad Sci U S A *77*, 1311-1315.

Ichimura, T., Yamamura, H., Sasamoto, K., Tominaga, Y., Taoka, M., Kakiuchi, K., Shinkawa, T., Takahashi, N., Shimada, S., and Isobe, T. (2005). 14-3-3 proteins modulate the expression of epithelial Na+ channels by phosphorylation-dependent interaction with Nedd4-2 ubiquitin ligase. J Biol Chem *280*, 13187-13194.

Inoki, K., Li, Y., Xu, T., and Guan, K.L. (2003). Rheb GTPase is a direct target of TSC2 GAP activity and regulates mTOR signaling. Genes Dev *17*, 1829-1834.

Inoki, K., Li, Y., Zhu, T., Wu, J., and Guan, K.L. (2002). TSC2 is phosphorylated and inhibited by Akt and suppresses mTOR signalling. Nat Cell Biol *4*, 648-657.

Inoue, H., Nojima, H., and Okayama, H. (1990). HIGH-EFFICIENCY TRANSFORMATION OF ESCHERICHIA-COLI WITH PLASMIDS. Gene *96*.

Jacinto, E., Facchinetti, V., Liu, D., Soto, N., Wei, S., Jung, S.Y., Huang, Q., Qin, J., and Su, B. (2006). SIN1/MIP1 maintains rictor-mTOR complex integrity and regulates Akt phosphorylation and substrate specificity. Cell *127*, 125-137.

Jacinto, E., Loewith, R., Schmidt, A., Lin, S., Rüegg, M.A., Hall, A., and Hall, M.N. (2004). Mammalian TOR complex 2 controls the actin cytoskeleton and is rapamycin insensitive. Nat Cell Biol *6*, 1122-1128.

James, S.R., Downes, C.P., Gigg, R., Grove, S.J., Holmes, A.B., and Alessi, D.R. (1996). Specific binding of the Akt-1 protein kinase to phosphatidylinositol 3,4,5-trisphosphate without subsequent activation. Biochem J *315 (Pt 3)*, 709-713.

Jemal, A., Bray, F., Center, M.M., Ferlay, J., Ward, E., and Forman, D. (2011). Global cancer statistics. CA Cancer J Clin *61*, 69-90.

Jewell, J.L., Russell, R.C., and Guan, K.-L. (2013). Amino acid signalling upstream of mTOR. Nat Rev Mol Cell Bio *14*, 133-139.

Johnson, L.N., Lowe, E.D., Noble, M.E., and Owen, D.J. (1998). The Eleventh Datta Lecture. The structural basis for substrate recognition and control by protein kinases. FEBS Lett *430*, 1-11.

Johnstone, C.N., Castellvi-Bel, S., Chang, L.M., Sung, R.K., Bowser, M.J., Pique, J.M., Castells, A., and Rustgi, A.K. (2005). PRR5 encodes a conserved proline-rich protein predominant in kidney: analysis of genomic organization, expression, and mutation status in breast and colorectal carcinomas. Genomics *85*, 338-351.

Jones, K.T., Greer, E.R., Pearce, D., and Ashrafi, K. (2009). Rictor/TORC2 Regulates Caenorhabditis elegans Fat Storage, Body Size, and Development through sgk-1. Plos Biol *7*, 604-615.

Jordan, V.C., and Koerner, S. (1975). Tamoxifen (ICI 46,474) and the human carcinoma 8S oestrogen receptor. Eur J Cancer *11*, 205-206.

Jun, X., Liu, D., Gill, G., and Zhou, S. (2001). Regulation of cytokine-independent survival kinase (CISK) by the Phox homology domain and phosphoinositides. J Cell Biol *154*, 699-705.

Kaizuka, T., Hara, T., Oshiro, N., Kikkawa, U., Yonezawa, K., Takehana, K., Iemura, S., Natsume, T., and Mizushima, N. (2010). Tti1 and Tel2 are critical factors in mammalian target of rapamycin complex assembly. J Biol Chem *285*, 20109-20116.

Karin, M. (2006). Nuclear factor-kappa B in cancer development and progression. Nature *441*, 431-436.

Kim, D.H., Sarbassov, D.D., Ali, S.M., King, J.E., Latek, R.R., Erdjument-Bromage, H., Tempst, P., and Sabatini, D.M. (2002). mTOR interacts with raptor to form a nutrient-sensitive complex that signals to the cell growth machinery. Cell *110*, 163-175.

Kim, D.H., Sarbassov, D.D., Ali, S.M., Latek, R.R., Guntur, K.V., Erdjument-Bromage, H., Tempst, P., and Sabatini, D.M. (2003). GbetaL, a positive regulator of the rapamycin-sensitive pathway required for the nutrient-sensitive interaction between raptor and mTOR. Mol Cell *11*, 895-904.

Kim, E., Goraksha-Hicks, P., Li, L., Neufeld, T.P., and Guan, K.-L. (2008). Regulation of TORC1 by Rag GTPases in nutrient response. Nature Cell Biology *10*, 935-945.

Kim, M.J., Chae, J.S., Kim, K.J., Hwang, S.G., Yoon, K.W., Kim, E.K., Yun, H.J., Cho, J.-H., Kim, J., Kim, B.-W*., et al.* (2007). Negative regulation of SEK1 signaling by serum- and glucocorticoid-inducible protein kinase 1. Embo J *26*, 3075-3085.

Kleinewietfeld, M., Manzel, A., Titze, J., Kvakan, H., Yosef, N., Linker, R.A., Muller, D.N., and Hafler, D.A. (2013). Sodium chloride drives autoimmune disease by the induction of pathogenic T(H)17 cells. Nature *496*, 518-+.

Knighton, D.R., Zheng, J.H., Ten Eyck, L.F., Ashford, V.A., Xuong, N.H., Taylor, S.S., and Sowadski, J.M. (1991). Crystal structure of the catalytic subunit of cyclic adenosine monophosphate-dependent protein kinase. Science *253*, 407-414.

Kobayashi, T., and Cohen, P. (1999). Activation of serum- and glucocorticoid-regulated protein kinase by agonists that activate phosphatidylinositide 3-kinase is mediated by 3-phosphoinositide-dependent protein kinase-1 (PDK1) and PDK2. Biochem J *339*, 319-328.

Kobayashi, T., Deak, M., Morrice, N., and Cohen, P. (1999). Characterization of the structure and regulation of two novel isoforms of serum- and glucocorticoid-induced protein kinase. Biochem J *344*, 189-197.

Kohn, A.D., Summers, S.A., Birnbaum, M.J., and Roth, R.A. (1996). Expression of a constitutively active Akt Ser/Thr kinase in 3T3-L1 adipocytes stimulates glucose uptake and glucose transporter 4 translocation. J Biol Chem *271*, 31372-31378.

Kokame, K., Kato, H., and Miyata, T. (1996). Homocysteine-respondent genes in vascular endothelial cells identified by differential display analysis - GRP78/BiP and novel genes. J Biol Chem *271*, 29659-29665.

Komander, D., Fairservice, A., Deak, M., Kular, G.S., Prescott, A.R., Peter Downes, C., Safrany, S.T., Alessi, D.R., and van Aalten, D.M. (2004). Structural insights into the regulation of PDK1 by phosphoinositides and inositol phosphates. The EMBO journal *23*, 3918-3928.

Koninki, K., Barok, M., Tanner, M., Staff, S., Pitkanen, J., Hemmila, P., Ilvesaro, J., and Isola, J. (2010). Multiple molecular mechanisms underlying trastuzumab and lapatinib resistance in JIMT-1 breast cancer cells. Cancer Lett *294*, 211-219.

Kops, G., de Ruiter, N.D., De Vries-Smits, A.M.M., Powell, D.R., Bos, J.L., and Burgering, B.M.T. (1999). Direct control of the Forkhead transcription factor AFX by protein kinase B. Nature *398*, 630-634.

Krebs, E.G., and Fischer, E.H. (1956). The phosphorylase b to a converting enzyme of rabbit skeletal muscle. Biochimica et biophysica acta *20*, 150-157.

Kurdistani, S.K., Arizti, P., Reimer, C.L., Sugrue, M.M., Aaronson, S.A., and Lee, S.W. (1998). Inhibition of tumor cell growth by RTP/rit42 and its responsiveness to p53 and DNA damage. Cancer Research *58*, 4439-4444.

Lahiry, P., Torkamani, A., Schork, N.J., and Hegele, R.A. (2010). Kinase mutations in human disease: interpreting genotype-phenotype relationships. Nat Rev Genet *11*, 60-74.

Lang, F., Artunc, F., and Vallon, V. (2009). The physiological impact of the serum and glucocorticoid-inducible kinase SGK1. Curr Opin Nephrol Hy *18*, 439-448.

Lang, F., Boehmer, C., Palmada, M., Seebohm, G., Strutz-Seebohm, N., and Vallon, V. (2006). (Patho)physiological significance of the serum- and glucocorticoid-inducible kinase isoforms. Physiological Reviews *86*, 1151-1178.

Lang, F., Eylenstein, A., and Shumilina, E. (2012). Regulation of Orai1/STIM1 by the kinases SGK1 and AMPK. Cell Calcium *52*, 347-354.

Lang, F., and Shumilina, E. (2013). Regulation of ion channels by the serum- and glucocorticoid-inducible kinase SGK1. Faseb J *27*, 3-12.

Lang, F., and Voelkl, J. (2013). Therapeutic potential of serum and glucocorticoid inducible kinase inhibition. Expert Opinion on Investigational Drugs *22*, 701-714.

Laplante, M., and Sabatini, D.M. (2012). mTOR signaling in growth control and disease. Cell *149*, 274-293.

Laplante, M., and Sabatini, D.M. (2013). Regulation of mTORC1 and its impact on gene expression at a glance. Journal of Cell Science *126*, 1713-1719.

Le, N.T.V., and Richardson, D.R. (2004). Iron chelators with high antiproliferative activity up-regulate the expression of a growth inhibitory and metastasis suppressor gene: a link between iron metabolism and proliferation. Blood *104*, 2967-2975.

Leroy, V., De Seigneux, S., Agassiz, V., Hasler, U., Rafestin-Oblin, M.-E., Vinciguerra, M., Martin, P.-Y., and Feraille, E. (2009). Aldosterone Activates NF-kappa B in the Collecting Duct. Journal of the American Society of Nephrology *20*, 131-144.

Liang, J., Zubovitz, J., Petrocelli, T., Kotchetkov, R., Connor, M.K., Han, K., Lee, J.H., Ciarallo, S., Catzavelos, C., Beniston, R.*, et al.* (2002). PKB/Akt phosphorylates p27, impairs nuclear import of p27 and opposes p27-mediated G1 arrest. Nature Medicine *8*, 1153-1160.

Liu, D., Yang, X.H., and Zhou, S.Y. (2000). Identification of CISK, a new member of the SGK kinase family that promotes IL-3-dependent survival. Current Biology *10*, 1233-1236.

Liu, M., Chen, L.L., Chan, T.H.M., Wang, J., Li, Y., Zeng, T.T., Yuan, Y.F., and Guan, X.Y. (2012). Serum and glucocorticoid kinase 3 at 8q13.1 promotes cell proliferation and survival in hepatocellular carcinoma. Hepatology *55*, 1754-1765.

Liu, P., Cheng, H., Roberts, T.M., and Zhao, J.J. (2009). Targeting the phosphoinositide 3-kinase pathway in cancer. Nature Reviews Drug Discovery *8*.

Livak, K.J., and Schmittgen, T.D. (2001). Analysis of relative gene expression data using real-time quantitative PCR and the 2(T)(-Delta Delta C) method. Methods *25*, 402-408.

Loewith, R., Jacinto, E., Wullschleger, S., Lorberg, A., Crespo, J.L., Bonenfant, D., Oppliger, W., Jenoe, P., and Hall, M.N. (2002). Two TOR complexes, only one of which is rapamycin sensitive, have distinct roles in cell growth control. Mol Cell *10*, 457-468.

Ma, L., Chen, Z., Erdjument-Bromage, H., Tempst, P., and Pandolfi, P.P. (2005). Phosphorylation and functional inactivation of TSC2 by Erk implications for tuberous sclerosis and cancer pathogenesis. Cell *121*, 179-193.

Manning, B.D., and Cantley, L.C. (2007). AKT/PKB signaling: Navigating downstream. Cell *129*, 1261-1274.

Manning, B.D., Tee, A.R., Logsdon, M.N., Blenis, J., and Cantley, L.C. (2002a). Identification of the tuberous sclerosis complex-2 tumor suppressor gene product tuberin as a target of the phosphoinositide 3-kinase/akt pathway. Mol Cell *10*, 151-162.

Manning, G., Whyte, D.B., Martinez, R., Hunter, T., and Sudarsanam, S. (2002b). The protein kinase complement of the human genome. Science *298*, 1912-1934.

Martina, J.A., Chen, Y., Gucek, M., and Puertollano, R. (2012). MTORC1 functions as a transcriptional regulator of autophagy by preventing nuclear transport of TFEB. Autophagy *8*, 903-914.

Mayo, L.D., and Donner, D.B. (2001). A phosphatidylinositol 3-kinase/Akt pathway promotes translocation of Mdm2 from the cytoplasm to the nucleus. Proc Natl Acad Sci U S A *98*, 11598-11603.

McCormick, J.A., Feng, Y., Dawson, K., Behne, M.J., Yu, B., Wang, J., Wyatt, A.W., Henke, G., Grahammer, F., Mauro, T.M.*, et al.* (2004). Targeted disruption of the protein kinase SGK3/CISK impairs postnatal hair follicle development. Mol Biol Cell *15*, 4278-4288.

Melotte, V., Qu, X., Ongenaert, M., van Criekinge, W., de Bruine, A.P., Baldwin, H.S., and van Engeland, M. (2010). The N-myc downstream regulated gene (NDRG) family: diverse functions, multiple applications. Faseb J *24*, 4153-4166.

Meng, F.M., Yamagiwa, Y., Taffetani, S., Han, J.H., and Patel, T. (2005). IL-6 activates serum and glucocorticoid kinase via p38 alpha mitogen-activated protein kinase pathway. Am J Physiol-Cell Physiol *289*, C971-C981.

Mikosz, C.A., Brickley, D.R., Sharkey, M.S., Moran, T.W., and Conzen, S.D. (2001). Glucocorticoid receptor-mediated protection from apoptosis is associated with induction of the serine/threonine survival kinase gene, sgk-1. J Biol Chem *276*, 16649-16654.

Milburn, C.C., Deak, M., Kelly, S.M., Price, N.C., Alessi, D.R., and Van Aalten, D.M.F. (2003). Binding of phosphatidylinositol 3,4,5-trisphosphate to the pleckstrin homology domain of protein kinase B induces a conformational change. Biochem J *375*, 531-538.

Miller, T.W., Rexer, B.N., Garrett, J.T., and Arteaga, C.L. (2011). Mutations in the phosphatidylinositol 3-kinase pathway: role in tumor progression and therapeutic implications in breast cancer. Breast Cancer Res *13*, 224.

Moran, T.J., Gray, S., Mikosz, C.A., and Conzen, S.D. (2000). The glucocorticoid receptor mediates a survival signal in human mammary epithelial cells. Cancer Research *60*, 867-872.

Morgenstern, J.P., and Land, H. (1990). ADVANCED MAMMALIAN GENE-TRANSFER - HIGH TITER RETROVIRAL VECTORS WITH MULTIPLE-DRUG SELECTION MARKERS AND A COMPLEMENTARY HELPER-FREE PACKAGING CELL-LINE. Nucleic Acids Research *18*.

Mosmann, T. (1983). Rapid colorimetric assay for cellular growth and survival: application to proliferation and cytotoxicity assays. J Immunol Methods *65*, 55-63.

Murakami, M., Ichisaka, T., Maeda, M., Oshiro, N., Hara, K., Edenhofer, F., Kiyama, H., Yonezawa, K., and Yamanaka, S. (2004). mTOR is essential for growth and proliferation in early mouse embryos and embryonic stem cells. Mol Cell Biol *24*, 6710-6718.

Murray, J.T., Campbell, D.G., Morrice, N., Auld, G.C., Shpiro, N., Marquez, R., Peggie, M., Bain, J., Bloomberg, G.B., Grahammer, F.*, et al.* (2004). Exploitation of KESTREL to identify NDRG family members as physiological substrates for SGK1 and GSK3. Biochem J *384*, 477-488.

Murray, J.T., Cummings, L.A., Bloomberg, G.B., and Cohen, P. (2005). Identification of different specificity requirements between SGK1 and PKBalpha. Febs Letters *579*, 991-994.

Musgrove, E.A., and Sutherland, R.L. (2009). Biological determinants of endocrine resistance in breast cancer. Nat Rev Cancer *9*, 631-643.

Myers, M.P., Pass, I., Batty, I.H., Van der Kaay, J., Stolarov, J.P., Hemmings, B.A., Wigler, M.H., Downes, C.P., and Tonks, N.K. (1998). The lipid phosphatase activity of PTEN is critical for its tumor supressor function. P Natl Acad Sci USA *95*, 13513-13518.

Najafov, A., Shpiro, N., and Alessi, D.R. (2012). Akt is efficiently activated by PIF-pocket- and PtdIns(3,4,5)P3-dependent mechanisms leading to resistance to PDK1 inhibitors. Biochem J *448*, 285-295.

Najafov, A., Sommer, E.M., Axten, J.M., Deyoung, M.P., and Alessi, D.R. (2011). Characterization of GSK2334470, a novel and highly specific inhibitor of PDK1. Biochem J *433*, 357-369.

Naray-Fejes-Toth, A., Canessa, C., Cleaveland, E.S., Aldrich, G., and Fejes-Toth, G. (1999). sgk is an aldosterone-induced kinase in the renal collecting duct - Effects on epithelial Na+ channels. J Biol Chem *274*, 16973-16978.

Nasir, O., Wang, K., Foller, M., Gu, S., Bhandaru, M., Ackermann, T., Boini, K., Mack, A., Klingel, K., Amato, R.*, et al.* (2009). Relative Resistance of SGK1 Knockout Mice Against Chemical Carcinogenesis. Iubmb Life *61*, 768-776.

Network, C.G.A. (2012). Comprehensive molecular portraits of human breast tumours. Nature *490*, 61-70.

Nojima, H., Tokunaga, C., Eguchi, S., Oshiro, N., Hidayat, S., Yoshino, K., Hara, K., Tanaka, N., Avruch, J., and Yonezawa, K. (2003). The mammalian target of rapamycin (mTOR) partner, raptor, binds the mTOR substrates p70 S6 kinase and 4E-BP1 through their TOR signaling (TOS) motif. J Biol Chem *278*, 15461-15464.

O'Reilly, K.E., Rojo, F., She, Q.B., Solit, D., Mills, G.B., Smith, D., Lane, H., Hofmann, F., Hicklin, D.J., Ludwig, D.L.*, et al.* (2006). mTOR inhibition induces upstream receptor tyrosine kinase signaling and activates Akt. Cancer Research *66*.

Okuzumi, T., Fiedler, D., Zhang, C., Gray, D.C., Aizenstein, B., Hoffman, R., and Shokat, K.M. (2009). Inhibitor hijacking of Akt activation. Nat Chem Biol *5*, 484-493.

Ortutay, C., Väliaho, J., Stenberg, K., and Vihinen, M. (2005). KinMutBase: a registry of disease-causing mutations in protein kinase domains. Hum Mutat *25*, 435-442.

Oshiro, N., Takahashi, R., Yoshino, K., Tanimura, K., Nakashima, A., Eguchi, S., Miyamoto, T., Hara, K., Takehana, K., Avruch, J.*, et al.* (2007). The proline-rich Akt substrate of 40 kDa (PRAS40) is a physiological substrate of mammalian target of rapamycin complex 1. The Journal of biological chemistry *282*, 20329-20339.

Pablo Arroyo, J., Lagnaz, D., Ronzaud, C., Vazquez, N., Ko, B.S., Moddes, L., Ruffieux-Daidie, D., Hausel, P., Koesters, R., Yang, B.*, et al.* (2011). Nedd4-2 Modulates Renal Na+-Cl- Cotransporter via the Aldosterone-SGK1-Nedd4-2 Pathway. Journal of the American Society of Nephrology *22*, 1707-1719.

Pao, A.C., Bhargava, A., Di Sole, F., Quigley, R., Shao, X., Wang, J., Thomas, S., Zhang, J., Shi, M., Funder, J.W.*, et al.* (2010). Expression and role of serum and glucocorticoid-regulated kinase 2 in

the regulation of Na+/H+ exchanger 3 in the mammalian kidney. Am J Physiol Renal Physiol *299*, F1496-1506.

Pao, A.C., McCormick, J.A., Li, H., Siu, J., Govaerts, C., Bhalla, V., Soundararajan, R., and Pearce, D. (2007). NH(2) terminus of serum and glucocorticoid-regulated kinase 1 binds to phosphoinositides and is essential for isoform-specific physiological functions. American Journal of Physiology-Renal Physiology *292*, F1741-F1750.

Park, H., Adams, M.A., Lachat, P., Bosman, F., Pang, S.C., and Graham, C.H. (2000). Hypoxia induces the expression of a 43-kDa protein (PROXY-1) in normal and malignant cells. Biochem Biophys Res Commun *276*, 321-328.

Park, H.S., Kim, M.S., Huh, S.H., Park, J.H., Chung, J.K., Kang, S.S., and Choi, E.J. (2002). Akt (protein kinase B) negatively regulates SEK1 by means of protein phosphorylation. J Biol Chem *277*, 2573-2578.

Park, J., Leong, M.L., Buse, P., Maiyar, A.C., Firestone, G.L., and Hemmings, B.A. (1999). Serum and glucocorticoid-inducible kinase (SGK) is a target of the PI 3-kinase-stimulated signaling pathway. Embo J *18*, 3024-3033.

Pasham, V., Rotte, A., Bhandaru, M., Eichenmuller, M., Frohlich, H., Mack, A.F., Bobbala, D., Yang, W.T., Pearce, D., and Lang, F.R. (2011). Regulation of gastric acid secretion by the serum and glucocorticoid inducible kinase isoform SGK3. Journal of Gastroenterology *46*, 305-317.

Pearce, L.R., Alton, G.R., Richter, D.T., Kath, J.C., Lingardo, L., Chapman, J., Hwang, C., and Alessi, D.R. (2010a). Characterization of PF-4708671, a novel and highly specific inhibitor of p70 ribosomal S6 kinase (S6K1). Biochem J *431*, 245-255.

Pearce, L.R., Huang, X., Boudeau, J., Pawłowski, R., Wullschleger, S., Deak, M., Ibrahim, A.F., Gourlay, R., Magnuson, M.A., and Alessi, D.R. (2007). Identification of Protor as a novel Rictor-binding component of mTOR complex-2. Biochem J *405*, 513-522.

Pearce, L.R., Komander, D., and Alessi, D.R. (2010b). The nuts and bolts of AGC protein kinases. Nat Rev Mol Cell Bio *11*, 9-22.

Pearce, L.R., Sommer, E.M., Sakamoto, K., Wullschleger, S., and Alessi, D.R. (2011). Protor-1 is required for efficient mTORC2-mediated activation of SGK1 in the kidney. Biochem J *436*, 169-179.

Peterson, T.R., Laplante, M., Thoreen, C.C., Sancak, Y., Kang, S.A., Kuehl, W.M., Gray, N.S., and Sabatini, D.M. (2009). DEPTOR is an mTOR inhibitor frequently overexpressed in multiple myeloma cells and required for their survival. Cell *137*, 873-886.

Podsypanina, K., Ellenson, L.H., Nemes, A., Gu, J.G., Tamura, M., Yamada, K.M., Cordon-Cardo, C., Catoretti, G., Fisher, P.E., and Parsons, R. (1999). Mutation of Pten/Mmac1 in mice causes neoplasia in multiple organ systems. P Natl Acad Sci USA *96*, 1563-1568.

Polyak, K., and Metzger Filho, O. (2012). SnapShot: breast cancer. Cancer Cell *22*, 562-562.e561.

Rao, A.D., Sun, B., Saxena, A., Hopkins, P.N., Jeunemaitre, X., Brown, N.J., Adler, G.K., and Williams, J.S. (2013). Polymorphisms in the serum- and glucocorticoid-inducible kinase 1 gene are associated

with blood pressure and renin response to dietary salt intake. Journal of Human Hypertension *27*, 176-180.

Rauhala, H.E., Porkka, K.P., Tolonen, T.T., Martikainen, P.M., Tammela, T.L.J., and Visakorpi, T. (2005). Dual-specificity phosphatase 1 and serum/glucocorticoid-regulated kinase are downregulated in prostate cancer. International Journal of Cancer *117*, 738-745.

Ring, A.M., Leng, Q., Rinehart, J., Wilson, F.H., Kahle, K.T., Hebert, S.C., and Lifton, R.P. (2007). An SGK1 site in WNK4 regulates Na+ channel and K+ channel activity and has implications for aldosterone signaling and K+ homeostasis. P Natl Acad Sci USA *104*, 4025-4029.

Roczniak-Ferguson, A., Petit, C.S., Froehlich, F., Qian, S., Ky, J., Angarola, B., Walther, T.C., and Ferguson, S.M. (2012). The Transcription Factor TFEB Links mTORC1 Signaling to Transcriptional Control of Lysosome Homeostasis. Science Signaling *5*.

Roderick, H.L., and Cook, S.J. (2008). Ca2+ signalling checkpoints in cancer: remodelling Ca2+ for cancer cell proliferation and survival. Nature Reviews Cancer *8*, 361-375.

Rodon, J., Dienstmann, R., Serra, V., and Tabemero, J. (2013). Development of PI3K inhibitors: lessons learned from early clinical trials. Nature Reviews Clinical Oncology *10*, 143-153.

Rodriguez-Viciana, P., Warne, P.H., Dhand, R., Vanhaesebroeck, B., Gout, I., Fry, M.J., Waterfield, M.D., and Downward, J. (1994). Phosphatidylinositol-3-OH kinase as a direct target of Ras. Nature *370*, 527-532.

Rodrik-Outmezguine, V.S., Chandarlapaty, S., Pagano, N.C., Poulikakos, P.I., Scaltriti, M., Moskatel, E., Baselga, J., Guichard, S., and Rosen, N. (2011). mTOR Kinase Inhibition Causes Feedback-Dependent Biphasic Regulation of AKT Signaling. Cancer Discovery *1*, 248-259.

Rozansky, D.J., Cornwall, T., Subramanya, A.R., Rogers, S., Yang, Y.-F., David, L.L., Zhu, X., Yang, C.-L., and Ellison, D.H. (2009). Aldosterone mediates activation of the thiazide-sensitive Na-Cl cotransporter through an SGK1 and WNK4 signaling pathway. Journal of Clinical Investigation *119*, 2601-2612.

Sabatini, D.M., Erdjument-Bromage, H., Lui, M., Tempst, P., and Snyder, S.H. (1994). RAFT1: a mammalian protein that binds to FKBP12 in a rapamycin-dependent fashion and is homologous to yeast TORs. Cell *78*, 35-43.

Sabers, C.J., Martin, M.M., Brunn, G.J., Williams, J.M., Dumont, F.J., Wiederrecht, G., and Abraham, R.T. (1995). Isolation of a protein target of the FKBP12-rapamycin complex in mammalian cells. J Biol Chem *270*, 815-822.

Sakoda, H., Gotoh, Y., Katagiri, H., Kurokawa, M., Ono, H., Onishi, Y., Anai, M., Ogihara, T., Fujishiro, M., Fukushima, Y.*, et al.* (2003). Differing roles of Akt and serum- and glucocorticoid-regulated kinase in glucose metabolism, DNA synthesis, and oncogenic activity. J Biol Chem *278*, 25802-25807.

Salker, M.S., Christian, M., Steel, J.H., Nautiyal, J., Lavery, S., Trew, G., Webster, Z., Al-Sabbagh, M., Puchchakayala, G., Foeller, M.*, et al.* (2011). Deregulation of the serum- and glucocorticoid-inducible kinase SGK1 in the endometrium causes reproductive failure. Nature Medicine *17*.

Sancak, Y., Bar-Peled, L., Zoncu, R., Markhard, A.L., Nada, S., and Sabatini, D.M. (2010). Ragulator-Rag Complex Targets mTORC1 to the Lysosomal Surface and Is Necessary for Its Activation by Amino Acids. Cell *141*, 290-303.

Sancak, Y., Peterson, T.R., Shaul, Y.D., Lindquist, R.A., Thoreen, C.C., Bar-Peled, L., and Sabatini, D.M. (2008). The Rag GTPases bind raptor and mediate amino acid signaling to mTORC1. Science *320*, 1496-1501.

Sancak, Y., Thoreen, C.C., Peterson, T.R., Lindquist, R.A., Kang, S.A., Spooner, E., Carr, S.A., and Sabatini, D.M. (2007). PRAS40 is an insulin-regulated inhibitor of the mTORC1 protein kinase. Mol Cell *25*, 903-915.

Sanchez, I., Hughes, R.T., Mayer, B.J., Yee, K., Woodgett, J.R., Avruch, J., Kyriakis, J.M., and Zon, L.I. (1994). ROLE OF SAPK/ERK KINASE-1 IN THE STRESS-ACTIVATED PATHWAY REGULATING TRANSCRIPTION FACTOR C-JUN. Nature *372*.

Sandu, C., Rexhepaj, R., Grahammer, F., McCormick, J.A., Henke, G., Palmada, M., Nammi, S., Lang, U., Metzger, M., Just, L*., et al.* (2005). Decreased intestinal glucose transport in the sgk3-knockout mouse. Pflugers Arch *451*, 437-444.

Sano, H., Kane, S., Sano, E., Mîinea, C.P., Asara, J.M., Lane, W.S., Garner, C.W., and Lienhard, G.E. (2003). Insulin-stimulated phosphorylation of a Rab GTPase-activating protein regulates GLUT4 translocation. J Biol Chem *278*, 14599-14602.

Sarbassov, D.D., Ali, S.M., Kim, D.H., Guertin, D.A., Latek, R.R., Erdjument-Bromage, H., Tempst, P., and Sabatini, D.M. (2004). Rictor, a novel binding partner of mTOR, defines a rapamycin-insensitive and raptor-independent pathway that regulates the cytoskeleton. Curr Biol *14*, 1296-1302.

Sarbassov, D.D., Guertin, D.A., Ali, S.M., and Sabatini, D.M. (2005). Phosphorylation and regulation of Akt/PKB by the rictor-mTOR complex. Science *307*, 1098-1101.

Schmidt, E.-M., Gu, S., Anagnostopoulou, V., Alevizopoulos, K., Foeller, M., Lang, F., and Stournaras, C. (2012a). Serum- and glucocorticoid-dependent kinase-1-induced cell migration is dependent on vinculin and regulated by the membrane androgen receptor. Febs Journal *279*.

Schmidt, E.-M., Kraemer, B.F., Borst, O., Muenzer, P., Schoenberger, T., Schmidt, C., Leibrock, C., Towhid, S.T., Seizer, P., Kuhl, D*., et al.* (2012b). SGK1 Sensitivity of Platelet Migration. Cellular Physiology and Biochemistry *30*.

Schnackenberg, C.G., Costell, M.H., Bernard, R.E., Minuti, K.K., Grygielko, E.T., Parsons, M.J., Laping, N.J., and Duddy, G. (2007). Compensatory role for Sgk2 mediated sodium reabsorption during salt deprivation in Sgk1 knockout mice. Faseb J *21*, A508-A508.

Schorr, K., and Furth, P.A. (2000). Induction of bcl-x(L) expression in mammary epithelial cells is glucocorticoid-dependent but not signal transducer and activator of transcription 5-dependent. Cancer Research *60*, 5950-5953.

Schwab, M., Lupescu, A., Mota, M., Mota, E., Frey, A., Simon, P., Mertens, P.R., Floege, J., Luft, F., Asante-Poku, S.*, et al.* (2008). Association of SGK1 gene polymorphisms with type 2 diabetes. Cellular Physiology and Biochemistry *21*, 151-160.

Settembre, C., De Cegli, R., Mansueto, G., Saha, P.K., Vetrini, F., Visvikis, O., Tuong, H., Carissimo, A., Palmer, D., Klisch, T.J.*, et al.* (2013). TFEB controls cellular lipid metabolism through a starvation-induced autoregulatory loop. Nature Cell Biology *15*, 647-+.

Settembre, C., Zoncu, R., Medina, D.L., Vetrini, F., Erdin, S., Erdin, S., Tuong, H., Ferron, M., Karsenty, G., Vellard, M.C.*, et al.* (2012). A lysosome-to-nucleus signalling mechanism senses and regulates the lysosome via mTOR and TFEB. Embo J *31*, 1095-1108.

Shah, O.J., Wang, Z.Y., and Hunter, T. (2004). Inappropriate activation of the TSC/Rheb/mTOR/S6K cassette induces IRS1/2 depletion, insulin resistance, and cell survival deficiencies. Current Biology *14*, 1650-1656.

Shan, Z.H., Haaf, T., and Popescu, N.C. (2003). Identification and characterization of a gene encoding a putative mouse Rho GTPase activating protein gene 8, Arhgap8. Gene *303*, 55-61.

Shanmugam, I., Cheng, G., Terranova, P.F., Thrasher, J.B., Thomas, C.P., and Li, B. (2007). Serurn/glucocorticoid-induced protein kinase-1 facilitates androgen receptor-dependent cell survival. Cell Death and Differentiation *14*, 2085-2094.

Shelly, C., and Herrera, R. (2002). Activation of SGK1 by HGF, Rac1 and integrin-mediated cell adhesion in MDCK cells: PI-3K-dependent and -independent pathways. Journal of Cell Science *115*, 1985-1993.

Shimono, A., Okuda, T., and Kondoh, H. (1999). N-myc-dependent repression of ndr1, a gene identified by direct subtraction of whole mouse embryo cDNAs between wild type and N-myc mutant. Mech Dev *83*, 39-52.

Shin, I., Yakes, F.M., Rojo, F., Shin, N.Y., Bakin, A.V., Baselga, J., and Arteaga, C.L. (2002). PKB/Akt mediates cell-cycle progression by phosphorylation of p27(Kip1) at threonine 157 and modulation of its cellular localization. Nat Med *8*, 1145-1152.

Shiota, C., Woo, J.-T., Lindner, J., Shelton, K.D., and Magnuson, M.A. (2006). Multiallelic disruption of the rictor gene in mice reveals that mTOR complex 2 is essential for fetal growth and viability. Developmental Cell *11*.

Sievers, F., Wilm, A., Dineen, D., Gibson, T.J., Karplus, K., Li, W., Lopez, R., McWilliam, H., Remmert, M., Soeding, J.*, et al.* (2011). Fast, scalable generation of high-quality protein multiple sequence alignments using Clustal Omega. Molecular Systems Biology *7*.

Simon, P., Schneck, M., Hochstetter, T., Koutsouki, E., Mittelbronn, M., Merseburger, A.S., Weigert, C., Niess, A.M., and Lang, F. (2007). Differential regulation of serum- and glucocorticoid-inducible kinase 1 (SGK1) splice variants based on alternative initiation of transcription. Cellular Physiology and Biochemistry *20*, 715-728.

Skolnik, E.Y., Margolis, B., Mohammadi, M., Lowenstein, E., Fischer, R., Drepps, A., Ullrich, A., and Schlessinger, J. (1991). Cloning of PI3 kinase-associated p85 utilizing a novel method for expression/cloning of target proteins for receptor tyrosine kinases. Cell *65*, 83-90.

Slagsvold, T., Marchese, A., Brech, A., and Stenmark, H. (2006). CISK attenuates degradation of the chemokine receptor CXCR4 via the ubiquitin ligase AIP4. Embo J *25*.

Slamon, D.J., Clark, G.M., Wong, S.G., Levin, W.J., Ullrich, A., and McGuire, W.L. (1987). Human breast cancer: correlation of relapse and survival with amplification of the HER-2/neu oncogene. Science *235*, 177-182.

Snyder, P.M., Olson, D.R., and Thomas, B.C. (2002). Serum and glucocorticoid-regulated kinase modulates Nedd4-2-mediated inhibition of the epithelial Na+ channel. J Biol Chem *277*, 5-8.

Sorlie, T., Perou, C.M., Tibshirani, R., Aas, T., Geisler, S., Johnsen, H., Hastie, T., Eisen, M.B., van de Rijn, M., Jeffrey, S.S.*, et al.* (2001). Gene expression patterns of breast carcinomas distinguish tumor subclasses with clinical implications. P Natl Acad Sci USA *98*, 10869-10874.

Sorlie, T., Tibshirani, R., Parker, J., Hastie, T., Marron, J.S., Nobel, A., Deng, S., Johnsen, H., Pesich, R., Geisler, S.*, et al.* (2003). Repeated observation of breast tumor subtypes in independent gene expression data sets. Proc Natl Acad Sci U S A *100*, 8418-8423.

Soukas, A.A., Kane, E.A., Carr, C.E., Melo, J.A., and Ruvkun, G. (2009). Rictor/TORC2 regulates fat metabolism, feeding, growth, and life span in Caenorhabditis elegans. Gene Dev *23*, 496-511.

Staal, S.P. (1987). Molecular cloning of the akt oncogene and its human homologues AKT1 and AKT2: amplification of AKT1 in a primary human gastric adenocarcinoma. Proc Natl Acad Sci U S A *84*, 5034-5037.

Stambolic, V., Suzuki, A., de la Pompa, J.L., Brothers, G.M., Mirtsos, C., Sasaki, T., Ruland, J., Penninger, J.M., Siderovski, D.P., and Mak, T.W. (1998). Negative regulation of PKB/Akt-dependent cell survival by the tumor suppressor PTEN. Cell *95*, 29-39.

Stehelin, D., Fujita, D.J., Padgett, T., Varmus, H.E., and Bishop, J.M. (1977). Detection and enumeration of transformation-defective strains of avian sarcoma virus with molecular hybridization. Virology *76*, 675-684.

Stephens, L., Smrcka, A., Cooke, F.T., Jackson, T.R., Sternweis, P.C., and Hawkins, P.T. (1994). A novel phosphoinositide 3 kinase activity in myeloid-derived cells is activated by G protein beta gamma subunits. Cell *77*, 83-93.

Stephens, P.J., Tarpey, P.S., Davies, H., Van Loo, P., Greenman, C., Wedge, D.C., Nik-Zainal, S., Martin, S., Varela, I., Bignell, G.R.*, et al.* (2012). The landscape of cancer genes and mutational processes in breast cancer. Nature *486*, 400-404.

Sun, S.Y., Rosenberg, L.M., Wang, X.R., Zhou, Z.M., Yue, P., Fu, H., and Khuri, F.R. (2005). Activation of Akt and eIF4E survival pathways by rapamycin-mediated mammalian target of rapamycin inhibition. Cancer Research *65*.

Sun, X.J., Rothenberg, P., Kahn, C.R., Backer, J.M., Araki, E., Wilden, P.A., Cahill, D.A., Goldstein, B.J., and White, M.F. (1991). Structure of the insulin receptor substrate IRS-1 defines a unique signal transduction protein. Nature *352*, 73-77.

Sutherland, E.W., Jr., and Wosilait, W.D. (1955). Inactivation and activation of liver phosphorylase. Nature *175*, 169-170.

Suzuki, A., de la Pompa, J.L., Stambolic, V., Elia, A.J., Sasaki, T., Barrantes, I.D., Ho, A., Wakeham, A., Itie, A., Khoo, W*., et al.* (1998). High cancer susceptibility and embryonic lethality associated with mutation of the PTEN tumor suppressor gene in mice. Current Biology *8*, 1169-1178.

Tai, D.J.C., Su, C.-C., Ma, Y.-L., and Lee, E.H.Y. (2009). SGK1 Phosphorylation of I kappa B Kinase alpha and p300 Up-regulates NF-kappa B Activity and Increases N-Methyl-D-aspartate Receptor NR2A and NR2B Expression. J Biol Chem *284*, 4073-4089.

Tanner, M., Kapanen, A.I., Junttila, T., Raheem, O., Grenman, S., Elo, J., Elenius, K., and Isola, J. (2004). Characterization of a novel cell line established from a patient with Herceptin-resistant breast cancer. Mol Cancer Ther *3*, 1585-1592.

Tannheimer, S.L., Rehemtulla, A., and Ethier, S.P. (2000). Characterization of fibroblast growth factor receptor 2 overexpression in the human breast cancer cell line SUM-52PE. Breast cancer research : BCR *2*, 311-320.

Taub, M., Wang, Y., Szczesny, T.M., and Kleinman, H.K. (1990). Epidermal growth factor or transforming growth factor alpha is required for kidney tubulogenesis in matrigel cultures in serum-free medium. P Natl Acad Sci USA *87*, 4002-4006.

Tee, A.R., Manning, B.D., Roux, P.P., Cantley, L.C., and Blenis, J. (2003). Tuberous sclerosis complex gene products, Tuberin and Hamartin, control mTOR signaling by acting as a GTPase-activating protein complex toward Rheb. Curr Biol *13*, 1259-1268.

Tessier, M., and Woodgett, J.R. (2006). Role of the Phox homology domain and phosphorylation in activation of serum and glucocorticoid-regulated kinase-3. J Biol Chem *281*, 23978-23989.

Thedieck, K., Polak, P., Kim, M.L., Molle, K.D., Cohen, A., Jenö, P., Arrieumerlou, C., and Hall, M.N. (2007). PRAS40 and PRR5-like protein are new mTOR interactors that regulate apoptosis. PLoS One *2*, e1217.

Tschopp, O., Yang, Z.Z., Brodbeck, D., Dummler, B.A., Hemmings-Mieszczak, M., Watanabe, T., Michaelis, T., Frahm, J., and Hemmings, B.A. (2005). Essential role of protein kinase B gamma (PKB gamma/Akt3) in postnatal brain development but not in glucose homeostasis. Development *132*, 2943-2954.

Tzatsos, A. (2009). Raptor binds the SAIN (Shc and IRS-1 NPXY binding) domain of insulin receptor substrate-1 (IRS-1) and regulates the phosphorylation of IRS-1 at Ser-636/639 by mTOR. The Journal of biological chemistry *284*, 22525-22534.

Tzatsos, A., and Kandror, K.V. (2006). Nutrients suppress phosphatidylinositol 3-kinase/Akt signaling via raptor-dependent mTOR-mediated insulin receptor substrate 1 phosphorylation. Mol Cell Biol *26*, 63-76.

Vallon, V., Schroth, J., Lang, F., Kuhl, D., and Uchida, S. (2009). Expression and phosphorylation of the Na+-Cl- cotransporter NCC in vivo is regulated by dietary salt, potassium, and SGK1. American Journal of Physiology-Renal Physiology *297*, F704-F712.

Vallon, V., Wyatt, A.W., Klingel, K., Huang, D.Y., Hussain, A., Berchtold, S., Friedrich, B., Grahammer, F., BelAiba, R.S., Gorlach, A.*, et al.* (2006). SGK1-dependent cardiac CTGF formation and fibrosis following DOCA treatment. Journal of Molecular Medicine-Jmm *84*, 396-404.

Vander Haar, E., Lee, S.I., Bandhakavi, S., Griffin, T.J., and Kim, D.H. (2007). Insulin signalling to mTOR mediated by the Akt/PKB substrate PRAS40. Nat Cell Biol *9*, 316-323.

Vanhaesebroeck, B., Guillermet-Guibert, J., Graupera, M., and Bilanges, B. (2010). The emerging mechanisms of isoform-specific PI3K signalling. Nat Rev Mol Cell Biol *11*, 329-341.

Vasudevan, K.M., Barbie, D.A., Davies, M.A., Rabinovsky, R., McNear, C.J., Kim, J.J., Hennessy, B.T., Tseng, H., Pochanard, P., Kim, S.Y.*, et al.* (2009). AKT-Independent Signaling Downstream of Oncogenic PIK3CA Mutations in Human Cancer. Cancer Cell *16*.

Vezina, C., Kudelski, A., and Sehgal, S.N. (1975). RAPAMYCIN (AY-22,989), A NEW ANTIFUNGAL ANTIBIOTIC .1. TAXONOMY OF PRODUCING STREPTOMYCETE AND ISOLATION OF ACTIVE PRINCIPLE. Journal of Antibiotics *28*, 721-726.

Viglietto, G., Motti, M.L., Bruni, P., Melillo, R.M., D'Alessio, A., Califano, D., Vinci, F., Chiappetta, G., Tsichlis, P., Bellacosa, A.*, et al.* (2002). Cytoplasmic relocalization and inhibition of the cyclin-dependent kinase inhibitor p27(Kip1) by PKB/Akt-mediated phosphorylation in breast cancer. Nat Med *8*, 1136-1144.

Virbasius, J.V., Song, X., Pomerleau, D.P., Zhan, Y., Zhou, G.W., and Czech, M.P. (2001). Activation of the Akt-related cytokine-independent survival kinase requires interaction of its phox domain with endosomal phosphatidylinositol 3-phosphate. Proc Natl Acad Sci U S A *98*, 12908-12913.

Volden, P.A., and Conzen, S.D. (2013). The influence of glucocorticoid signaling on tumor progression. Brain Behavior and Immunity *30*, S26-S31.

Vukicevic, S., Kleinman, H.K., Luyten, F.P., Roberts, A.B., Roche, N.S., and Reddi, A.H. (1992). Identification of multiple active growth factors in basement membrane Matrigel suggests caution in interpretation of cellular activity related to extracellular matrix components. Exp Cell Res *202*, 1-8.

Walsh, D.A., Perkins, J.P., and Krebs, E.G. (1968). An adenosine 3',5'-monophosphate-dependant protein kinase from rabbit skeletal muscle. The Journal of biological chemistry *243*, 3763-3765.

Wan, M., Leavens, K.F., Hunter, R.W., Koren, S., von Wilamowitz-Moellendorff, A., Lu, M., Satapati, S., Chu, Q., Sakamoto, K., Burgess, S.C.*, et al.* (2013). A Noncanonical, GSK3-Independent Pathway Controls Postprandial Hepatic Glycogen Deposition. Cell Metab *18*, 99-105.

Wang, K., Gu, S., Nasir, O., Foller, M., Ackermann, T., Klingel, K., Kandolf, R., Kuhl, D., Stournaras, C., and Lang, F. (2010). SGK1-dependent Intestinal Tumor Growth in APC-deficient Mice. Cellular Physiology and Biochemistry *25*, 271-278.

Wang, L., Harris, T.E., Roth, R.A., and Lawrence, J.C. (2007). PRAS40 regulates mTORC1 kinase activity by functioning as a direct inhibitor of substrate binding. J Biol Chem *282*, 20036-20044.

Wang, R.C., Wei, Y., An, Z., Zou, Z., Xiao, G., Bhagat, G., White, M., Reichelt, J., and Levine, B. (2012). Akt-Mediated Regulation of Autophagy and Tumorigenesis Through Beclin 1 Phosphorylation. Science *338*, 956-959.

Wang, Y.Z., Zhou, D.J., Phung, S., Masri, S., Smith, D., and Chen, S.A. (2011). SGK3 Is an Estrogen-Inducible Kinase Promoting Estrogen-Mediated Survival of Breast Cancer Cells. Molecular Endocrinology *25*, 72-82.

Waterhouse, A.M., Procter, J.B., Martin, D.M.A., Clamp, M., and Barton, G.J. (2009). Jalview Version 2-a multiple sequence alignment editor and analysis workbench. Bioinformatics *25*, 1189-1191.

Webster, M.K., Goya, L., and Firestone, G.L. (1993a). Immediate-Early Transcriptional Regulation and Rapid Messenger-Rna Turnover of a Putative Serine Threonine Protein-Kinase. J Biol Chem *268*, 11482-11485.

Webster, M.K., Goya, L., Ge, Y., Maiyar, A.C., and Firestone, G.L. (1993b). Characterization of Sgk, a Novel Member of the Serine Threonine Protein-Kinase Gene Family Which Is Transcriptionally Induced by Glucocorticoids and Serum. Mol Cell Biol *13*, 2031-2040.

Weigelt, B., and Downward, J. (2012). Genomic Determinants of PI3K Pathway Inhibitor Response in Cancer. Front Oncol *2*, 109.

Willems, L., Tamburini, J., Chapuis, N., Lacombe, C., Mayeux, P., and Bouscary, D. (2012). PI3K and mTOR Signaling Pathways in Cancer: New Data on Targeted Therapies. Current Oncology Reports *14*.

Woo, S.-Y., Kim, D.-H., Jun, C.-B., Kim, Y.-M., Haar, E.V., Lee, S.-i., Hegg, J.W., Bandhakavi, S., Griffin, T.J., and Kim, D.-H. (2007). PRR5, a novel component of mTOR complex 2, regulates platelet-derived growth factor receptor beta expression and signaling. J Biol Chem *282*, 25604-25612.

Wu, C., Yosef, N., Thalhamer, T., Zhu, C., Xiao, S., Kishi, Y., Regev, A., and Kuchroo, V.K. (2013). Induction of pathogenic T(H)17 cells by inducible salt-sensing kinase SGK1. Nature *496*, 513-517.

Wu, W., Chaudhuri, S., Brickley, D.R., Pang, D., Karrison, T., and Conzen, S.D. (2004). Microarray analysis reveals glucocorticoid-regulated survival genes that are associated with inhibition of apoptosis in breast epithelial cells. Cancer Research *64*, 1757-1764.

Wu, W., Zou, M., Brickley, D., Pew, T., and Conzen, S. (2006). Glucocorticoid receptor activation signals through forkhead transcription factor 3a in breast cancer cells. Molecular Endocrinology *20*, 2304-2314.

Wu, Y., Dowbenko, D., Spencer, S., Laura, R., Lee, J., Gu, Q., and Lasky, L.A. (2000). Interaction of the tumor suppressor PTEN/MMAC with a PDZ domain of MAGI3, a novel membrane-associated guanylate kinase. J Biol Chem *275*, 21477-21485.

Wulff, P., Vallon, V., Huang, D.Y., Volkl, H., Yu, F., Richter, K., Jansen, M., Schlunz, M., Klingel, K., Loffing, J.*, et al.* (2002). Impaired renal Na+ retention in the sgk1-knockout mouse. Journal of Clinical Investigation *110*.

Wullschleger, S., Loewith, R., and Hall, M.N. (2006). TOR signaling in growth and metabolism. Cell *127*, 5-19.

Xu, J., Liao, L., Qin, J., Xu, J., Liu, D., and Songyang, Z. (2009). Identification of Flightless-I as a Substrate of the Cytokine-independent Survival Kinase CISK. J Biol Chem *284*.

Xu, J., Liu, D., Gill, G., and Songyang, Z. (2001). Regulation of cytokine-independent survival kinase (CISK) by the Phox homology domain and phosphoinositides. J Cell Biol *154*.

Xu, J., Wan, M., He, Q., Bassett, R.L., Jr., Fu, X., Chen, A.C., Shi, F., Creighton, C.J., Schiff, R., Huo, L.*, et al.* (2012). SGK3 is associated with estrogen receptor expression in breast cancer. Breast Cancer Research and Treatment *134*.

Yang, Q., Inoki, K., Ikenoue, T., and Guan, K.-L. (2006). Identification of Sin1 as an essential TORC2 component required for complex formation and kinase activity. Gene Dev *20*, 2820-2832.

Yang, S., Zhang, J.J., and Huang, X.-Y. (2009). Orai1 and STIM1 Are Critical for Breast Tumor Cell Migration and Metastasis. Cancer Cell *15*, 124-134.

Yang, Z.Z., Tschopp, O., Hemmings-Mieszczak, M., Feng, J., Brodbeck, D., Perentes, E., and Hemmings, B.A. (2003). Protein kinase B alpha/Akt1 regulates placental development and fetal growth. J Biol Chem *278*, 32124-32131.

Yao, L.J., McCormick, J.A., Wang, J., Yang, K.Y., Kidwai, A., Colussi, G.L., Boini, K.M., Birnbaum, M.J., Lang, F., German, M.S.*, et al.* (2011). Novel Role for SGK3 in Glucose Homeostasis Revealed in SGK3/Akt2 Double-Null Mice. Molecular Endocrinology *25*, 2106-2118.

You, H., Jang, Y.J., You-Ten, A.I., Okada, H., Liepa, J., Wakeham, A., Zaugg, K., and Mak, T.W. (2004). P53-dependent inhibition of FKHRL1 in response to DNA damage through-protein kinase SGK1. P Natl Acad Sci USA *101*, 14057-14062.

Yu, J., Zhang, Y., McIlroy, J., Rordorf-Nikolic, T., Orr, G.A., and Backer, J.M. (1998). Regulation of the p85/p110 phosphatidylinositol 3'-kinase: stabilization and inhibition of the p110alpha catalytic subunit by the p85 regulatory subunit. Mol Cell Biol *18*, 1379-1387.

Yu, Y., Yoon, S.-O., Poulogiannis, G., Yang, Q., Ma, X.M., Villen, J., Kubica, N., Hoffman, G.R., Cantley, L.C., Gygi, S.P.*, et al.* (2011). Phosphoproteomic Analysis Identifies Grb10 as an mTORC1 Substrate That Negatively Regulates Insulin Signaling. Science *332*, 1322-1326.

Zemtsova, I.M., Heise, N., Frohlich, H., Qadri, S.M., Kucherenko, Y., Boini, K.M., Pearce, D., Shumilina, E., and Lang, F. (2010). Blunted IgE-mediated activation of mast cells in mice lacking the serum- and glucocorticoid-inducible kinase SGK3. Am J Physiol-Cell Physiol *299*, C1007-C1014.

Zeng, X., Xu, H.M., and Glazer, R.I. (2002). Transformation of mammary epithelial cells by 3-phosphoinositide-dependent protein kinase-1 (PDK1) is associated with the induction of protein kinase C alpha. Cancer Research *62*.

Zhang, L.P., Cui, R.W., Cheng, X.D., and Du, J. (2005). Antiapoptotic effect of serum and glucocorticoid-inducible protein kinase is mediated by novel mechanism activating I kappa B kinase. Cancer Research *65*, 457-464.

Zhang, W., Xia, X., Reisenauer, M.R., Rieg, T., Lang, F., Kuhl, D., Vallon, V., and Kone, B.C. (2007). Aldosterone-induced Sgk1 relieves Dot1a-Af9-mediated transcriptional repression of epithelial Na+ channel alpha. Journal of Clinical Investigation *117*, 773-783.

Zhao, B., Lehr, R., Smallwood, A.M., Ho, T.F., Maley, K., Randall, T., Head, M.S., Koretke, K.K., and Schnackenberg, C.G. (2007). Crystal structure of the kinase domain of serum and glucocorticoid-regulated kinase 1 in complex with AMP PNP. Protein Sci *16*, 2761-2769.

Zhou, B.P., Liao, Y., Xia, W., Zou, Y., Spohn, B., and Hung, M.C. (2001). HER-2/neu induces p53 ubiquitination via Akt-mediated MDM2 phosphorylation. Nat Cell Biol *3*, 973-982.

Zhou, D., Salnikow, K., and Costa, M. (1998). Cap43, a novel gene specifically induced by Ni2+ compounds. Cancer Research *58*, 2182-2189.

Zhou, R., and Snyder, P.M. (2005). Nedd4-2 phosphorylation induces serum and glucocorticoid-regulated kinase (SGK) ubiquitination and degradation. J Biol Chem *280*, 4518-4523.

Zoncu, R., Bar-Peled, L., Efeyan, A., Wang, S., Sancak, Y., and Sabatini, D.M. (2011). mTORC1 Senses Lysosomal Amino Acids Through an Inside-Out Mechanism That Requires the Vacuolar H+-ATPase. Science *334*, 678-683.